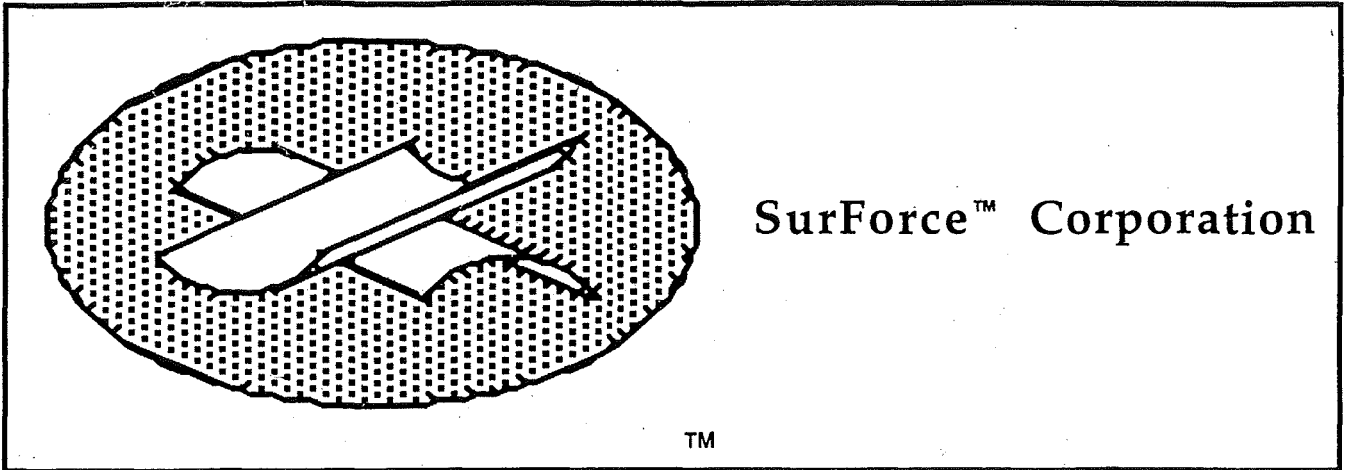


Tonyza



## SURFACE FORCES APPARATUS 3™

### USER'S MANUAL

This manual is the Property of SurForce™ Corporation.

© 1996 SurForce™ Corporation.

All rights reserved.

No part of this manual may be reproduced or used in any form or by any means, graphic, electronic or mechanical, including photocopying, recording, taping, or information storage and retrieval systems without written permission of SurForce™ Corporation.

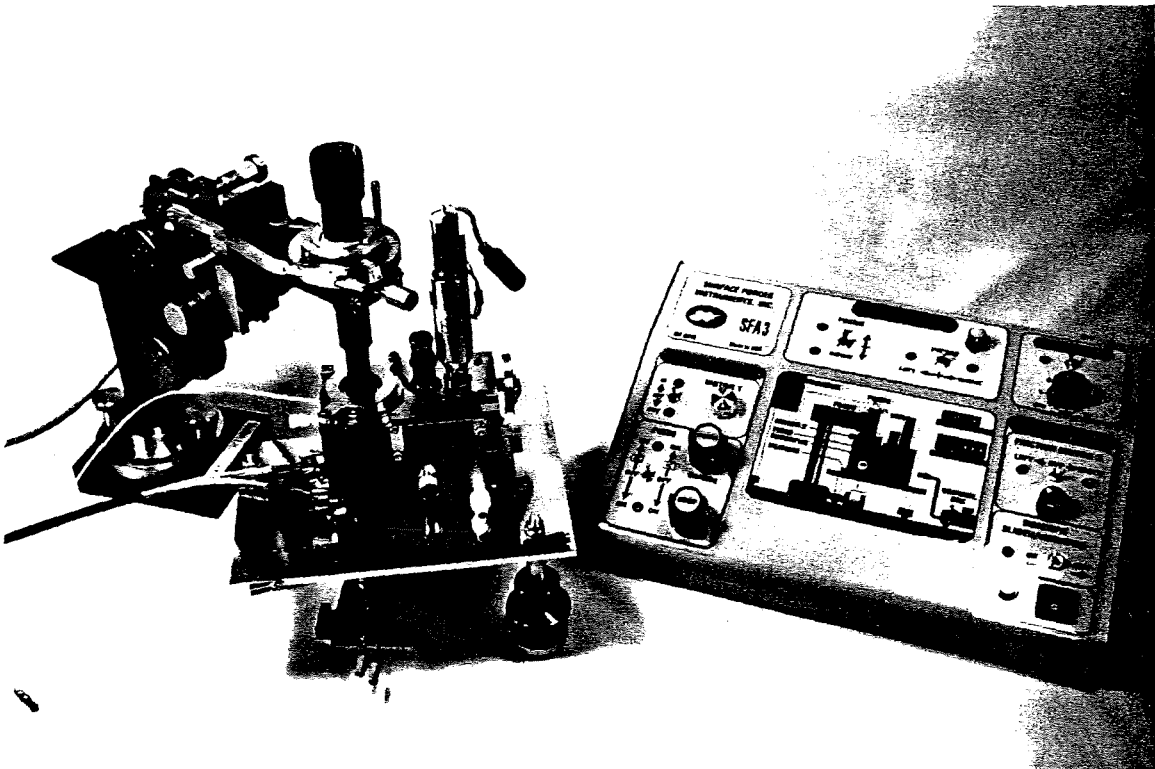
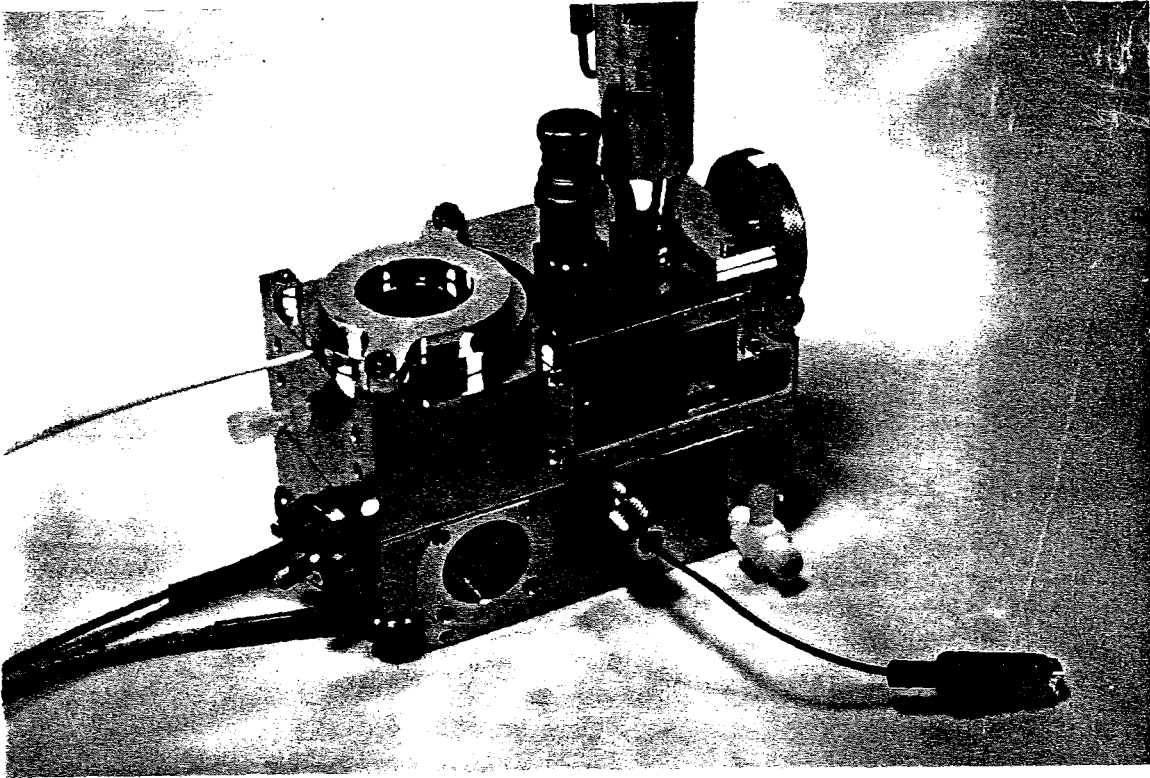


Figure 1. Surface Forces Apparatus 3.

## Surface Forces Apparatus 3

Surface Forces Apparatuses (SFAs) are research instruments for directly measuring the static and dynamic forces between surfaces, and for studying other interfacial and thin film phenomena at the molecular level. Although useful for both basic and applied research, the SFA 3 is essentially a research tool, intended for investigations of new phenomena and the unexpected, rather than for routine measurements. To this end, the SFA 3 has been designed to be highly versatile, allowing for improvisation and the ability to choose different measuring techniques during experiments.

### What it does

The SFA 3 measures the forces between two surfaces in vapors or liquids with a sensitivity of a few millidynes (10 nN) and a distance resolution of 1 Å (0.1 nm). It can also be used to measure the refractive index of the medium between the surfaces, molecular orientations in thin films (under certain conditions), adsorption isotherms, capillary condensation, surface deformations arising from surface forces, dynamic interactions such as viscoelastic and frictional forces, and other time-dependent phenomena in real time. Though mica surfaces are the primary surfaces used for these measurements, it is possible to deposit or coat these surfaces with surfactants, lipids, polymers, proteins, metals, metal oxides, silica, etc., so as to alter the nature and chemistry of the interacting surfaces while keeping them smooth by virtue of the molecularly smooth mica substrate surface underneath.

### How it works

The picture opposite shows an assembled *basic apparatus* ready for use. The shapes of the interacting surfaces and the separation between them are measured by analyzing the optical interference fringes produced when white light passes normally through the two surfaces. The distance between the surfaces can be controlled over a range of 5 mm with a resolution of 1 Å by a four-stage mechanism of increasing sensitivity. The stiffness of the *force-measuring spring* can be adjusted during experiments by moving the dove-tailed clamp along the length of the spring. This enables forces of greatly differing magnitudes to be measured. Dynamic measurements are conducted with surfaces in motion by vibrating the piezoelectric crystal supporting the upper surface, or using one of the attachments described in Part II.

### Additional features

The SFA 3 employs similar techniques to those used in SFA Mk 2 and other SFAs, but it is easier to operate and is generally more user-friendly. The first three stages of the four-stage distance control can be controlled directly by hand and allow for rapid manual control of surface separation to within 10 Å. All four distance controls have been specially designed to produce perfectly linear displacements of the surfaces without backlash (there are no moving shafts or sliding dovetails in any of the distance control mechanisms – only springs). The SFA 3 is also more robust, less susceptible to thermal drifts, easier to clean, and requires smaller quantities of liquid than conventional SFAs. A number of facilities that appeared as accessories in earlier models are now part of the Basic Unit, and new attachments allow for dynamic measurements to be made of friction, lubrication and viscoelastic forces over a large range of shear rates and sliding speeds.

## **PART 1: ASSEMBLY OF BASIC UNIT**

1.1	Setting up and equipping a surface forces measurement laboratory.....	6
1.2	Brief description of UNITS and PARTS, with figures.....	18
1.3	Handling the SFA: cleaning and assembly (Basic Unit only).....	48

## **PART 2: GENERAL OPERATING PROCEDURES**

2.1	Preparation of surfaces for force measurements or interferometric experiments .....	59
2.2	Installation of surfaces into the SFA 3.....	69
2.3	Initial observation of surfaces with Newton's rings .....	72
2.4	Observation of surfaces with FECO fringes and initial measurements and calibrations .	73
2.5	Filling the SFA chamber with liquid.....	76
2.6	General operating procedures.....	77
2.7	Distance measurements with FECO fringes.....	79
2.8	Other measurements with FECO fringes .....	87
2.9	Measuring equilibrium forces.....	90
2.10	Measuring viscous forces and other dynamic interactions .....	93
2.11	Calibrations .....	93
2.12	Analyzing the results.....	97
2.13	Miscellaneous hints and troubleshooting; servicing your SFA .....	99

## **PART 3: ATTACHMENTS & ACCESSORIES**

3.1	Syringe injection unit .....	103
3.2	Friction device.....	104
3.3	Bimorph slider.....	108
3.4	Bimorph vibrator.....	119
3.5	Other (optional) attachments and customized modifications .....	121

## **PART 4: FURTHER INFORMATION, SPECIFICATIONS, REFERENCES**

4.1	Performance specifications of SFA 3 and attachments .....	124
4.2	Complete list of parts .....	126
4.3	References to SFA technology and literature on force measurements, videos.....	131
4.4	APPENDIX 1 (Copy of the original publication describing the SFA3) .....	134
4.5	APPENDIX 2 (Example of an SFA experiment).....	135
4.6	APPENDIX 3 (Force-measuring capabilities of SFA and AFM compared).....	136

## FIGURES (DRAWINGS & PHOTOGRAPHS)

Fig. No.		Page
1	Surface Forces Apparatus 3 (SFA3).....	2
2	SFA3 (schematic) showing parts controlled by the CONTROL BOX.....	6
3	Plan of small surface forces laboratory.....	10
4	Units and attachments.....	18
5	Assembly drawing of SFA 3 – BASIC UNIT showing key parts.....	19
6	Sub-units 1 – 5 of BASIC UNIT.....	20
7	Assembly drawing of UPPER CHAMBER.....	21
8	Assembly drawing of Motor Housings.....	22
9	Assembly drawing of LOWER CHAMBER and heater connections.....	23
10	Assembly drawing of VARIABLE SPRING.....	24
11	Assembly drawing of SYRINGE INJECTOR.....	24
12	Assembly drawing of PIEZO MOUNT.....	25
13	Assembly drawing of BASE.....	25
14	Assembly drawing of MIRROR.....	26
15	Assembly drawing of FRICTION DEVICE.....	27
16	Assembly drawing of BIMORPH SLIDER.....	28
17	Assembly drawing of BIMORPH VIBRATOR.....	29
18	Photographs of dismantled BASIC UNIT showing key parts.....	30
19	Photographs of UPPER CHAMBER.....	31
20	Photographs of LOWER CHAMBER and VARIABLE SPRING.....	32
21	Photographs of BASE.....	33
22	Photographs of PIEZO MOUNT.....	34
23	Photographs of MIRROR.....	35
24	Photographs of OPTICS STAND.....	36
25	Photographs of SYRINGE INJECTOR.....	37
26	Photographs of FRICTION DEVICE.....	38
27	Photographs of BIMORPH SLIDER.....	39
28	Photographs of BIMORPH VIBRATOR and FIXED SPRING MOUNT.....	40
29	Photographs/drawings of CONTROL BOX (front, back and inside wiring).....	41-43
30	Photographs of MISCELLANEOUS SUPPLY ITEMS, TOOLS, etc.....	44-47
31	Soaking of apparatus parts under cover.....	50
32	Types of screws used in the SFA 3.....	52
33	Tweezers used in various mica-handling operations.....	59
34	Stages in the preparation of mica sheets.....	60
35	Controlling the mutual crystallographic orientation of mica sheets.....	64
36	Langmuir-Blodgett deposition of surfactant layers on mica and other surfaces.....	68
37	Views through window of assembled Basic Unit after installation of the disks.....	70-71
38	FECO optical system.....	74
39	FECO fringe patterns (numerical example).....	83
40	Measuring surface radii from the shapes of FECO fringes.....	88
41	Various types of FECO patterns obtained on different systems.....	89
42	Basic mechanics of the force-measuring spring system.....	91
43	Optical path length for non-normally incident light.....	101
44	Friction Device attachment.....	105
45	Different mounting configurations of the Friction Device.....	106
46	Bimorph Slider attachment.....	109
47	Electrical wiring and connections of Bimorph Slider.....	111
48	Shear elements of the Bimorph Slider attachment.....	113
49	Equivalent mechanical circuit of the Bimorph Slider and Friction Device.....	115
50	Bimorph Vibrator assembly.....	120
51	Small volume lower chamber with height-adjustable lower window.....	122
52	Dove-tailed disks and disk mounts.....	123
53	SFA and AFM force-measuring techniques compared.....	137-138

# PART I

## ASSEMBLY OF BASIC UNIT

PART 1 describes the design of a surfaces forces measurements laboratory and the tools and facilities that are required for assembling and servicing the SFA 3 Basic Unit (most of these are supplied). PART 2 describes procedures for carrying out normal force measurements. Additional attachments and modifications to the Basic Unit are described in PART 3. PART 4 provides more detailed information including a complete parts list, performance specifications and a bibliography.

### 1.1 SETTING UP AND EQUIPPING A SURFACE FORCES MEASUREMENT LABORATORY

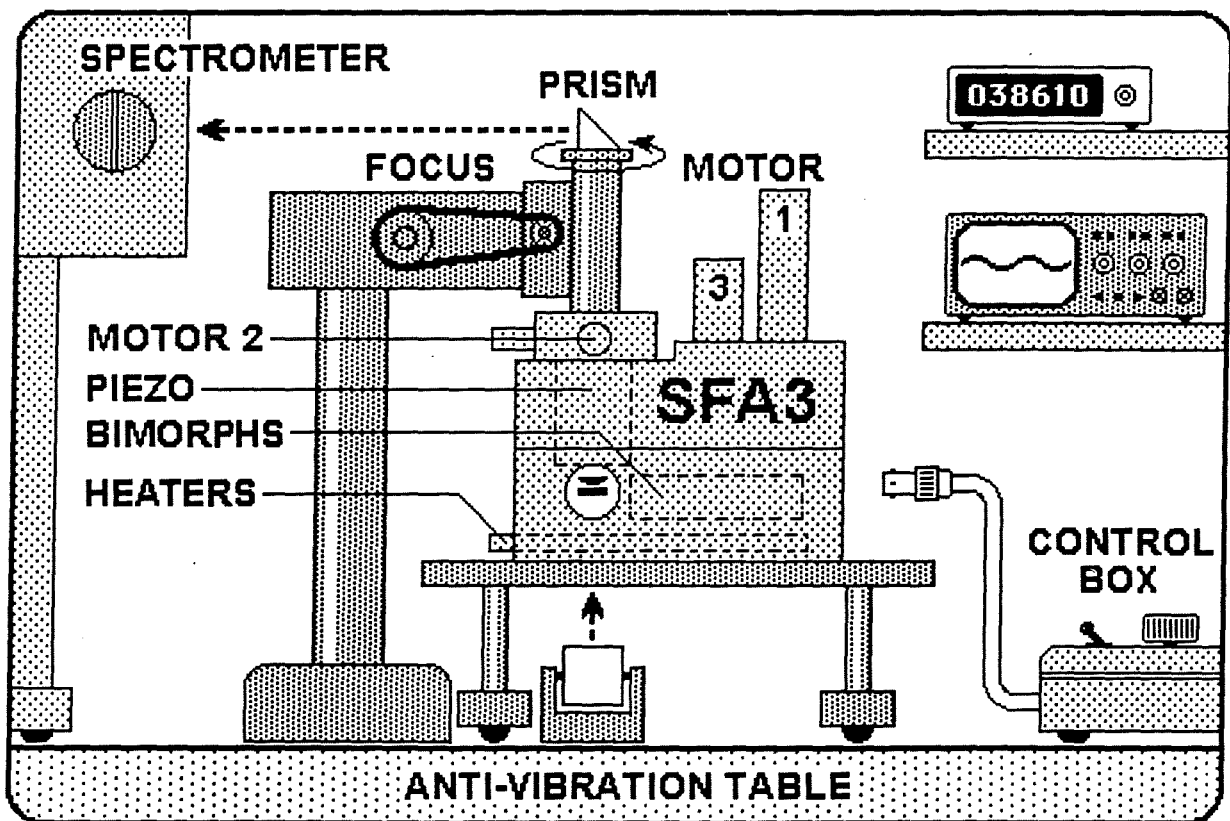


Figure 2. Schematic of SFA 3 setup, also showing those parts that are controlled by the CONTROL BOX. Recommended horizontal distance from prism to spectrometer entrance slit: 50 cm. Recommended vertical distance from prism to table top: 30 cm. Height of centre of mirror from table top: 4.6 cm.

## SFA 3 BASIC UNIT

You should have received the following items in your SFA package:

UPPER CHAMBER
LOWER CHAMBER
VARIABLE SPRING
BASE
PIEZO MOUNT
OPTICS STAND
MIRROR
CONTROL BOX
ENCODER DISPLAY COUNTERS
TOOL KIT (SEE LIST BELOW)
SUPPLY BOX (SEE LIST BELOW)
ELECTRIC CABLES (SEE LIST BELOW)
FRICITION DEVICE

See Table II in Part 4 for further details on individual parts and components.

### ASSEMBLY TOOLS (TOOL KIT)

Screw drivers, flat type – 11 sizes (mm): 1.5, 2.0, 2.5, 3.0, 4.0, 4-in-one, two large  
Screw drivers, hex type, Allen keys – 9 sizes (mm): 0.9 1.3, 1.5, 2.0, 2.5, 3.0, 4.0, 0.028", 0.035"  
Screw drivers, Philips type – 3 sizes: 00, 0, 1  
Nut driver – 1 size: 4.0 mm, for adjusting limit switch positions on motor housings  
Tweezers (1 flat tipped, 1 Teflon coated, for handling small parts and polished surfaces)  
Tweezers – specially shaped, for picking up cylindrical silica disks  
Forceps (stainless steel, 2 sizes: 4" and 6", for handling parts, helical springs, etc.)  
Forceps (1 angled, 1 pointed, for handling platinum wire, mica and small parts)  
Spatula (steel, for inserting/removing main spring of Upper Chamber)  
Cleaning brushes (15) – for cleaning threaded holes with water or alcohol only  
Mini wrenches (3/16" – for mirror cables, 1/8" – for micro electric connectors)  
Adjustable spanner/wrench (for micrometer, motor housings, etc.)  
Double-ended right angled screw driver (for bolting main spring in Upper Chamber)

## SUPPLY ITEMS (SUPPLY BOX)

Base pads/kinematic mounts (three, for base legs)  
Belts (two, for Optics Stand)  
Eyepiece (X10 wide-angle, *Nikon CFWE 10XA*)  
Force-measuring springs (4 spare)  
Friction Device clamping screws (two)  
Friction Device restrainer with short 3.5 mm screw  
Glass disk for sealing apparatus without using piezo mount and for leak tests.  
Glue (some crystals of Shell EPON RESIN 1004 and 1009)  
Graticule / reticule with cross-hair (for eyepiece)  
Kel-F tubing with Luer connectors at ends (two)  
Luer fittings (2 fem-fem, 2 male-male, 2 fem-male, 3 caps, 2 male ports, 2 female ports, 1 valve, O-rings size -003 for Luer threads, Teflon Luer filter)  
Microscope tube (for use with Friction Device) with X10 objective installed  
Microscope tube (normal, for use with Optics Stand) with X5 objective  
Mirror control cables (3, with thumb screws, end clamps and washers)  
Mirror knobs (3)  
Needles (3, for cleaving mica)  
O-rings (30 spare): -003, -006, -007, -008, -010, -012, -015\*, -020, -222, -224, -236  
Perspex window (1 spare)  
Potentiometer dials (two, for coarse and fine Piezo controls on Control Box)  
Prism (1 inch, for placing on top of Optics Stand)  
Screws (spares, unusual sizes only)  
Self-adhesive vernier scale for motor housing (spare strip)  
Silica disks (8): 3.5 mm high (2), 4.0 mm (2), 4.5 mm (1), 2.5 mm for friction device mount only (3).  
Small Kel-F tipped 1.6 mm stainless steel screws (3 spare)  
Spanners (two) for bellows ring clamps  
Spirit level (for placing on Base)  
Stand for Upper Chamber (flat base with 4 supporting legs, tapered on top)\*  
Syringe (50 ml, for filling SFA chamber)  
Teflon bellows (1 spare)  
Thermistor port  
Thermistor (wired to connecting cable, plus one spare)  
Thumb screws (two, brass, for Optics Stand base)  
Upper Chamber stainless-steel helical spring (alternatives, with lower stiffness)

\* Optional, requires separate order.

## ELECTRIC CABLES AND CONNECTORS

Check that the Control Box and Apparatus are electrically earthed or 'grounded' before switching on. The Apparatus should be earthed via a hole on the front of the Base Plate. See comments on avoiding 'earth loops' or 'ground loops' on page 43.

Numbers refer to those marked on cables. Note: 1 metre (m)  $\approx$  3 feet.

### POWER

1. POWER STATION: surge-protected, to suit local voltage supply.
2. POWER INPUT CABLE (2 m): Three-pin chord from Station to Control Box.

### OPTICS STAND

3. OPTICS CABLE (mini-DIN, 2–3 m): 8-pin cable from Control Box Optics Output to Optics Stand. In some models, one end of this cable is already attached to the Optics Stand.

### APPARATUS MOTOR 1

4. MOTOR 1 CABLE (mini-DIN, 2 m): Six-pin cable from Control Box Output to Motor 1.
5. ENCODER CABLE (2 m): 8-pin silver steel connector leading to two 4-pin cables each terminating in a 21-pin connector to be plugged into display counters for Motors 1 and 2.

### PIEZO

6. PIEZO INPUT CABLE (1 m): Connect free end to low-voltage ( $\pm 5$ –10 V) regulated DC power supply or function generator (ripple  $< 1$  mV). Turn Piezo switch to EXT. When using internal power supply, switch to INT.
7. PIEZO OUTPUT CABLE (BNC–BNC, 1 m): From Control Box Piezo Output to high gain DC amplifier (X50–100 TREK type, with BNC input socket).
8. PIEZO MOUNT CABLE (BNC–BNC coax cable, 2 m): From high gain amplifier to Piezo Mount on apparatus via BNC–LEMO connector.

### FRICTION DEVICE

9. FRICTION DEVICE CABLE (2 m). Connect free end to strain gauge detector/bridge, the other end to the 4-pin LEMO receptacle on the Friction Device.
10. MOTOR 2 CABLE (mini-DIN, 2 m): Six-pin cable from Control Box Output to Motor 2.
11. ENCODER CABLE (2 m): 8-pin silver steel connector leading to two 4-pin cables each terminating in a 21-pin connector to be plugged into display counters for Motors 1 and 2.

### BIMORPH SLIDER / VIBRATOR (optional)

12. BIMORPH INPUT CABLE (1 m): Connect free end to DC power supply or function generator.
13. BIMORPH OUTPUT CABLE (BNC–BNC, 1 m): From Bimorph Output on Control Box to low gain amplifier or directly to Bimorph Slider.
14. BIMORPH MOUNT CABLE (BNC–LEMO coax connector, 2 m): From low gain amplifier or directly from Bimorph Output on Control Box to LEMO connector on Bimorph Slider. This cable can also be used to connect the BIMORPH VIBRATOR to a lock-in amplifier or oscilloscope.

### MISCELLANEOUS

15. HEATER CABLE (2 m): Connect from Control Box Heater Output to heater rods in Lower Chamber.
16. FUSES: Spare 0.5 and 1.0 Amp fuses for Control Box fuse holders (fast action fuses).
17. THERMISTOR: Connect thermistor leads to resistance input on multimeter (not supplied).
18. EARTHING LEAD: Single wire connection from front of Base plate to earth (ground).

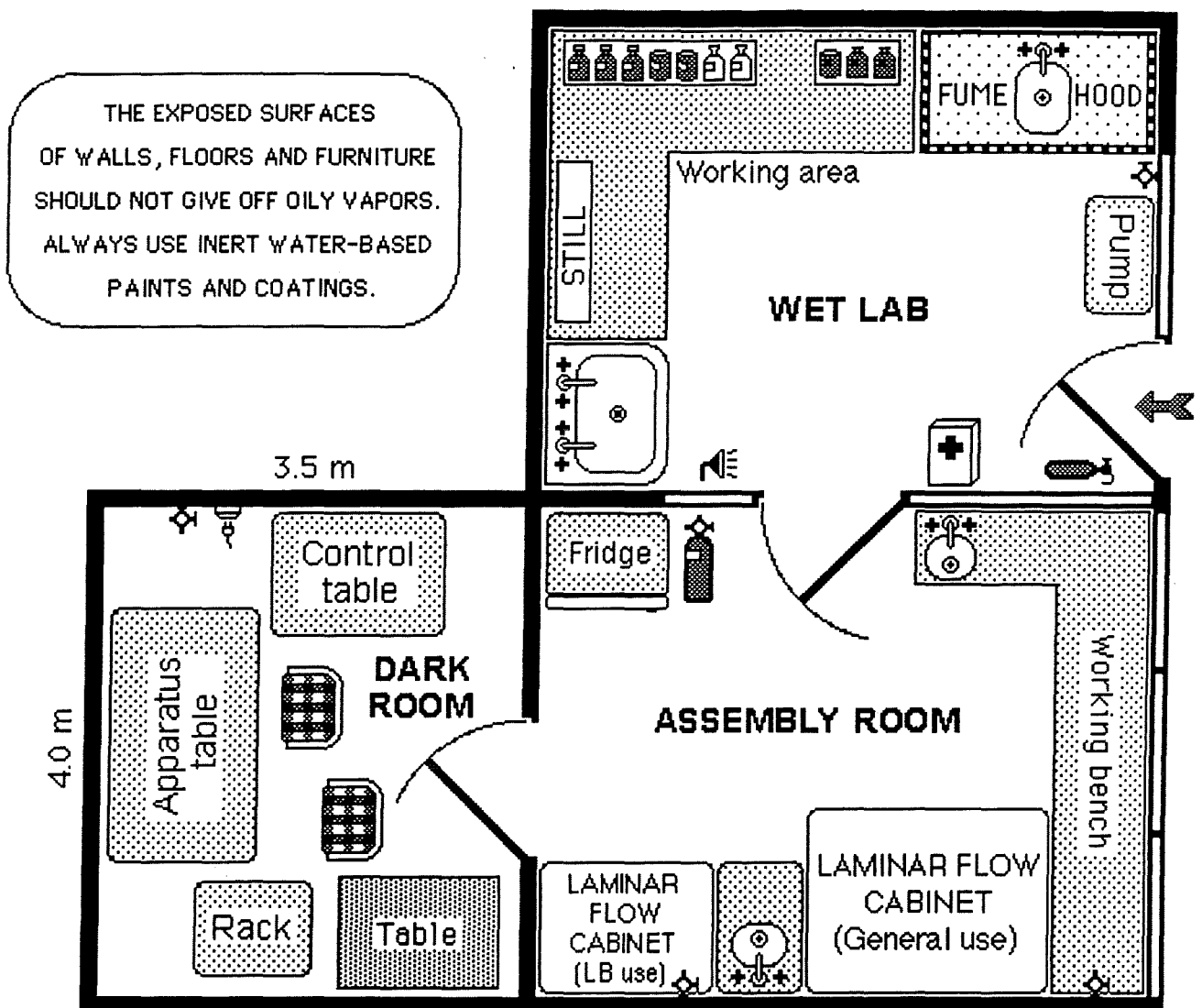


**Figure 3.** Small self-contained surface forces laboratory. Additional experimental rooms (dark rooms) may be added at a later date.

## IMPORTANT CONSIDERATIONS IN PLANNING A SURFACE FORCES MEASUREMENT LABORATORY

Figure 3 shows a suitable layout for a small surface forces laboratory, indicating convenient locations for a WET LAB (for liquid purification, solvent distillation, etc.) an ASSEMBLY ROOM (for assembling and cleaning the apparatus) and one DARK ROOM (for performing experiments). Ideally, the laboratory should be located in a basement or ground floor – well away from vibration-producing machinery such as large pumps or air-conditioning units. The walls, furniture and floor should never be coated or cleaned with oil-based polishes that give off surface active contaminants into the atmosphere (these can usually be smelled if present). All laboratory surfaces, including floors and work benches, should be cleaned with warm water only. The dark room(s) should be thermostatically controllable to  $\pm 0.1^\circ\text{C}$ , if possible, and the thermostating air-conditioning or air-ducting system should not be connected to other laboratories so as not to introduce air-borne contamination into the lab atmosphere. Ideally, the air pressure of the experimental rooms should be slightly higher than of the adjoining rooms, ensuring a steady flow of (clean and thermostatted) air from that room outwards.

### **Recommended laboratory hardware and fittings (see Table I for complete list)**

Your SFA3 package should arrive in a condition ready for immediate use in experiments – all necessary apparatus parts, assembly tools, electrical items and cables being provided with your unit (see lists on pages 7-9). However, a number of additional laboratory hardware items (not provided in the package) are needed for carrying out experiments. These are described in the following paragraphs (essential items are underlined). A full list of items is given in Table I below.

The following major laboratory hardware items and facilities are recommended for most routine experiments, some of which are shown in Figure 3: Work benches with sinks, tables and chairs. Storage cabinets. Clean inert gas supply outlets in each room (such as clean, dry nitrogen gas from boil off source, not cylinders). Laminar flow cabinet(s) for cutting mica, apparatus assembly, and for other preparations under dust-free conditions. Fume hood. Distillation units for water and solvent purification. Anti-vibration table for placing apparatus (optional, but essential for laboratories located above ground-level). Small fridge. Evaporator vacuum pump for silvering and surface deposition (ducted to the outside through the wall). Additional laboratory and apparatus-associated items are listed in Table I below.

**Optical items (see Table I for details)**

Grating spectrometer with 90° prism at entry slit on adjustable turntable, one exit port with movable reticulated eyepiece and a second exit port for normal or video camera, recommended grating dispersion 32Å/mm (spare gratings of 16Å/mm and 64Å/mm optional). White light source – tungsten-halogen or xenon-arc lamp, with collimating lens and IR heat-absorbing filter. Sodium lamp and mercury pen-ray light sources. Rotating image dove prism. Light polarizers. Video camera-recorder system (optional for dynamic measurements).

---

**Electronic items (see Table I for details)**

General purpose 5-digit multimeter. High voltage power supply and/or amplifier for driving piezoelectric crystals and bimorphs (low voltage power supplies for driving DC motors are supplied with the Basic Unit). Other equipment and electronic devices such as function generators, amplifiers, strain-gauge bridges, frequency counters, lock-in amplifiers, chart recorders and storage scopes may be required for specialized experiments (see Table I).

**Miscellaneous items (see Table I for details)**

Mica cutting stage and small hot plate for gluing mica sheets and other substrates to silica disks. Langmuir-Blodgett trough for depositing organic layers on surfaces. Miscellaneous laboratory supplies and materials: glassware, filters, mica (Ruby Muscovite clear, thick large sheets, about 6"x6" square), glues, chemicals, etc.

**TABLE I – COMPLETE LIST OF LABORATORY ITEMS REQUIRED**

Table I on the following few pages is a list of laboratory equipment, supplies and facilities that – with the few exceptions indicated – are not provided with the Basic SFA 3 or its Attachments but which are required for conducting routine static and dynamic force measurements. Essential items for measuring forces with the Basic Unit are starred in black – ★, those required additionally for dynamic measurements using the dynamic attachments are starred in white – ☆. The unstarred items are optional or required only for specialized measurements, for example, involving *in-situ* spectroscopic techniques that may require even additional equipment and facilities not shown here. Columns 1 and 2 give the main specifications and uses of the equipment item. Columns 3 – 6 provide the name of a product that has been found suitable for these purposes, although other products may be equally or more suitable, depending on the experiments. Column 5 gives the number of units that are normally required. Surface Forces Instruments, Inc., will be pleased to advise on and, when feasible, provide any of the items (or similar items) listed here as part of the purchase of a SFA 3 and/or attachments. These items will appear under the category ADDITIONAL EQUIPMENT ITEMS in the Sales Contract.

**TABLE I**  
**SPECTROMETER**

1 Equipment Item	2 Required for	3 Supplier	4 Model	5 No.	6 Price*
★ <b>Spectrometer</b> 1/2 or 1/4 meter grating spectrometer with grating (32Å/mm dispersion - 1200 grooves/mm, 550 nm blaze), adjustable entrance slit, fixed exit slit, camera port.	Measuring surface separations, surface shapes, and thin film thickness, via FECO fringe interferometry	Scientific Measurements Systems	MonoSpec (1/2 m).....00-000	1	8,000
			or MonoSpec (1/4 m).....82-497	1	or 3,430
			Grating (550nm blaze).....11-080	1	590
			Adjustable Entrance Slit.....15-3000	1	600
			Fixed Exit Slit .....12-525	1	90
			Operator's Manual.....00-4167	1	?
			Installation & Demonstration.....	1	?
★ <b>Translation Stage</b> Traveling eyepiece with manual drive encoder	Fitted to replace the spectrometer exit slit	Newport-Klinger	Translation Stage (25mm).....426A	1	500
			Encoder Motor.....850 B-1	1	500
			Installation (16 hrs labor).....	1	?
★ <b>Display Counter</b> with power supply	Translation Stage encoder readout	Klinger	Display Counter with Power Supply 110V/220V....CV 100-1 or CV 200-1	1	550
★ <b>Wide field Eyepiece</b> 10X adjustable focus with 10X10X1mm sq. grid reticle	Translation Stage at spectrometer exit slit	A. G. Heinz	CFW-N 10X Nikon Eyepiece....84220	1	172
			with 10X10X1mm squares grid reticle (installed).....SO 75962	1	60
★ <b>Prism</b>	Entrance slit	Rolyn Optics	Right Angle Prism 90°, 25mmX25mm.....40.0060	2	2x41=82
★ <b>Prism turntable</b> with 3-axis rotational controls	Entrance slit	Klinger	Turntable.....PO 32N Clamp.....	1 1	350 ?

★ Essential items for the Basic Unit.

☆ Essential items for the Friction Device, Bimorph Slider and/or Bimorph Vibrator.

\* Prices are estimates in US \$ and do not include TAX, SHIPPING and HANDLING.

**LIGHT SOURCES & OPTICAL ITEMS**

1 Equipment Item	2 Required for	3 Supplier	4 Model	5 No.	6 Price*
★ <b>White light source</b> 100W Tungsten-Halogen Lamp, or Xenon Arc Lamp. Powered by Low Voltage Power Supply - see LVPS.	White light source for FECO interferometry	Ealing	Projection Lamphouse.....27-1007	1	900
			Leveling Base.....27-1049	1	500
			100W tungsten-halogen lamps (bulbs).....27-8427	20	250
			or Xenon Arc Lamp unit.....	1	or 1,500
★ <b>Condenser lens</b>	Focus incoming light	Ealing	Condenser Lens Assembly....22-7959	1	180
★ <b>XY transverse slide</b> with pillar	For mounting condenser lens	Ealing	Transverse Slide.....22-4071	1	96
			Vertical Slide.....22-4089	1	85
★ <b>IR filter</b>	Absorb heat-producing IR light	Ealing or Edmund	45° Hot mirror.....35-6881 or Hot mirror.....J43,453	1 1	116 or 43
★ <b>Dove prism</b> in rotary holder	For rotating image	Oriel or Edmund	Dove prism, mounted.....46420	1	261
			or Dove prism, unmounted....J32,554	1	or 75
★ <b>Sodium Lamp</b> with power supply and extra lamp	Observe Newton's rings with SFA	Fisher		1	1,500
★ <b>Mercury Lamp</b> thin pen-ray type (~5 W)	Calibrate wavelength, cure glue		Sycon 100	1	

Stage micrometer	Calibrating Spectrometer magnification	Ealing			
Calibration microscope (Micrometer eyepiece)	Calibrating springs (with XYZ stage)	Edmund	Measuring Microscope 45X with reticle scale.....J38,840	1	390
Widefield Eyepiece 10X with adjustable focus and built in cross-hair reticle	Optics Stand & misc. (spare item – one supplied with SFA)	Various: Rolyn Optics, McBain	Typical 10X widefield eyepiece.....	1	50-150
			Cross-wire reticle (graticule).....	1	35-55
10X objective (spare / alternative)	Replace Ealing 5X objective (24-9722) on Optics Stand tube	Ealing	10X objective in housing.....24-9748 (Lens can be readily removed from housing to replace 5X lens on tube)	1	250
Polarizer	Analyze FECO fringe polarization			1 pair	
Abbé refractometer	Refractive index calibrations	Edmund	Abbé Refractometer.....J38,581	1	1,000

### VACUUM COATING UNIT

1 Equipment Item	2 Required for	3 Supplier	4 Model	5 No.	6 Price*
★ Vacuum Coating Unit with 12" diam. bell jar	Deposit Ag, SiO <sub>2</sub> , etc., on mica	Cooke	Vacuum Pump Station.....CVE301	1	8,415
			Evaporation Module.....CV-301-EPS	1	2,500
★ Thickness monitor	Measuring thickness of deposited films on surfaces	Maxtech Cooke	TM-200 Thickness Monitor.102208-1	1	1,250
			SH-100 Sensor Head.....123205-1	1	574
			IF-110 Feedthru 1".....130200-1	1	295
			or Sycon 100 Thickness Monitor with Feed through and Head (installed)...	1	or 3,000
★ Molybdenum or tungsten boats	For evaporating silver shot / wire	Ladd Research	Molybdenum (Moly) Boats: 1-7/8" total length.....8-30730	6	34
★ Silver shot	For evaporating 500-550Å films on mica	Alfa (Johnson Matthey)	Ag 99.999% (3mm diam).....14153	50 gm	179

### MICA CUTTING

1 Equipment Item	2 Required for	3 Supplier	4 Model	5 No.	6 Price*
★ Mica: Thick, large sheets of Clear Ruby Muscovite	Used as substrate surfaces	S&J Trading AIM (Australia)	Clear Ruby Muscovite Grade 2 – V2	4 lb	1,000
★ Platinum wire 0.006" or 0.2 mm diameter	For melt-cutting mica	Fisher	Pt wire (0.006" diam).....13-766-10A	36"	100
★ Mica cutting stage	For supporting and cutting mica sheets (powered by low V DC power supply – LVPS)	Constructed in-house (Edmund) or by SFI.	Parts for in-house construction: mica sheet holders, XYZ positioning stage (Edmund J3607, J3608 or J37,603), electrodes, clamps, 10 hr labor.		est. 1,000
★ Small Hot-Plate	For melting thermosetting glues			1	
★ Thermosetting Glues	Gluing mica sheets for aqueous solutions	Shell	Shell 'resins' EPON 1004, EPON 1007, EPON 1009, . . . (for aqueous)	1/4 lb	30
Thermosetting Glues	Gluing mica sheets for organic solvents	Misc. chemical suppliers	Sym-diphenylcarbazide (for inert liquids), Glucose (for toluene), cf text	1/4 lb	
UV-curing Glues	Gluing mica sheets in flattened contact	Edmund Scientific	Norland Optical Adhesive #61		

## ELECTRICAL

1 Equipment Item	2 Required for	3 Supplier	4 Model	5 No.	6 Price*
★ ☆ Low Voltage DC Power Supply (LVPS). Dual Outputs: 0 to ±24V, 0.5 Amp. [This item may be included in the Control Box]	Driving DC motors on Upper Chamber and Friction Device	Electro Industries, or BK-Maxtec	Triple Power Supply.....Model 2555A Triple Power Supply.....Model 1651 Various models (need low ripple)	1 1	200 or 429
★ Low Voltage DC Power Supply (LVPS) – 12V, 8A	For 100 W lamp, mica cutting stage, and small gluing hot-plate	Ealing..... BK-Maxtec... Electro Ind...	Stabilized Power Supply.....27-3540 Power Supply.....Model 1688 or 1686 Various models.....	1 1 1	865 or 300 or 200
★ Multimeter (4-5 digit)	AC/DC V-I-R measurements	Ealing Keithley	Various models available	1-2	2x750 = 1,500
★ High voltage DC power supply (HVPS). ±500V to ±1,000V, usable with the FG. Alternatively, use LVPS and amplify with VA.	Driving piezo crystal on piezo mount.	Various e.g., Trek	Various models available, e.g., Trek Model 605A (but not usable with FG). Alternatively, use low voltage DC power supply (LVPS) regulated to ±1mV and amplify X50-100 with VA.	1	~1,000
☆ Function Generator (FG) mHz, ramp, sine, square, triangular, sawtooth, ±5 to ±10 DC offset, low ripple.	For driving piezos and bimorphs, after amplifying X100 with VA.	Hewlett-Packard  Various other	Function Generator.....HP33120A  Various other models available	1	1,725
★ ☆ Voltage amplifier (VA)	Amplify outputs from FG and LVPS to piezos/bimorphs	Trek	Amplifier (1 channel).....601B-1 or (2 indep. channels).....601B-2	1 —	1,830 or 2,480
☆ Strain Gauge Bridge	Measure friction strain gauge output	Measurements Group or Yokogawa (Y)	Signal Conditioning Amplifier.....2311 or Signal Conditioner (Y).....345810 or Strain Amplifier (Y).....313401	1 1 1	1,655 or ? or ?
☆ Chart Recorder	Recording friction traces	Soltec Corp.	Flatbed Recorder – 1 pen: 1mV, 750 mm/s.....Model 1241 or Flatbed Recorder – 2 pen: 1mV, 750 mm/s.....Model 1242	1 or 1	1,895 or 2,850
Storage O-Scope	Recording/storing fast friction transients	Fluke	Fluke CombiScope.....PM 3380 A (analog/digital with 8-32 memory)	1	~3,300
Multimeter (high precision)	High accuracy instr., e.g., for thermocouple	Fluke	Various advanced models available	1	3,000
Lock-in amplifier	Measure amplitude-phase relationships in dynamic experiments	EG & G or Stanford Instruments	Dual phase lock-in amplifier .....SR 830 DSP	1	~5,000

★ Essential items for the Basic Unit.

☆ Essential items for the Friction Device, Bimorph Slider and/or Bimorph Vibrator.

\* Prices are estimates in US \$ and do not include TAX, SHIPPING and HANDLING.

### GENERAL LABORATORY SUPPLIES

1 Equipment Item	2 Required for	3 Supplier	4 Model	5 No.	6 Price*
Silica disks and windows	Replacement or spare	ESCO, N. J.; see QUARTZ in Thomas Register	ESCO silica disks & windows, various sizes and shapes..... Note: SFI, Inc. will supply at market value or below if in stock .	—	\$ 20-100 per item, depends on number
★ Miscellaneous small tools and disposable items needed for cleaning and assembly	Tool kit (provided), forceps, tweezers, glassware, filters, tubing, syringes, etc.	Various: Fisher, Berg, Pic, Edmund, etc.		—	2,500
★ Pressure rinsers or ethanol squirt guns	Ethanol squirt cleaning of SFA parts	Baxter	Gelman 1L Pressure Rinser....F3100	2	2X272 = 544
★ Laminar Flow Cabinet or Work Station: Outward horizontal air-flow type	Mica cutting, SFA assembly, water distillations	ISEC, Gelman		1-2	2X4500 = 9000
★ Glass Desiccators	For storing mica sheets, samples, etc.	Fisher		2	2X250 = 500
★ Nitrogen gas supply (from liq. nitrogen)	Purging apparatus, blow dry cleaning			—	—
★ Syringes, needles, Luer connectors, PTFE tubing	Injection filling, purg-ir and draining the SFA	Hamilton, Ornifit	Some items supplied with apparatus	—	500
Water Aspirators	Aspirating chamber during cleaning/filling	Fisher?		2	100
Spirit level (supplied)	Leveling SFA when placed on Base Plate	Edmund	Calibrated circular level.....J42,763	1	28
Domes (transparent covers)	Covering apparatus parts	Edmund	Transparent dome (7").....J71,710 Transparent dome (12").....J80,179 Transparent dome (16").....J85,216	1 1 1	24 35 55
Langmuir-Blodgett Deposition Trough	Depositing organic layers on surfaces			1	15,000 - 45,000
Anti-vibration table (1 per SFA system/room)	Reducing vibrations during experiments			1/SFA	2,500
Balance	General purpose balances	Shimadzu, Mettler		1-3	1,500 - 6,000
Centrifuge	Purifying solutions of dust / particulates	Beckman, DuPont		1	
Conductivity cell/pH meter	Electrodes can be inserted into SFA		Conductivity cell..... pH meter.....	1 1	1,000 500
Distillation Units	Purifying water and organic liquids	Labconco, Millipore		1-2	2,000
Drying oven	For glassware, etc.			1	1,000
Fridge - laboratory type	General purpose	Fisher		1	1,000
Normal/stereo microscope	General purpose			1	5,000
Oil-less pumps	Aspirating liquids, evacuating desiccators	Gelman		1-2	1,000

### VIDEO CAMERA – RECORDING SYSTEM

1 Equipment Item	2 Required for	3 Supplier	4 Model	5 No.	6 Price*
Video Camera (SIT)	Visualizing moving FECO fringes	DAGE MTI Hamamatsu		1	10,000
Video Recorder with single and variable frame speed, & freeze frame capabilities	Recording moving FECO fringes	JVC	Video Cassette Recorder.....HR S5200 U	1	900
Video Micrometer	Analyzing positions of FECO fringes	Colorado Instruments		1	7,000
Video Monitor	Observing FECO fringe patterns	Sony		1-2	1,000 – 2,000
Video Timer	Recording exact times of events	For-A		1	700
Polaroid Camera for pre-recorded videos	Making B&W photos of single video frames			1	1,200
Video Camera small, CCD	Top view of surfaces with normal microscope		Needs additional monitor, and tube adaptors for changing magnification	1	1,500

★ Essential items for the Basic Unit.

☆ Essential items for the Friction Device, Bimorph Slider and/or Bimorph Vibrator.

\* Prices are estimates in US \$ and do not include TAX, SHIPPING and HANDLING.  
as already described.

## 1.2 BRIEF DESCRIPTION OF UNITS AND PARTS, WITH FIGURES

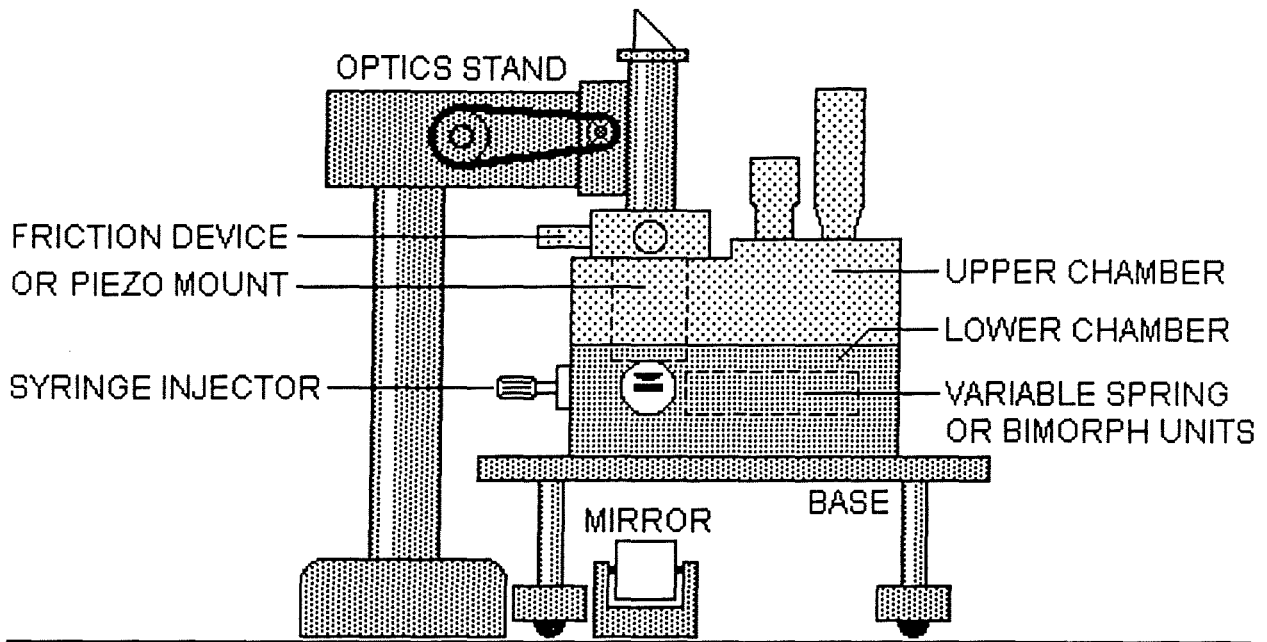


**Figure 4.** Units and attachments of the SFA3.

The SFA 3 is composed of the following numbered UNITS and ATTACHMENTS:

<b>BASIC UNIT</b>	<ul style="list-style-type: none"> <li>0 – MISCELLANEOUS</li> <li>1 – UPPER (CONTROL) CHAMBER</li> <li>2 – LOWER (LIQUID) CHAMBER</li> <li>3 – BASE AND LEGS</li> <li>4 – VARIABLE SPRING</li> <li>5 – PIEZO MOUNT</li> <li>6 – MIRROR</li> <li>7 – OPTICS STAND</li> </ul>
<b>ATTACHMENTS</b>	<ul style="list-style-type: none"> <li>8 – SYRINGE INJECTOR</li> <li>11 – FRICTION DEVICE</li> <li>12 – BIMORPH SLIDER</li> <li>13 – BIMORPH VIBRATOR</li> </ul>

Each UNIT is composed of a number of machined PARTS, usually between 10 and 30, together with special screws, electric connections and other small fittings. All of these come together to produce the final assembled apparatus. The apparatus is normally delivered fully assembled and functional, that is, UNITS 1–5 will be assembled and fitted together. UNITS 6 and 7, which are used separately from each other, will also be pre-assembled before delivery. Some parts and supply items do not belong to any obvious unit or are used in a number of different units, these have been placed in the MISCELLANEOUS UNIT category.

Table II in Section 4.2 lists the names and numbers of all the parts and units of the SFA 3 and its attachments. This list can be folded out for referencing when reading the sections on cleaning, assembly and operations, or when referring to the figures and drawings.

The following pages contain many figures, assembly drawings and photographs of different units, key parts and supply items. Additional figures and drawings, especially of ATTACHMENTS, appear at other places in this brochure – see page 5 for a complete list of figures.

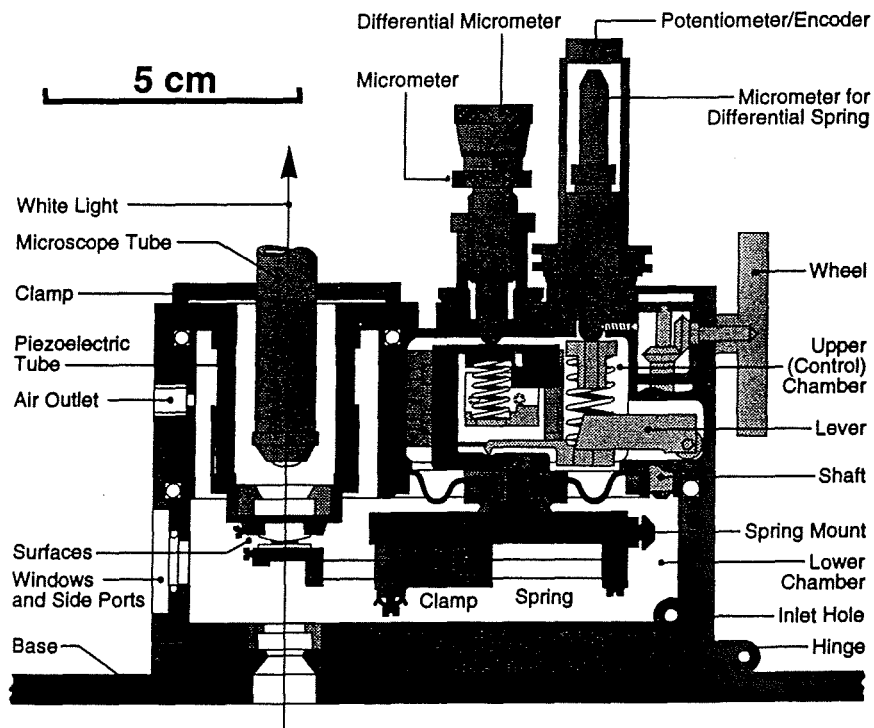


**Figure 5.** Assembly drawing of SFA 3 BASIC UNIT showing key parts.

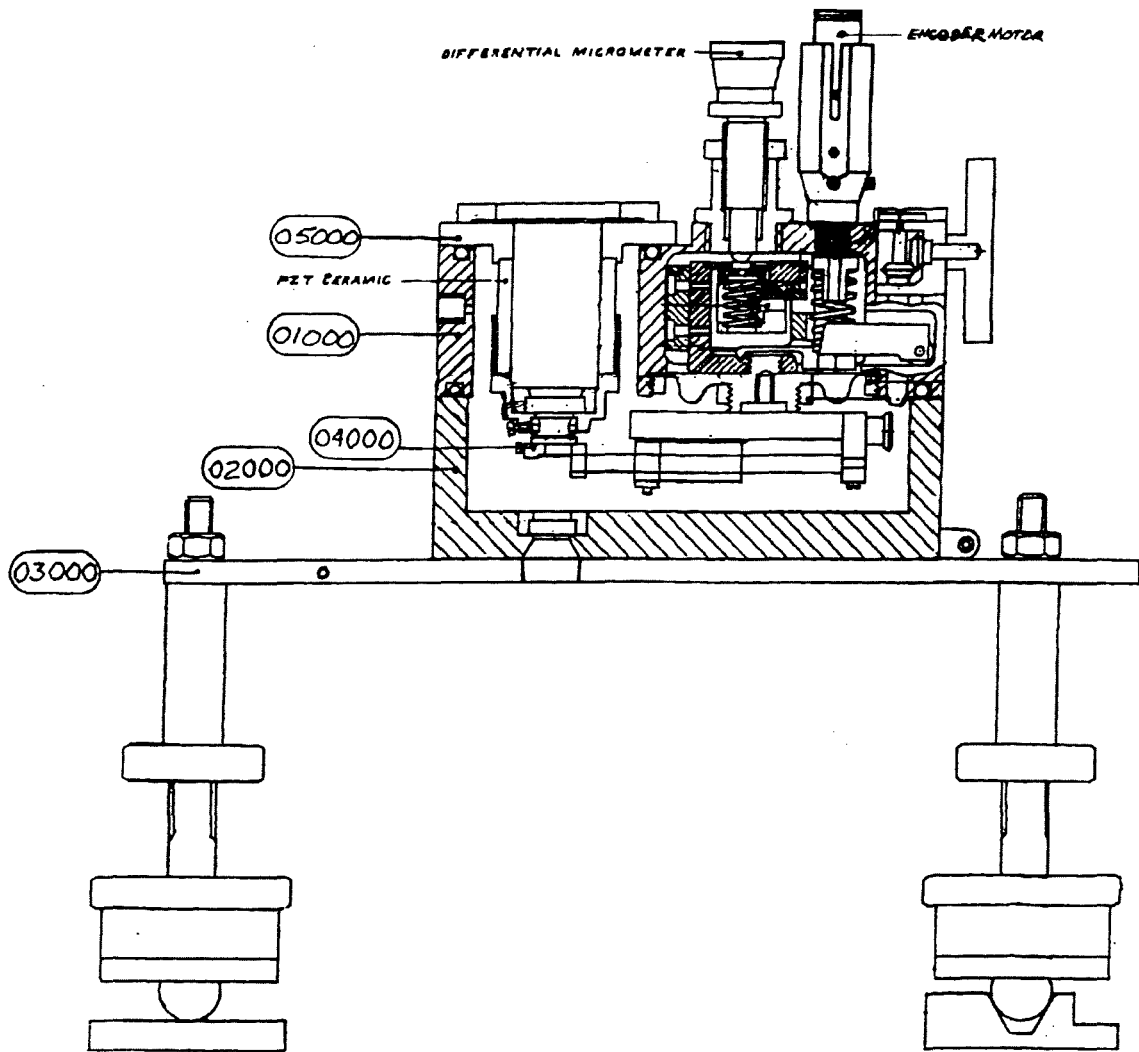


Figure 6. SUB-UNITS 1 to 5 of SFA3 BASIC UNIT.

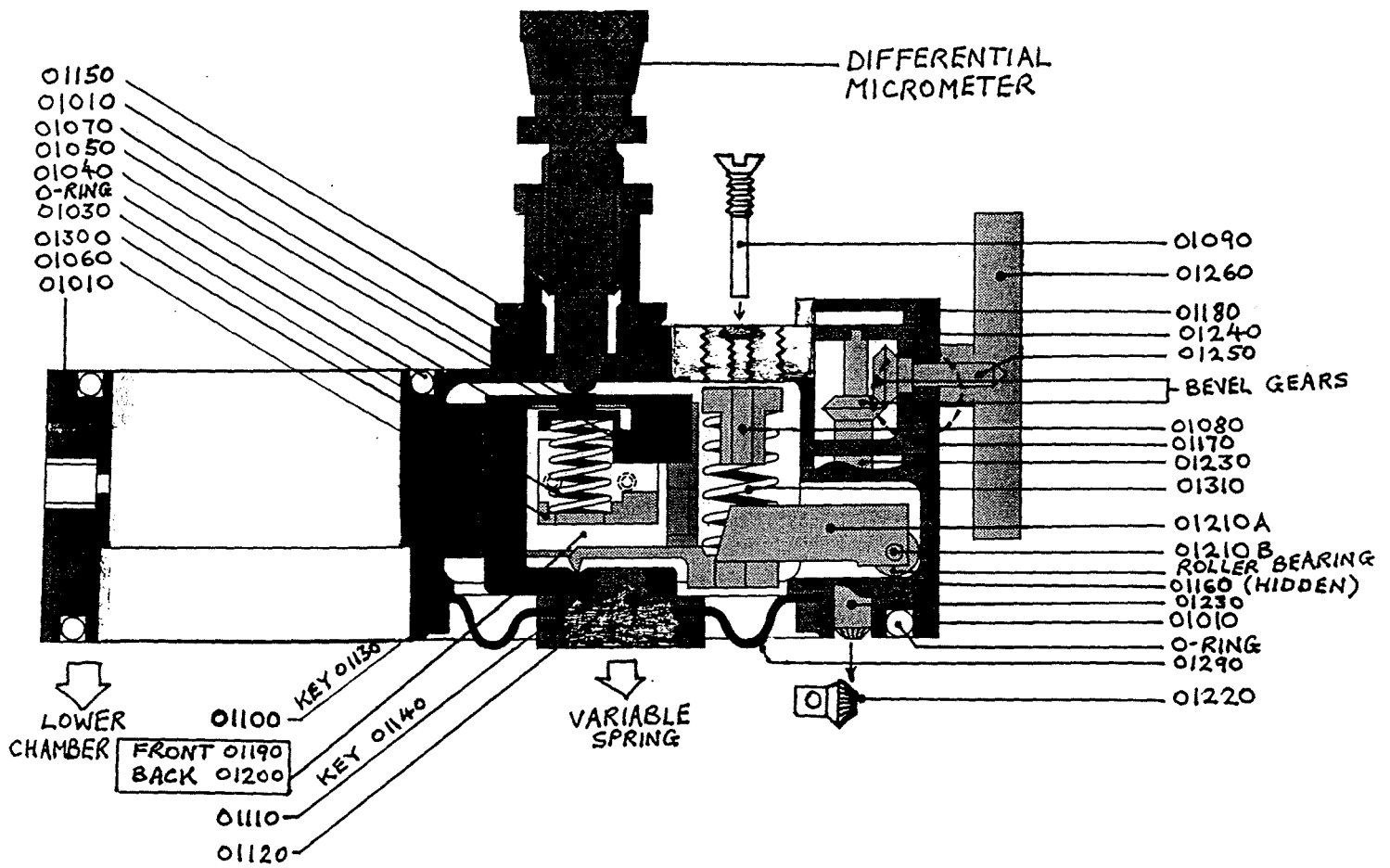
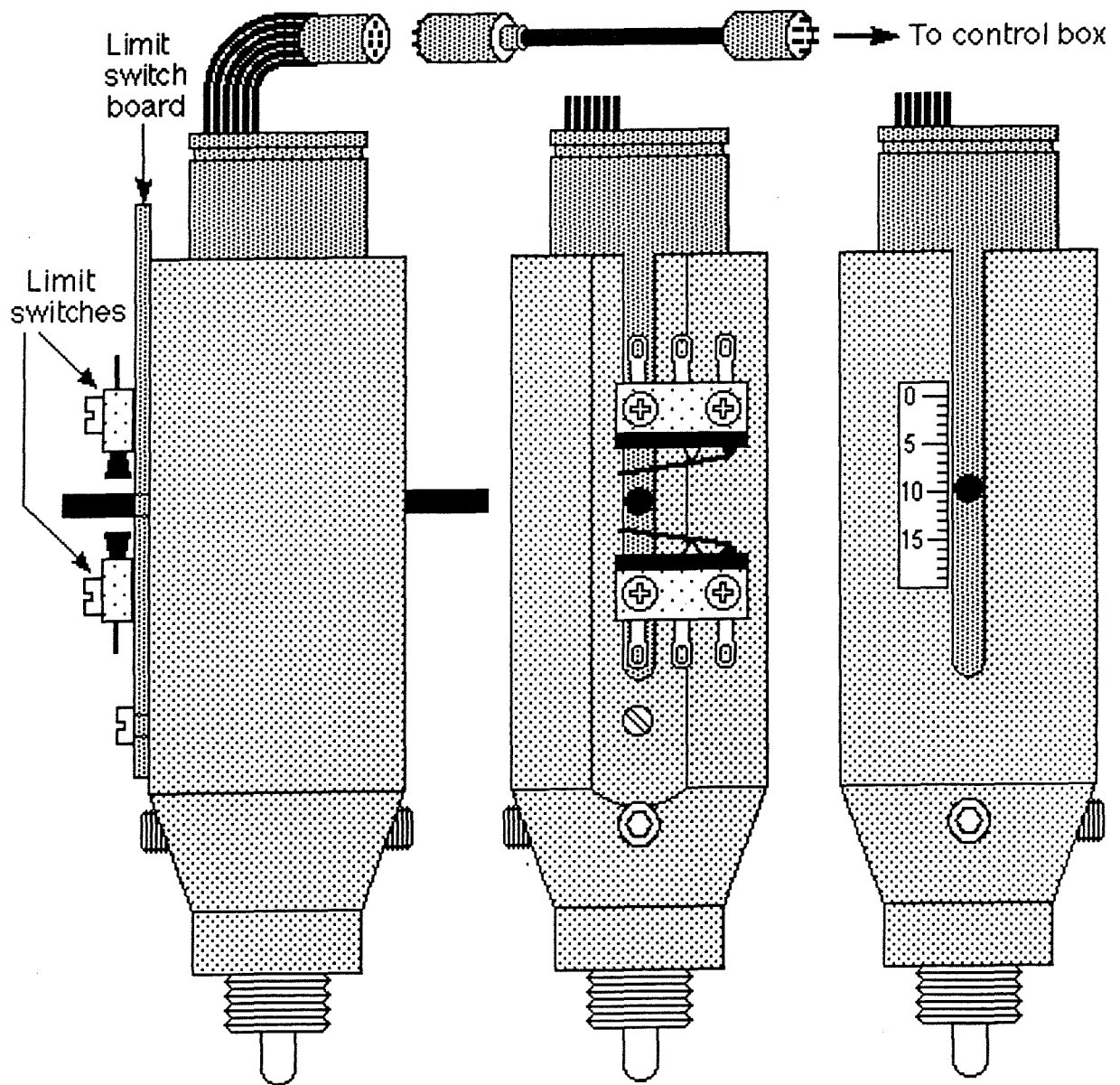
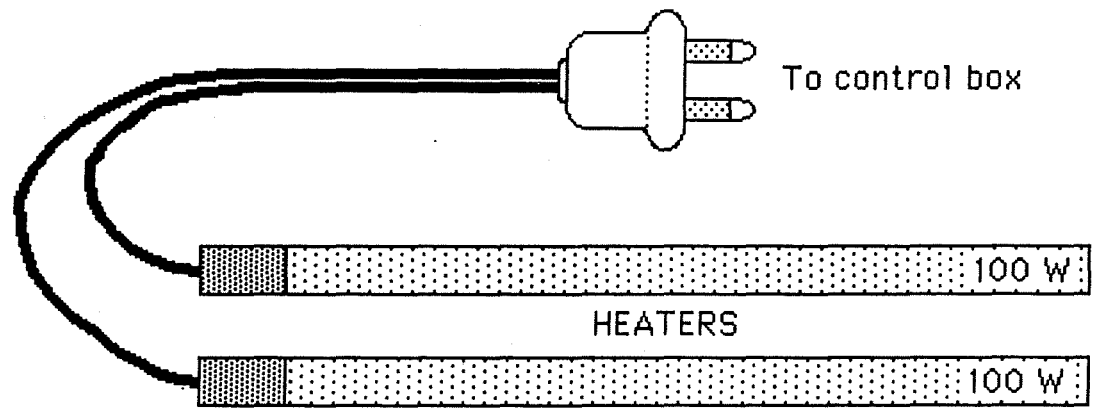
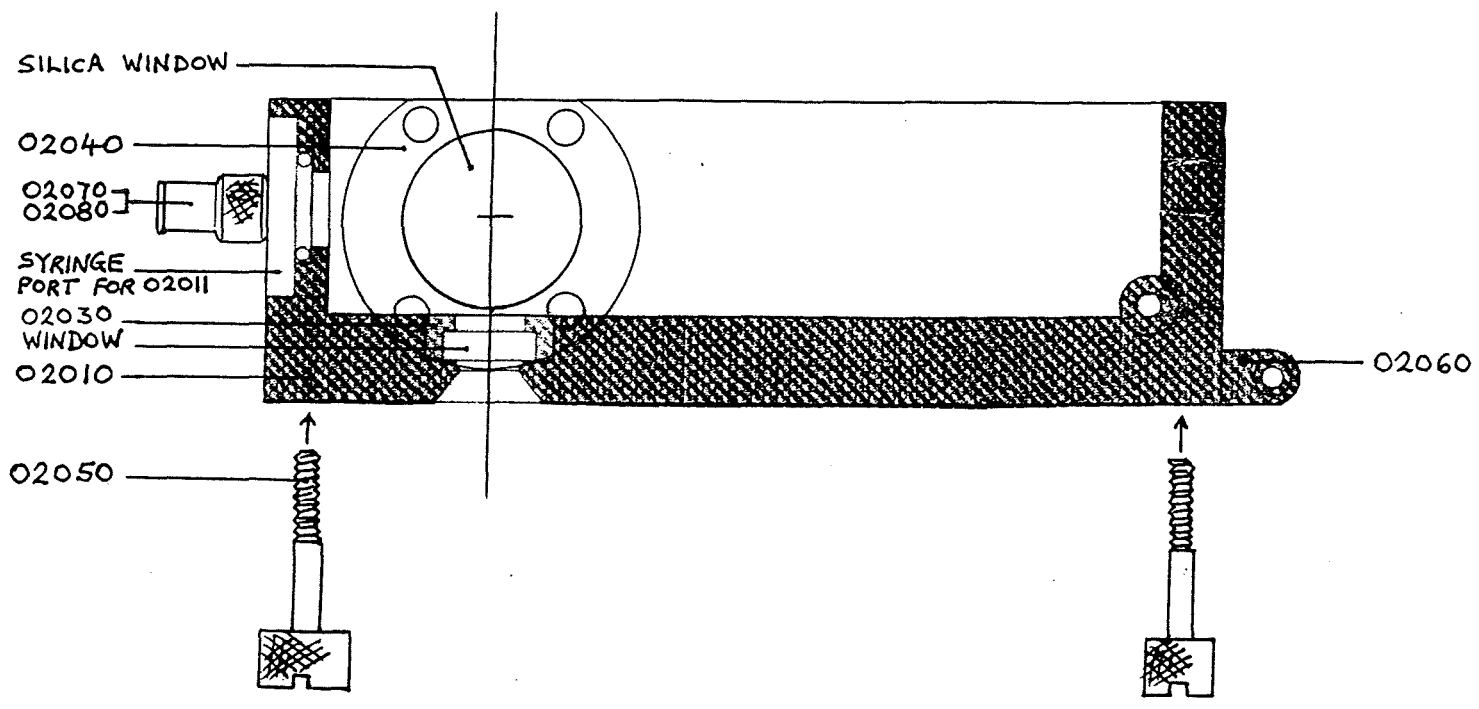


Figure 7. Assembly drawing of UPPER CHAMBER.



**Figure 8.**  
 Assembly drawing of motor housing on UPPER CHAMBER (and FRICTION DEVICE).



**Figure 9.** Assembly drawing of LOWER CHAMBER and HEATERS. Heater cables may be connected in parallel or in series, depending on local voltage.

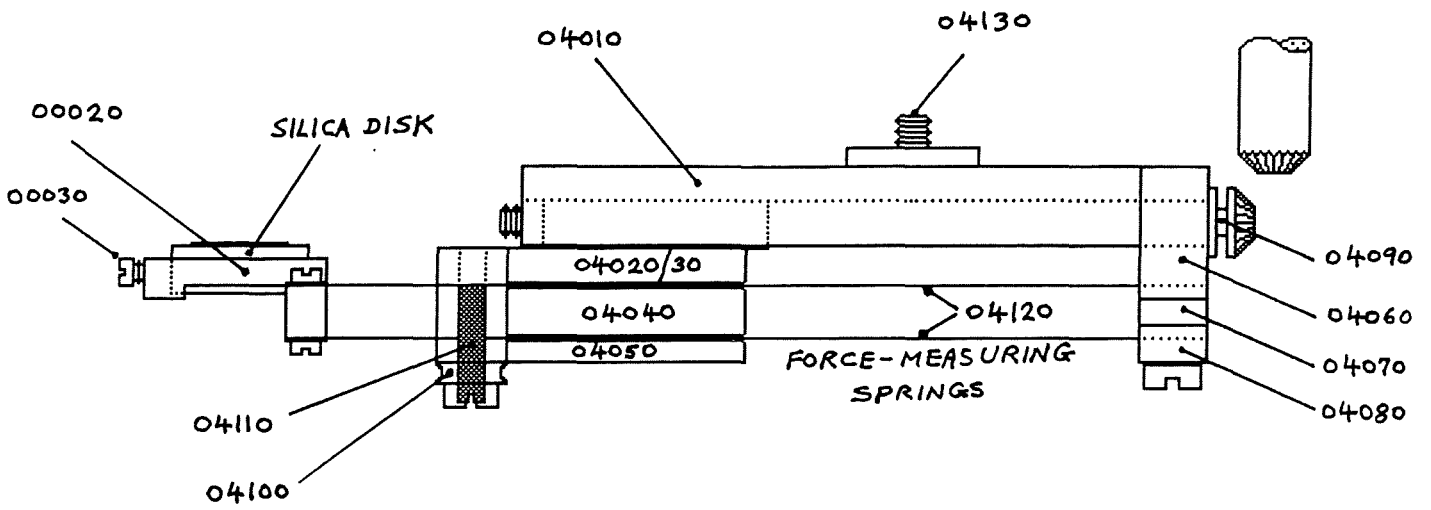


Figure 10. Assembly drawing of VARIABLE SPRING.

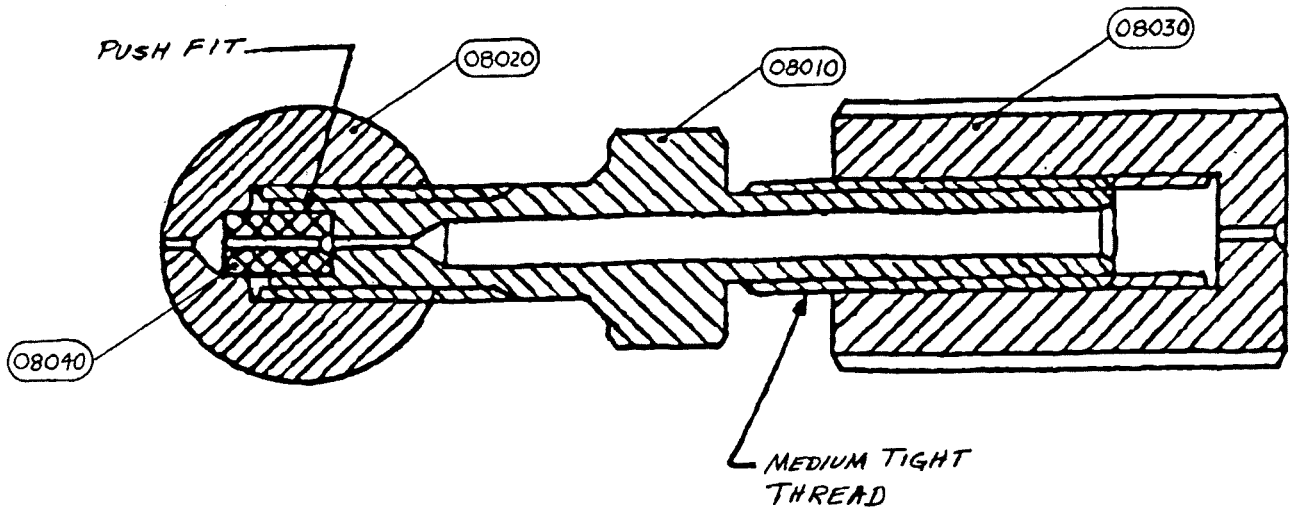
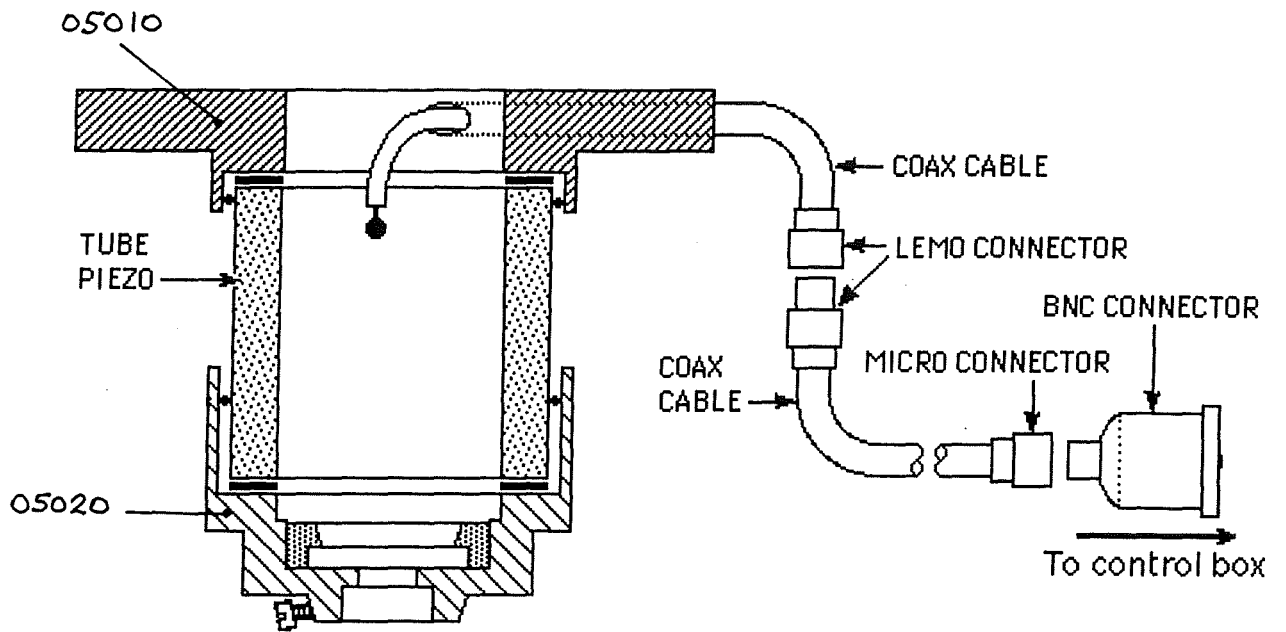
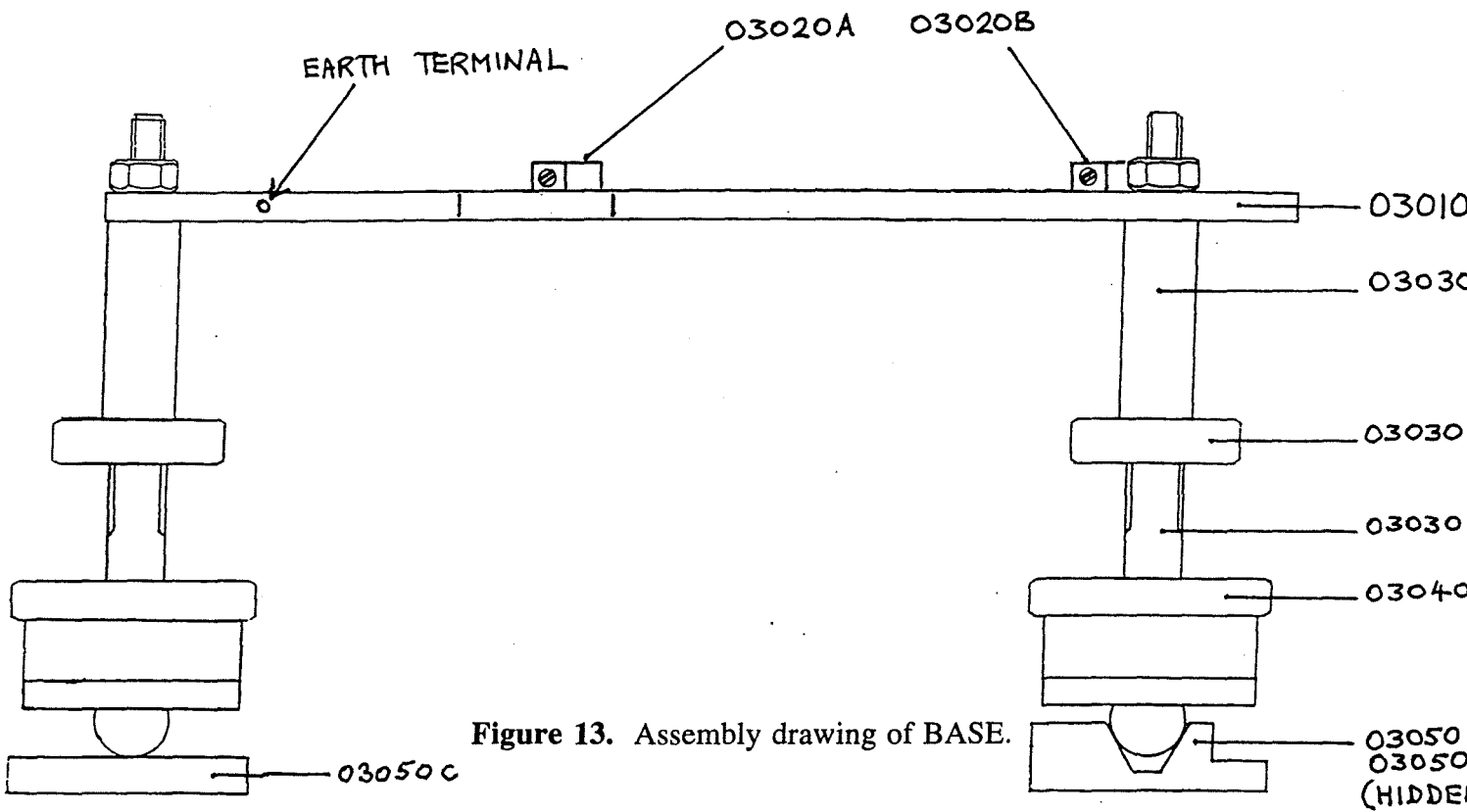


Figure 11. Assembly drawing of SYRINGE INJECTOR.



**Figure 12.** Assembly drawing of PIEZO MOUNT.

Note: when handling the micro-connectors, do not push or pull the thin coaxial cable – always connect and disconnect by turning and pushing or pulling the brass hex head.



**Figure 13.** Assembly drawing of BASE.

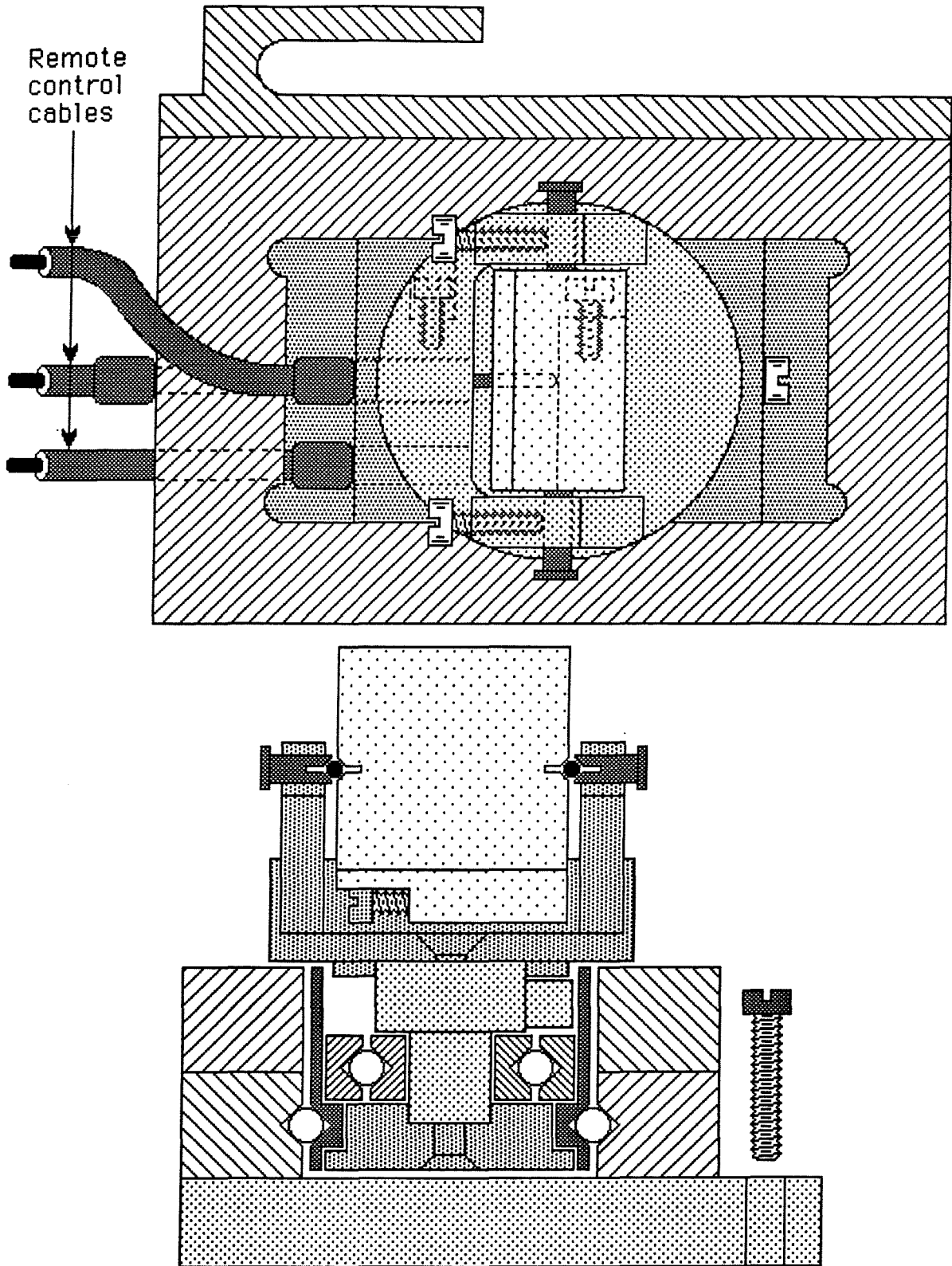


**Figure 14.** Assembly drawings of MIRROR.

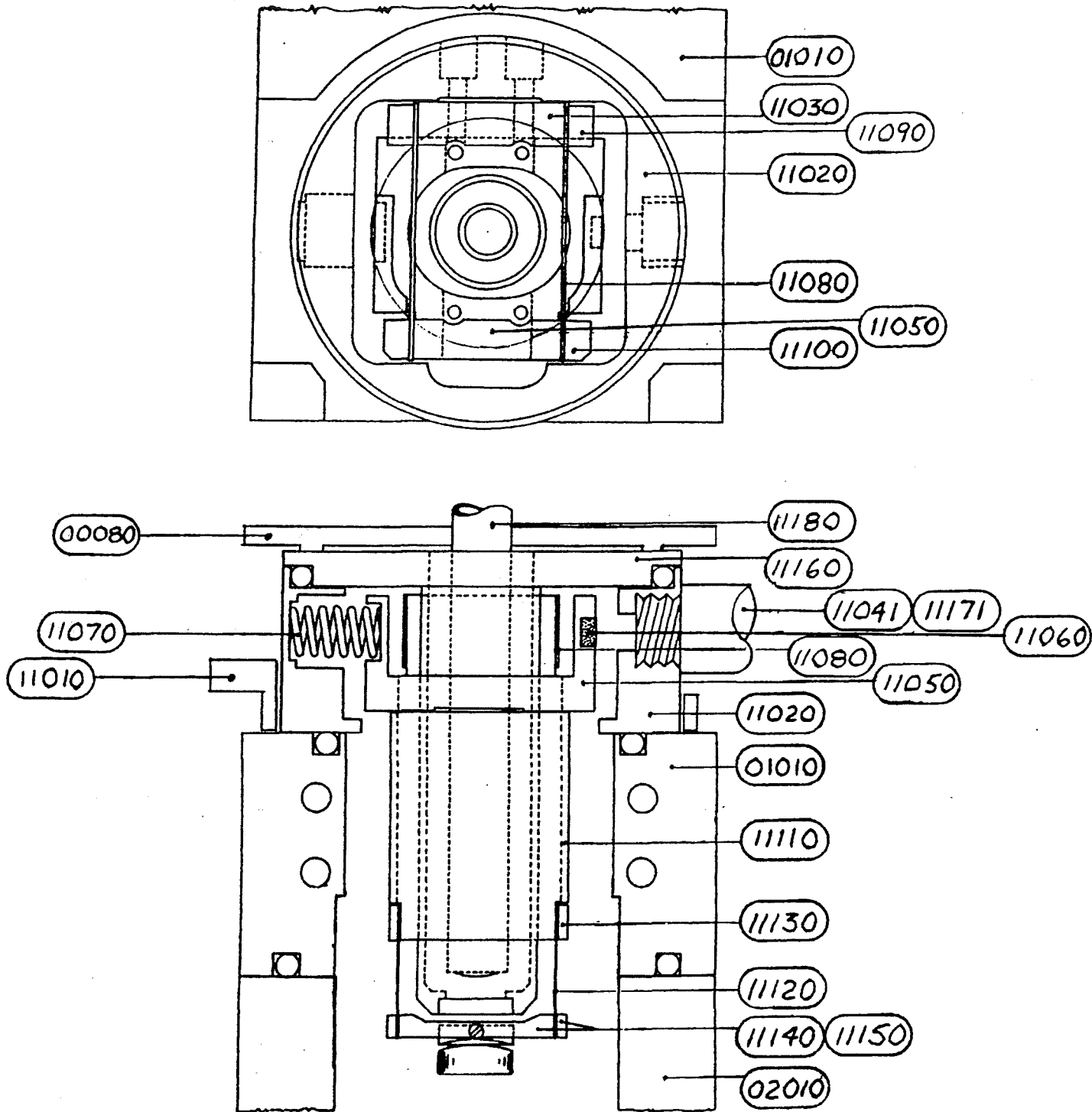
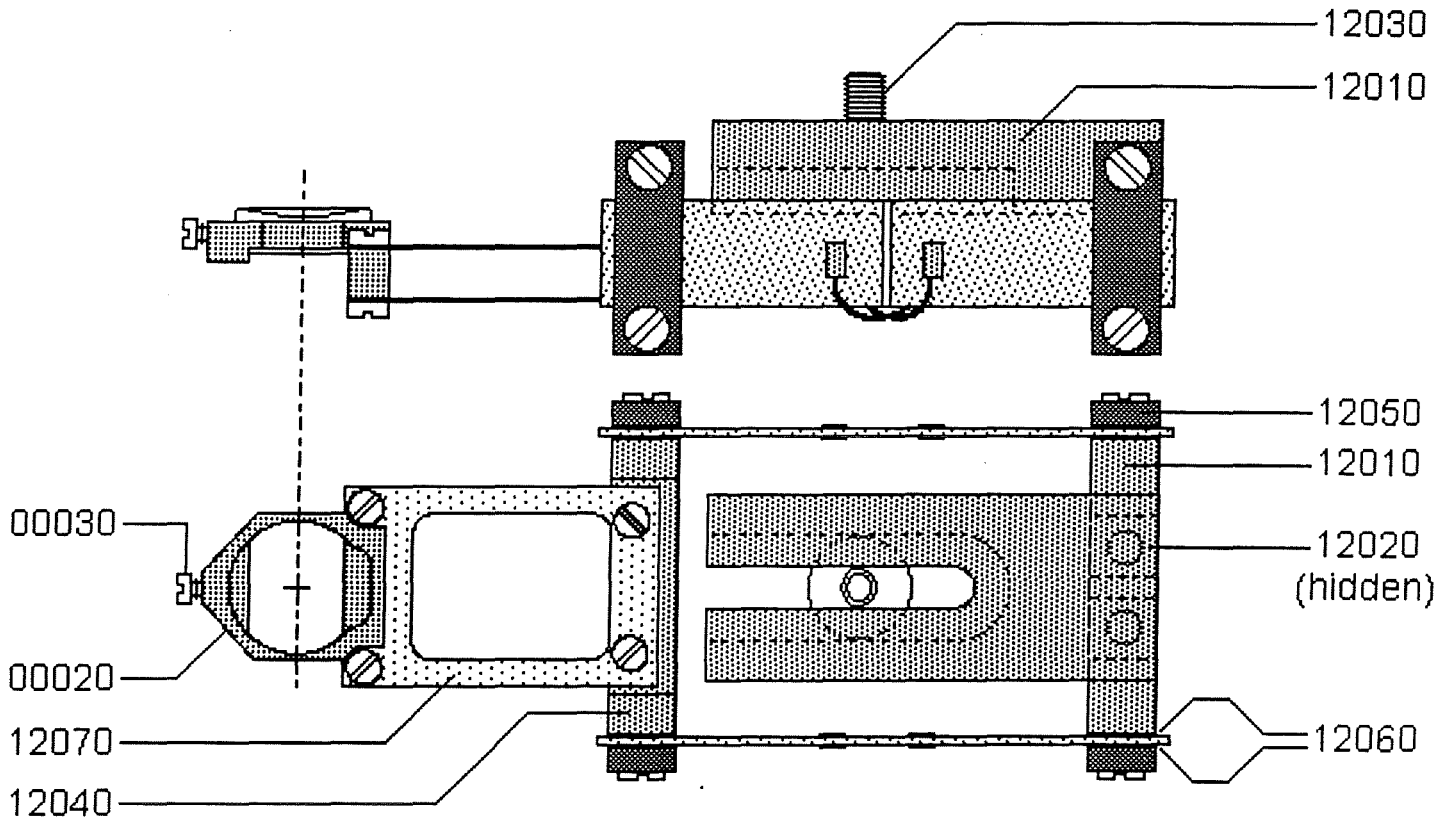
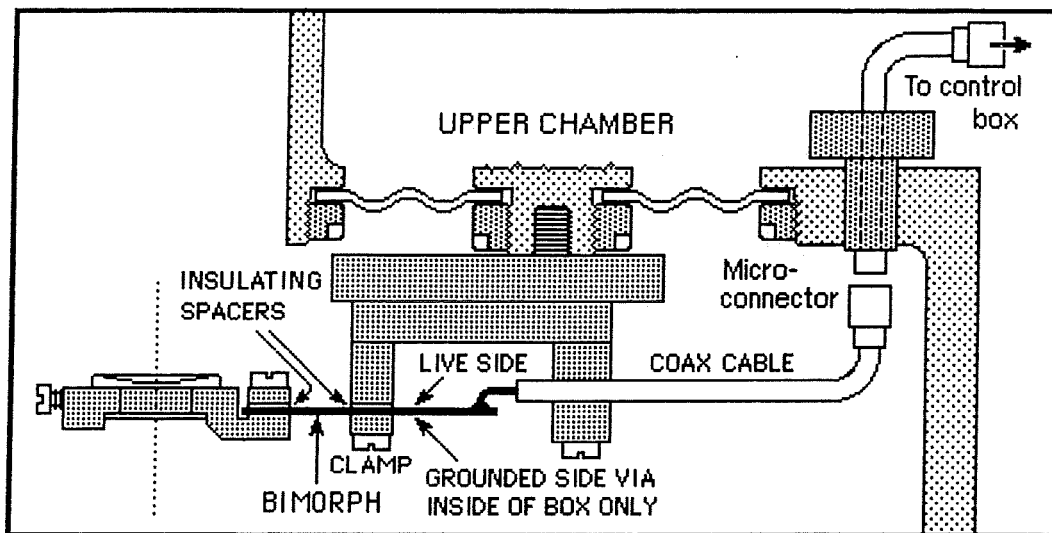


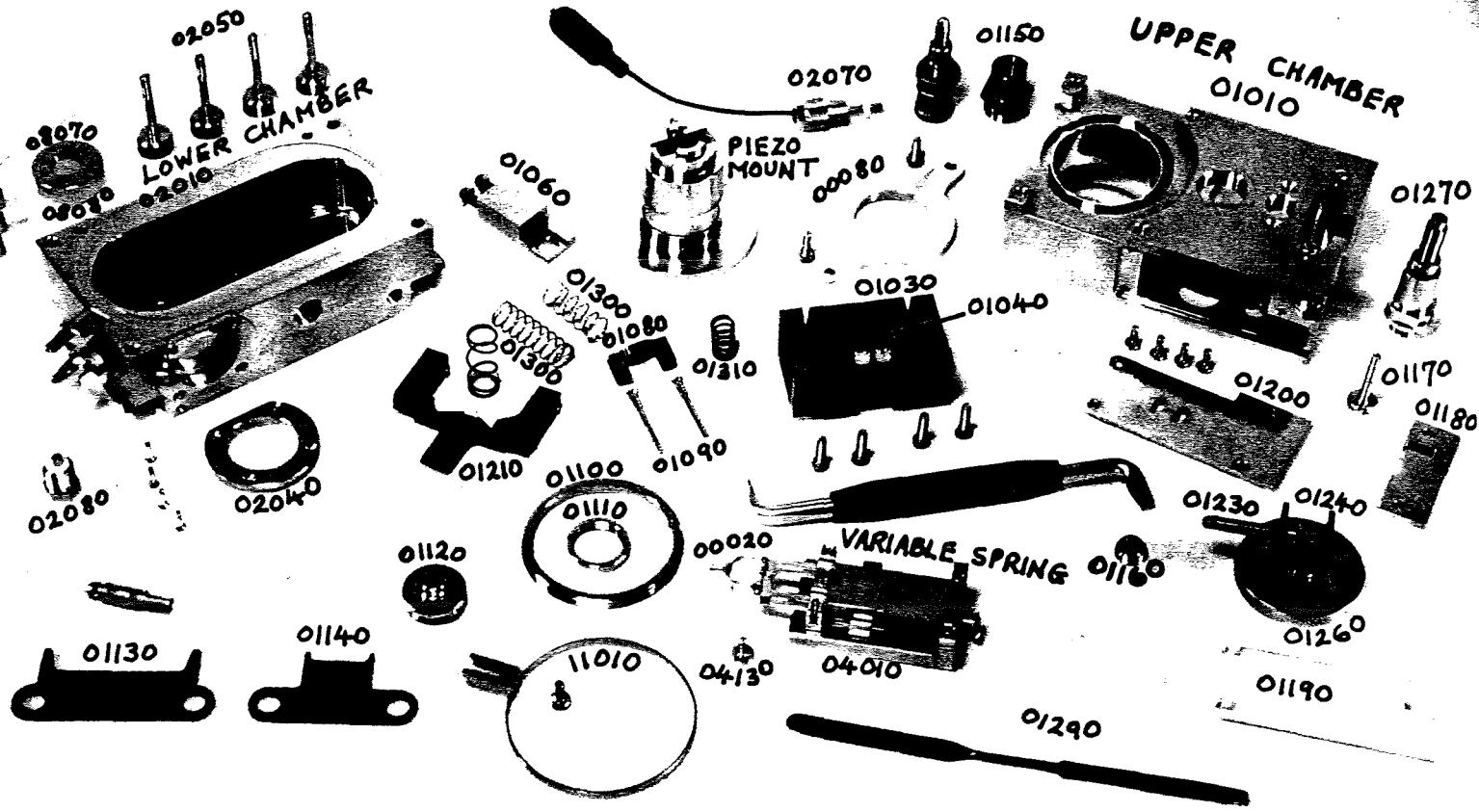
Figure 15. Assembly drawing of FRICTION DEVICE.



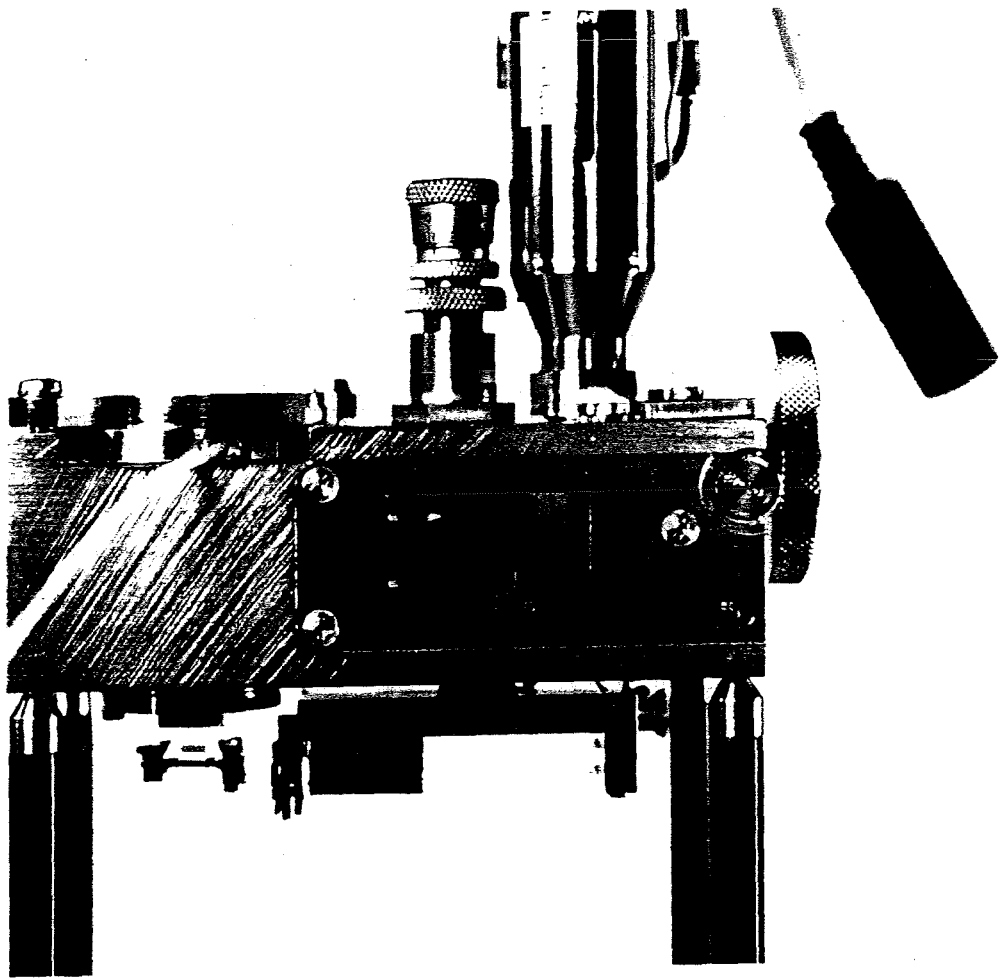
**Figure 16.** Assembly drawing of BIMORPH SLIDER.



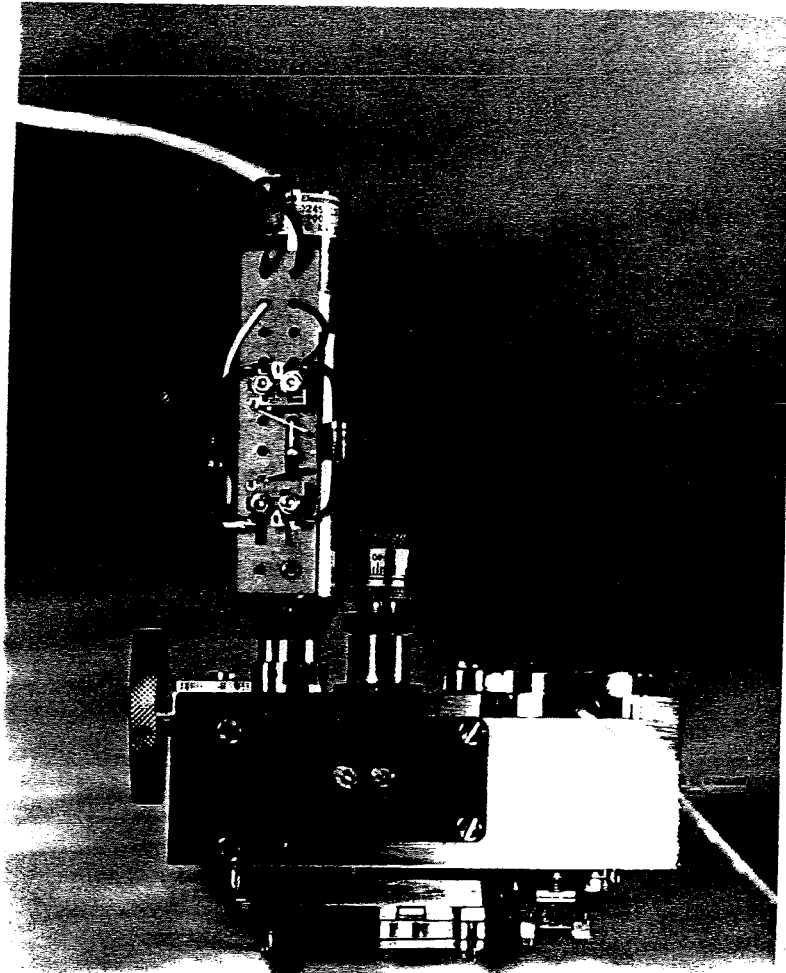
**Figure 17.** Assembly drawing of BIMORPH VIBRATOR.



Figures 18. Photographs of dismantled BASIC UNIT showing key parts.

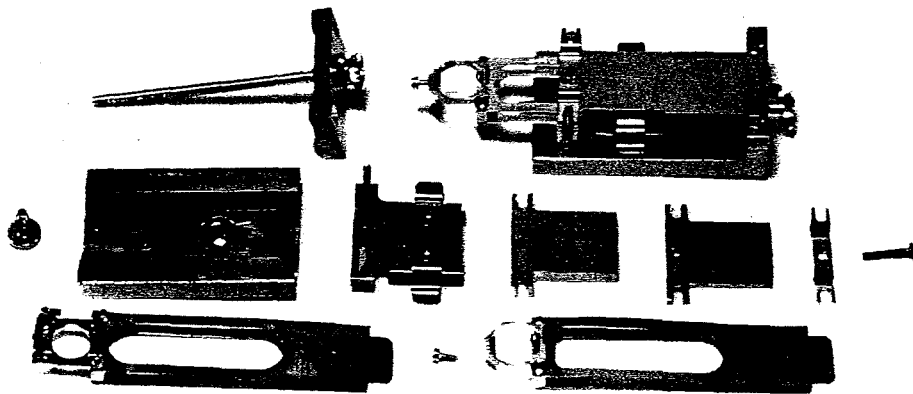
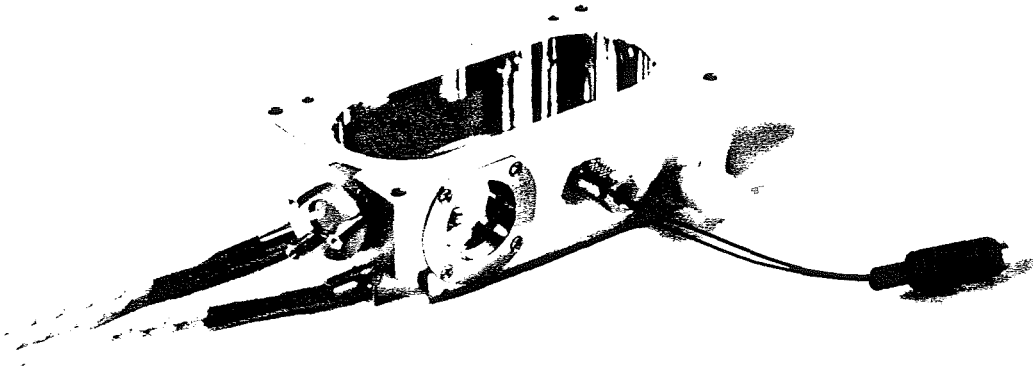


**Figures 19. Photographs of UPPER CHAMBER.**

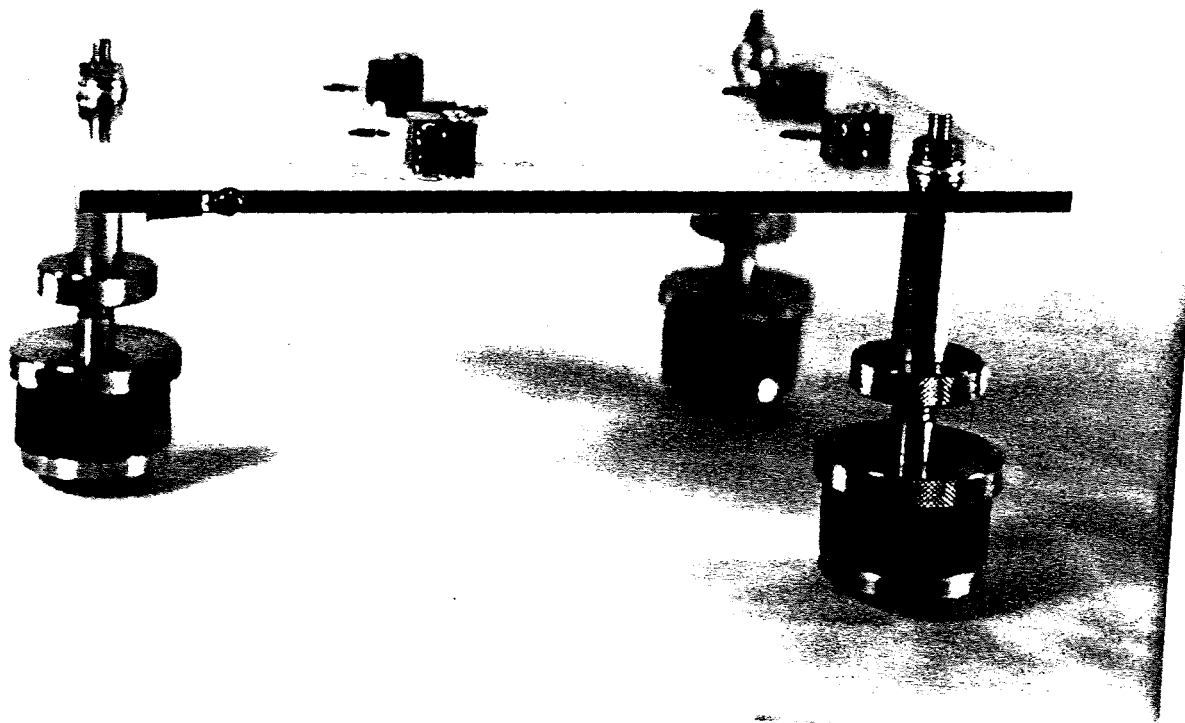


Figures 19. Photographs of UPPER CHAMBER.

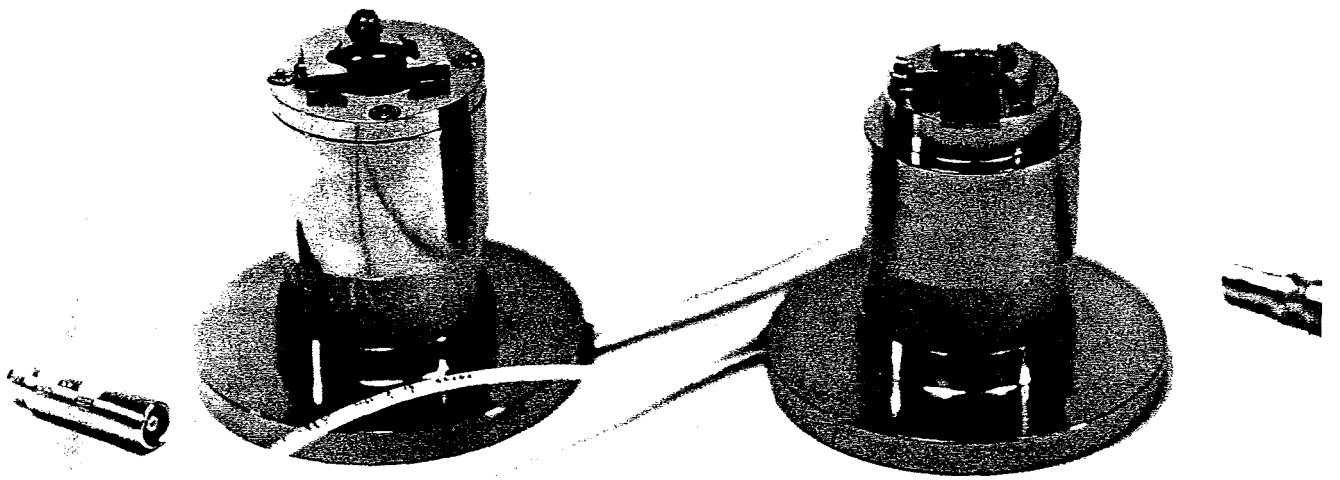
31a



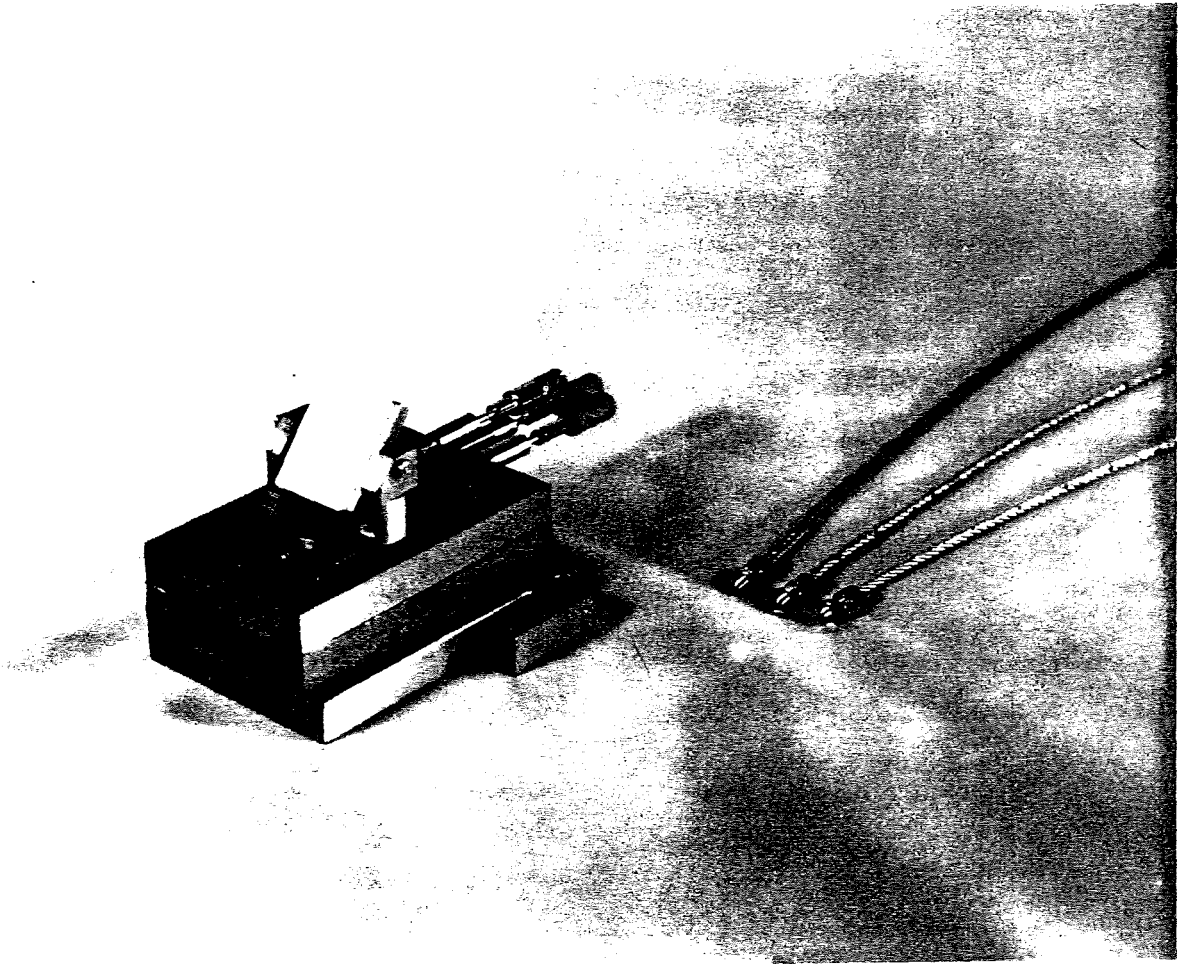
**Figures 20.** Photographs of LOWER CHAMBER and VARIABLE SPRING.



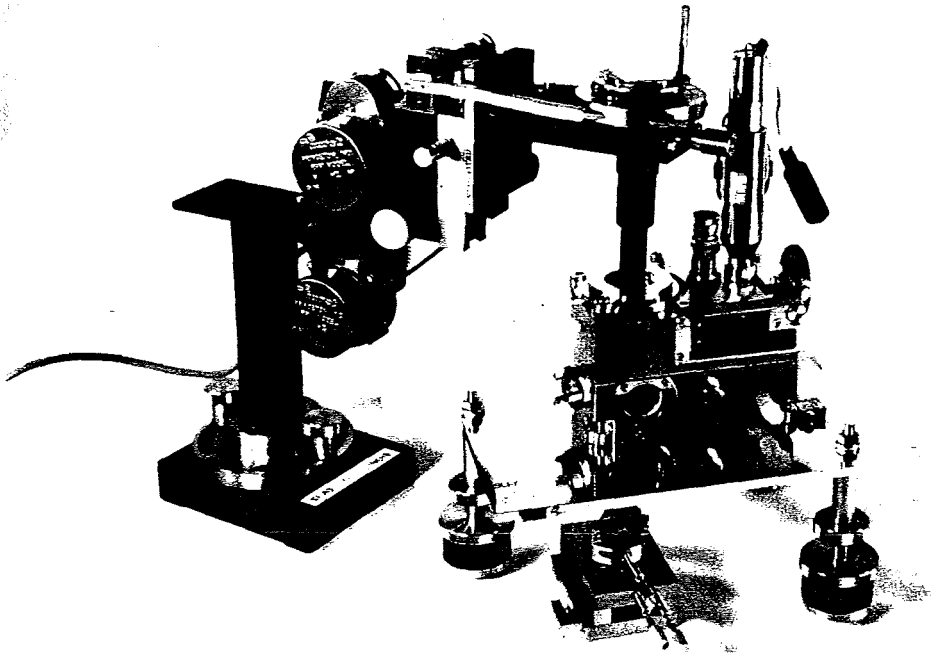
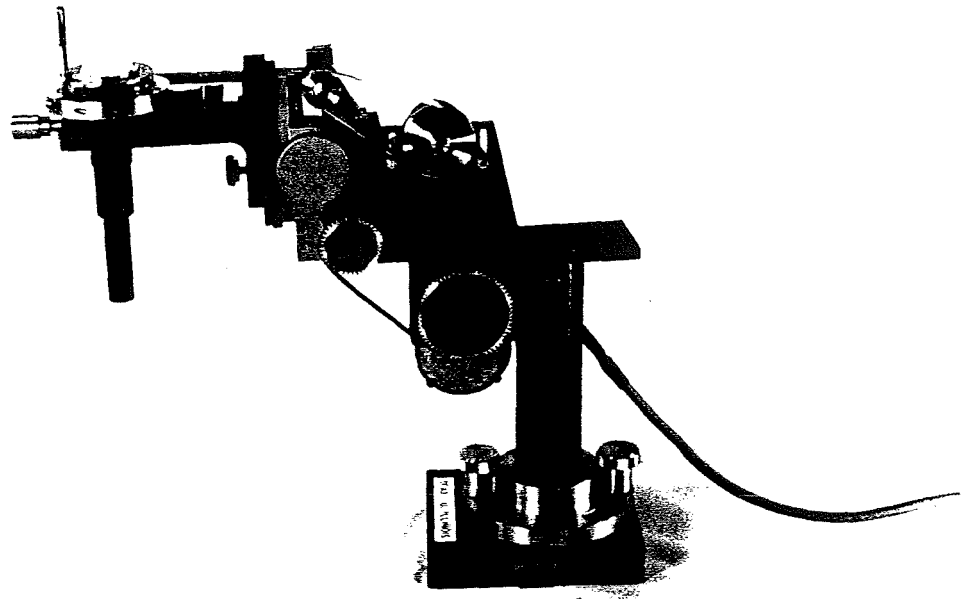
**Figures 21.** Photograph of BASE. The small screw hole on the front of the base plate is for electrically connecting the apparatus to earth (ground).



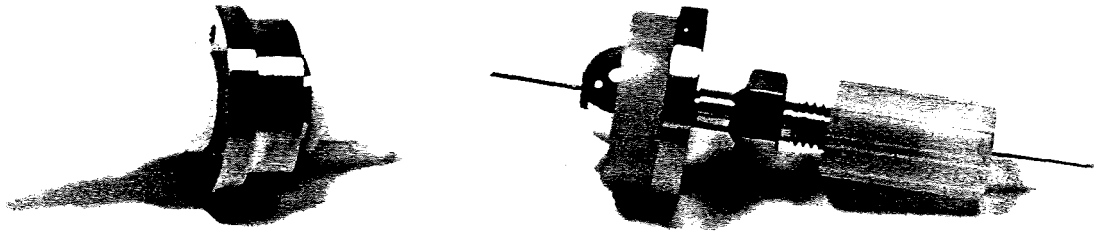
**Figures 22.** Photograph of PIEZO MOUNT.



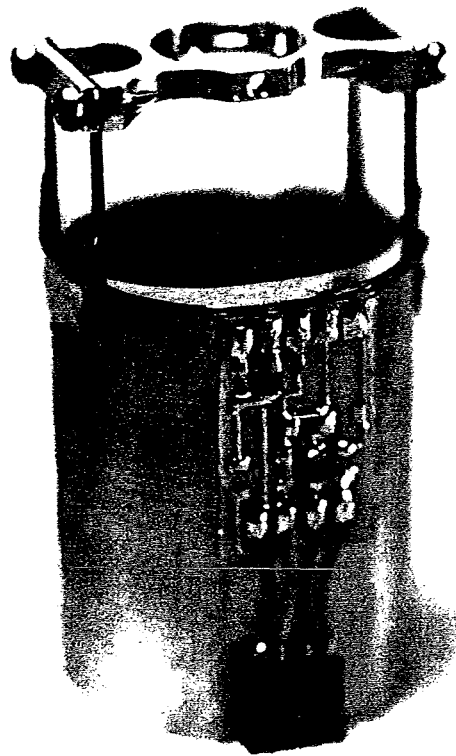
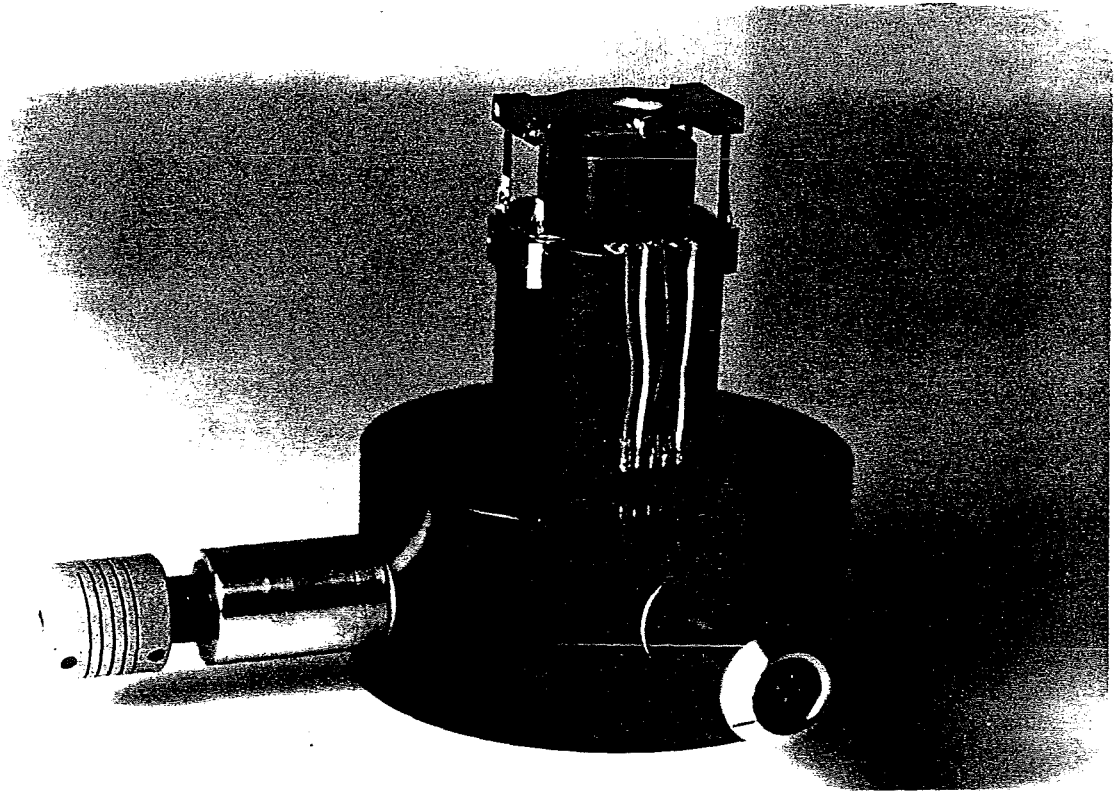
**Figures 23.** Photograph of MIRROR.



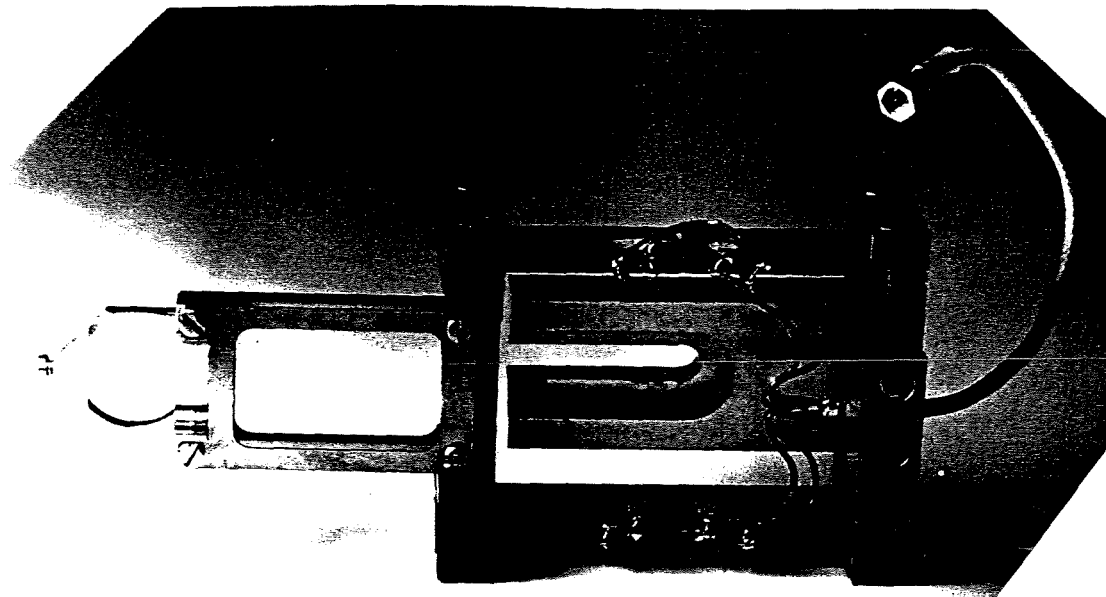
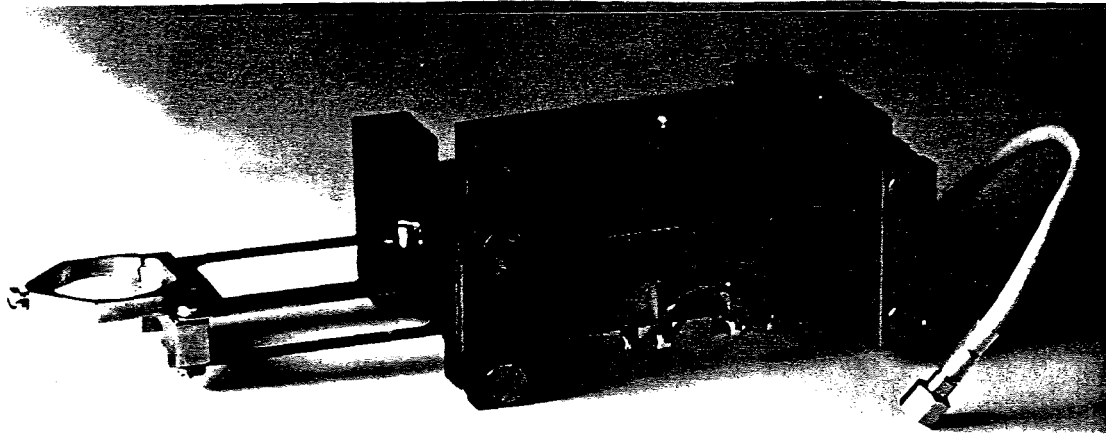
Figures 24. Photograph of OPTICS STAND.



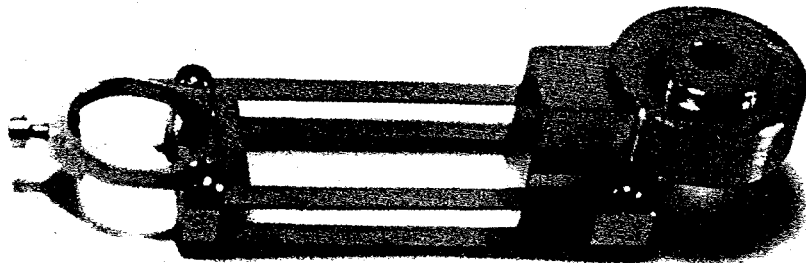
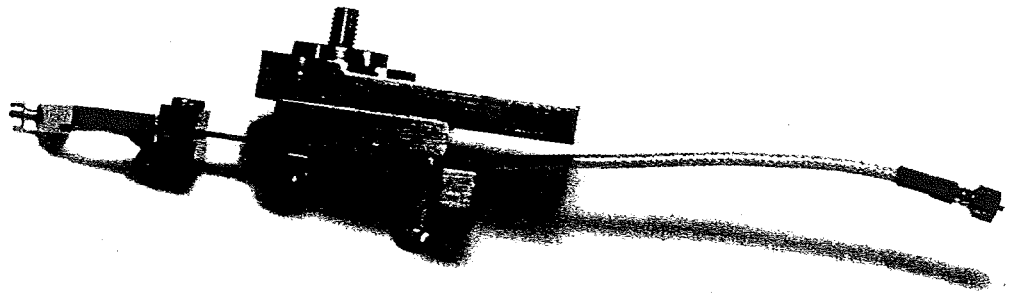
**Figures 25.** Photograph of SYRINGE INJECTOR.



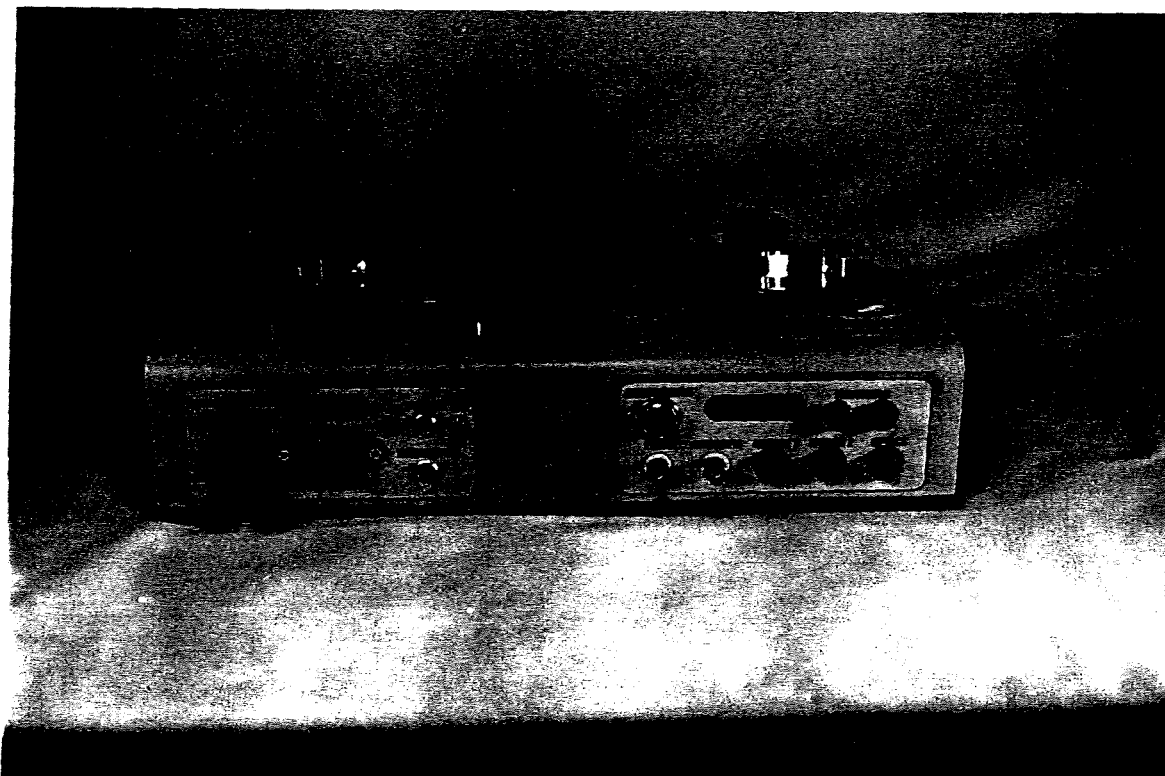
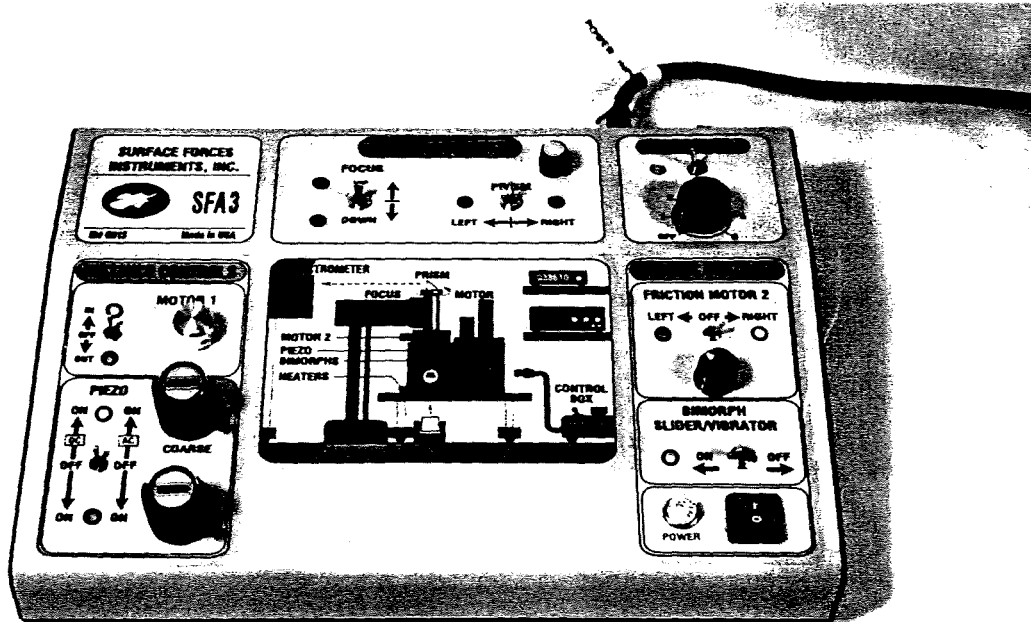
**Figures 26.** Photograph of FRICTION DEVICE and removable/exchangeable barrel.



Figures 27. Photograph of BIMORPH SLIDER.



Figures 28. Photograph of BIMORPH VIBRATOR and FIXED SPRING MOUNT.



**Figures 29.**

Drawings and photographs of CONTROL BOX (front and back, and inside wiring).

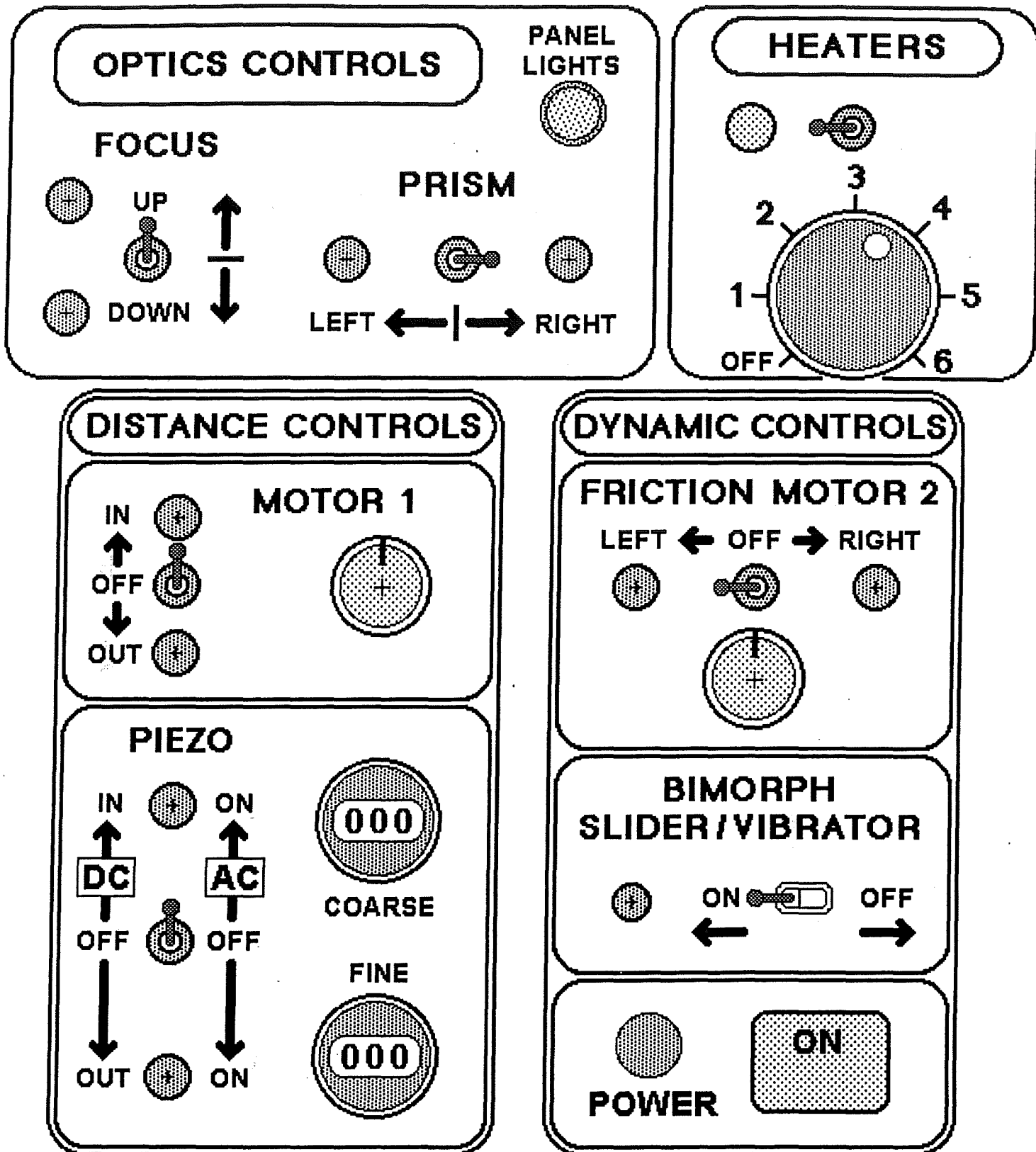
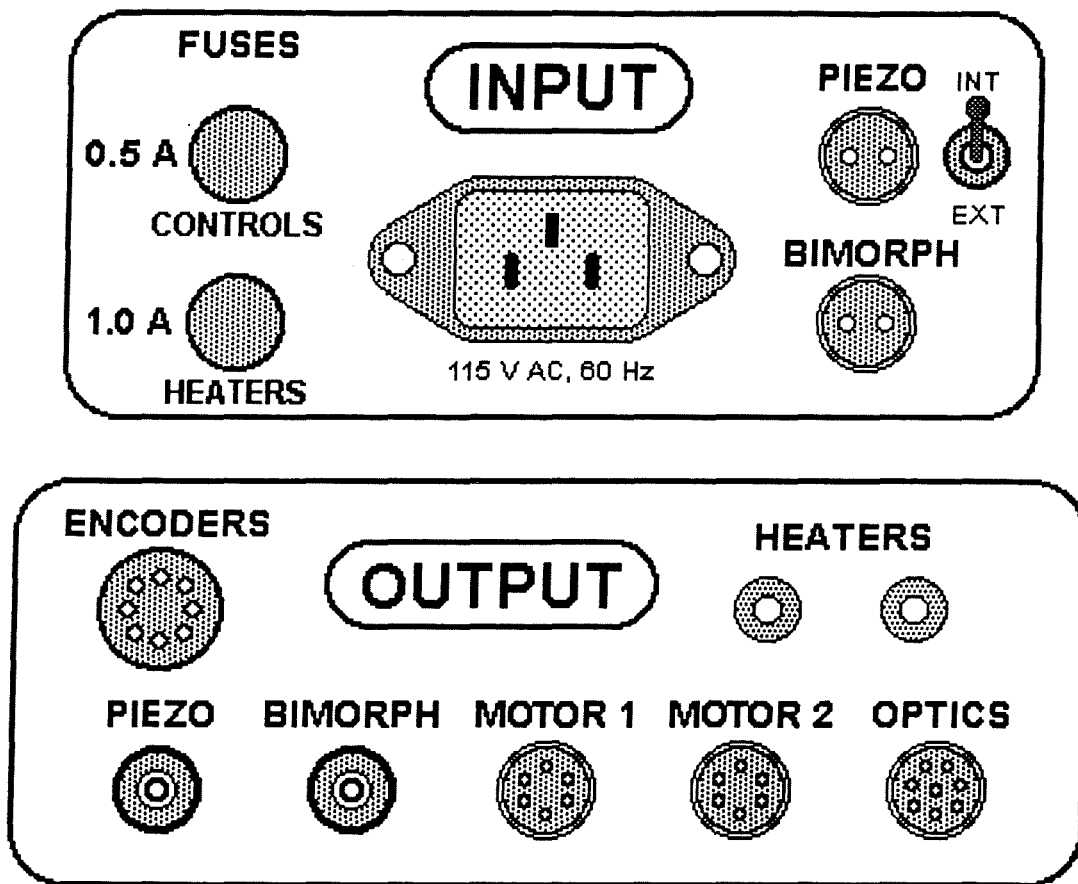


Figure 29a. CONTROL BOX – Front panels.

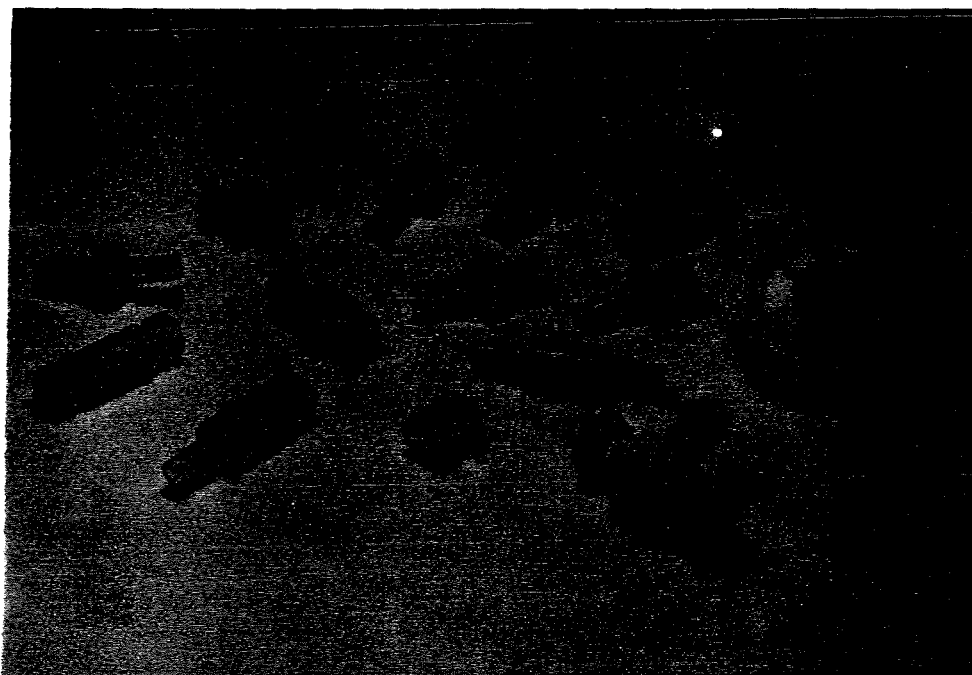
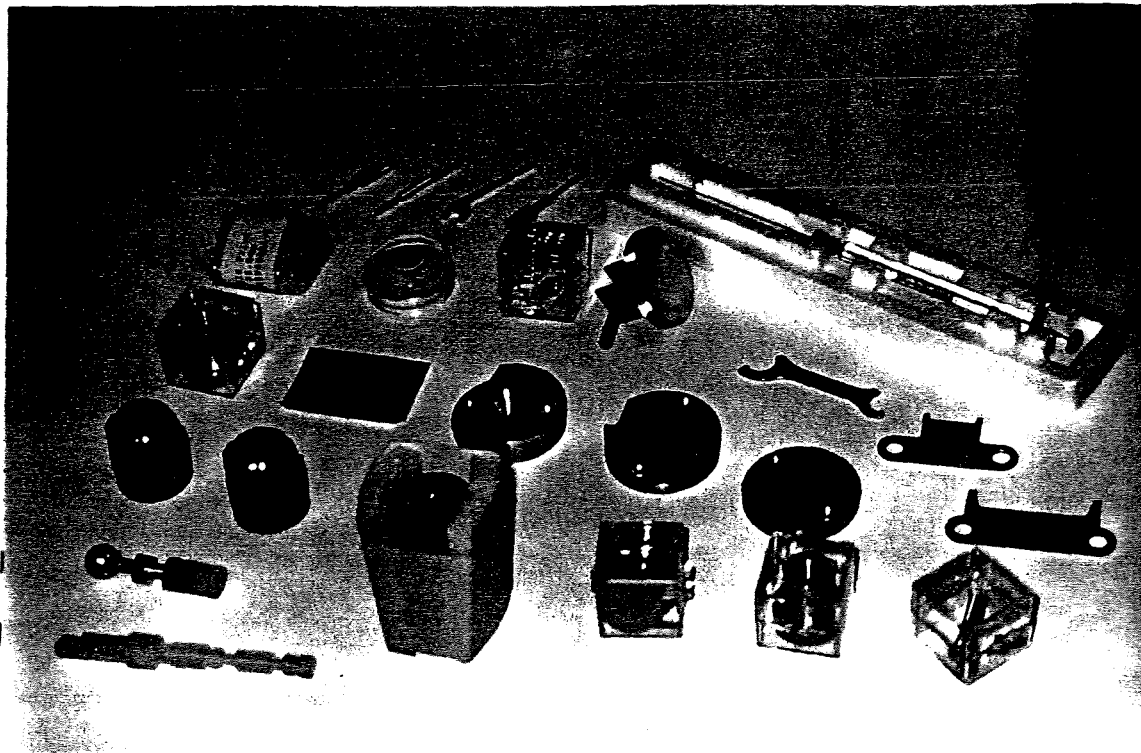


**Figure 29b.** CONTROL BOX – Back INPUT and OUTPUT panels. Power input and output voltages are 110–115 V @ 60Hz for the US, 220V @ 50Hz for Europe, and 100V @ 50 Hz for Japan. Each control box has been adjusted for the local mains voltage supply.

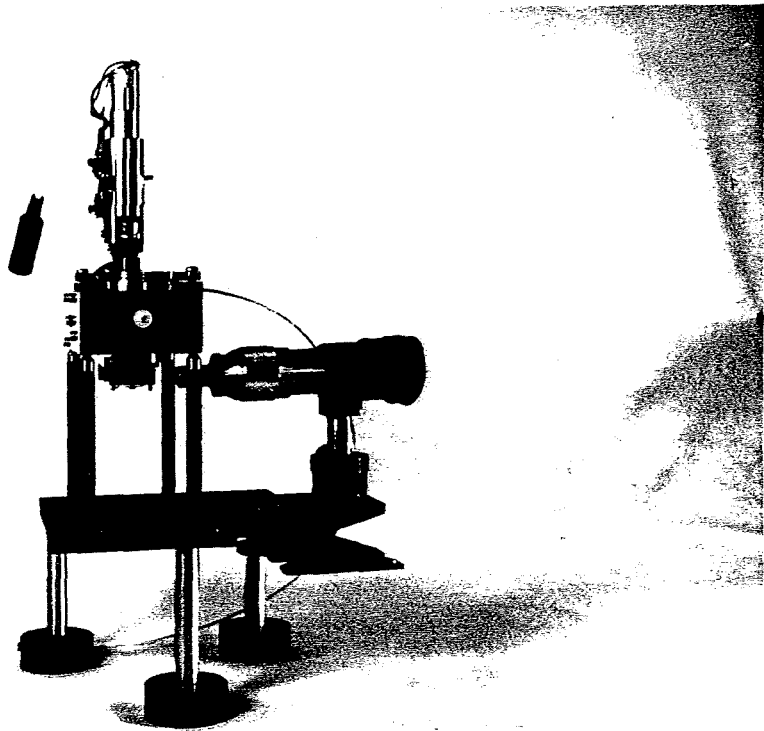
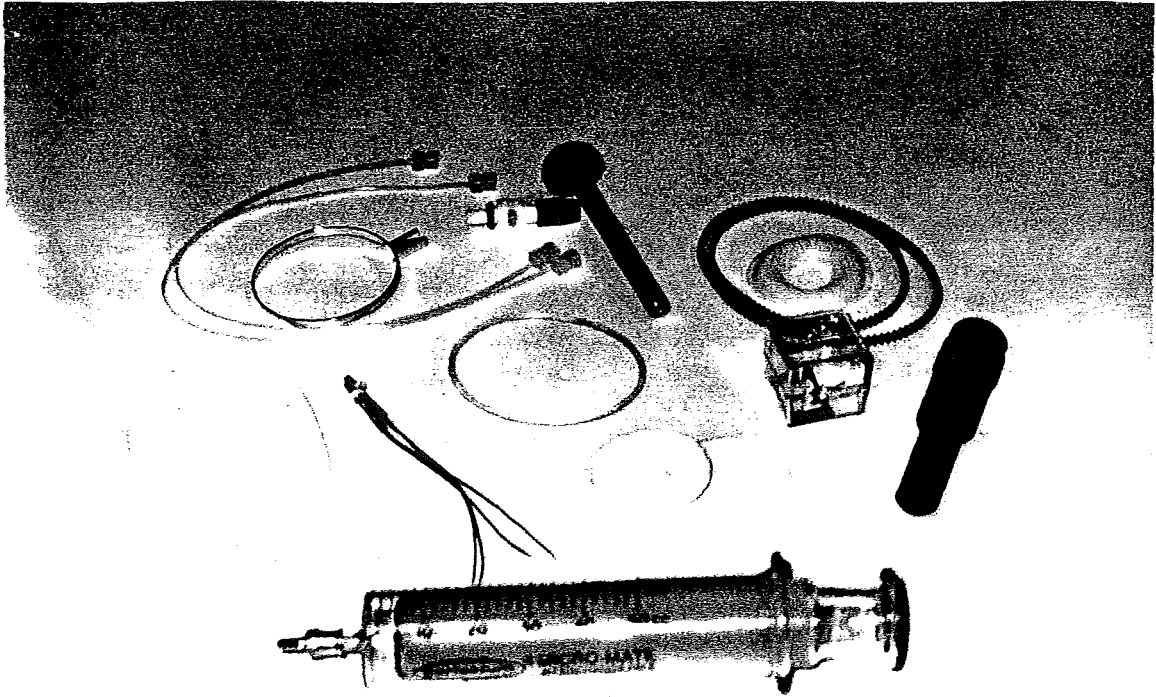
### Earth loops / ground loops

When wiring up the control box and other instruments to the apparatus, one must never earth the apparatus in more than one place or else one is liable to pick up electric noise from "earth loops" or "ground loops" (you may read up on this important phenomenon in any electrical engineering handbook). The earthing contact for the apparatus is a small hole on the front of the base plate, which should be used as the common terminal for connecting the apparatus and all electric units requiring a ground terminal (piezos, bimorphs, motors, etc.). Thus, the outer surfaces of the Piezo Mount is earthed through the electric contact of its housing with the apparatus when it is bolted into place (check that all conducting metal parts of the piezo housing are indeed electrically connected to the outer *earthed* wall of the piezo tube but not the inner *live* wall). Likewise, all bimorphs should have their earthed sides connected to the steel wall of the apparatus and not independently through the outer shield of its coaxial cable.

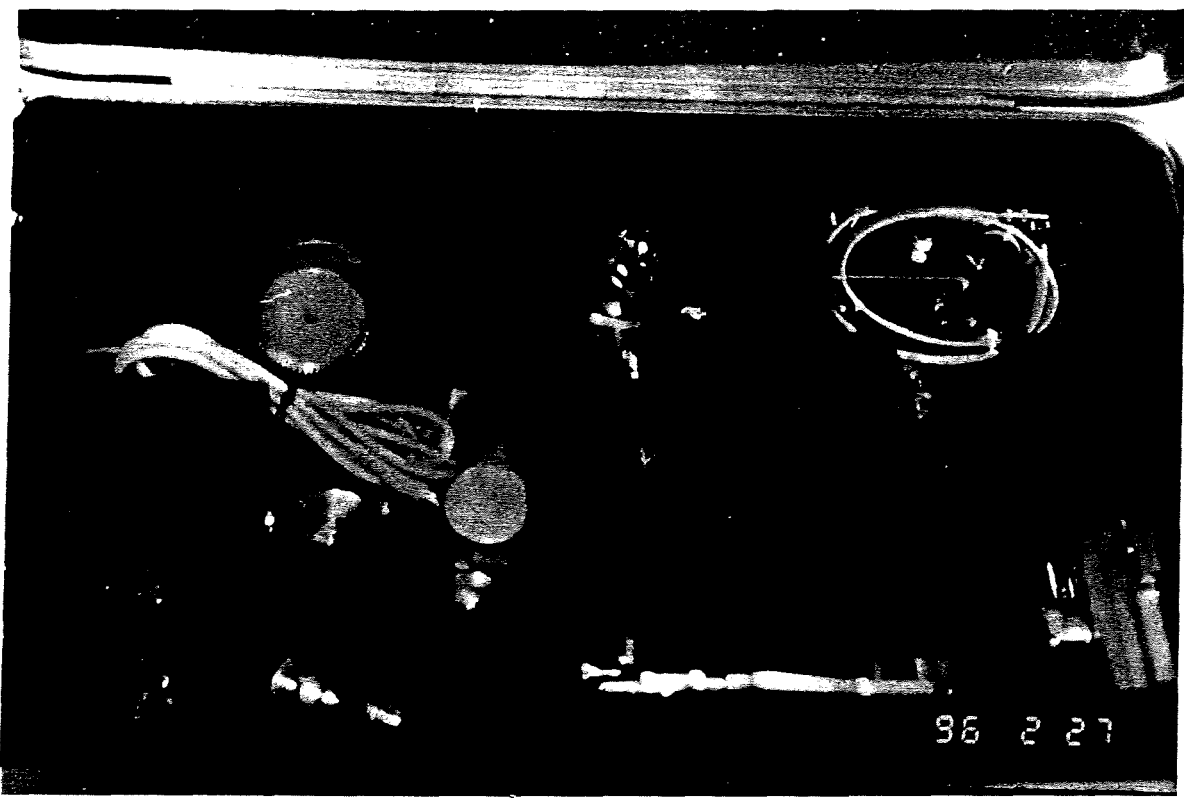
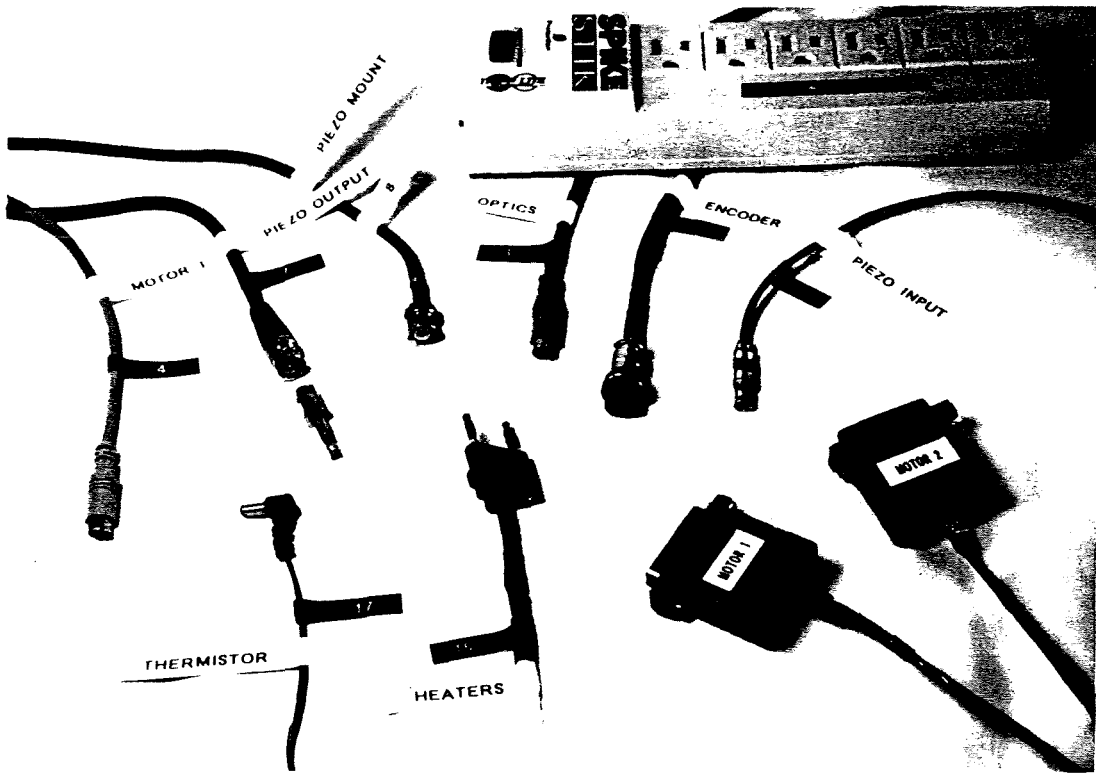




**Figures 30 (continued).**  
MISCELLANEOUS PARTS, SUPPLY ITEMS, ELECTRIC CABLES, ASSEMBLY  
TOOLS, LUER FITTINGS, etc.



**Figures 30 (continued).**  
MISCELLANEOUS PARTS, SUPPLY ITEMS, ELECTRIC CABLES, ASSEMBLY  
TOOLS, LUER FITTINGS, etc.



Figures 30 (continued).  
MISCELLANEOUS PARTS, SUPPLY ITEMS, ELECTRIC CABLES, ASSEMBLY  
TOOLS, LUER FITTINGS, etc.

### 1.3 HANDLING THE SFA: CLEANING AND ASSEMBLY (BASIC UNIT ONLY)

#### Assembly/disassembly between experiments

When not in use, i.e., between experiments, the Basic Unit can be left assembled, or it can be partially disassembled into its different UNITS, or selected UNITS can be fully disassembled into their individual PARTS. All UNITS are already assembled on delivery, and most will not require any special attention, such as disassembly, between experiments. However, it is wise to check that they are functioning properly before each new experiment (these checks are described in Section 2). Only the LOWER CHAMBER and VARIABLE SPRING UNIT need to be regularly disassembled, cleaned (each part at a time), and reassembled before each new experiment, although this may not be necessary if a series of similar experiments are being conducted one after the other, for example, if each experiment involves filling the apparatus with the same liquid or solution. In this case, simply draining the box and flushing it out with clean ethanol a few times should be sufficient. The apparatus can then be left, closed and filled with ethanol, until the next experiment. As a general rule, full disassembly of a UNIT should not be necessary between experiments unless (1) a thorough cleaning is called for, as might occur after an experiment with strongly adsorbing compounds or after an accidental spill, (2) the internal stainless steel surfaces need to be passivated – a type of 'servicing' that is recommended once every 6–12 months depending on the corrosiveness of the aqueous solutions used, or (3) a faulty part needs to be fixed or replaced.

The following small tools and glassware are needed for cleaning and assembly, some of which are shown in Figures 30 on pages 44-47 (starred items ★ are supplied with each SFA). Before proceeding, make sure that all tools needed for cleaning and/or assembly are clean and ready for use inside the laminar flow cabinet.

- ★ SFA3 supply items, assembly tools kit, and electric cables (see list on Pages 8-9).
- ★ Luer fittings and stop-cocks for inlets and outlets.
- ★ Syringes and needles.
- ★ Thermistor.
- ★ Micrometers.
- ★ O-rings.
- ★ Screws, nuts and washers.
- ★ Spatulas (both Teflon-coated and stainless-steel).
- ★ Various miniature cleaning brushes (toothbrush-type, pipe-cleaning type).

- ★ Screw driver set, including Philips-head, hex-head and nut-head types.
- ★ Allen keys: metric and English.
- ★ Stainless steel and Teflon-tipped tweezers and forceps – various sizes and types.
- ★ Spanners and wrenches.

Acetone.

Ethanol (clean liquid in sealed bottle or squirt bottle).

Ethanol gun (pressure rinser).

Air gun: compressed clean dry nitrogen gas gun (compressed gas should come from liquid nitrogen tank, not compressed gas cylinder, and all connecting tubes should be made of clean Teflon tubing or stainless steel).

Beakers: 2 large flat-bottomed (6" or 15 cm diameter).

Beakers: 8 small (100-200 ml).

Petri dishes (can also be used as beaker covers).

Beaker covers for all of the above (petri dishes will do).

Lint-free absorbing tissues.

Small files and de-burring tools.

### **Passivation of stainless steel parts**

All internal steel parts have already been passivated in 30% conc.  $\text{HNO}_3$ . Repassivation of those steel parts whose surfaces come into contact with the experimental solution is recommended every 12 months or more often if experiments routinely involve strong aqueous salt solutions, especially chlorides, or if the internal surfaces have become scratched. To passivate, immerse the stainless steel parts (but *not* any protruding electrical connections such as the piezo crystal) in 30%  $\text{HNO}_3$  at 60°C for 30 minutes (note: Kel-F is inert to conc.  $\text{HNO}_3$ ), then remove all excess acid by thorough washing in clean distilled water.

### **Degreasing, deburring and sonication**

If some parts have become visibly dirty or greasy, for example, if a part has been sent to the machine shop, a degreasing in acetone is recommended. Use small scrubbing brushes if necessary, making sure that the bristles are not dissolved by acetone. This could be followed by sonication, especially if new thread holes have been tapped. All threaded holes and other cavities should have any debris or burr finally removed by air-blasting or squirting ethanol into the holes using an ethanol gun.

### **Cleaning of fully disassembled parts before assembly**

The following describes the recommended cleaning procedure of individual parts. All cleaning and drying should be done in a clean air, dust-free atmosphere, e.g., in a laminar flow cabinet.

First, thoroughly clean all glassware and tools (glass beakers, stainless-steel forceps, etc.) with clean ethanol (absolute alcohol). Carefully place all non-electric, non-piezo parts into ethanol-filled glass beakers. The larger parts may all be placed into the 15 cm diameter flat bottomed beaker. The smaller parts, including small screws and O-rings, should be placed into well-marked smaller beakers. You may wish to identify different beakers for the small parts, otherwise you may confuse different screws and O-rings that look similar. Use Teflon-coated tweezers to pick up the parts and carefully place (not drop) them into the beakers. When handling the parts, be particularly careful not to scratch any of the smooth polished surfaces, particularly the O-ring grooves and sealing surfaces. Teflon O-rings need particular care when being handled.

While still immersed in ethanol, scrub metal parts with a *soft* chemically inert brush (fine toothbrush type). Use the miniature pipe-cleaning type brushes to clean inside screw holes. Note that vigorous scrubbing should be avoided since this will remove the protection afforded by the passivation layer causing possible contamination by  $\text{Cr}^{3+}$  leaching. One by one, remove parts from beaker, squirt ethanol from a hand-held 'ethanol gun' directly onto all sides and into holes of each part. Direct the ethanol jet outwards, being careful to ensure that the reflected ethanol spray does not land inside the laminar-flow cabinet or on surfaces that need to remain clean. When all sides of a part have been squirted, place the part in a second ethanol-filled beaker. Cover the beakers, then cover everything with a transparent glass globe (Figure 31) and leave to 'soak' until ready for assembly.

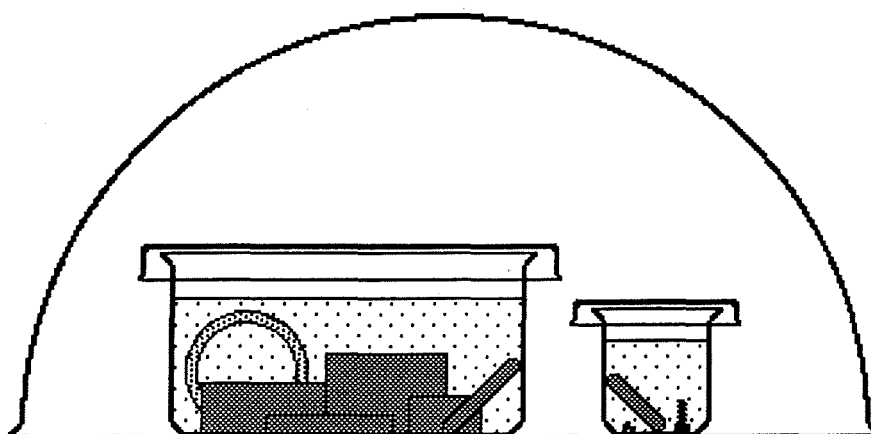


**Figure 31.** Soaking of metal, glass and Teflon parts in ethanol prior to assembly or between experiments. Round transparent perspex (plexi-glass) domes or flat-faced boxes are readily available from a number of suppliers (see table I).

Prior to assembly, remove each part from the beakers, rapidly blow-drying (especially the small holes and threads) with a nitrogen jet as they are taken out. Direct the nitrogen jet outwards, being careful not to blow away small parts. Note: blow drying is essential; if apparatus parts are simply left to dry by allowing the ethanol to evaporate, only the ethanol is removed leaving behind undesirable contaminants. By blowing the surfaces dry with a pressurized N<sub>2</sub>-gun both the ethanol and contaminants are swept away quickly (the pressure rinser by Gelman is recommended; plastic squirt bottles are not since they suck in air contaminants continuously as they are used). Place dry parts on a clean stainless-steel surface or clean Teflon-coated paper sheet inside the laminar flow-cabinet. When all the parts (or units) have been cleaned and dried, proceed with the assembly, as described below.

### **Routine cleaning between experiments (requiring no disassembly)**

The following describes the recommended cleaning procedure between experiments when full disassembly is not required, for example, during a series of experiments using similar liquids. In most cases, it is only necessary to rinse the apparatus a few times with ethanol: each time filling the apparatus then draining, aspirating and blow-drying, following the instructions given in the above paragraphs. For a more thorough cleaning, especially after experiments with polymer and surfactant solutions, a preliminary light scrubbing with soft brushes in ethanol or chloroform (CHCl<sub>3</sub>) is recommended followed by soaking in chloroform, depending on the polymer (see above). When all units have been cleaned and dried, proceed with the next experiment (described in PART 2 of this manual). Alternatively, fill the chamber with clean ethanol, close the apparatus and all outlets (using the large glass disk instead of the piezo mount), and leave until required.

### **Greasing of micrometer threads**

The two micrometers on the Upper Chamber and the one on the Friction Device do not come into contact with the internal chamber and so can be greased with any suitable low VP grease. For greasing the micrometers of motors 1 or 2, remove the motor housing by unscrewing it (you may have to loosen the limit switch board first). Note the position of the protruding shaft and then loosen the two set screws on the housing and gently unscrew the threaded micrometer shaft until it comes away from the housing. Clean the thread by rubbing with acetone or alcohol. Rub some grease between your thumb and index finger, then rub your fingers round the thread only. Reinsert shaft and lock back into place in exactly the same position as before. For greasing the Differential Micrometer, first remove the micrometer housing by unbolting nut 01150 (Fig. 7), then turn the top knob all the way until the small part comes out. Grease both threads separately. Don't over grease and don't use force in any of the above operations.

## ASSEMBLY OF BASIC UNIT

Make sure that all tools needed for assembly are clean, dry and placed ready for handling inside the laminar flow cabinet (cf. Figures 30). Newly machined parts and screws may sometimes be difficult to fit together or screw into. This may be because a small piece of metal (burr) is still lodged in a hole or thread or screw head. Rather than force the parts together, use a small needle file or deburring tool to remove such pieces of metal until the parts fit together smoothly.

### BASE (Figures 13, 21)

Attach the three legs 03030 into the base plate 03010 using the hex nuts and washers provided. Screw on the four base hinges 03020 with the 8 flathead screws provided. Place base on flat table and check that it is level using the spirit level.

You may adjust the level and height of the base plate by turning the legs (parts 03040) and tightening with the leg nuts (parts 03030 B). Later, screw in the three locating disks (kinematic mounts) 03050A, B and C to your experimental table using threaded machine screws or wood screws so that the base will always settle at precisely the same place each time you put it down.

### LOWER CHAMBER (Figures 9, 20)

The following operations should be carried out by use of clean forceps, tweezers and screwdrivers, without touching any of the parts by hand and with care so as not to scratch the surfaces (this procedure should always be adopted when handling parts that will come into contact with the chamber fluids and internal surfaces).

Put into place the following:

- **Side window** – part 02040 against the round silica window and O-ring (size –020), using 4 Philips head screws.

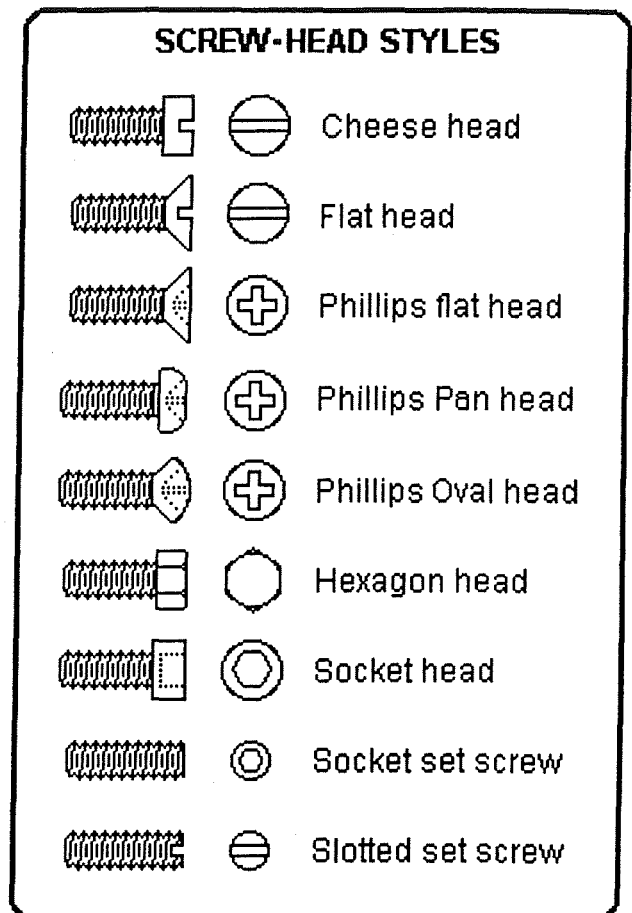


Figure 32. Types of screws used in the SFA 3.

- **Thermistor** – part 02070 against thermistor and O-ring (size –006 or –007). Alternatively, the thermistor hole may be sealed (plugged) with part 02080 and the same O-ring.
- **Syringe port plug** – place O-ring (size –012) in hole, then press in and screw on plug 08080 with three screws (or using the three threaded studs 08090 and hex nuts 08100). Do not overtighten. If you have a syringe unit, assemble as per Figure 11, page 24. If you want to use the syringe port for controlling the vapor pressure inside the chamber, screw on 08110 instead of 08080 with three ordinary nuts or the hex nuts 08100 without tightening, then press in part 08051 and tighten the three nuts gently (a light pressure will ensure a good seal). Close off the end of 08051 with a Luer plug. If you want to use the syringe, after inserting the O-ring, press in syringe housing assembly 08010 with the steel ball 08020 against the O-ring, and tighten with three ordinary nuts or the hex nuts 08100 (tighten gently – enough to ensure a good seal but not too much that turning the syringe holder becomes difficult). Insert a 7.5–9.0 cm long, 0.071" diameter flat-ended needle (supplied), and observe that it just comes out from the other end. Turn part 08010 to tighten the sealing grip around the needle inside the syringe unit (see Figures 11 & 25). To seal (plug up) the needle hole, plug the exposed end with a Luer plug (e.g., male-male connector and end-cap).
- **Inlet hole** – screw in male Luer connector into the inlet hole. To ensure a good seal, you may insert a –003 O-ring first and/or wrap some Teflon tape around the thread before screwing in the Luer connector. Close end with Luer cap.
- **Hinge** – screw part 02060 with the two oval-head screws provided.
- **Heaters** – insert after the apparatus has been fully assembled and placed on the base.

### UPPER CHAMBER (Figures 7, 19)

Place the parts to be assembled also in the laminar flow cabinet as shown in Figure 18. Fit main and top O-rings into Upper Chamber [01010]. Tightly bolt steel part 01050 to the Cu-Be part 01040 using the two flathead screws provided. Tightly bolt 01040 to the Cu-Be spring 01030 using two cheese-head screws (ensure the right orientation and parallelism). Press the helical spring 01310<sup>†</sup> into the recessed holes in the two Cu-Be parts 01210 and 01080 and slide assembly into position in the Upper Chamber. Slide the Cu-Be assembly 01030 into place using the thin metal spatula to part and ease the slippage between the cantilever springs of parts 01030 and 01210 while gently pressing down the sharp edge of 01210 (no force should be required during this operation). Bolt 01030 into the Upper Chamber 01010 using four screws and the special right-angled screw driver provided. Screw in the two guiding pins 01090

---

<sup>†</sup> Different helical springs may be used, depending on the range and sensitivity required for the differential spring control (the third distance control) which is currently set at about 1000:1. An alternative spring having a lower stiffness is supplied with each SFA3.

through the roof of the Upper Chamber (do not tighten yet), passing them through the two slots of part 01080. Check for smoothness of motion of 01080 by pressing it in and out through the top hole using the flat end of a soft rod (the flat end of a pencil or the soft plastic end of the steel spatula). Tighten guiding pins 01090 while ensuring perfect smoothness of motion when tight.

Centralize part 01210 by hand. Screw part 01120 into part 01040 tightly but carefully (without scratching or bending any of the surfaces): Part 01120 should not be touched by hand. Slip or screw in the Teflon bellows 01290 into place, ensuring that the inner and outer lips are pressed all the way in and are lying flat against the steel seats. Screw in rings 01100 and 01110 using the two key spanners 01130 and 01140: this operation must be done incrementally by tightening each ring alternately a little at a time so that there is no residual stress on the bellows.

Screw part 01150 into place, then insert and screw in the differential micrometer and locking nut. Turn both the coarse and differential heads to test for smoothness of rotation over their full ranges (6 mm for the coarse, limited by the Cu-Be part 01030 touching the ceiling and floor, respectively, of the inner chamber). The fine control head should not be turned beyond the red ring. Turn the coarse head on the differential micrometer anti clockwise until the rounded end of the micrometer shaft is above the flat ceiling of the internal chamber. Loosely bolt 01060 to 01200 using two screws with washers, then bolt 01200 to the Upper Chamber from the back with 4 screws. Loosen 01060 by loosening the two screws holding it from the back. Raising part 01050 to the ceiling and part 01060 as low as possible, insert helical spring 01300 using the medium sized serrated forceps provided so that each end 'clicks' into place in the recessed holes on 01060 and 01050 (protect yourself during this delicate operation: the spring may suddenly fly out in your face). From the back of the chamber, gently tighten the two screws but allow enough space for them to be moved up and down the two slots. Raise both screw heads with the back edge of the steel forceps and tighten fully\* so that part 01060 is level and horizontal and positioned so that the micrometer and the cantilever springs of 01030 can move the whole way from the chamber ceiling to the floor without hindrance (a total distance of 6 mm, or  $\pm 3$  mm from the mean position). Set the coarse control so that the cantilever springs of 01030 are horizontal, that is, at the mean position. Set the differential (fine) control at the black ring, which is at the middle of the recommended range of travel (do not go beyond the red ring).

---

\* An alternative way to tighten the two screws is to push part 00000 up until the spring assembly touches the ceiling, then tighten 01200, ensuring that 01060 is level.

Screw on part 01270 and insert the normal micrometer barrel through it, pressing it in to the end. Tighten the barrel with the two set screws on 01270 (not too tight). Test the micrometer for smoothness of rotation and absence of backlash by hand over the whole range of travel – about 10 mm from top to bottom – but do not force it beyond either end. Limit switches on the driving motor will ensure that you will not be able to exceed the safe travel range during experiments. However, before using for the first time, check that the micrometer and limit switches are working properly and smoothly over the desired range by moving the micrometer electrically or by hand (in case the limit switches are not going to be used).

Assemble the bevel-gear unit and wheel: place small –007 O-ring into the shaft hole and screw in part 01160, gently tightening it against the O-ring. Slip shaft 01230 of the bevel-gear unit into the hole, and close up the top with part 01180 using two screws. Test the up-down movement of the unit and smoothness of wheel rotation. The positive pressure of the O-ring on the shaft should be felt. Screw in the locking screw 01170 almost to the end, but do not lock.

Press dovetail part 04010 of the variable spring unit into the recess hole in 01120 and align perfectly parallel to the long axis of the upper chamber. Tighten with screw 04130. Neither of these parts should be touched by hand – special gloves should be worn.

Place upper chamber on lower chamber 02010, positioning the two together with the dowel pins. Screw in male Luer connector into air-outlet port on 01010 and close with a Luer cap. Blow clean internal chamber of Upper Chamber to remove dust, then close off with transparent side window 01190 using three screws (making sure that it does not press against the locking screw 01170). You may also close the piezo hole by placing the Piezo Mount into it and clamping it in place with the clamping plate 00080 (at this stage, it doesn't matter if you align the clamp in the NE or NW directions). Remember to screw on the small disk-locking screw 00030 into the disk mount 05020 before inserting the piezo mount. It is also worth checking, every now and again, that the piezo crystal connections are in order, that is, having infinite resistance across the coax cables, and closed circuit between the outer cable, the crystal mount (05010), the outer piezo wall, the upper disk mount (05020), and ground. The base should be grounded by connecting a ground wire to a screw on the front side of the base plate.

Slip in the four chamber tightening screws 02050 upwards at the four corners of the lower chamber and rotate by hand until the lower and upper chambers are sealed together. Place apparatus on base with the lower window on top of the oval hole. Tighten the two pointed locating screws on base hinges 03020A into the two grooved holes in hinge 02060 at the back of the Lower Chamber, and test that SFA can be tilted about the hinge 02060. Lower the SFA

back onto the base and tighten the other two locating screws (on base hinges 03020B) into the two grooved holes at the front of the Lower Chamber. The apparatus should be sitting comfortably on the base plate.

### **FORCE-MEASURING SPRING (Figures 10, 20)**

The following operations should be carried out by use of clean forceps, tweezers and screwdrivers, without touching any of the parts by hand and with care so as not to scratch the surfaces (this procedure should always be adopted when handling parts that will come into contact with the chamber fluids and internal surfaces). Attach part 04030 to 04020 using two screws. Screw on the small disk-locking screw 00030 into the disk mount 00020. Screw the holed ends of the two cantilever springs 04120 to the lower disk mount 00020 using the four screws provided, but do not tighten fully. Tighten the two rods 04110 into part 04020 and slip in parts 04040 and 04050 between them. Slip the two cantilever springs 04120 on either side of 04040, and screw in the clamping spring 04100 with the long screw provided. Tighten the clamping screw very slightly, so that the two cantilever springs can still slide easily.

Assemble parts 04060, 04070 and 04080 with two screws, ensuring that all 4 beveled edges point inwards, but do not tighten the double cantilever spring so that it cannot be slid out. The double threaded screw 04090 should already be attached to part 04060 and bevel gear 01220. Thread screw 04090 into part 04020 from the 'correct' end until it protrudes from the other side. Slip the two cantilever spring ends between parts 04060, 04070 and 04080 and very gently tighten the two screws on 04080. Slip the whole spring assembly, part 04020 first, into the dove tail 04010 (which is already attached to the underside of the Upper Chamber) from right to left, and bolt part 04060 to 04010 tightly with two flathead screws.

Test whether the shaft 01230 engages the level gear 01220 exactly at its centre. If not, do not turn wheel 01260. Remove the whole sliding assembly from the dovetail slide 04010, readjust and reclamp it with screw 04130. Only when it is perfectly centered with the shaft 01230 will it be safe to rotate the wheel to initiate sliding of the double-cantilever force-measuring spring clamp. To test for good fit, lower the shaft via wheel 01260 until it engages the bevel gear. Press the wheel down until positive engagement is felt (do not press too hard – excess force will cause difficult, uneven motion of the bevel gears), then lock the shaft in place with locking screw 01170. Turn the wheel slowly in both directions, checking that the wheel turns easily and evenly as the dove-tail slides smoothly in either direction.

It is important that the double cantilever springs 04120 are also properly clamped with respect to parts 04060, 04070 and 04080. Turn the wheel counterclockwise until the clamping unit on

04020 starts pushing against the lower disk mount 00020. While pressing the disk mount against 04040 with a steel rod, tighten the screw on the clamp shim 04100 about 2 turns beyond the point where the clamp shim just starts to bend/deform. Now turn the wheel 01260 clockwise until the far ends of the cantilever springs 04120 just start to buckle against parts 04060, 04070, 04080. Reverse the wheel to relieve the buckling, then tighten the two screws on 04080. Now loosen the screw on 04100 by 1 turn, that is, to 1 turn beyond the point where the clamp shim starts to bend. The above procedure should ensure that during reclamping, the two cantilever springs 04120 remain parallel (and therefore that the silica disks do not bend) during the sliding of the dovetail 04020 over the whole range of clamping distances (from 0 to 32 mm).

Now test that the wheel 01260 can be turned (slowly) and the clamp unit moved (smoothly) without the cantilever springs 04120 buckling. Buckling will occur if the clamp shim is bent too much by the clamping screw. However, if an experiment at a fixed spring stiffness is being planned, especially a high stiffness (as might be required for experiments at high loads only), it is worth tightening this screw more than for experiments where the stiffness will be varied.

Set the clamp about 1.5 cm from the lower disk mount (requiring about 30 rotations of the wheel) so that it is roughly in the position shown in Figure 5. Unlock the locking screw 01170 and raise the wheel and shaft to the top, then relock the shaft in this position. You may now adjust the height of the spring mount via either micrometer. **IT IS IMPORTANT NEVER TO FORGET TO UNLOCK THE LOCKING SCREW 01170 AND RAISE THE SHAFT BEFORE MOVING THE SURFACES UP OR DOWN. FAILURE TO DO THIS WILL PUT LARGE STRESSES ON THE SPRINGS AND MECHANICAL PARTS.**

### **Final assembly**

Purge SFA chamber with a gentle flow of clean, dry N<sub>2</sub> gas for 1 hour, letting the gas in through a cleaned Teflon filter attached to the Luer inlet in the Lower Chamber and out through the Luer outlet on the Upper Chamber, or vice versa. Remove gas feed and plug up both holes with Luer caps.

Fit motor housing 00040 with reversible DC motor and encoder to the micrometer head on part 01270 in the upper chamber. Attach limit switches at the appropriate positions. Connect electric cables to Control Box and encoder display panel, and test motorized micrometer for smoothness of motion, absence of backlash, and proper working of encoder display, motor speed control and limit switches.

The apparatus may now be filled with clean ethanol up to about the rim of the lower chamber, but not so high that the liquid will wet the piezo tube, and sealed. Various additional tests and calibrations could be done at this stage: (1) You may calibrate the liquid volume of your assembled chamber by filling/injecting up to a particular level, as seen through the window, and noting the volume injected. (2) When sealing the piezo hole with the round glass cover (supplied) test that the bellows and other seals do not 'leak' by tilting the SFA until it is upright and examine for leaks – but first remove front window on Upper Chamber and be prepared to soak up any leaking fluid immediately, before it has time to spread. Tilt back and continue checking for leaks. Test overnight by noting whether the liquid level – as seen through the window – has dropped; if so, then some ethanol must have evaporated out through a small hole somewhere, in which case you should further tighten all the seals. The apparatus can now be left as it is, preferably covered as in Figure 31, until it is used.

### **OPTICS STAND AND MIRROR (Figures 14, 23, 24)**

These arrive fully assembled. They require no maintenance and their use is fairly self-explanatory. Connect the 6-pin cable from the optics stand to the Control Box OUT panel. Before each experiment, make sure that the dot on the fine focusing stage is positioned between the two horizontal lines on the translation stage. Also make sure that the micrometer is set at the midway point of the scale, i.e., at about 5 mm. Coarse focusing can be done by hand (large round knob). Fine focusing and the prism turntable angle can be controlled from the front panel via two 'momentary' switches. The standard objective fitted at the end of the optics tube is a modified Ealing Electro-Optics X5 objective. If a higher image magnification is required, a X10 objective can be used instead: Ealing Objective (Cat. No. 24-9748) is recommended: the encased X10 objective lens can be readily removed from the housing and screwed directly to the end of the optics tube, part 07290, after removing the X5 objective.

### **MIRROR (Figures 14, 23)**

The two mirror angles and position can be controlled by hand using the three finger screws. Extension cables and replaceable finger screws are provided for remote control.

END OF PART 1

## PART II

# GENERAL OPERATING PROCEDURES

### PREPARATION OF MICA SURFACES FOR FORCE MEASUREMENTS OR INTERFEROMETRIC EXPERIMENTS

Prepare the laminar flow cabinet for cleaving by laying out clean tweezers and mini-forceps (Figure 33), the metal blocks for holding mica sheets during cutting, the hot wire cutter connected to a low voltage DC power supply, platinum wire (0.2 mm or 0.006"–0.008" diameter), large scissors, petri dish (10 cm or 4" diameter), ethanol cleaning liquid, a few large mica sheets, and 5 dangling clips from the ceiling of the cabinet for hanging mica sheets from.

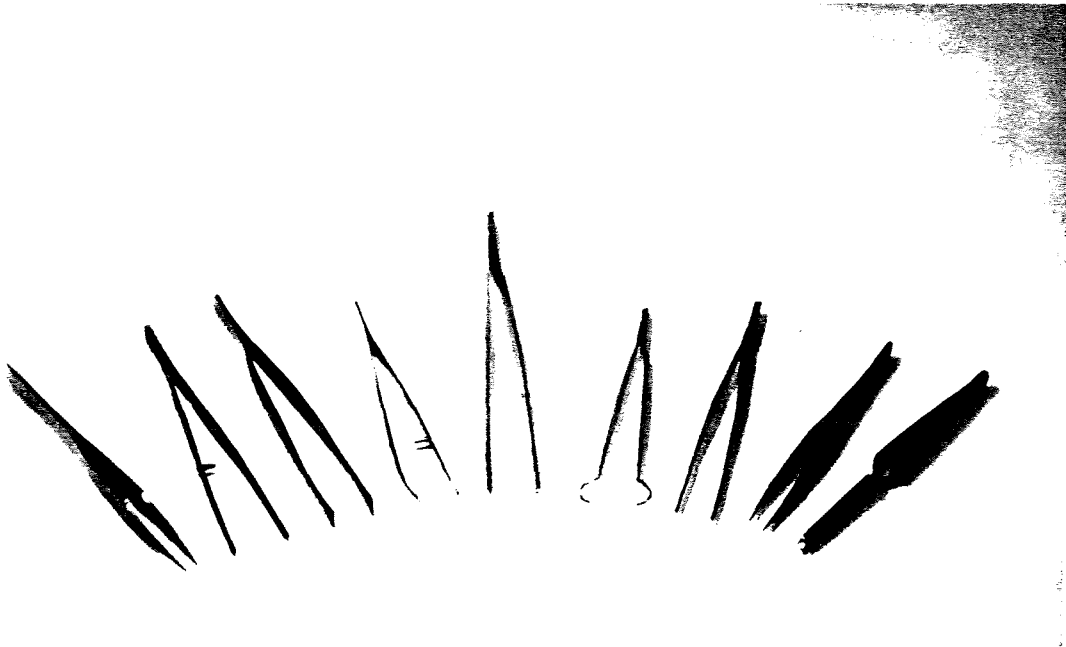


**Figure 33.** Tweezers and other small tools used in various mica-handling operations such as cutting, gluing and mounting (see also Fig. 30). Tools should be cleaned before each stage.

Select a 15cm X 20cm X 0.5 mm thick sheet of Ruby Muscovite mica, trim its edges with large strong scissors, and remove all excess edge flakes, beat sheet a few times to allow edge flakes to disperse (don't do this near delicate surfaces). From this sheet a semi-thick sheet is cleaved (peeled) *slowly* to expose two smooth surfaces that are largely step-free as ascertained by eye. Step-free surfaces are usually obtained when the bifurcation line moves smoothly, without jerking or 'cracking' during the peeling. Cleavage may be initiated by inserting the tip of a sharp needle into the edge of the thick sheet, opening up the crack by gentle lateral movement

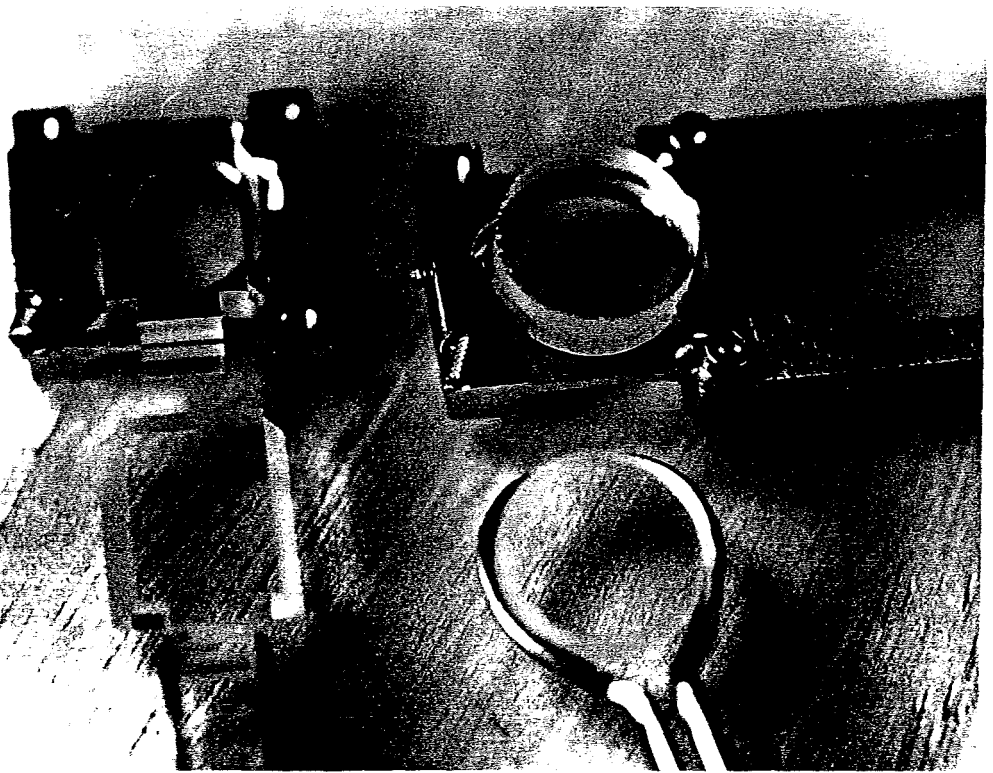
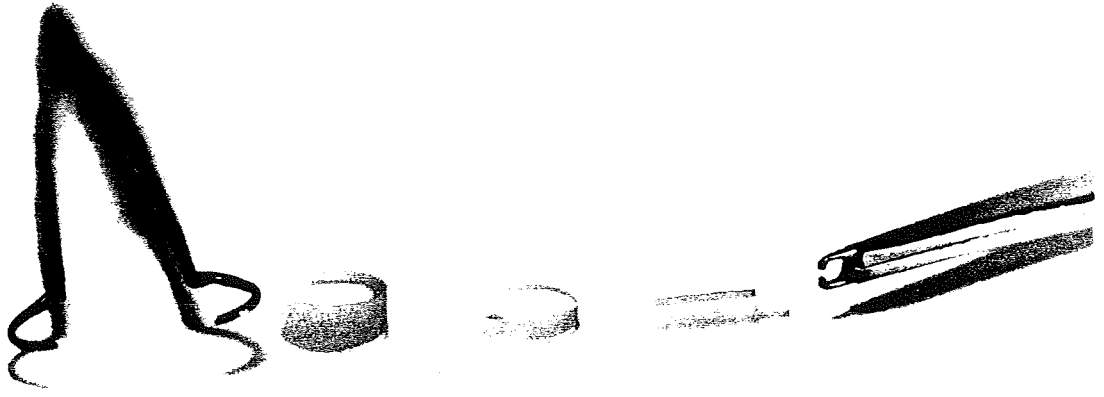
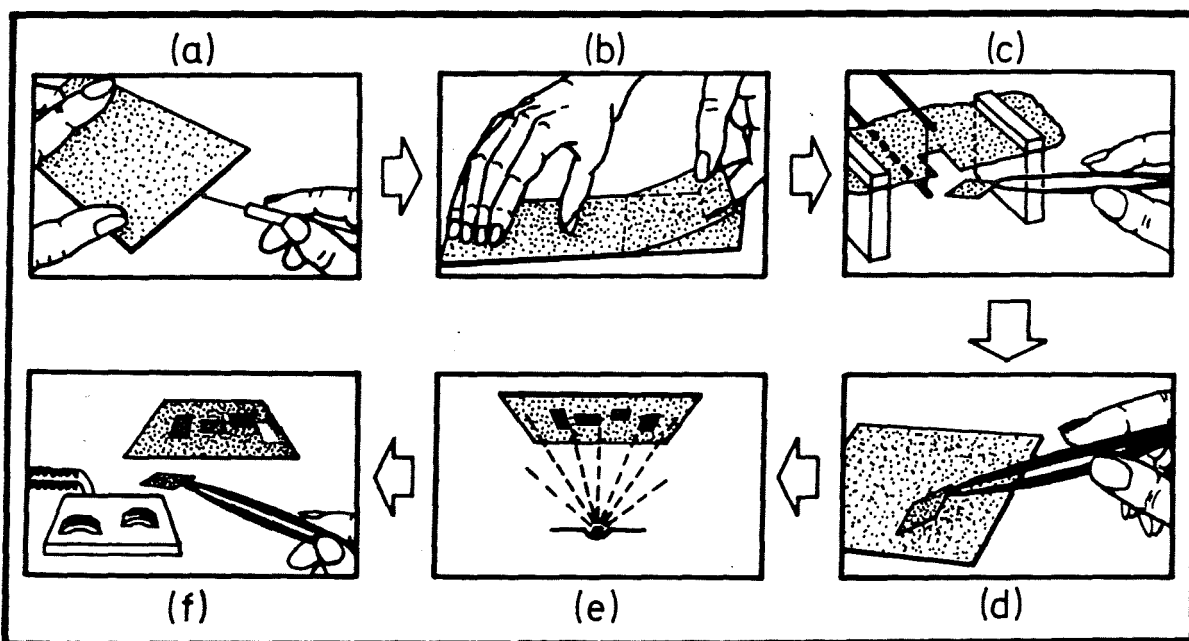
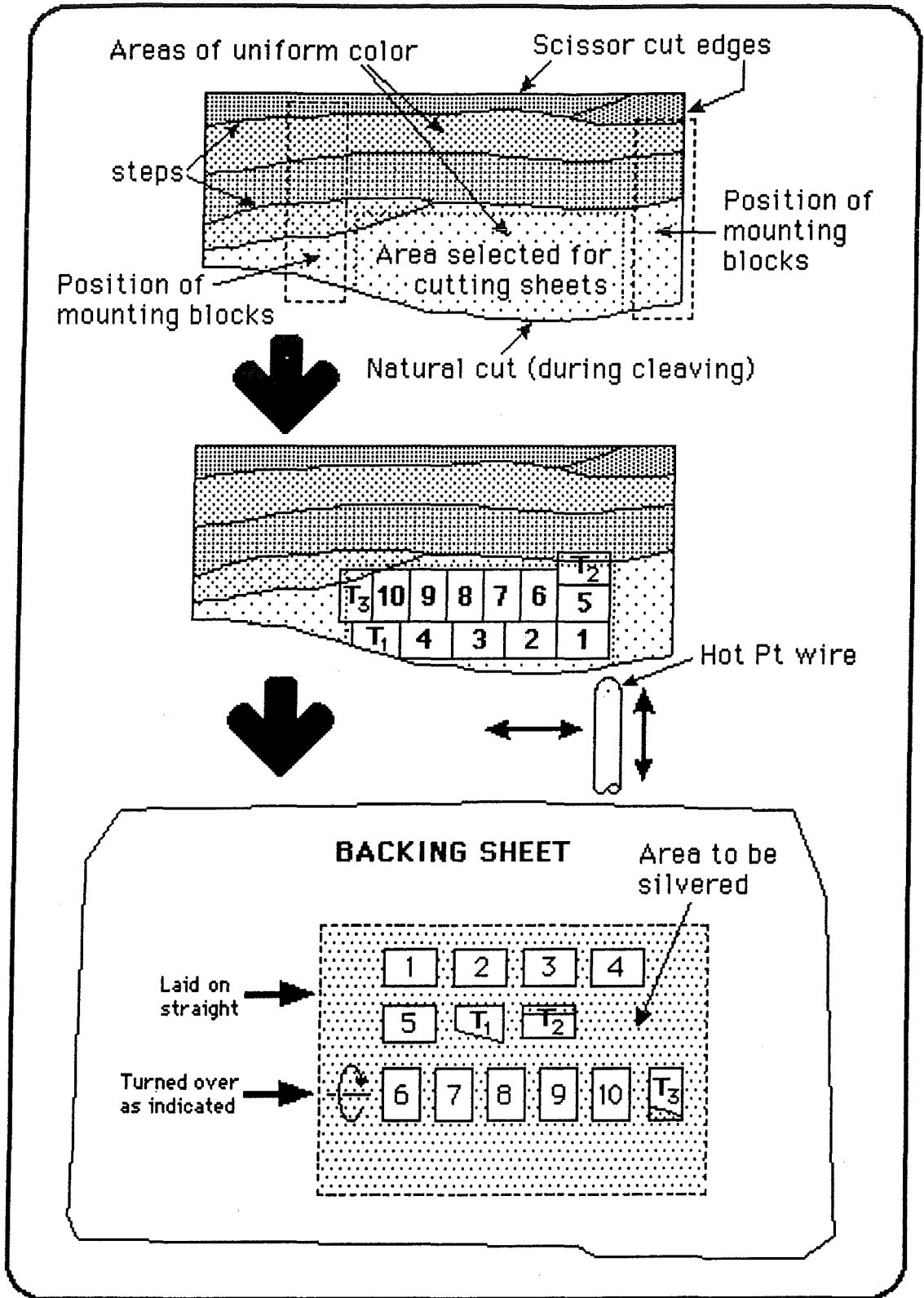


Fig. 33 - continued.

of the needle, followed by careful peeling away of the two sheets. The freshly cleaved sheets are examined in the neon light of the laminar flow cabinet for the number/location and direction of the steps. One of the two sheets (the best or thinnest) is chosen as the 'backing sheet' and hung vertically from a clip parallel to the air-flow direction and well away from the cleaving area to avoid flakes from settling on its freshly cleaved surface. The other is chosen for further cleaving of much thinner and smaller sheets to be used as the substrate surfaces in experiments. When cleaving/peeling, insert the needle as close to the freshly cleaved surface as possible and try to cleave in a direction *parallel* to the step lines. If a sheet is sufficiently thin (2-3  $\mu\text{m}$  thick) interference colors are seen reflected by the surface. These colors change abruptly at cleavage steps, but remain uniform over regions of constant thickness. Thinner sheets (<1-2  $\mu\text{m}$ ) have brighter colors that change less with the angle, and these sheets also flap about more in the flowing air stream. When cleaving thin mica sheets from a thick sheet, it is essential to do it in as stress-free way as possible. This is usually best achieved by slowly peeling a thin sheet from the thick sheet, *parallel* to the direction of the steps. The thin sheet should be peeled away very slowly, at a uniform rate of about 5mm/sec, without tearing or sticking occurring.



**Figure 34 (Continued on next page).** Stages in the preparation of mica sheets: (a)-(b) cleaving (sheets should peel away slowly and smoothly, *along* the steps), (c) cutting (fairly rapid movement of the hot wire is recommended), (d) placing cut sheets on backing sheet to which they should immediately adhere, (e) silvering, followed by storage in dessicator or (f) gluing (do not overheat). Stages (a)-(d) and (f) must be carried out in a laminar flow cabinet (horizontal air flow type); stage (e) is carried out in a vacuum coating unit or evaporator.



**Figure 34** (continued). When pairs of sheets (1 and 6, 2 and 7, etc.) are cut and placed on the backing sheet as shown above, after gluing and mounting into the apparatus, the sheets will be in crystallographic register, displaying maximum birefringence of the FECO fringes (see Figure 35).

With experience it is possible to cleave sufficiently large regions (approx. 1 sq. inch or 10 cm<sup>2</sup>) that are a few microns thick and free of steps on either side. If a large enough step-free region is found, place it across two clean metal blocks and hold it in place with two smaller block, as shown in Figure 34(c). The platinum wire cutter should have a short ~7 mm long platinum wire of diameter 0.2 mm or 0.006"–0.008" vertically mounted between two parallel rods as shown in Figure 34(c). The rods are attached to an X–Y translation carriage. The wire is heated above the melting point of mica by passing a low voltage current through it.

Adjust the height of the platinum wire so that the centre of the wire, which will be the hottest part, is exactly at the level of the mica sheet, which should be stretched taught between the two blocks so as to be completely flat (this can be done by gentle moving the blocks apart once the mica sheet is held down on each block by the smaller block). Place the large backing sheet, face up, somewhere in the laminar flow cabinet well away from the cutting area, and note where you intend to place the small mica sheets (preferably away from steps). Check that the tips of your sharp tweezers are not bent and that they meet symmetrically. Place the wire cutter well away from the mica. Gradually increase the current through the wire until it becomes yellowish-white. After the wire has 'outgassed' (a few seconds) bring the translation stage up to the mica, position it 'correctly', and start cutting (burning) the sheets. Cut each sheet one side at a time by moving the hot wire at a uniform-but fairly rapid rate of about 1-2 seconds per side. As each rectangular sheet is cut free from the main sheet it is immediately picked up with the straight, sharp tweezers and placed on the freshly cleaved surface of the backing sheet (but see Figure 35). At once, molecular contact should take place across the whole rectangular contact area, except at the edges which have been damaged during the melting; but this is to advantage as it allows the sheets to be picked up again later with tweezers. If the cut sheets do not adhere well, try turning them over; if they still adhere poorly, it is wise to reject them.

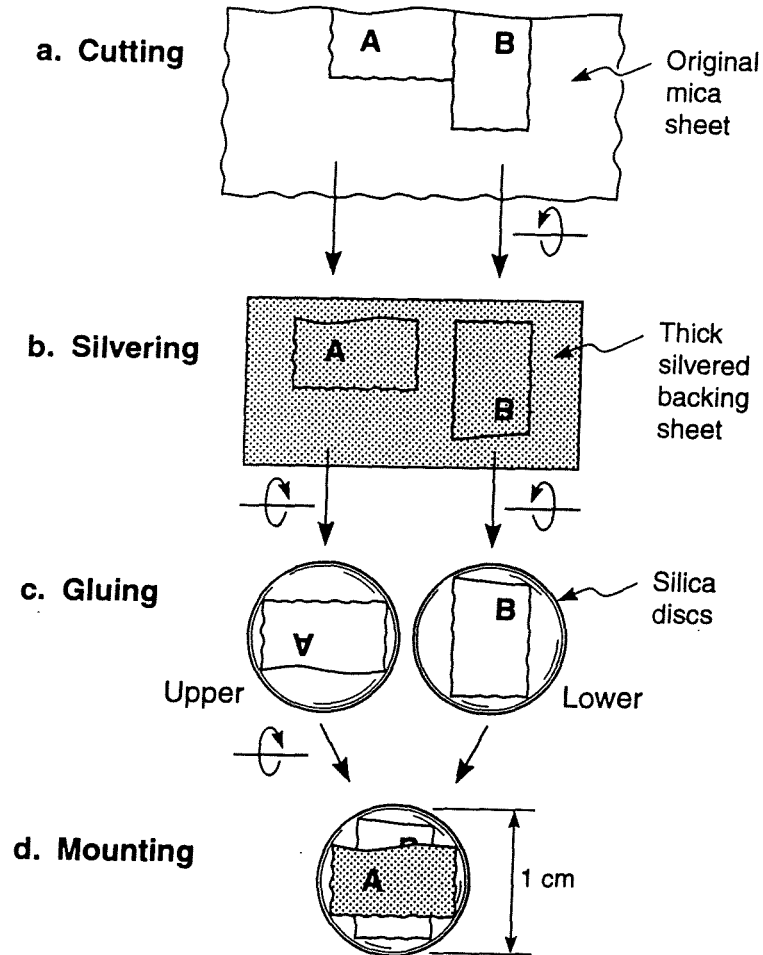
In this way, six or more small rectangular sheets (about 6 mm × 9 mm) are cut out in pairs, some length-wise, some width-wise, and placed on the same backing sheet, as shown in Figure 34. In this way the surfaces of the rectangular sheets in contact with the large sheet are protected from contamination as long as they remain there. It is advisable to keep track of each sheet, its orientation relative to the other sheets, whether it was turned over before being placed on the backing sheet and about which axis. Figure 35 gives further details on how to cut and place sheets so that their relative crystallographic orientation is preserved or rotated by a known angle during experiments. After making a sketch of the disposition and orientation of all the pieces on the backing sheet, it can be turned over and placed, like a cover, on the clean petri dish for transporting out of the laminar flow cabinet.

It is also wise to cut a few "test" sheets (labelled T in Figure 34) which can be used for measuring the thickness and orientation of the mica sheets prior to using them in an experiment. After silvering the backing sheet (see below), one of the test sheets can be glued onto a glass plate (a microscope cover slip is ideal) and another laid on it as in a normal experiment, ensuring that the silvered surfaces are on the outside in both cases. This test piece can then be stuck directly onto the entrance slit of the spectrometer and the fringes observed by directing a light beam from a small flashlight (torch) onto the surfaces by hand. Alternatively, the fringe positions can be more accurately measured by placing the glass plate below the microscope tube of the Optics Stand, aligning the optics and adjusting the position and angle of the surfaces as in a normal experiment, and measuring the fringes accurately.

All the above operations should be carried out in a laminar flow dust-free laminar flow cabinet (hood) to prevent dust and mica flakes from settling on the freshly cleaved surfaces (the flow of air should be *horizontal* and *outwards* towards the worker). Surgical gloves may be worn to prevent oily secretions from spreading onto the surfaces. The mica should always be handled at its edges only. It should be remembered that inhalation of fine particles is a health hazard, so precautions are advisable for protection of both lungs and eyes when cleaving the mica.

Next, the exposed surfaces are silvered in a vacuum coating unit at a pressure of  $\sim 10^{-5}$  torr (allow 1-2 hrs for outgassing) as shown in Figure 34(e). Standard precautions should be taken to ensure that a uniform layer of pure silver (about 550 Å thick and/or of  $\sim 98\%$  reflectivity) is deposited at  $\sim 1$  Å/sec at a pressure of  $\sim 10^{-6}$  atm. In particular, the mica backing sheet should be at least 40 cm away from the crucible (e.g., molybdenum boat) to avoid overheating of the deposited silver layer. An overheated layer will look brownish rather than bluish and have a lower reflection coefficient. After silvering, the large sheet is returned to the dust free cabinet for gluing, as shown in Figure 34(f), or stored in a dessicator for later use. The adhering surfaces will be protected from environmental contaminants so long as the sheets remain on the backing sheet, but it is also important to prevent deterioration of the silver layers by ensuring that the dessicator atmosphere is dry and free of oily vapors (otherwise the silver surface may not adhere well when the sheets are later glued onto the glass surfaces).

**Figure 35.** The birefringence of the FECO fringes varies as  $\cos\theta$ , being maximum for  $\theta=0^\circ$  and zero for  $\theta=\pm 90^\circ$ , as described later. This figure gives the procedure for preparing and mounting mica sheets so as to preserve or control the mutual crystallographic orientation, or twist angle  $\theta$ , of the two sheets (refer also to Figure 34).



First, a mica sheet is cleaved to produce an area with a uniform thickness of about one micron. Two rectangular pieces, A and B, are carefully cut from this area so that all the edges are either parallel or perpendicular to each other as in (a). One piece, say B, is turned over before it is put on the backing sheet to which it adheres. The other sheet, A, is also placed on the backing sheet but without being rotated (b). After silvering, the mica sheets are peeled off from the backing sheet and glued, silver sides down, onto the cylindrically curved surfaces of two silica disks as shown in (c). The longer side of each rectangular sheet is positioned parallel to the

principle cylindrical axis of each disk. Inside the apparatus chamber, the lower disk, supporting B, is mounted at the end of the force-measuring spring, while the upper is attached to the end of the piezoelectric tube. The aim is to make the two mica surfaces face each other at the same angle as in the uncleaved mica, that is, at  $\theta=0$ , as shown in (d), although other, non-zero orientations can also be achieved. Final alignment is done by viewing the surfaces via the microscope tube that passes through the piezoelectric tube. Exact crystallographic matching is established visually by rotating the piezo tube mount until the corners and edges of the rectangular sheets are aligned, very much as one would align two pieces of paper. This method generally allows for rough initial alignment to within  $\pm 2^\circ$ .

A special ring attachment (provided with each Friction Device) can be fitted snugly around the circular Piezo Mount. This allows the upper mica sheet to be rotated by any desired 'twists' angle around a fixed vertical axis during an experiment. For very precise angular rotations, a rigid horizontal arm can be attached to the top of the Piezo Mount, and a micrometer positioned at the end of the arm. This allows the twist angle  $\theta$  to be controlled to better than  $0.01^\circ$ . Due to the fact that the two surfaces are cylindrical, it may be impractical to rotate them by more than  $\pm 30^\circ$  from zero in any one experiment.

A video is available showing all stages of mica preparation.

## **PREPARATION OF APPARATUS FOR FORCE MEASUREMENTS**

Having previously cut, silvered and treated the mica sheets as described above, they are now ready for gluing on the silica disks and mounting into the apparatus.† The following assembly tools should be clean and ready for use inside the laminar flow cabinet: hot-plate, needle-sharp 'biological grade' tweezers (for lifting up mica sheets), various small forceps and tweezers, screw-drivers, glue, ethanol squirt gun.

Switch on sodium lamp in the experimental room. Blow a filtered nitrogen gas jet into all parts of main chamber, piezoelectric mount, silica discs, tools, etc., to finally get rid of dust, concentrating on holes, outlets, inlets, etc. Attach filter to Luer outlet of Upper Chamber, then close off with Luer cap. Close off the Luer inlet on the Lower Chamber with Luer cap (attach filter first, if required). Depending on the type of experiment to be conducted, a Teflon tap (supplied) may be screwed into the Lower Chamber instead of the Luer connector. Place the Piezo Mount on the working area, facing 'up'. Note that there is also an all-steel replacement mount 00010 without the piezo tube – this can be useful for experiments in which the fine sensitivity of the piezoelectric crystal is not required. This part is also less sensitive to temperature drifts than the crystal mount. Unscrew screws 00030 on both the piezo mount 05020 and the lower disk mount 00020 just enough that there is space to slip in the silica disks.

### **GLUING**

Gluing of mica is done by putting two silica discs on a small electrically heated hot-plate and placing some crystals of EPON RESIN, sym-diphenylcarbazine or sugar (total volume ~1 mm<sup>3</sup>) on the top curved surfaces of the discs. As the crystals melt, the liquid is spread evenly over the surfaces with curved tweezers, and a mica sheet is then peeled off the large backing sheet with straight pointed tweezers and placed on top of the glue, silvered side down. Ensure that the mica lays down out evenly over the glue layer, exposing a smooth, unbuckled surface of uniform (cylindrical) curvature. To do this, you may need to press the edges and sides gently into the glue with Teflon-tipped tweezers. The disc should be removed from the hot-plate as soon as good adhesive contact is established (underheating of the glue can cause bad adhesion, but overheating can cause small bubbles to form or even deterioration of the silver layer). On removing the disk from the hot-plate, inspect the surfaces at grazing incidence to see that no edges or flakes are sticking up. The other mica sheet of the 'matching pair' (cf. Figures

---

† For experiments requiring 'treated' surfaces, for example, two different surfaces, or surfaces other than mica, or mica surfaces that are first coated with a layer of surfactant, polymer, metal or biological material, a number of additional stages are required before the surfaces are mounted into the apparatus. One of these is shown in Figure 36.

34 and 35) is now glued similarly to the second disc. If anything goes wrong (e.g., a mica sheet tearing on being stripped off) other sheets from the remaining pairs on the large sheet can be used instead.

If a 1 mm cube crystal of glue is used in the gluing, which after melting spreads out over an area of, say, 6 mm x 8 mm (~50 mm<sup>2</sup>), the final thickness of the glue layer will be 1/50 mm or 20 μm. In some experiments it is important to know this thickness, which can be deduced at the end of an experiment by first estimating the glued area per sheet, then weighing each glass disk with the mica sheets still glued on, and again after the mica and glue have been removed (see below). The density of the glue is also needed (Shell EPON RESIN series glues have a density of about 0.61 g/cm<sup>3</sup>). Sym-diphenylcarbazine (a white powder of M.P. 176°C) may also be used as a glue; it is suitable for work in inert non-polar (but not aromatic) solvents, and aqueous solutions (so long as the temperature remains at room temperature). But it is slightly soluble in water, and more so in solutions containing divalent cations, so that after a few days dissolves away or becomes opaque. Most glues are also sensitive to high concentrations of chloride salts. The polymers EPON RESIN 1004 or 1009 (Shell) – also thermosetting glues – are better suited for work in water: they are not affected by water even at higher temperatures (60°C). However, they are more viscous than the carbazine – they have a glass transition,  $T_g$ , rather than a true melting point – and are therefore more difficult to handle. For room temperature aqueous experiments, the EPON 1004 ( $T_g \approx 90-100^\circ\text{C}$ ) is recommended; at elevated temperatures, a higher  $T_g$  resin, such as EPON 1009, would be more suitable. Other glues can be used for work in strong organic solvents such as acetone, chloroform and toluene. Sugars are particularly good for this purpose, such as a mixture of dextrose and galactose for toluene. UV-curing glues can also be used such as Norland Optical Adhesive #61 from Edmund Scientific (see also Table I and, for example, S. M. Kilbey, F. S. Bates, M. Tirell, R. Hill, H. Yoshizawa, J. Israelachvili. *Macromolecules* **28** (1995) 5626–5631). Such glues are particularly useful for producing two flat, parallel surfaces (rather than curved surfaces), which may be desirable for some experiments. To achieve this, after gluing the mica sheets, they are brought into flattened contact inside the apparatus and the glue is then cured (set) by UV irradiation (5 Watt Hg pen-ray lamp at a distance of 3-5 cm from the surfaces) for 5-10 minutes inside the SFA chamber while the surfaces are still in contact. After curing, the two surfaces remain flat and parallel on separation. This glue dissolves in chloroform.

To remove glued mica from the discs at the end of an experiment, place in acetone or chloroform for an hour or overnight then peel off sheets.

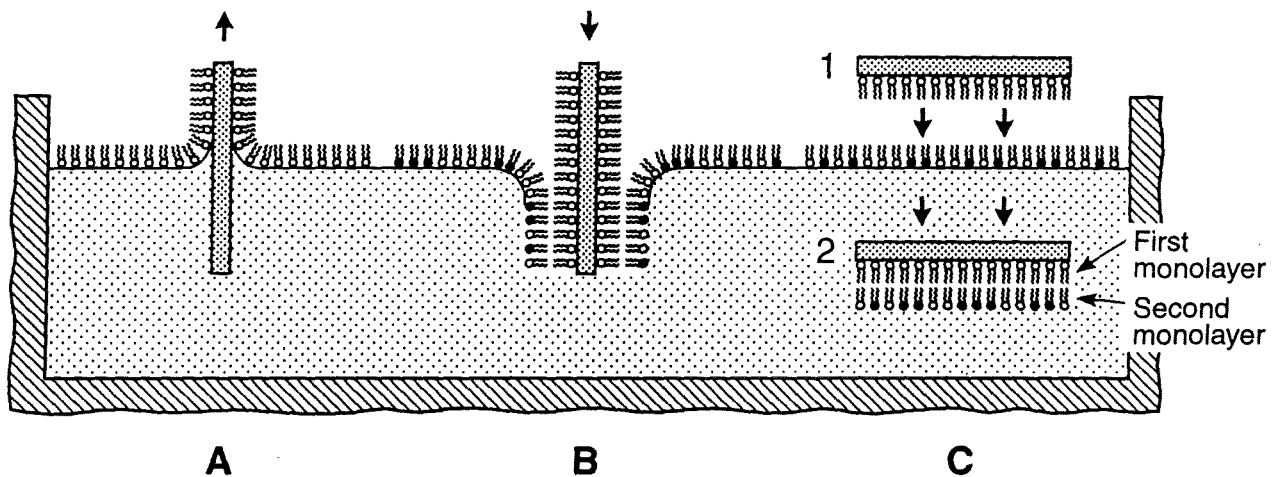
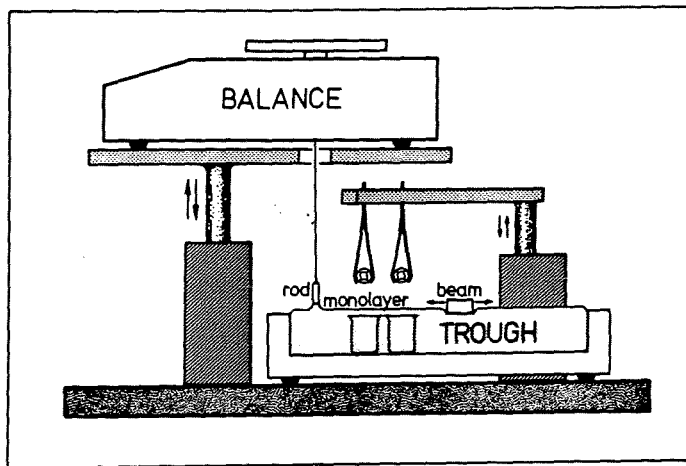


**Figure 36.** Langmuir-Blodgett deposition trough set-ups suitable for pre-coating mica (and other) surfaces with insoluble surfactant or lipid monolayers or bilayers prior to their installation into the apparatus. The mica sheets are shown glued to the two silica discs ready for depositing a (second) monolayer followed by insertion into the two beakers in which they will be transferred (under water) to the apparatus and mounted into position through the large front window (the apparatus must be placed on its side during this operation). A special Teflon DEPOSITION CELL may also be used for transferring the disks under water to the apparatus for insertion through the side window. Depositions may also be done in the straight contact (Langmuir-Schaeffer) method, as shown. For good, clean depositions, the trough should be fully enclosed.

### INSTALLATION OF SURFACES INTO THE SFA 3

Carefully choose the 'right' disks for your experiment. Disk heights vary from 2.5 mm to 5.5 mm and can be used in various combinations (two 4 mm disks are considered 'standard'). The optimum choice depends partly on the vertical setting of the two bolting screws on part 01200 at the back of the apparatus, which in turn depends on the type of experiment being conducted – whether normal force measurement, friction experiment, bimorph sliding experiment, deposition 'under water' experiment, etc.

Glue on mica sheets on two silica discs as described in the previous section. Any additional surface treatment of the mica surfaces could be done now, for example, coating of surfactant layers (cf. Figure 36) or of metal oxide, silica or polymer layers via some other deposition, evaporative or spin-coating method. Some types of surface treatments may have to be done before the gluing.

Establish which disks and at what angles they will be mounted into their respective disk mounts so that the final configuration is the desired one (cf. Figure 37) and that the coaxial cable on the Piezo Mount protrudes at a convenient direction. Using straight but curved-ended tweezers, pick up lower disk and place into hole on the Disk Mount 00020 and tighten into place with a hex head (Alan key) or Philips head screw driver. Check that the disk is really sitting firmly in place by gently trying to lift the disk with a spatula or screw-driver and establishing that the disk does not move. Turn the coarse micrometer control to ensure that the lower surface is sufficiently low that it will not touch the upper surface when it is installed (see \* below). A specially constructed STAND for supporting the UPPER CHAMBER during these operations is highly recommended (see photo of STAND in Figure 30).

Place upper silica disk and place into hole on top of the piezo mount and tighten into place. Again, check that the disk is firmly in place by gently trying to lift the disk with a thin spatula or screw-driver and establishing that the disk does not move (this will avoid making this discovery when you turn the piezo mount upside down). Turn the piezo mount over and place into position on top of the Upper Chamber without hitting the lower surface (see \* above). Rotate and centralize piezo mount in its hole so that coaxial cable comes out at a convenient direction. Clamp 00080 into place in the 1:30 – 7:30 clock directions using the two Philips head screws provided (do not clamp tightly at this stage).

Position two dowel pins of Upper Chamber on holes of Lower Chamber and lower Upper Chamber gently into place. Bolt the two chambers firmly together with the four screws 02050.

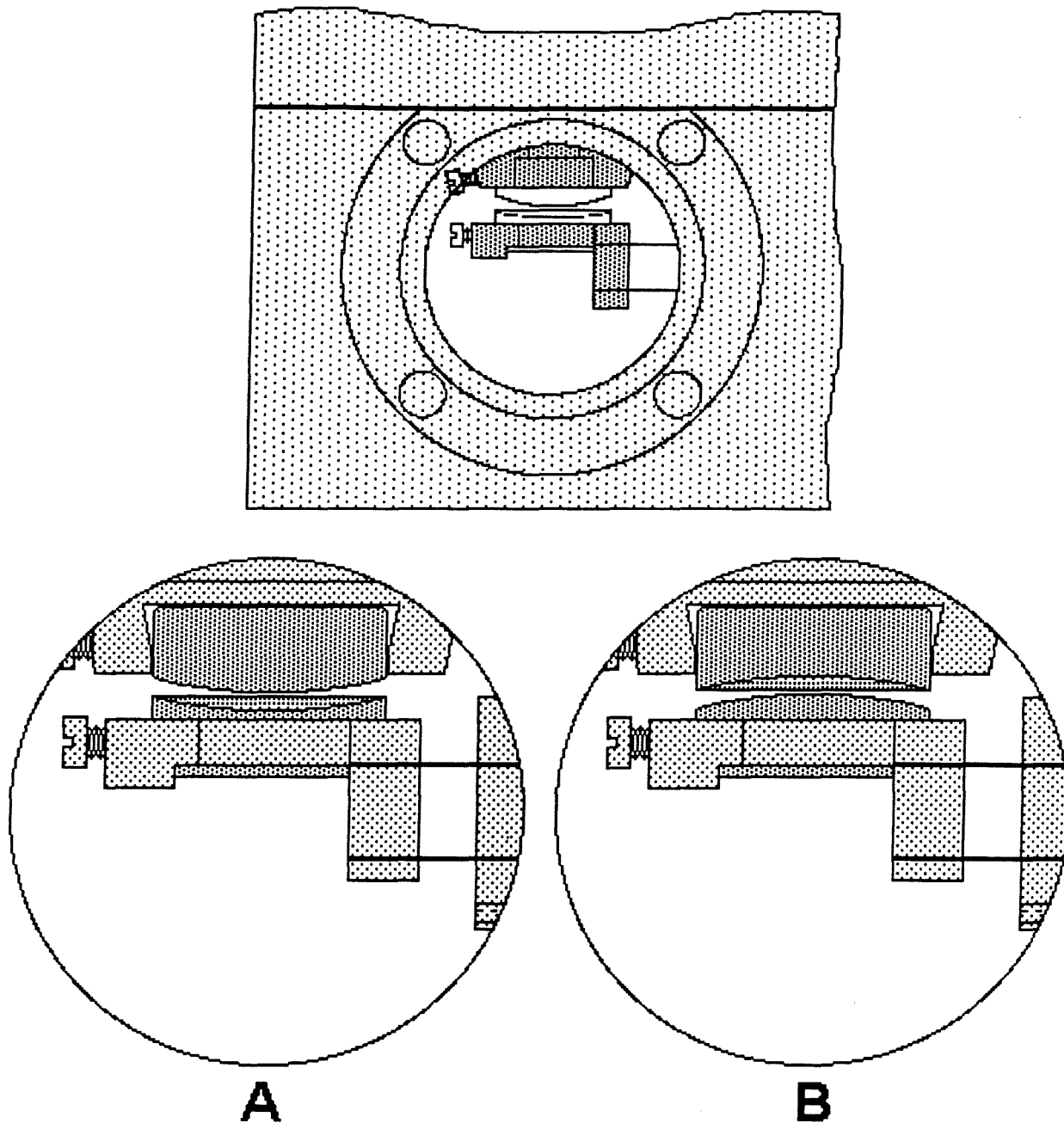


**Figure 37.** View through window of assembled Basic Unit after installation of the two disks (see also next page). Note that the disks may be positioned in two different ways, as shown above (angles other than 0 or 90° are also possible). In experiments involving frictional sliding this difference is important. For example, in geometry A the FECO fringes will remain centered in the field of view during in-out sliding of the upper surface but move during left-right sliding, whereas in geometry B they will move away from the centre during in-out sliding but remain fixed during left-right motion. The situation is different again when the lower surface is the one that moves, as occurs with the Bimorph Slider. One should avoid having the contact area that move away from the center of the eyepiece during sliding since this will complicate the accuracy of the optical measurements.

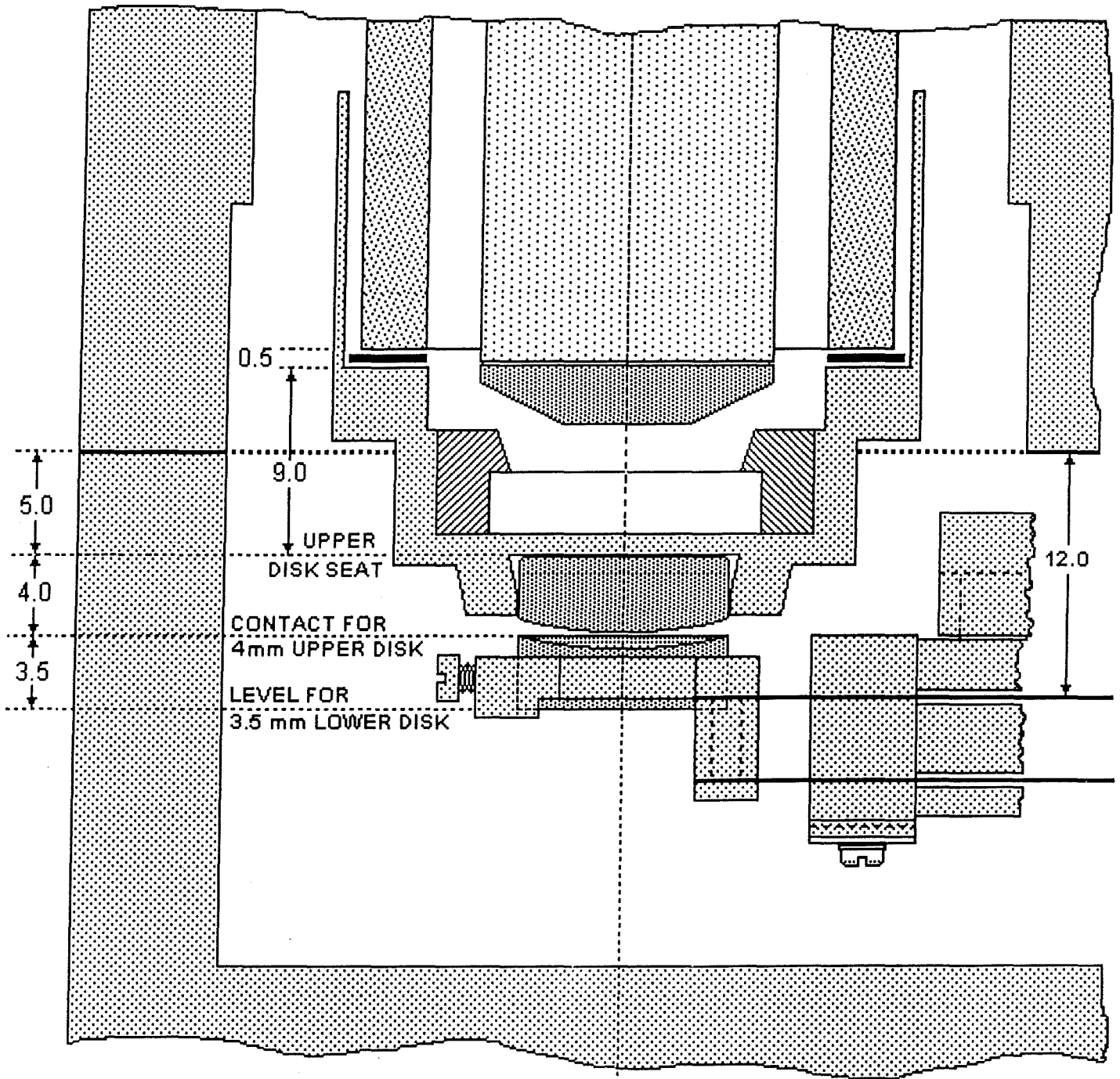


Figure 37C.

## **INITIAL OBSERVATION OF SURFACES WITH NEWTON'S RINGS**

Flush out chamber with dry, clean N<sub>2</sub> gas for 10–30 minutes via one of the filtered inlets and outlets as previously described.

Place apparatus on a table (preferably an anti-vibration table) and place sodium lamp under lower window. Place microscope tube with X5 or X10 objective through piezoelectric tube and place eyepiece on top. Bring lower surface close to upper surface ( $\ll 1$  mm) by rotating the coarse micrometer head by hand while viewing the approaching surfaces through the front plate window (a torch light beamed at the surfaces from one of the windows helps).

After moving the surfaces close together but not into contact, observe the Newton's rings. Loosen the two clamping screws, move and rotate the piezo mount and bring the surfaces closer together manually until the Newton's Rings appear clear and central (or near central) in the field of view, and circular (or near circular). Test for reversibility *with no backlash* of differential micrometer controls, Establish that, on bringing the surfaces *very* gently together, good contact occurs and that on separation an abrupt jump apart is seen. Good contact is seen by the sudden absence of vibrations, sharpened circular rings, and fixed radius of the Newton's rings when the load is further increased (unless the force-measuring spring stiffness is high). Separate the surfaces to about 1 mm (2 turns of the coarse micrometer) and carefully (without joggling the Piezo Mount or clamp 00080) tighten the two clamping screws on 00080 that will lock the piezo mount in place. Recheck contact and note the approximate contact position on the coarse micrometer head as well as by checking the disposition of the cantilever springs on part 01030.

Flush out the apparatus with dry Nitrogen gas for at least one hour (depending on how dry or inert an atmosphere is required) then close the Luer taps and/or plug up inlets and outlets with Luer caps.

Bring surfaces into contact once again and separate to ensure that all is well (still viewing them via the Newton's rings). Separate surfaces about 0.5 mm (one full turn of the coarse micrometer).

**Note:** One turn of the coarse micrometer head corresponds to 0.5 mm displacement of the surfaces. The differential (fine) micrometer head provides about 0.07 mm (70  $\mu$ m) per turn.

## **OBSERVATION OF SURFACES WITH FECO FRINGES and INITIAL MEASUREMENTS AND CALIBRATIONS**

Check that the mirror, when placed in position to direct the light beam into the apparatus, reflects the light beam vertically up and brings it into focus roughly where the surfaces will be. This can be tested with a piece of paper.

Place the three legs of the Base on the three kinematic mounts 03050 (A, B, C) previously fixed onto the experimental table (preferably an anti-vibration table) suitably positioned for FECO viewing with a spectrometer, as shown in Figure 2. The entry slit of the latter should be about 50 cm from the microscope tube (or prism) and about 30 cm above the table floor. Place the Optics Stand into position.

### **CONNECTING THE SFA3 TO THE CONTROL BOX (Figure 29)**

The Control Box provides access to the various electrically driven parts of the apparatus: the motors and piezoelectric elements for driving the surfaces together or laterally shearing them, the focusing microscope and prism turntable for optimizing the light beam from the apparatus to the spectrometer, and the heaters of the lower chamber.

All necessary electric cables for the Control Box have been supplied. Plug in the Control Box to a 3-pin power line outlet via the multi-terminal surge protector provided. Connect the optics stand cable to the OPTICS OUTPUT terminal at the back of the control box. Connect motor 1 to the MOTOR 1 OUTPUT terminal via the 2 m (6 ft) cable with the two 6-pin DIN plugs at either end (motor 2 is connected in the same way). Connect two cables from one of the independent outputs of a  $\pm 25\text{V}$  (or greater) dual or triple output DC power supply to the + and - INPUT terminals for MOTOR 1 (the inputs for motor 2 are connected in the same way to the second output of the power supply). Connect one end of the ENCODER cable to the ENCODER OUTPUT terminal and the other two ends to the two encoders for motors 1 and 2. Connect a  $\pm 5\text{V}$  or  $\pm 10\text{V}$  fixed DC power supply outputs (no ground) to the + and - PIEZO INPUT terminals using the two PIEZO cables. Connect the PIEZO OUTPUT terminal to a high voltage  $\pm\text{DC}$  amplifier (see Table 1) via a BNC-BNC cable and set the gain at X50 to X100 so that the piezo will receive a maximum of  $\pm 500\text{ V DC}$  under normal operations (the piezo can easily take  $\pm 1000\text{V}$  or more, but this can cause stress-induced drifts afterwards). Connect the amplifier output to the PIEZO MOUNT via the PIEZO cable (BNC-LEMO type). Connect Function Generator output to BIMORPH BNC INPUT using a BNC-BNC cable, and the BIMORPH BNC OUTPUT to the bimorph mini-coax connection on the apparatus via the

BIMORPH cable. Connect the HEATER cable to the Control Box through the dual banana plug HEATER OUTPUT. Connect the thermistor leads to a multimeter and set for resistance readings. Ground (earth) the base via the threaded hole at the front thin edge of the base plate.

Test all the Control Box switches, knobs, indicator lights, motors (Upper Chamber motor 1, Friction motor 2, prism turn-table and focus control sync. motors), bimorph and piezo voltage controls (coarse and fine), reversibility of all switches, etc.

Place mirror under lower window (it may already be there) and direct white light from tungsten-halogen or arc-lamp (see Table 1) vertically upward through the surfaces and focused on the surfaces (an I.R. filter or cold mirror is recommended for reducing heating due to the white light, this may be positioned just before or after the collimating lens). Look under the apparatus to see that the light beam is indeed entering the apparatus through the centre of the window. View surfaces with 10X eyepiece, moving the microscope tube so that the contact region is in the center of the field of view. Play with lamp focus (collimating lens), light angle, and the three mirror controls until light intensity is maximum. Bring surfaces very close together but not touching, as viewed through front window or from the known position of contact on the coarse micrometer head.

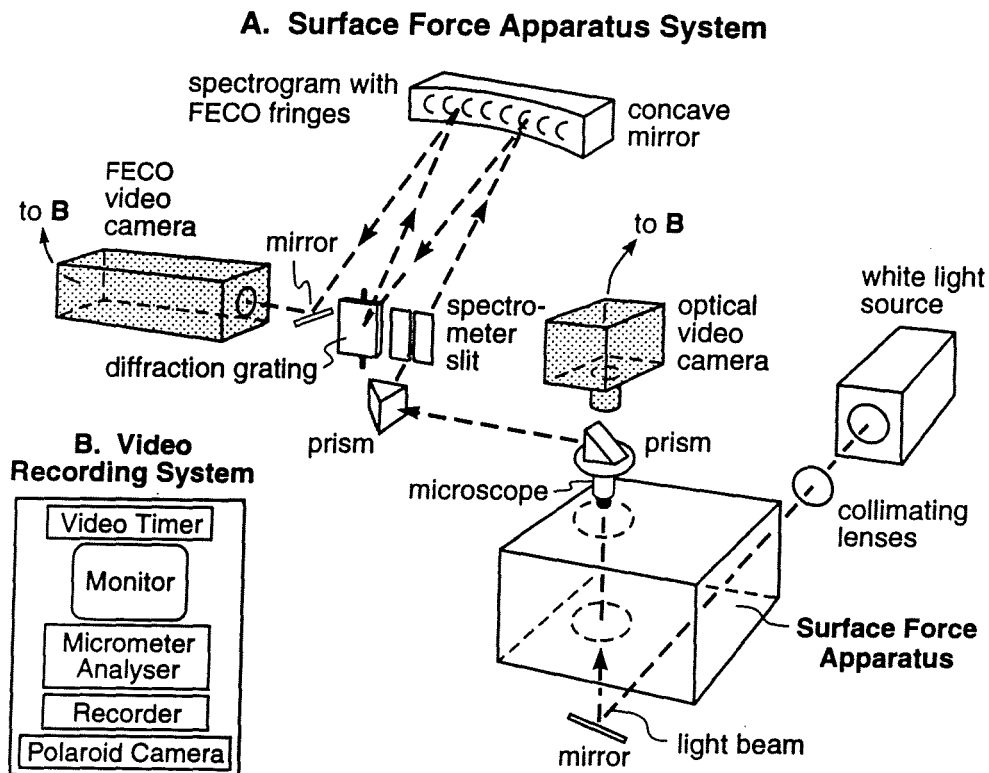


Figure 38. FECO optical system.

Replace eyepiece on turn-table by prism, darken room, focus and direct outcoming light onto spectrometer slit by adjusting the coarse focus, tilting the prism stage and rotating the turn-table. Observe FECO fringes in spectrometer exit eyepiece. When performed in air, vibrations will cause fringes to be very blurred. Mounting the apparatus on an anti-vibration table will greatly reduce this. These vibrations disappear almost totally when the box is filled with liquid, especially at surface separations below 2000 Å, so that an anti-vibration table is not essential for experiments in liquids at small separations. Vibrations also disappear in air once the surfaces come into adhesive contact.

Very gradually bring surfaces into contact. Once in contact finally adjust all the optics – lamp focus, mirror angles, prism turn-table control, prism tilt angle, microscope fine focus, slit width, etc. to make the fringes bright, sharp and as far to the *red-end* of the spectrum as possible (see Figure 43). Ensure that the contact remains flat on ‘scanning’ the surfaces by rotating the prism turn-table. Note whether alternate fringes have similar shapes over a wide spectral range (this establishes equality of the thickness of the two mica sheets).

Pick a suitable odd-shaped fringe (see Figure 39) and wavelength range (normally between the green and yellow mercury calibration lines) for measurements. Measure fringe contact positions, and mercury calibration lines. Take photos or record fringes on video, if required. Separate surfaces manually, slowly with the coarse and fine differential micrometer and note sudden and clean jump apart. Repeat contact-separation if necessary. Test for proper functioning and reversibility, with no backlash, of micrometer controls, DC motor, encoder readout and piezoelectric controls (although this is easier to do after the apparatus has been filled with liquid). Test that thermistor and heaters are working properly. Check that the apparatus is electrically earthed (grounded).

The OPTICS STAND has been designed specially for use with the surface forces apparatus. It has the following controls, which should also be tested:

- (i) Two focus controls: manual knob and motorized. Start each new experiment with fine control at the center of the total range – the dot should be positioned mid way between the two parallel lines.
- (ii) Two prism turn-table controls: manual for coarse and motorized for fine. Start each new experiment with the micrometer reading at about 5 mm. To manually rotate turn-table, first unscrew or ‘ease’ slotted screw on side of turn-table.
- (iii) Linear movement (manual screw).
- (iv) Rotation of stand about main pillar (manual).
- (v) Prism tilt angle control (vertical manual screw).

### **Addition of a second camera**

One can employ a second camera at the same time as looking at the FECO fringes by simply splitting the emerging beam by 90° using a normal 50-50 beam-splitter. The vertical (undeflected) beam can then be directed to a "top-view" camera, such as a CCD camera or fluorescence microscope, and the horizontal (deflected) beam is directed to the spectrometer, as in normal operations. For a description, with pictures, of how to combine normal optical microscopy with FECO interferometry see "Direct Visualization of Cavitation and Damage in Ultrathin Liquid Films", T. Kuhl, M. Ruths, Y-L. Chen, J. Israelachvili, *Journal of Heart Valve Disease* 3 (1994) S117-S127.

---

## **FILLING THE SFA CHAMBER WITH LIQUID**

---

It is recommended that the chamber be filled from a 75–100 ml gas-tight syringe (the total internal volume is about 75 ml, but this depends on which attachment is installed). Aqueous solutions should be de-aerated well before filling with a suction pump or vacuum for ~1 hour. An inert material such as a piece of Teflon may be placed inside the liquid during de-aeration to aid the nucleation of bubbles. Once the liquid is ready, it should be placed in the experimental room together with the apparatus for some hours to allow both to reach the same temperature; this will reduce thermal drifts of the surfaces after filling. The room itself should be thermostatted at the desired temperature of the experiment ( $\pm 0.1^\circ\text{C}$ ) a few hours before starting. Before filling, the chamber should be flushed out (purged) with a gentle stream of clean, dry  $\text{N}_2$  gas through one of the inlets (open other outlet). This is always advisable, especially prior to experiments with nonaqueous liquids where trace amounts of water could prove detrimental. The surfaces should be  $<0.1$  mm apart during the flushing (close enough to keep particles from settling on them) which should continue for about 1 hour. The chamber is now ready for filling with liquid through the right inlet on the lower chamber.

Separate surfaces about 0.25 mm and tilt apparatus on hinge 02060 so that on filling, the liquid will rise vertically past the surfaces (a supporting block may have to be inserted under the apparatus to keep it upright). Open air-outlet tap. Remove inlet Luer cap or open stop-cock and attach syringe or Teflon feed tube from filling flask. Inject liquid slowly, holding syringe and apparatus steady with both hands. The liquid surface may also be aspirated during filling through the syringe port to remove any surface-active matter before the liquid surface passes across the surfaces (this should be done inside the Laminar flow cabinet and preferably by a second person). Close syringe port (if open) and bring apparatus down onto base. Liquid level

should be above upper disk surface, as viewed through window. If all 'looks good', close or plug inlet and outlet ports. Manually bring surfaces closer together but not yet into contact.

Check that there are no leaks by noting that the liquid level does not drop over time (every few hours).

## GENERAL OPERATING PROCEDURES

Manually bring surfaces to within a few microns separation using the coarse and fine (differential) micrometer heads. The fine head should be close to the mid-point of its travel range. Observe the FECO fringes in the spectrometer or video monitor, and optimize the optics (focus, mirror angles, mercury calibration lines, prisms, etc.). Fully tighten the coarse micrometer nut making sure that the surfaces are not forced into contact. From now on, only the differential (fine) micrometer, the differential spring micrometer (motor 1) and the piezo crystal controls will be used. Move surfaces closer together and test all three distance controls for smoothness and absence of backlash and drift (thermal drifts may take one hour or more to die down after filling the chamber - longer if the liquid and/or apparatus are initially at a different temperature from the room temperature, which should be thermostatically controlled to  $\pm 0.1^\circ\text{C}$ ).

Measure forces, record fringes, etc., as described below.

The range of operation of the differential micrometer is  $\pm 3$  mm (coarse) and  $\pm 1$  mm (fine). The fine movement is reduced by a factor of about 8 between the surfaces.

The range of operation of motor 1 is 10.5 mm. This movement reduced by a factor of about 1,000 between the surfaces (i.e., 1  $\mu\text{m}$  movement results in a  $10\text{\AA}$  displacement of the spring supporting the lower surface). However, other helical springs with higher or lower spring rates (stiffnesses) can be used instead of the standard one 01310, which will result in a lower or higher 'gearing ratio' of the differential spring control (note: using *stiffer* helical springs is not recommended).

For changing the concentration of electrolyte, surfactant or polymer in the liquid, keep surfaces  $\lesssim 1$   $\mu\text{m}$  apart (not more). Open air-outlet (with filter attached). Remove some liquid through liquid inlet on front-plate and close, always ensuring that the level stays above the mica surfaces. Slowly inject new solution through syringe inlet ensuring that no bubbles are injected. Mix contents by inwards and outwards movements of syringe. Close air-outlet tap. Allow to settle for 10–30 minutes. Rapidly separate surfaces with coarse micrometer to 1–2

mm and bring them back again, repeating a few times – the final motion being in the 'in' direction. Now allow surfaces to equilibrate with the solution at a separation of a few  $\mu\text{m}$ , though for polymer solutions a much larger separation of 1–2 mm may be required.

The above procedure minimizes the probability that any impurity particles coming in with the injected liquid will settle on the surfaces, while ensuring that the solution is properly mixed.

If a particle does come between the surfaces this is readily apparent from the way the surfaces abruptly stop approaching each other at some finite (usually large) separation, and distort, as readily seen on the fringes. On other occasions a large steeply repulsive force may be measured close in which is clearly not the force that is being investigated. When this happens it is best to look for a new position of the two surfaces as follows: separate the surfaces, then loosen the two clamping screws on 00080. Replace the prism with the eyepiece and focus the microscope tube so that you can see the contact region. As you look down onto the surfaces, move the piezoelectric mount 05010 in both z and y directions to ensure that both the upper and lower surfaces have moved to a new 'contact' area. Reclamp and proceed as before. At each contact position, measure the radii of curvature of the surfaces from the FECO fringes in two perpendicular directions, using a rotating DOVE prism.

At the end of an experiment, disconnect leads (motor, piezo, friction or bimorph attachment, ground). Carefully lift off upper part of Optics Stand without moving the base (see \* below). Switch off white light and mercury lamps. Remove apparatus and place in laminar flow cabinet. Attach Teflon feed tube to liquid inlet and drain chamber, tilting the box if necessary, with air outlet open and filter removed.

Calibrate the spring 04120 with weights and a traveling microscope or vernier eyepiece. One calibration should be enough – all subsequent values should be the same if the spring is clamped in the same way each time. However, if the spring is exchanged or the unit is disassembled, or if the clamping screw has been adjusted, it should be recalibrated.

Calibrate the lateral magnification of the microscope, as seen in the spectrometer, as follows: First, return the microscope tube to the same vertical position it had in the experiment (see \* above). Then, place a graticule where the mica surfaces were. Focus and view the graticule markings (as dark horizontal lines) on the spectrometer entrance slit and view them in the exit eyepiece. Repeat for the perpendicular magnification with the graticule rotated by  $90^\circ$  and the beam rotated by  $90^\circ$  using the DOVE prism. Again, one calibration for the normal and perpendicular magnifications should suffice if the apparatus and microscope stand are positioned in the same way each time (relative to the spectrometer).

If the chamber is to be used again soon with a similar liquid, there is no need to dismantle the apparatus after an experiment: fill with ethanol and drain; refill with ethanol and leave overnight. You may replace the piezo mount with the special thick round glass disk supplied for this purpose. Drain and aspirate out alcohol and pass dry N<sub>2</sub> gas for a few hours. Never dry the inside walls by 'wicking' with filter paper, aspirate or blow dry only. When leaving the apparatus for a long time, relieve some of the pressure on the O-rings.

Alternatively, dismantle all parts that come into contact with liquid and place in an ethanol bath; cover bath, and keep until needed again. Most O-rings need not be removed, but they should be changed once they have flattened too much after many experiments (this occurs more often with the smaller, thinner O-rings). The inlet and outlet windows are permanently press fitted into place and should never need replacing unless a leak develops.

Loosen or disconnect microscope belts when not in use for a long time.

## **DISTANCE MEASUREMENTS WITH FECO FRINGES**

### **Unique features of the SFA-FECO force-measurement technique**

The SFA technique for measuring forces, when used together with the FECO optical technique for visualizing two surfaces, allows for the unambiguous measurements of the following parameters that cannot be independently measured by any other combination of techniques: (i) simultaneous measurement of the static and dynamic forces, both normal and lateral, between two surfaces, (ii) independent measurement of the separation between the two surfaces at their point of closest approach at any time during the approach, separation or shearing of two surfaces, (iii) quantitative visualization of the local surface geometry and how it changes or evolves with time, for example, due to force-induced elastic deformations or damage during an interaction or during frictional sliding, and (iv) the ability to visualize contamination, trapped particles and cavitation in thin films between the surfaces from the deformed shapes of the FECO fringes in combination with refractive index measurements.

---

The limits of resolution of FECO fringes using modern optical techniques make it possible to measure film thicknesses to better than 1 Å (using, for example, a 32 Å/mm spectrometer), and this sets the effective limit to which distances (and refractive indices) may be measured by the method.

But to achieve this degree of accuracy, careful attention must be paid to the collimation and alignment of the light – the light must pass normally through the surfaces.

FECO fringe patterns are normally observed using a spectrometer. The microscope focuses the light emerging from the surfaces onto the spectrometer slit (ideally, the light must enter the slit at exactly 90°), and the fringes appear as a series of bright colored fringes in the spectrogram. The *lateral* magnification is, therefore, no better than that of the microscope used and, in practice, rarely exceeds 500. In any case, there is a theoretical limit to the *lateral* resolution that is possible, and is of the order of a wavelength of light.

The experimental conditions needed to obtain optimum results with multiple beam interferometry using "Fringes of Equal Chromatic Order" (FECO), have been described by S. Tolansky in *Multiple Beam Interferometry of Surfaces and Films*, Oxford University Press, 1948, and *An Introduction to Interferometry*, Longmans, Green & Co., London, 1955. The theory and use of FECO interferometry in surface studies has been described by Israelachvili in *J. Colloid & Interface Sci.* **44**, 259 (1973), and Horn, Israelachvili & Pribac in *J. Colloid and Interface Sci.* **115**, 480 (1987). For a review of modern deposition techniques, see Hass, Heaney & Hunter in *Physics of Thin Films* **12**, 1 (1982).

### Introduction to FECO interferometry

If two back silvered sheets of mica or other transparent material are in contact, and if white light is passed normally through them, the emerging light consists of discrete wavelengths  $\lambda_n^0$  ( $n = 1, 2, 3, \dots$ ) which can be separated and measured as sharp fringes (FECO) in an ordinary grating spectrometer. If the two sheets have the same thickness,  $T$ , and if the surfaces are then separated by a distance  $D$ , these fringes shift to longer wavelengths  $\lambda_n^D$  given by

$$\tan(2\pi\mu D / \lambda_n^D) = \frac{2\bar{\mu} \sin \left[ \frac{1 - \lambda_n^0 / \lambda_n^D}{1 - \lambda_n^0 / \lambda_{n-1}^0} \pi \right]}{(1 + \bar{\mu}^2) \cos \left[ \frac{1 - \lambda_n^0 / \lambda_n^D}{1 - \lambda_n^0 / \lambda_{n-1}^0} \pi \right] \pm (\bar{\mu}^2 - 1)} \quad (1)$$

where + refers to odd order fringes ( $n$  odd), and – refers to even order fringes ( $n$  even).  $\bar{\mu} = \mu_{\text{mica}} / \mu$ , where  $\mu_{\text{mica}}$  is the refractive index of mica at  $\lambda_n^D$ , and  $\mu$  is the refractive index of the medium between the two mica surfaces at  $\lambda_n^D$ . For separations less than 300Å, the above equation simplifies to the following two approximate equations

$$D = \frac{n F_w (\lambda_n^D - \lambda_n^0)}{2\mu_{\text{mica}}} \quad \text{for } n \text{ odd (positive sign in Eq. 1)} \quad (1a)$$

$$D = \frac{n F_n (\lambda_n^D - \lambda_n^0) \mu_{\text{mica}}}{2\mu^2} \quad \text{for } n \text{ even (negative sign in Eq. 1)} \quad (1b)$$

where  $(n)F_n = \frac{\lambda_{n-1}^0}{(\lambda_{n-1}^0 - \lambda_n^0)}$  (1c)

*check w/ Tonya, it's there in examples*

from which the refractive index can be calculated from

$$\mu = \left( \frac{(\lambda_{n-1}^D - \lambda_{n-1}^0)(n-1)F_{n-1}}{(\lambda_n^D - \lambda_n^0)nF_n} \right)^{1/2} \mu_{\text{mica}} \quad (1d)$$

which requires a simultaneously measurement of  $\lambda_n^D$  and  $\lambda_{n-1}^D$ .

By use of the above equations both the distance  $D$  and the medium refractive index  $\mu$  can be determined independently by measuring the shifts in wavelengths of an odd and adjacent even fringe. The accuracy is about  $\pm 0.1$  nm for measurements of  $D$  in the range 0–200 nm, while for  $\mu$  it is better than 1% at large  $D$  but is less accurate as  $D$  falls below 10 nm. To use the above equation we only require an accurate prior determination of the refractive index of the mica. The refractive index and dispersion of mica can be measured with an Abbé Refractometer using Hg and Na light.<sup>†</sup> The accuracy is  $\pm 0.0002$  – more than adequate for most purposes. Mica is birefringent, so that each fringe appears as a doublet – its exact location in the spectrum being determined by the refractive indices of the two components, known as the  $\gamma$  and  $\beta$  components. Typical values for the refractive indices, which vary from mica to mica, are

$$\left. \begin{aligned} \mu_\gamma &= 1.5846 + 4.76 \times 10^5 / \lambda^2 (\text{\AA}) \\ \mu_\beta &= 1.5794 + 4.76 \times 10^5 / \lambda^2 (\text{\AA}) \end{aligned} \right\} \mu_{\text{mean}} = 1.5820 + 4.76 \times 10^5 / \lambda^2 (\text{\AA}) \quad (2)$$

for red or brownish micas, and

$$\left. \begin{aligned} \mu_\gamma &= 1.5953 + 4.76 \times 10^5 / \lambda^2 (\text{\AA}) \\ \mu_\beta &= 1.5907 + 4.76 \times 10^5 / \lambda^2 (\text{\AA}) \end{aligned} \right\} \mu_{\text{mean}} = 1.5930 + 4.76 \times 10^5 / \lambda^2 (\text{\AA}) \quad (2)$$

<sup>†</sup> Because mica is birefringent, these measurements can be tricky and require that the rectangular or square mica sheet used in the refractometer have its edges cut parallel to the two optic axes (this can be established with crossed polaroids) and polished flat. Two measurements are made at each wavelength (e.g., Hg and Na), with each axis respectively parallel and perpendicular to the light, which give the  $\gamma$  and  $\beta$  components at that wavelength.

for greenish micas. These values correspond to a birefringence of  $\Delta\mu = \mu_\gamma - \mu_\beta = 1.5846 - 1.5794 = 0.0052$  for brownish micas, and  $\Delta\mu = 1.5953 - 1.5907 = 0.0046$  for greenish micas. When two equally thick mica sheets are in contact, the resulting fringes will have an 'effective' birefringence (Figure 39) given by

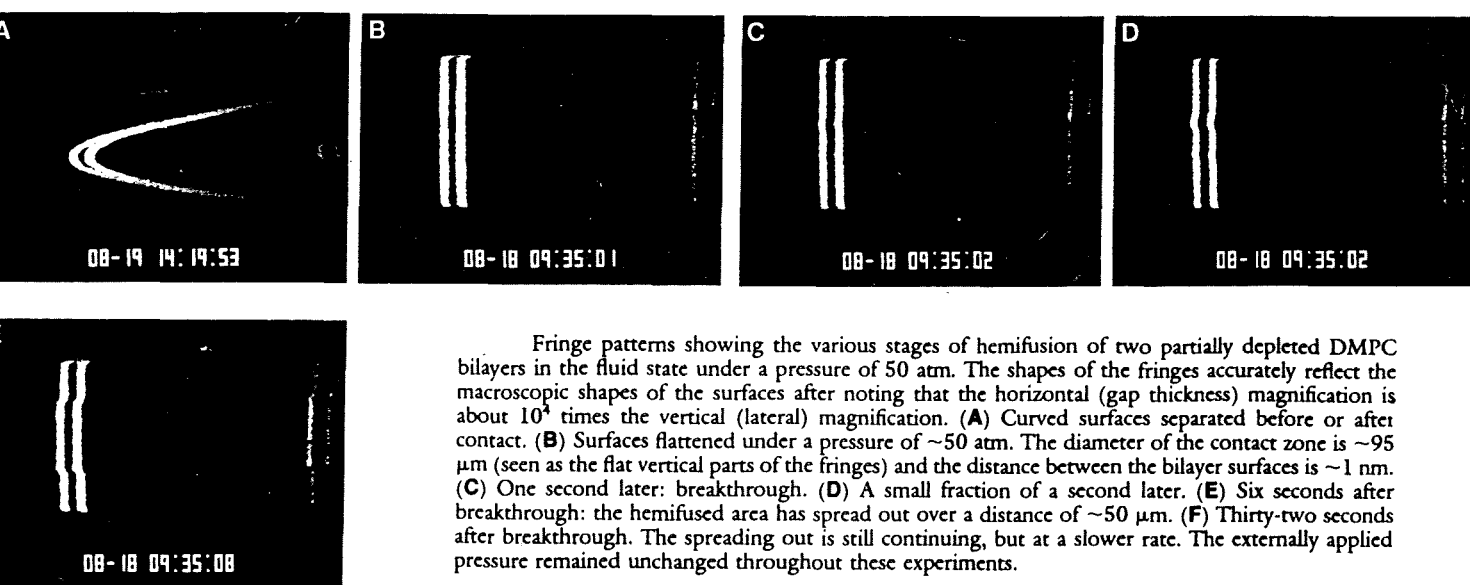
$$\Delta\mu_\theta = \Delta\mu \cos\theta \quad (3)$$

where  $\Delta\mu$  is the intrinsic, or maximum, birefringence of the sheet material, obtained for a single sheet or for two perfectly aligned sheets (as given above), and where  $\theta$  is the 'twist' angle between the crystallographic axes of two misaligned sheets (see example below). When the effective birefringence is less than the maximum, the refractive index of the  $\beta$  and  $\gamma$  components is then given by

$$\begin{aligned} \mu_\gamma &= \mu_{\text{mean}} + \frac{1}{2}\Delta\mu_\theta && \text{for the } \gamma\text{-components} \\ \text{and} \quad \mu_\beta &= \mu_{\text{mean}} - \frac{1}{2}\Delta\mu_\theta && \text{for the } \beta\text{-components} \end{aligned} \quad (4)$$

which are the values that must be used in Equation 1.

As an example of the use of Equation 1, consider an experiment where the contact wavelengths of the  $\beta$  and  $\gamma$  components of three adjacent fringes,  $\lambda_n^0$ ,  $\lambda_{n-1}^0$  and  $\lambda_{n-2}^0$ , are measured and found to be as given in the upper set of boxes in Figure 39. After separating the surfaces, the positions of the curved tips of the  $n$  and  $(n-1)$  order fringes are measured and the corresponding wavelengths,  $\lambda_n^D$  and  $\lambda_{n-1}^D$ , are given in the lower set of boxes in Figure 39.



Fringe patterns showing the various stages of hemifusion of two partially depleted DMPC bilayers in the fluid state under a pressure of 50 atm. The shapes of the fringes accurately reflect the macroscopic shapes of the surfaces after noting that the horizontal (gap thickness) magnification is about  $10^4$  times the vertical (lateral) magnification. (A) Curved surfaces separated before or after contact. (B) Surfaces flattened under a pressure of ~50 atm. The diameter of the contact zone is ~95  $\mu\text{m}$  (seen as the flat vertical parts of the fringes) and the distance between the bilayer surfaces is ~1 nm. (C) One second later: breakthrough. (D) A small fraction of a second later. (E) Six seconds after breakthrough: the hemifused area has spread out over a distance of ~50  $\mu\text{m}$ . (F) Thirty-two seconds after breakthrough. The spreading out is still continuing, but at a slower rate. The externally applied pressure remained unchanged throughout these experiments.

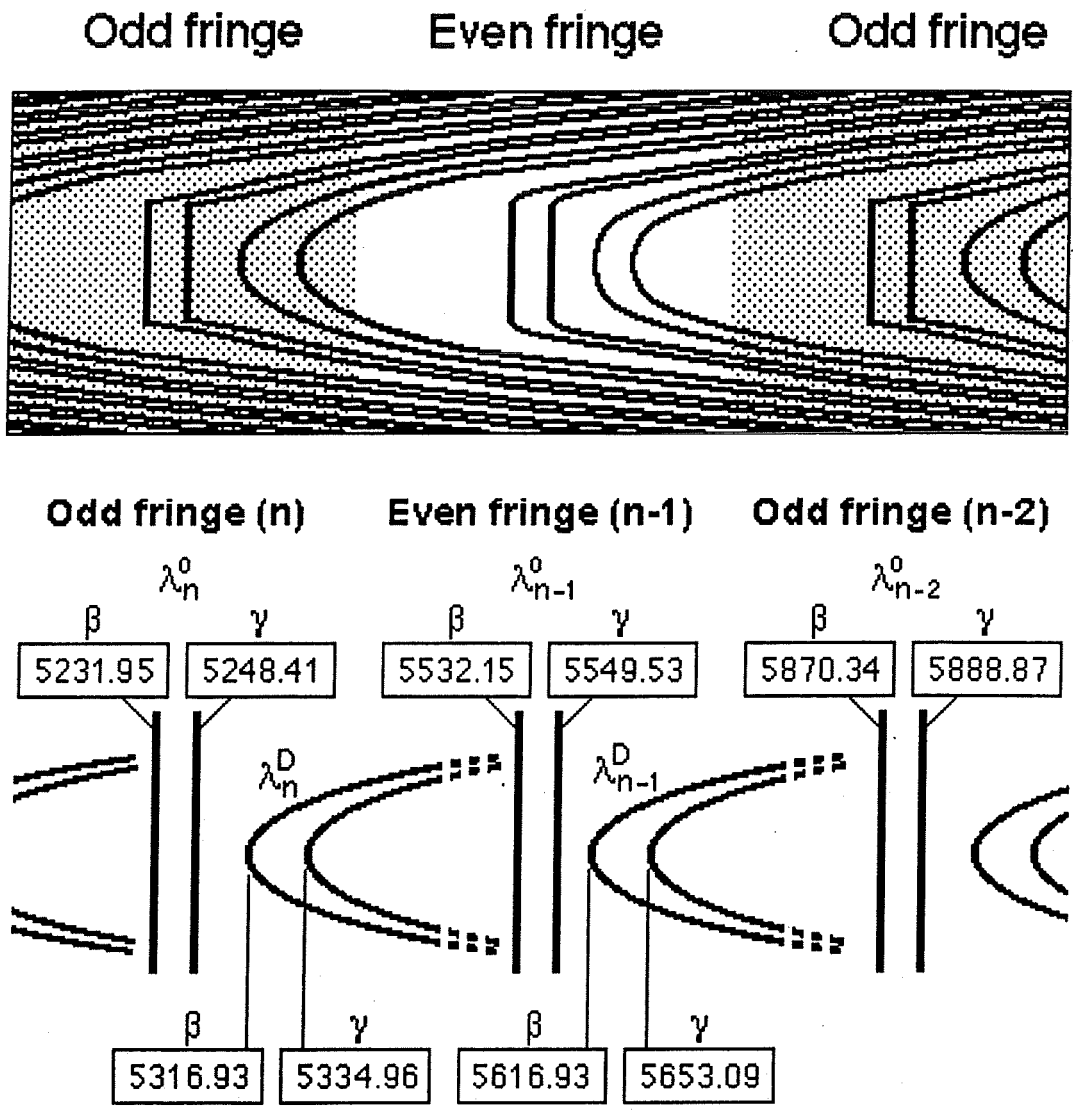
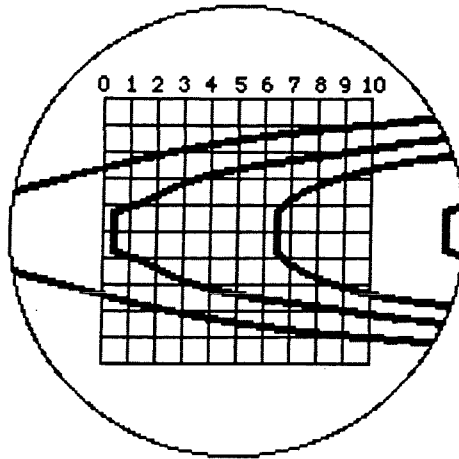


**Figure 39.** Numerical example of analysis of FECO fringe patterns. To measure the positions of the flat or curved tips of fringes, it is recommended that the movable eyepiece on the spectrometer exit have a graticule placed in the focal plane with a 10 X 10 grid of vertical and horizontal lines 1 mm apart, as shown below and in Figure 40.



The effective birefringence of two mica sheets in contact can be calculated from the contact wavelengths at  $\lambda$  according to

$$\Delta\mu_{\theta} \approx \frac{(\lambda_{\gamma}^0 - \lambda_{\beta}^0)\mu_{\text{mica}}}{\lambda} \quad (5)$$

which for the above values gives  $\Delta\mu_{\theta} \approx 1.60 \times (5248.41 - 5231.95) / 5240 = 0.0050$ . For this brownish mica  $\Delta\mu \approx 0.0052$ , which implies that  $\theta \approx 0$ , i.e., that the two sheets are well aligned. From Equations 2–5, the refractive indices of the  $\gamma$  and  $\beta$  components at different wavelengths are therefore:  $\mu_{\gamma} = 1.5845 + 4.76 \times 10^5 / \lambda^2 (\text{\AA})$  and  $\mu_{\beta} = 1.5795 + 4.76 \times 10^5 / \lambda^2 (\text{\AA})$ . Using these values, Equation 1 can be solved simultaneously for the pair of adjacent odd ( $n$ ) and even fringes ( $n-1$ ) – independent solutions being obtained for the  $\gamma$  and  $\beta$  components – to give

for the  $\beta$ -component:  $D = 493 \pm 1 \text{ \AA}$ ,  $\mu_{\text{medium}} = 1.540$ ,

for the  $\gamma$ -component:  $D = 493 \pm 1 \text{ \AA}$ ,  $\mu_{\text{medium}} = 1.717$ .

The above values were measured in an experiment across a thin film of the birefringent liquid crystal 5CB whose bulk refractive index components are very close to the above two values.

Normally, however,  $\mu_{\text{medium}}$  is known and the intervening liquid is not birefringent, so that Equation (1) can be solved directly for one fringe only (normally the  $\beta$ -component of an odd fringe) without iteration for odd and even fringes or simultaneous measurements of  $\beta$  and  $\gamma$  fringes.

The method for measuring  $D$  described above is recommended for distances up to 5,000–10,000  $\text{\AA}$  (but can be used at all distances). For larger separations, above about 10,000  $\text{\AA}$ , we

may note that on bringing the surfaces into contact, and counting the number of fringes that have to pass the contact wavelength  $\lambda_n^0$  in the process, one can readily obtain the separation: each time a fringe passes  $\lambda_n^0$ , the distance moved until the next fringe passes  $\lambda_n^0$  is exactly  $\lambda_n^0/2\mu$  where  $\mu$  is the refractive index of the medium (liquid, vapor) between the surfaces. Thus if ~9.3 fringes are moved until contact, the original separation is therefore  $9.3 \lambda_n^0/2\mu$ . This method is not exact, but is rapid and accurate to at least 1%.

The following formula gives the exact surface separation for an arbitrary fringe shift and requires only that the contact positions ( $\lambda_n^0, \lambda_{n-1}^0$ ) of two adjacent (odd and even) fringes be measured: At some large surface separation where two adjacent fringes of unknown order  $p$  and  $p-1$  having wavelengths  $\lambda_p$  and  $\lambda_{p-1}$  are situated between  $\lambda_n^0$  and  $\lambda_{n-1}^0$  (i.e.,  $\lambda_n^0 < \lambda_p < \lambda_{p-1} < \lambda_{n-1}^0$ ) the surface separation  $D$  is given by

$$D = \frac{\lambda_p \lambda_{p-1}}{2\mu(\lambda_{p-1} - \lambda_p)} + \frac{\lambda_{p-1} T_p}{\lambda_{p-1} - \lambda_p} - \frac{\lambda_p T_{p-1}}{\lambda_{p-1} - \lambda_p}$$

$$= \frac{1}{(\lambda_{p-1} - \lambda_p)} \left[ \frac{\lambda_p \lambda_{p-1}}{2\mu} + \lambda_{p-1} T_p - \lambda_p T_{p-1} \right] \quad (6)$$

where  $T_p$  and  $T_{p-1}$  are the distances calculated assuming that  $\lambda_p$  and  $\lambda_{p-1}$  have shifted from  $\lambda_n^0$ , i.e., by using  $\lambda_p$  and  $\lambda_{p-1}$  for  $\lambda_n$  in Equation (1). If  $\lambda_p = \lambda_n^0$ , then  $T_p = 0$  and the above equation simplifies to

$$D = \frac{1}{(\lambda_{p-1} - \lambda_p)} \left[ \frac{\lambda_p \lambda_{p-1}}{2\mu} - T_{p-1} \lambda_p \right] \quad (7)$$

For very large separations, above 10  $\mu\text{m}$  and out to hundreds of microns, a third method of distance measurement becomes more practicable whose accuracy is of the order of 1%. At such large separations the FECO fringes are very close together. If the wavelengths of any two adjacent fringes are measured as  $\lambda_p$  and  $\lambda_{p-1}$  then the separation of the surfaces is given by

$$D = \left[ \frac{\lambda_p \lambda_{p-1}}{\lambda_{p-1} - \lambda_p} - \frac{\lambda_n^0 \lambda_{n-1}^0}{\lambda_{n-1}^0 - \lambda_n^0} \right] / 2\mu \quad (8)$$

where  $\lambda_n^0, \lambda_{n-1}^0$  are the wavelengths of any two adjacent fringes at contact, and  $\mu$  is the refractive index of the medium, as above. (Values of  $\lambda_p$  and  $\lambda_{p-1}$  may be obtained more

accurately by averaging over a number of, say, ten fringes in the field of view.) The derivation of the above formula is straightforward, viz.

$$2 \frac{\lambda_p \lambda_{p-1}}{(\lambda_{p-1} - \lambda_p)} = 2T\mu_{\text{mica}} + D_{\text{medium}} \quad (9)$$

where T is the (single) mica sheet thickness, given by

$$2T\mu_{\text{mica}} = \frac{\lambda_n^0 \lambda_{n-1}^0}{2(\lambda_{n-1}^0 - \lambda_n^0)} \quad (9a)$$

### Some useful hints and rules of thumb

(1) When using a grating with a dispersion of about 32Å/mm (the standard value) the thickness of the mica *in microns* may be quickly estimated from the spacing between adjacent contact fringes as measured in the eyepiece *in millimeters* (see Figure 40a): thickness (μm) = 14/spacing (mm). Thus, a spacing of 7 mm between fringes means that the mica is about 2 μm thick.

(2) When looking into the eyepiece before two surfaces are far from contact, a series of faint vertical bands (cos<sup>2</sup> fringes) will be seen. When final contact occurs, the odd fringes will be at the centers of the dark regions, and the even fringes will be at the centers of the bright regions.

(3) When two surfaces are brought towards each other from a large distance, very time a fringe passes a contact wavelength, say λ<sub>n</sub><sup>0</sup>, the surfaces will have been moved by λ<sub>n</sub><sup>0</sup>/2μ<sub>medium</sub>, which for typical values of λ<sub>n</sub><sup>0</sup> ≈ 5,500Å and μ ≈ 1.33 (water) means a displacement of about 2,000 Å.

### Additional notes

Note that the optical method for measuring the surface separation actually measures the distance between the two outer silvered layers on the far sides of the mica sheets. For sheets having a typical thickness of T=2.5 μm, one can verify that no error greater than ±0.1 nm in the surface separation is caused by normal temperature variations (±0.5°C) and applied pressures of the experiments (unless these are higher than a few hundred atmospheres, which can be directly measured using the Hertz or JKR theories). For temperature variations above about 1°C, a correction to 2T has to be made. The thermal expansion of mica is (9–12) 10<sup>-6</sup>/°C; thus, for example, a 10°C rise in temperature of the liquid will expand the composite mica sheets (2T) by ~ 6 Å if 2T = 6 μm. However, since μ also increases with temperature, the *apparent* increase in T, as measured by an odd fringe, is about twice this value. It is recommended that the effect of temperature on the contact fringe positions be simply calibrated before or after an experiment

with two mica sheets in contact. This allows one to establish what correction is required for  $D=0$  in a force measurements at different temperatures using the same type of mica.

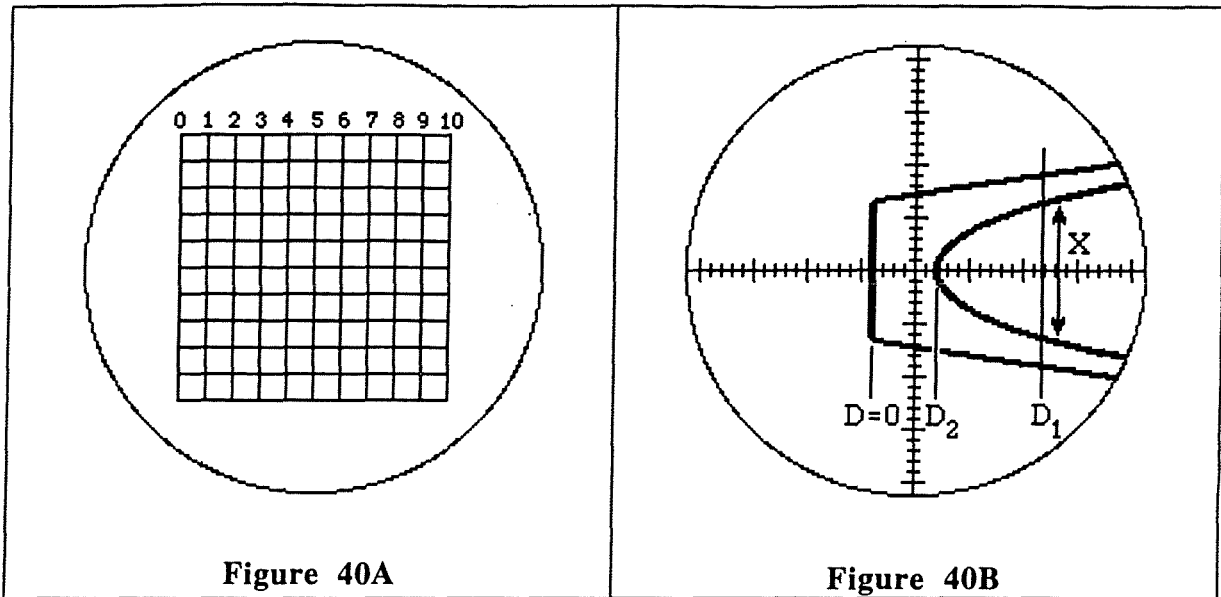
During force measuring experiments it is advisable to periodically check and readjust the position of the Hg (or other) calibration lines in the spectrometer, since temperature drifts in the room can cause the spectrometer to expand and slightly move the Hg line with time. This is particularly important when measurements requiring accuracy at the sub-ångstrom level are being carried out.

---

## OTHER MEASUREMENTS AND OBSERVATIONS WITH FECO FRINGES

---

FECO interferometry is a powerful technique for measuring not only surface separations but also a host of other surface and thin-film phenomena both at equilibrium (static measurements) and as a function of real time (dynamic measurements). All that is required is a good 1/2 metre grating spectrometer (a 1/4 m can be just as good) with a grating of dispersion  $32\text{\AA}/\text{mm}$  that has been calibrated for both normal and lateral magnification (spare gratings having half and/or twice the nominal dispersion may sometimes be useful for certain types of measurements). A wide-field focusing eyepiece (see Table 1) should be attached at the exit slit, supported on a translation stage that can be moved laterally across the focal plane of the spectrogram over a distance of about 20 mm. An encoder readout on the translation stage allows lateral distance measurements to be later transformed into wavelengths. The eyepiece should have a 10 mm X 10 mm grid in the focal plane (Figure 39 and 40A), although other interchangeable eyepieces with different graticules may sometimes be more useful, such as one with a simple cross-wire or a cross-wire with 0.1 or 0.2 mm graduations on the vertical line (for measuring the length of the flat parts of FECO fringes which give the contact area, as illustrated in Figure 40B). For dynamic measurements, an SIT video camera with monitor, recorder and video analyzer may be attached to the second exit port (camera port) on the spectrometer. This, and other optical accessories that are required or are optional for dynamic optical measurements are listed in Table 1.



### Measuring surface radii (refer to Figure 40B)

The local radius of curvature in one direction  $R_{||}$  may be obtained from the shape of the FECO fringes. Measure the two distances  $D_1$  and  $D_2$ , as well as the lateral distance  $X$  on any one fringe. If the spectrometer-microscope magnification factor is  $f$ , the radius  $R_{||}$  is given by

$$R_{||} = \frac{(X/f)^2}{8(D_1 - D_2)} \quad (10)$$

The mean radius of curvature is given by  $\bar{R} = \sqrt{R_{||}R_{\perp}}$ , where  $R_{\perp}$  is the radius measured perpendicular to  $R_{||}$  using a DOVE prism.

### Bibliography

The following references provide useful examples of how FECO interferometry can be used to measure surface shapes and deformations, and other surface phenomena (cf. Figure 41).

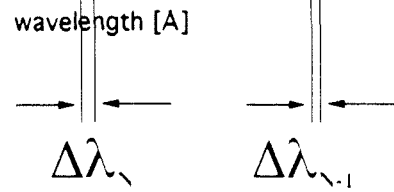
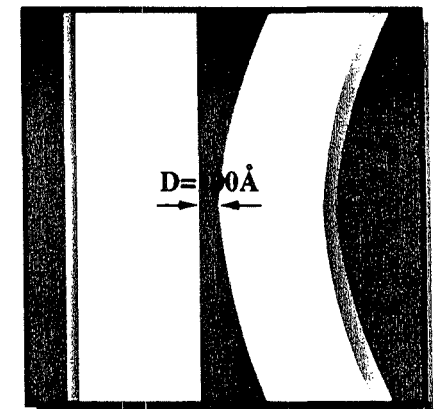
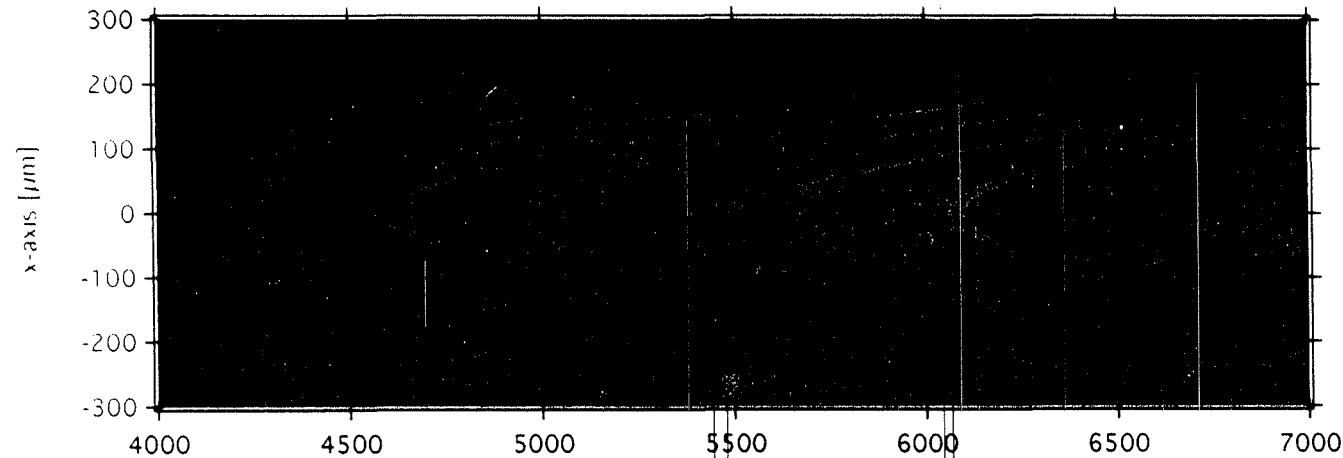
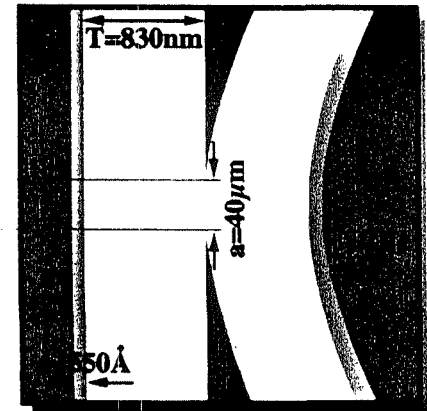
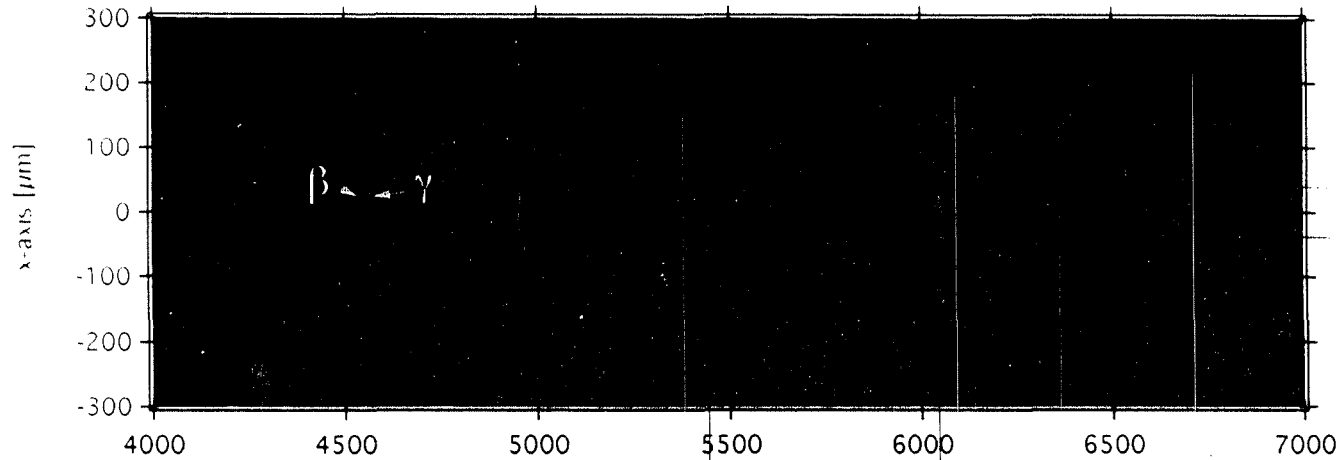
#### General papers

- *Thin Film Studies Using Multiple Beam Interferometry.*, J. N. Israelachvili, *J. Colloid Interface Sci.* **44** (1973) 259-272.
- *Multiple-beam interferometry with thin metal films and unsymmetrical systems.* M. T. Clarkson, *J. Phys. D* **30** (1989) 475-482.
- *Analytic solution for the three-layer multiple beam interferometer.* Roger Horn and Douglas Smith, *Applied Optics* **30** (1991) 59-65.

#### Surface shape analysis (topology)

- *Measurement of the Deformation and Adhesion of Solids in Contact* R. G. Horn, J. Israelachvili, F. Pribac, *J. Colloid & Interface Sci.* **115** (1987) 480-492.
- *Topographic information from multiple beam interferometry in the Surface Forces Apparatus.* M. Heuberger, G. Luengo and J. Israelachvili (*in preparation*).

# Multiple Beam Interferometry in the Surface Forces Apparatus

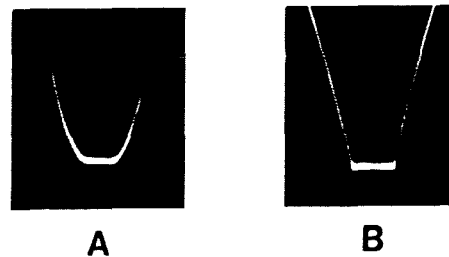
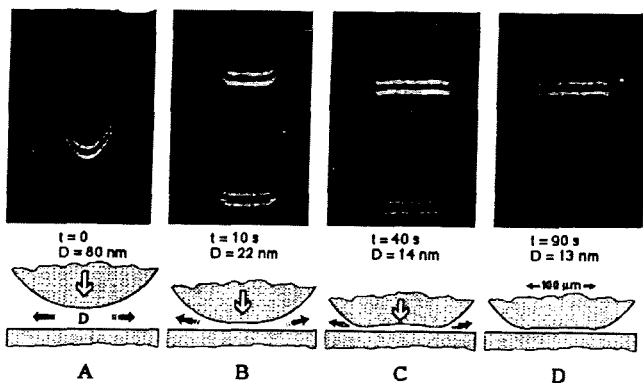


**Surface deformations with time due to viscous forces, bilayer fusion, etc.**

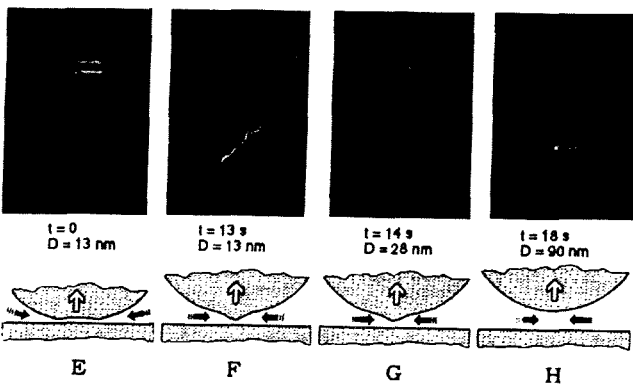
- *Direct visualization of cavitation and damage in ultrathin liquid films.*  
Tonya Kuhl, Marina Ruths, You-Lung Chen, Jacob Israelachvili, *Journal of Heart Valve Disease* 3 (1994) S117–S127.
- *Role of Hydrophobic Forces in Bilayer Adhesion and Fusion.*  
C. A. Helm, J. N. Israelachvili, P. M. McGuiggan, *Biochemistry* 31 (1992) 1794–1805.

**FECO spectroscopy: measuring molecular structure and dynamics in thin films**

- *Enhanced absorption within a cavity: a study of thin dye layers with the Surface Forces Apparatus.* C. Müller, P. Mächtle and C. A. Helm, *J. Phys. Chem.* 98 (1994) 11119–11125.
- *A thin absorbing layer at the center of a Fabry-Pérot interferometer.*  
P. Mächtle, C. Müller and C. A. Helm, *J. Phys. II France* 4 (1994) 481–500.
- *Eigenvalue analysis of the surface forces apparatus interferometer.*  
P. Rabinowitz, *J. Optical Soc. America A* 12 (1995) 1593–1601.



Fringe pattern for two curved mica surfaces (A) in compressive contact in water in the absence of adhesion, and (B) in adhesive contact in air. The shapes of the fringes accurately reflect the macroscopic shapes of the surfaces after noting that the vertical magnification is about  $10^4$  times the horizontal magnification (6). In both cases the diameter of the contact zone is about  $50 \mu\text{m}$  (seen as the flat horizontal parts of the fringes).



Changing FECO fringe pattern over time for two curved surfaces with initial (undeformed) radii of  $R = 1 \text{ cm}$  approaching and separating from each other in liquid polybutadiene (PBD) at a velocity  $v < 10 \mu\text{m}/\text{sec}$ .

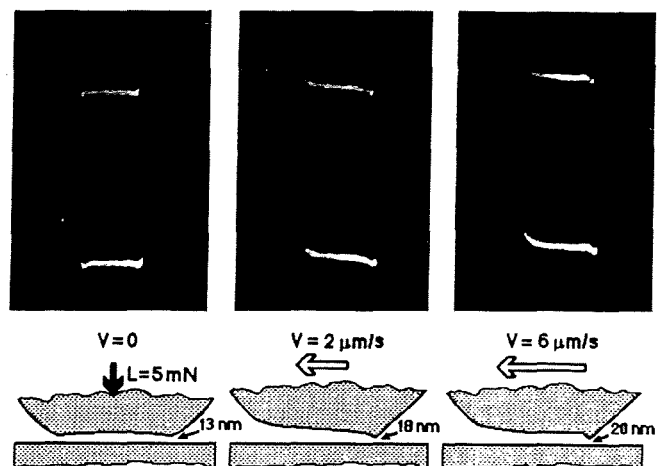


**Figure 41.** Various types of FECO fringe patterns obtained on different systems.

## MEASURING EQUILIBRIUM FORCES

Forces may be measured in a variety of ways depending on their magnitude. For measuring weak forces or for the tail end of a long-ranged force where high sensitivity is required, it is recommended that the piezoelectric crystal be used as follows:

The silica disc supporting the lower mica sheet is suspended at the end of a double cantilever spring of variable stiffness,  $K$ , which should be adjusted to some low value, say  $K=10^2 \text{ Nm}^{-1}$ . The forces are measured by suddenly reversing the voltage of the piezoelectric crystal, which expands or contracts it by a known (previously calibrated) amount. The resulting change in the separation between the two surfaces is then measured optically and any difference in the two values, when multiplied by the stiffness of the spring  $K$ , gives the force difference, whether attractive or repulsive, between the initial and final separations. The theoretical basis for this method is as follows: referring to Figure 42, let  $x = 0$  define the zero (or laboratory reference) position of the lower surface when the two surfaces are a large distance apart and there is no interaction force between them. As the upper surface is moved downwards to  $x=D_0$  the interaction force between the surfaces causes the spring to deflect by  $(D-D_0)$  causing the lower surface to move to a new equilibrium position at  $x=-(D-D_0)$ . For attractive forces the spring deflects upwards towards the upper surface and so  $D < D_0$ , whereas for repulsive forces the spring deflects downwards and  $D > D_0$ . At the new equilibrium separation  $D$ , the interaction force between the surfaces  $F(D)$  is balanced by the restoring force of the spring  $K(D-D_0)$ , so that at equilibrium we have

$$F(D) = K(D - D_0) \quad (11)$$

where  $F(D) > 0$  and  $D > D_0$  for repulsion.

Let the piezoelectric crystal expand by a finite amount  $\Delta D_0$ , so that  $D_0 \rightarrow D_0 - \Delta D_0$ , leading to a new equilibrium surface separation at  $D - \Delta D$ , then from the above equation we have

$$F(D - \Delta D) = K(D - \Delta D - D_0 + \Delta D_0) = K(\Delta D_0 - \Delta D) + F(D) \quad (12)$$

This shows that if an expansion of the crystal by an amount  $\Delta D_0$  causes the surface separation to change by  $\Delta D$  then the difference in the force at the initial position  $F(D)$  from that at the final position  $F(D - \Delta D)$  equals  $K(\Delta D_0 - \Delta D)$ . If  $\Delta D_0 = \Delta D$  there is no force difference. At large separations, this also implies that there is no force,  $F=0$ , so that this condition allows for calibration of the piezoelectric crystal, providing its expansion/contraction per volt.

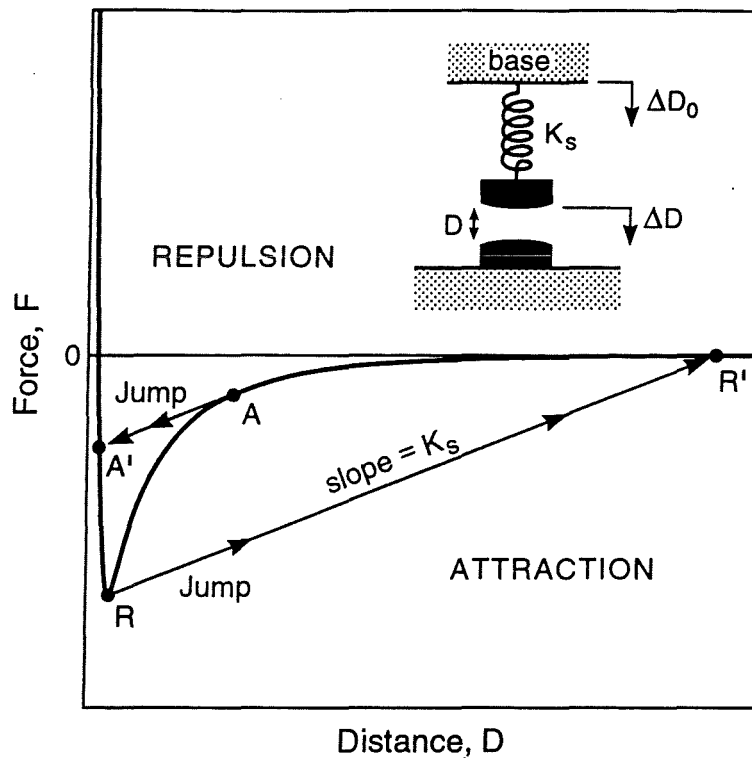


**Figure 42.** Basic mechanics of the force-measuring spring system.

For example, consider a system as in Figure.41 where the spring stiffness is  $K= 10^2 \text{ N/m}$  ( $10^5 \text{ dyne/cm}$ ). If the surfaces are initially  $100 \text{ nm}$  apart, where there is no measurable force, and the crystal is expanded by  $10 \text{ nm}$ ; then if the surfaces come to equilibrium at  $90 \text{ nm}$  there is, therefore, no force between the surfaces at  $90 \text{ nm}$ . However, if the two surfaces come to equilibrium at  $91 \text{ nm}$  there is a repulsive force at  $91 \text{ nm}$  equivalent to bending the spring by  $1 \text{ nm}$ , i.e., a force of  $K(\Delta D_0 - \Delta D) = 10^2(10 - 9)10^{-9} = 10^{-7} \text{ N}$ . For two cylindrical surfaces of radii  $R=1\text{-}2 \text{ cm}$  the time taken for them to reach equilibrium is about  $1 \text{ s}$  in water (viscosity  $\sim 1 \text{ cP}$ ). By this method one can start at large separations, where no force is detected, and work one's way down to smaller separations, and thus measure the force over any region of interest down to contact. Thus to measure the force  $F(D)$  between the two surfaces using the optical technique we need only to know

- (i) the force-measuring spring stiffness,  $K$ . This can be calibrated to within  $1\%$  after each experiment by placing small weights at the place where the mica surfaces were contacting and measuring the deflection with a traveling microscope or vernier eyepiece or simply an eyepiece with a graduated graticule in inserted.

- (ii) the amount the piezoelectric crystal expands or contracts,  $\Delta D_0$ , when the voltage is changed or reversed. This is measured optically at large separations where no forces are detected, before each force run.

The above method is the most accurate, but is time-consuming. Over certain distance regimes (usually below 10 nm) repulsive forces are often very large and rapidly varying with separation. In these regions of rapidly varying forces a second method of force measurement is more suitable: in this method the lower surface is moved *continuously*, either by applying a steadily increasing DC voltage to the piezo crystal or by use of MOTOR 1, stopping every now and again to measure the piezo voltage (or motor encoder reading) and surface separation. In this way much larger displacements  $\Delta D_0$  may be attained than possible with the crystal. This method is also much faster. When very strong repulsive forces are measured, the mica sheets will eventually deform (flatten) elastically so that their radius  $R$  is no longer constant. Under large compressive forces, one may measure the flattened contact area  $A$  and then plot the pressure ( $P=F/A$ ) against distance  $D$ , rather than the force  $F$  or  $F/R$  against  $D$ .

It is recommended that forces be measured both on approach (inward run) and separation (outward run). This will establish whether the force is reversible and, if not, the nature of the hysteresis in the force law. Hysteretic forces often arise with polymer systems where the hysteresis is time-dependent, depending both on the rate of approach and separation as well as on the previous history of the surfaces. It is therefore also recommended that force runs be measured at a given (measured) rate of approach and that the time allowed for equilibration between different points on a force curve also be recorded (and varied, if necessary). When measuring forces on separation, the procedure is as on approach but in reverse. In particular, after the surfaces have reached a separation of zero force one must continue to measure the force out to larger distances since these measurements constitute the piezo or motor calibration for the outward force-run.

Before starting a new force run, always check the mercury calibration line and reenter the optics (PRISM control and PRISM turntable) and focus (FOCUS control). Photographing the fringes or measuring the two radii may also be done at this point (with the surfaces outside the force field). A centering check should also be done when the surfaces are closest to each other.

On separating two surfaces from adhesive contact or from a potential minimum they usually jump out to large distance apart, from which the adhesion force may be obtained by multiplying the spring constant  $K$  by the distance jumped. Be careful that the 'jump' out is not an apparent one due to viscous forces arising from moving the surfaces apart too rapidly before they jump.

## MEASURING VISCOUS FORCES AND OTHER DYNAMIC INTERACTIONS

Various dynamic interactions can be measured, some employing the Basic Unit, others requiring an attachment such the Friction Device, Bimorph Slider or Bimorph Vibrator, which are described in Part III of the manual. The following references provide additional information on different types of dynamic measurements using the SFA technique:

- **The Drainage of Thin Liquid Films Between Solid Surfaces**  
Chan, D. Y. C. and Horn, R. G., *J. Chem. Phys.* **83** (1985) 5311-5324.
- **Measurement of the Viscosity of Liquids in Very Thin Films**  
J. N. Israelachvili, *J. Colloid and Interface Sci.* **110** (1986) 263-271.
- **Measurements of the Viscosity of Thin Films Between Two Surfaces With and Without Adsorbed Polymers**  
J. N. Israelachvili, *Colloid and Polymer Science* **264** (1986) 1060-1065.
- **Measurements of Dynamic Interactions in Thin Fluid Films: the Transition from Simple to Complex (Non-Newtonian) Behavior**  
J. N. Israelachvili, S. J. Kott, L. Fetters, *J. Polymer Sci., Part B: Polymer Physics* **27** (1989) 489-502.
- **Measurements of and Relation between the Adhesion and Friction of Two Surfaces Separated by Molecularly Thin Liquid Films**  
A. M. Homola, J. N. Israelachvili, M. L. Gee, P. M. McGuigan, *J. Tribology* **111** (1989) 675-682.
- **Motions and Relaxations of Confined Liquids**  
Granick, S., *Science* **253** (1991) 1374-1379.
- **Viscoelastic Dynamics of Confined Polymer Melts**  
Hu, H-W., Granick, S., *Science* **258** (1992) 1339-1342.

## CALIBRATIONS

A number of calibrations, mostly of a straightforward nature, have to be carried out before, during or after an experiment, or at any convenient time. Some need to be done only once, others need to be done repeatedly with each experiment.

- (1) **Thermistor.** This is straightforward to calibrate anytime and need only be done once. Hang the lower 3/4 of the steel body of the thermistor into cold water in a beaker, and insert a thermometer and magnetic stirring bar. Place on a hot plate and heat while stirring.

Calibrate between 5°C and 80°C using a standard multimeter. Fit the data to an exponential function. During experiments, the resistance can be measured anytime, preferably with the same multimeter. For thermistors such as SENSOR SCIENTIFIC, Part No. G198WM103C, that have a nominal resistance of 10,000Ω at 25°C, their resistance at different temperature is approximately as follows:

Temperature °C	Resistance Ω
20	12,500
25	10,000
30	8,050
35	6,550
40	5,300
45	4,350
50	3,600

- (2) **Heaters.** The two identical heaters are rated at 100 Watt each and may be connected in parallel or in series. Voltages of 10–50 VAC across each heater (20–100 VAC across both heaters when connected in series) should raise the temperature of the lower chamber, when filled with liquid, by 10–70°C above ambient, but this is very rough – the heater power controller is non-linear and the voltage-temperature characteristic should be calibrated with liquid in the chamber and the thermistor in place before it is used in an experiment for the first time. There is really no need to calibrate the heaters accurately since the thermistor will measure the temperature in the chamber at any time. Note that once the temperature is stabilized the drifts of the surfaces will die down. It is recommended that when using the heater power controller, the voltage output (the AC voltage across the heaters) is continually monitored with a multimeter. At low voltages, solid state power controllers can sometimes cut-off. This can be adjusted by opening the control box and turning the trimming pot on the heater controller. Variac power controllers do not have this problem.
- (3) **Piezoelectric crystal and MOTOR 1.** These should be calibrated (in distance vs volts for the piezo, distance vs encoder reading for the motor) using the FECO fringes as part of each force run at large distances where there is no force between the surfaces.
- (4) **Spectrometer dispersion.** Calibrate with the mercury green line and two yellow lines using a mercury pen lamp (see below).
- (5) **Mercury green or yellow lines.** Choose one reference line, say the green line, and check frequently, e.g., every hour or so, during the course of an experiment, resetting the

mercury green line to zero on the spectrometer encoder each time (the mercury calibration line can 'drift' due to a temperature change in the room, and also if any part of the optical alignment has been moved or adjusted, for example, if the prism or mirror have been inadvertently jogged). Do not change the mirror angle controls after starting an experiment since this could artificially shift the positions of the fringes, including their contact positions relative to the Hg lines by a small but not insignificant amount. However, if you do make any adjustments to the optics, always reset the Hg line to zero before proceeding further.

- (6) **Force-measuring spring (K variable from 30 to  $5 \times 10^5$  N/m)**. The SFA3 is unique in allowing you to vary the force-measuring spring stiffness by more than 4 orders of magnitude, thanks to the robustness of the dove-tail design (the maximum is set by the stiffness of the beryllium-copper cantilever spring,  $K \approx 1.5 \times 10^6$  N/m, on Part 01040 of the Upper Chamber – see spring  $S_2$  in Figure 2 of Appendix 1).

Calibrate once by adding small weights placed at the center of the disk mount (you may remove the disk first) and measuring the deflection using, for example, a vertical traveling microscope or micrometer eyepiece or normal microscope with a scaled graticule installed. Calibrate with force-measuring spring fully clamped (to avoid slip which may occur with the heavier weights or loads than are normally encountered in experiments). The spring constant should not vary from experiment to experiment if it is clamped in the same position each time, except for the stiffest clamping position where  $K \approx 5 \times 10^5$  N/m ( $5 \times 10^8$  dyne/cm) and where the contribution from the finite stiffness of the glue supporting the mica sheets (which depends on the type of glue and thickness of the glue layer) may no longer be ignored. This contribution to the effective stiffness of the force-measuring spring system is typically around  $10^6$  N/m ( $10^9$  dyne/cm), and it reduces the maximum effective stiffness as given by the following equation:  $1/K_{\text{eff}} = 1/K_{\text{spring}} + 1/K_{\text{glue}}$ . During experiments, one may calibrate the maximum effective stiffness  $K_{\text{eff}}$  by measuring the jumps apart of the surfaces from adhesive contact under full and weak clamping conditions (where  $K$  is known), and comparing the two values to obtain  $K_{\text{eff}}$  at full clamping (note that when the jump apart is small, a small correction has to be made for the elastic deformation of the surfaces at contact).

During experiments, one may also calibrate the spring stiffness by measuring the natural frequency of the lower support. This can be readily done by separating the surfaces a large distance (many microns) in air or liquid and vibrating the piezo over a range of frequencies until the blurred fringes become suddenly sharp. This will occur at a particular frequency,

$\nu$ , which is the resonant frequency of the lower support at that spring stiffness,  $K$ . Pre- or post-experiment calibrations (with the same disk installed) can be done using this method with Newton's rings to calibrate  $K$  as a function of  $\nu$ . The calibration should obey the equation:  $\omega = 2\pi\nu = \sqrt{K/m}$ , where  $m$  is the mass of the support with disk.

- (7) **Lateral magnification of surfaces as seen in spectrometer eyepiece.** This calibration is needed especially for measuring the radii of the surfaces from the shapes of the FECO fringes. Calibrate with a vernier graticule for  $0^\circ$  and  $90^\circ$  angles of the DOVE PRISM. A one-off calibration should suffice if the apparatus / optics stand / spectrometer positions remain unchanged from one experiment to the next.
- (8) **Liquid volume in chamber.** Note that, on draining chamber, some liquid (~5-10 ml) can remain trapped inside, at edges, holes, cracks, etc. Thus calibrate by filling, not by emptying.
- (9) **Bimorph slider.** For calibrating the bimorph stiffness,  $K$ , place upper chamber with bimorph attached on the side and calibrate with as you would the force-measuring spring (item 6) with small weights and a calibrated eyepiece (cf. Figure 40). The lateral movement of the bimorph slider ( $\text{\AA}$  per volt) may be calibrated by top viewing with a calibrated eyepiece and measuring the lateral deflection due to applying a low voltage (40 Volts max) trying both AC and DC. The deflection should be easily detectable. Alternatively, during experiments, with the surfaces in contact, you may calibrate the movement per volt from the measured displacement of the friction spring as recorded by the Friction Device.
- (10) **Friction device.** For calibrating the friction spring stiffness,  $K$ , clamp attachment firmly on the side and calibrate as you would the force-measuring spring (item 6) with small weights and a calibrated microscope.

## ANALYZING THE RESULTS

As a general rule, it is wise to analyze the results of your last experiment before proceeding with the next one. Analysis depends to some extent on how the data was recorded – whether by hand, on video tape, on a chart-recorder, fed directly into a computer, or a combination of these. This procedure in turn will depend on the type of experiment being conducted, on the experimental plan, and on the number of people participating. Team work, involving two or three people, is always preferable: it increases the 'brain power' of the planning and observation, reduces the possibility of mistakes, and allows for independent measurements to be made). This section does not deal so much with these aspects of how to conduct experiments, but more with what should be done before, during, and after an experiment. Keep a bound laboratory note book or record book, carefully distinguishing between entries made during an experiment from those made afterwards. For example, use different colors for the planning, actual recording and subsequent analysis or processing of the data (as well as even and odd page numbers for data entry and analysis, respectively).

### **Before an experiment**

Plan each experiment in detail from start to finish. Some experiments may be one-day experiments, others may go on for two weeks. Careful planning of what will be measured and what to look for (and alertness to what is not being looked for) is crucial to a successful experiment.

- ☆ Prepare the substrate surfaces (mica sheets or other supporting material): deposit a silver layer of known thickness and note the thickness and orientation of each sheet on the backing sheet. Carefully plan any surface treatment / deposition and how the treated surfaces will be installed into the apparatus.
- ☆ Perform any needed pre-calibrations, such as checking the mica thickness (with a 'test-piece'), checking all the motors and piezo crystal, checking the electrical instruments and connections, checking that you have the right grating in the spectrometer, etc. (See CALIBRATIONS).
- ☆ Have all tools and liquid solutions ready before starting. Remember easy-to-forget items such as spare light bulbs, photographic films or video tapes, chart-recorder paper, small torch (flash light), alternative grating, etc.

### **During experiments**

Start by perfecting the optical alignment, adjusting the mirror, lamp, base legs and prism turntables, as already described. In particular, try to make sure that the light passes normally (at  $90^\circ$ ) through the surfaces (see Figure 42). This will require adjusting the mirror controls but may also require adjusting the heights of the three legs of the Base.

It is important to record everything that may conceivably be relevant, even if it may not seem so at the time. This includes a complete record of the contact fringes (at least three successive order fringes and their birefringence), continuous or periodic measurements of the contact area (for flattened surfaces), measuring the adhesion force of adhering surfaces, checking the mercury calibration lines, reentering and refusing, noting any inward or outward drifts, measuring the temperature, checking for leaks, taking photographs or video recordings, measuring the refractive index at different film thicknesses, measuring forces on the way in as well as on the way out (calibrating the piezo or motor in both directions), recording the rates of approach and separation and the equilibration times between data points, noting the time between force runs and how far the surfaces were kept during the waiting period – and last but not least – repeating measurements at new positions and measuring the birefringence and two surface radii at each new position (Figure 40). When aligning the optics at each position, try to make sure that the light passes normally (at  $90^\circ$ ) through the surfaces (see Figure 42).

Being a 'good observer' is essential, as is the habit of following up all unexpected phenomena. Record everything and trust your measurements – by not clearing up loose ends you may miss an important discovery.

### **Analysis of results after an experiment**

Appendix 2 is an example of a complete experiment where all stages of a real experiment were noted down, including data recorded, subsequent analysis, and plotting of the results.

## MISCELLANEOUS HINTS & TROUBLESHOOTING; SERVICING YOUR SFA

### **Droplet experiments**

Distill and dry the fluid to be injected before sucking it up into a small 500  $\mu\text{l}$  syringe. Never expose the liquid to lab air after the distillation (to avoid it picking up dust particles). Once it is in the syringe, it should be injected between the surfaces under conditions of a positive clean-nitrogen gas pressure in the chamber (and then only after a few drops have been placed within or just outside the chamber to ensure that any impurities from the syringe come out first). Separate the surfaces about  $<0.5$  mm and direct the syringe needle to the top surface but well away from the centre. Inject a small quantity of liquid gently onto the top surface and allow the liquid to flow down until it bridges the two surfaces. Immediately bring the surfaces together, but not into contact. Close the syringe port, and fill the small receptacle or boat, part 08051, with a few drops of the liquid to ensure saturated vapor pressure within the chamber. The vapor pressure will actually be below saturation because the surfaces are usually slightly hotter than the liquid in the boat due to the light passing through them; however, if the liquid is placed in a flat-bottomed beaker just above the window so that the incoming light passes through it, this will heat the liquid 'reservoir' enough to significantly reduce the evaporation rate of the droplet between the surfaces. The liquid in the boat (but not the beaker) can be changed at any time from outside the apparatus via the Luer opening on its exposed side. The receptacle can also be used for placing  $\text{P}_2\text{O}_5$  in it to completely dry the internal chamber and any non-aqueous liquid droplet between the surfaces. For complete drying, allow the system to equilibrate overnight. If there is a leak that lets water vapor come into the chamber (see below) the  $\text{P}_2\text{O}_5$  will look wet, or have a shiny or glazed appearance.

### **Liquid condensation on glass surfaces**

This problem can arise in droplet experiments where small lenses condense on the surfaces of the glass windows and silica disks causing blurring of the fringes. This problem can be avoided in one of three ways: (1) By injecting bulk liquid into the thin gap between the window and upper disk. (2) By ensuring that the upper window and silica disk are at a slightly higher temperature than the rest of the chamber. This can be done by placing a small flat metal washer, suitably wired at two ends, into the piezo mount so that it sits on the glass window. Gently heat the washer and window by passing a low voltage current through it. (2) A special upper mount exists where there is no gap between the window and upper disk (see Figure 51).

## **Leaks**

It is amazing how a very small leak can allow atmospheric water and organic vapors to enter the internal chamber from outside. In some cases this can have a dramatic effect on the forces between the surfaces. For example, a small leak can totally prevent a non-polar liquid droplet from remaining completely dry; if the surfaces are hydrophilic, water will condense on the surfaces and give rise to strongly attractive capillary forces as well as change the "boundary conditions" for other types of interactions.

A small leak does not mean that liquid will be seen to flow out from the leaking hole. It will usually evaporate on emerging so that there is no obvious sign that a leak is occurring. Leaks often become apparent during experiments, for example, by noting that the liquid level is falling with time, or that  $P_2O_5$  in the receptacle is becoming wet (see above). To check for leaks, fill the box with a volatile liquid such as ethanol or cyclohexane up to a level that can be clearly measured through the window. Close the apparatus in the usual way (with no surfaces installed), and see whether the liquid level falls overnight.

Leaks are most often due to: (1) flattened O-rings, especially small ones, that need replacing, (2) insufficient tightening of the Teflon bellows, (3) forgetting to put an O-ring into one of the small holes, such as the thermistor hole or pinion shaft hole, (4) a hair or scratch on some smooth surface that contacts an O-ring, (5) a crack in the piezoelectric tube or the glue holding the piezoelectric tube to its support (contact SFI, Inc. if the piezo tube feels loose).

## **Fringe brightness**

If the fringes are not bright enough to be observed comfortably, due to oversilvering, one may attach a lens ( $f \approx 3.5$  cm) under the light entry port on the lower chamber. This will brighten the fringes but at the expense of some blurring.

## **Drifts**

It is strongly recommended that the experimental room be thermostatted to  $\pm 0.1^\circ\text{C}$ . This will reduce drifts to negligible levels (about  $1\text{\AA}/\text{min}$  may be considered). However, the apparatus may need to 'equilibrate' in the room for many hours. It is also wise to have the liquid solution and the apparatus inside the thermostatted room for a few hours before filling.

## **Mercury light**

Position of Hg lines in spectrogram varies with placement of Hg lamp, so don't move it once you have calibrated the FECO contact fringes during an experiment. At the beginning, make sure it is coming in from the same direction as the FECO beam. This can be done by removing the spectrometer prism and looking back into the microscope prism from the direction of where

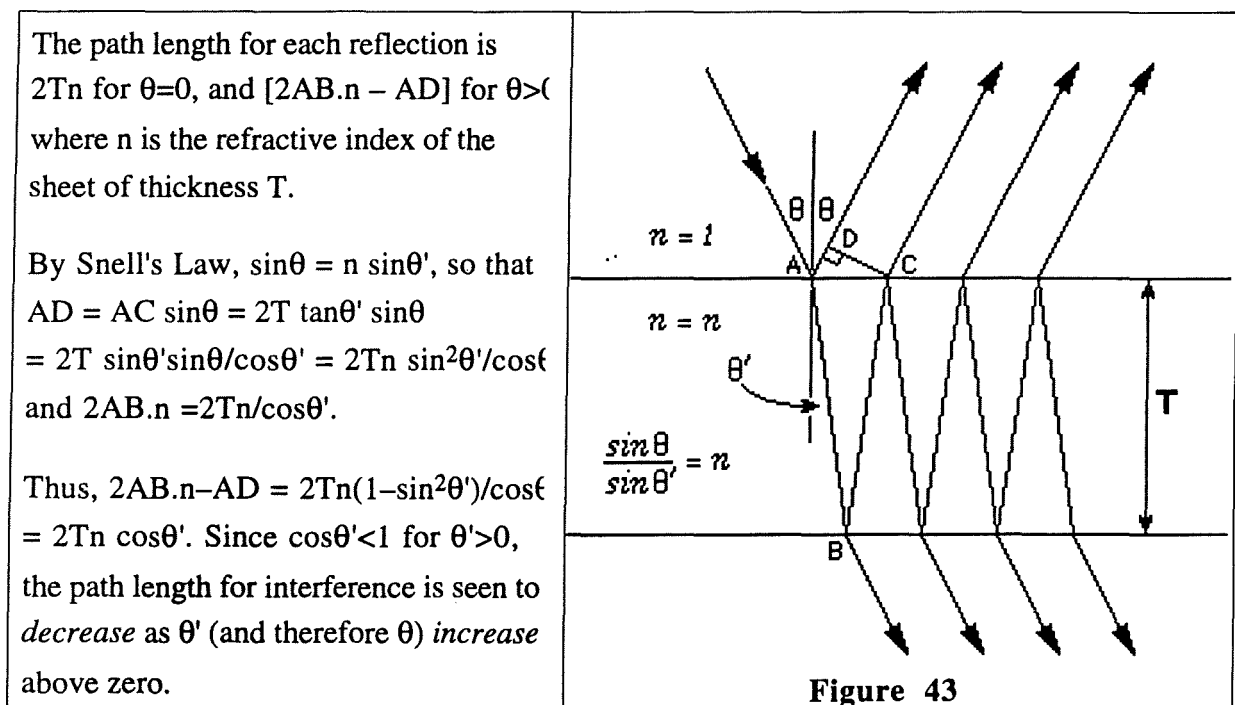
the center of the spectrometer prism will be located, and noting that both beam spots come from the same point.

### Achieving high local pressures

Use small radius disks ( $R \sim 1 \text{ mm}$ ) with little glue to get high local pressures – up to 0.5 GPa can be achieved in this way. See *The shear properties of Langmuir-Blodgett layers*. B. J. Briscoe and D. C. B. Evans, *Proc. Roy. Soc. (Lond.) A* 380 (1982) 389–407.

### Optical alignment

Sharpest fringes are obtained when the white light beam is passing normally through the surfaces at their point of closest approach (which is usually at the center of the interaction zone). If the light is passing at some finite angle  $\theta$  to the normal, the fringes will become blurred and also shift to SHORTER wavelengths. The reason for the shift to shorter, rather than longer, wavelengths as the mica sheets are tilted relative to the normal, i.e., for  $|\theta| > 0$ , is shown in Figure 43.



Try to ensure that the light comes through at  $\theta=0$  at each new position. This will also ensure that your fringe calibration, and hence your definition of  $D=0$ , remain valid. If you have rotated the two surfaces during the search for a new position, even though you have kept  $\theta=0$ , you must compare the *mid-points* of the  $\beta$  and  $\gamma$  doublets since these are the 'conserved' wavelengths at the different positions. The birefringence varies as  $\cos\theta$ .

### **Particle contamination**

Particulate contamination can be eliminated by better purification of the solutions: ensure that from the final stages of the distillation up to filling, the liquid never becomes exposed to atmospheric air, however momentarily. High speed spinning (centrifuging) a viscous liquid at an elevated temperature helps remove particulates. Reducing the surface radius,  $R$ , also reduces the *probability* of trapping a particle between two surfaces.

### **Motor speed controls**

If movement of the surfaces is too rapid or slow when using motor 1 (differential spring control), replace motor-encoder assembly with another having a different gear ratio. Complete motor-gearhead-encoder units are available from Micro Mo. It is possible to add another motor (Motor 3) to control the differential micrometer. However, this micrometer is usually controlled by hand, although its graduated head can be read to give the displacement of the spring support.

### **Do-it-yourself modifications**

The SFA3 is a versatile modular unit that can have parts interchanged and new attachments added. Some of these are described in Part III of this manual. Others can be designed by the user. An excellent book that provides useful hints on designing small machine components is *Foundations of Ultraprecision Mechanism Design* by S. T. Smith and D. G. Chetwynd, Gordon and Breach Science Publishers, Amsterdam (1992, 1994).

END OF PART 2

## PART III

# ATTACHMENTS & ACCESSORIES

---

### SYRINGE INJECTION UNIT

---

#### MAIN FEATURES

- ☆ Syringe injection facility
- ☆ Boat for vapor pressure control

The Syringe Injector (see Figures 11 and 25) is an attachment for injecting small quantities of liquid directly between the surfaces or into the apparatus main chamber during experiments without opening the chamber or exposing its atmosphere to the outside – essential for performing certain types of experiments, such as 'droplet experiments' with very small volumes of liquid. Includes rotating ball-and-socket fixture for directing syringe needle to any desired point near or between the two surfaces. Also provided: small liquid bath (receptacle or boat) that can be interchanged with the syringe fixture – for controlling the vapor pressure of the chamber during experiments – useful to controlling the concentration (activity) of solutes in the liquid. If neither syringe nor small bath are being used, the entry port may be plugged with a Kel-F plug (also provided). Customers should consider ordering this unit with the initial order rather than later since the Lower Chamber has to be shipped back to for modifications before the syringe unit can be used (in some models the syringe port is already machined into the Lower Chamber, at no extra cost). The syringe injector port may also be used for feeding liquids, other attachments and certain probes into the chamber, for example, a pH probe or a UV mercury pen-ray lamp for oxidizing surface organic groups.

#### COMPONENTS

- Injector port with plug.
- Ball-and-socket syringe fixture.
- Small liquid bath with female Luer port.
- Syringe with 7.5 cm-long needles, Luer connectors and end caps.

## **FRICION DEVICE (for SFA 3)**

### **MAIN FEATURES**

- ☆ Smooth lateral motion of upper surface
- ☆ Large lateral displacement (5 mm total traverse)
- ☆ Constant or variable speed in either direction
- ☆ Simultaneous measurement of normal and shear or friction forces
- ☆ Simultaneous measurement of surface deformations
- ☆ Friction force measuring sensitivity:  $10^{-5}$  N.
- ☆ Can measure friction coefficients as low as 0.0001

The FRICTION DEVICE for the SFA3, shown in Figures 15 and 26, is a 'complete unit' – both producing and measuring shear motion. It is an improved version of the unit originally described by A. M. Homola, J. N. Israelachvili, M. L. Gee and P. M. McGuiggan, in *J. Tribology* 111 (1989) 675-682 for use with the SFA Mk 2. Sliding motion of the upper surface is produced via a digital encoder-controlled motor-driven micrometer, and the shear/friction force is measured from the deflection of a double-cantilever friction-force-measuring spring assembly supporting the upper surface. The spring deflection is measured with a Wheatstone Bridge or strain gauge bridge connected to resistance or semiconductor strain gauges attached to the friction-force-measuring springs (semiconductor gauges are about 100 times more sensitive but more fragile than the resistance gauges). The assembled FRICTION DEVICE includes: spring-loaded anti-backlash translation stage driven by micrometer and reversible DC motor with digital encoder and display counter. Friction force-measuring double-cantilever springs with strain gauges mounted and wired to an output terminal. Clamping ring for attaching to SFA 3 Basic Unit and rotating upper surfaces about a fixed axis.

### **Operation and description of lateral sliding attachment**

Lateral (transverse) movement is achieved by the FRICTION DEVICE attachment (see Figures 15 and 26) which replaced the piezoelectric crystal tube mount supporting the upper silica disk of the basic apparatus. Figures 44 show the basic parts of the Friction Device as mounted into the SFA3. Lateral motion is initiated by a reversible, variable speed, DC motor-driven micrometer shaft which presses against the translation stage which is connected via two horizontal, double-cantilever, Cu-Be springs to the rigid mounting plate. One of these springs acts as a frictional force detector by having four strain gauges attached to it, forming the four arms of a Wheatstone bridge, and is electrically connected to a chart recorder or storage oscilloscope (see Table 1). This spring-loaded arrangement ensures perfect linear motion of the

translation stage without backlash. The Friction device is rigidly clamped on top of the main chamber in the same way as the piezo mount it replaces, and an additional circular clamping ring can be inserted that allows for the moving direction of the upper surface to be rotated about a fixed vertical axis.

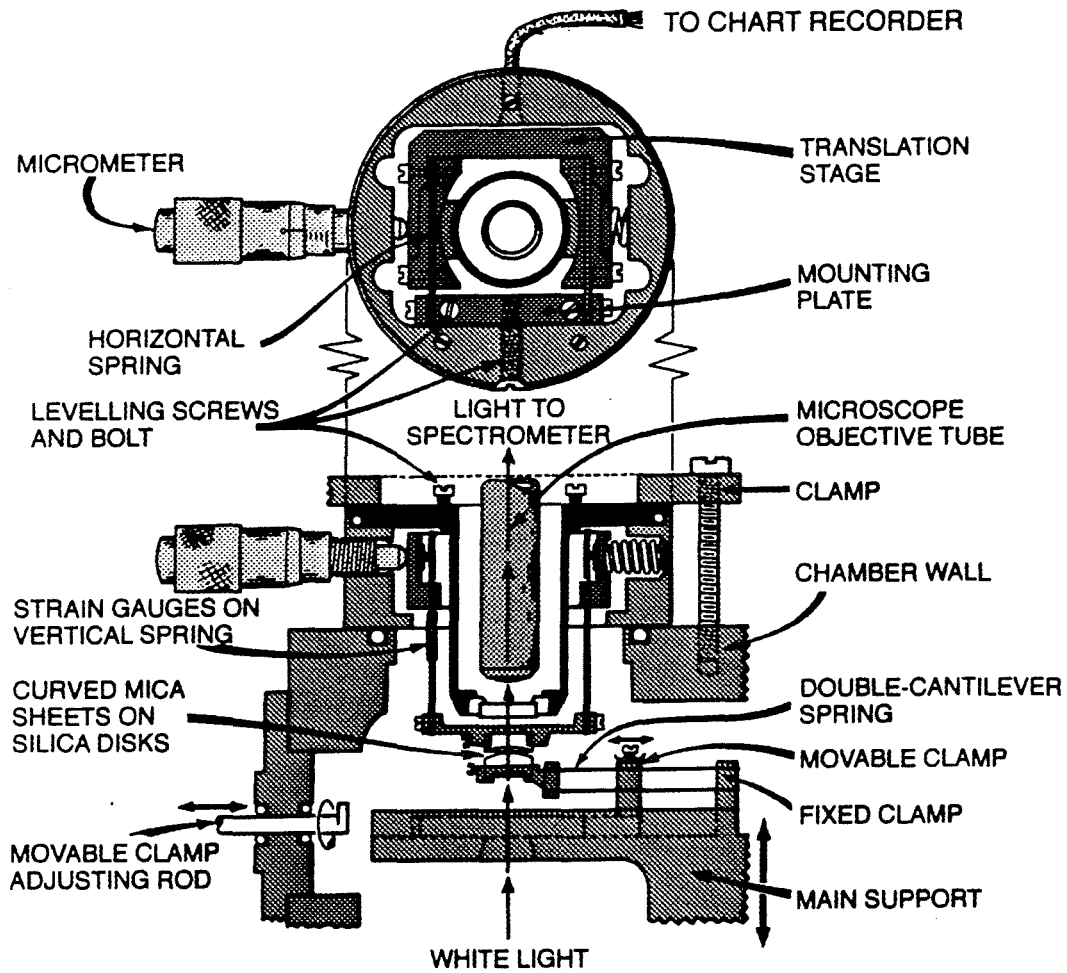


**Figure 44.** Assembly drawing of the FRICTION DEVICE.

Sliding motion is initiated by driving the micrometer, which deflects the translation stage causing the upper surface to move linearly and horizontally. If the upper mica surface experiences a transverse frictional or viscous shearing force due to its contact with, or proximity to, the lower surface the vertical springs will deflect. This deflection can be measured by the strain gauges attached to the springs. The stiffness of the double-cantilever spring unit can be varied but is typically  $3 \times 10^6$  dyne/cm ( $3 \times 10^3$  N/m). At this stiffness, a four-arm resistance strain gauge system has a sensitivity in measuring transverse forces of about 10

dynes ( $10^{-4}$  N) which corresponds to a displacement of the upper surface of about 300 Å. Semi-conductor gauges are more than an order of magnitude more sensitive, the practical limit of detection being determined by electrical noise in the instrumentation. Good results can be obtained using strain-gauge amplifier Model 2311 from MEASUREMENTS GROUP, chart recorder Model 1242 from SOLTEC and/or storage scope recorder Model 2232 from TEKTRONIX (see Table 1).

By suitably mounting the two cylindrical surfaces so that they are oriented as shown in Figure 37, the contact zone can be made to remain in the same place (at the center of the eyepiece) during the sliding of the upper surface. Note, too, that the Friction Device can be attached in either one of two perpendicular directions (Figure 45), thereby allowing for the upper surface to be moved in either the in-out or left-right directions. This, in turn, will determine the way the two silica disks are mounted.

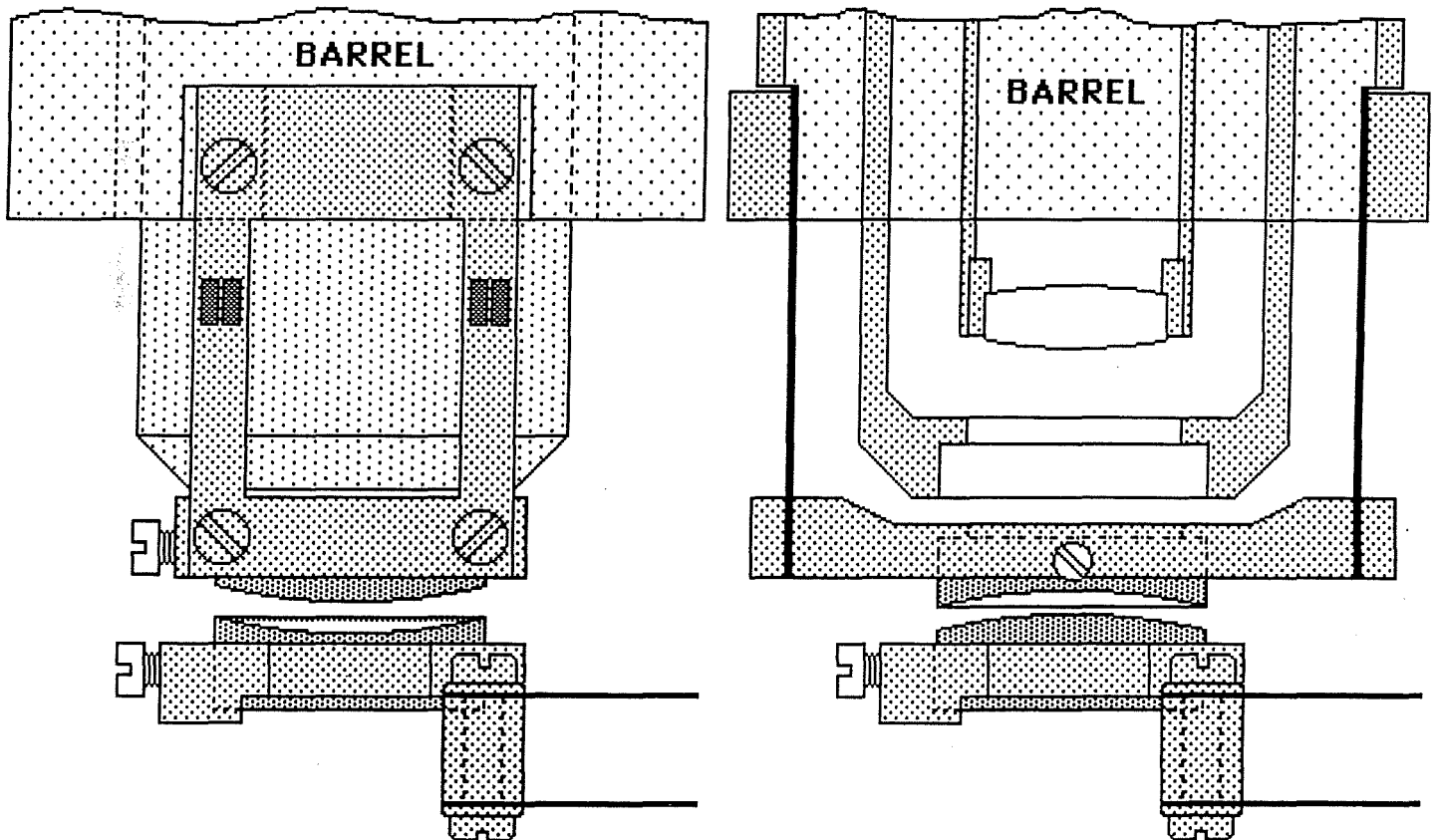


**Figure 45.** Different mounting configurations of the Friction Device as viewed from the front window. Note: Before using the Friction Device, check that the friction barrel, part 11110, is truly vertical. If it is not, you can adjust its angle by applying a medium force with your fingers to bring it back into vertical alignment.

The Friction Device attachment allows for the two surfaces to be sheared past each other at sliding speeds which can be varied continuously from 0.01-100  $\mu\text{m s}^{-1}$  while simultaneously measuring the transverse (shear) force  $F$  between them. At the same time the normal force or load  $L$  can be controlled and varied by moving the lower surface vertically, as in normal Basic Unit operations. The load  $L$  is given by multiplying this displacement by the (adjustable) spring constant of the horizontal double-cantilever force-measuring spring supporting the lower surface. The range of positive or negative loads that can be applied varies from 0 to  $\pm 100$  gm. Finally, the distance between the surfaces  $D$ , their true molecular contact area  $A$ , their elastic (or viscoelastic or elastohydrodynamic) deformation, and their lateral motion can all be simultaneously monitored by recording the moving FECO fringe pattern using a video camera (SIT type) and recording this on tape for later analysis with a video micrometer analyzer and single freeze-frame camera (Polaroid Freezeframe Video Image Recorder).

Note: Before using the Friction Device, check that the barrel, part 11110, is truly vertical. If it is not, you can adjust its angle by applying a medium force with your fingers to bring it back into vertical alignment.

For a review on shear studies using the Friction Device see the Chapter entitled **Surface Forces and Microrheology of Molecularly Thin Liquid Films** by J. N. Israelachvili, in *CRC Handbook of Micro & Nanotribology*, Ch. 8, 1995.

## BIMORPH SLIDER

### MAIN FEATURES

- ☆ Provides smooth lateral motion of lower surface.
- ☆ Total traverse: 1 mm ( $\pm 0.5$  mm).
- ☆ Constant, sinusoidal or programmable motion in either direction.
- ☆ Large dynamic range of frequencies, sliding speeds, shear rates.
- ☆ Simultaneous measurement of normal forces and surface deformations.
- ☆ Should be used simultaneously with the FRICTION DEVICE.

The BIMORPH SLIDER (see Figures 16 and 27) produces only lateral (or shear) motion of the lower surface via two parallel sectored bimorphs in a 'double-cantilever' geometry. Sinusoidal, saw-tooth, step-function and other types of displacement-time functions can be generated over a frequency range from micro-Hertz to 100 Hz, corresponding to sliding speeds from 10 cm/s to 10 Å/s. This dynamic range is much greater than can be attained with the motor-driven Friction Device. The assembled unit includes bimorphs and coaxial wiring to an external supply (function generator – see Table 1), a fixed-stiffness normal force-measuring double-cantilever spring with disk mount, and a means for mounting the unit to a SFA3. The BIMORPH SLIDER attachment allows for simultaneous lateral and normal forces to be measured. In addition, the surfaces may be imaged using the FECO optical interference technique which gives the surface separation and a direct visualization of the local surface geometry at all times during sliding. The BIMORPH SLIDER can be used simultaneously with the FRICTION DEVICE, which *must* be used if shear/friction forces are also to be measured.

For more information on the Bimorph Slider, see the following article

**Thin film rheology and tribology of confined polymer melts: contrast with bulk properties**, in *Macromolecules* (submitted), by Gustavo Luengo, Franz-Josef Schmitt and Jacob Israelachvili.

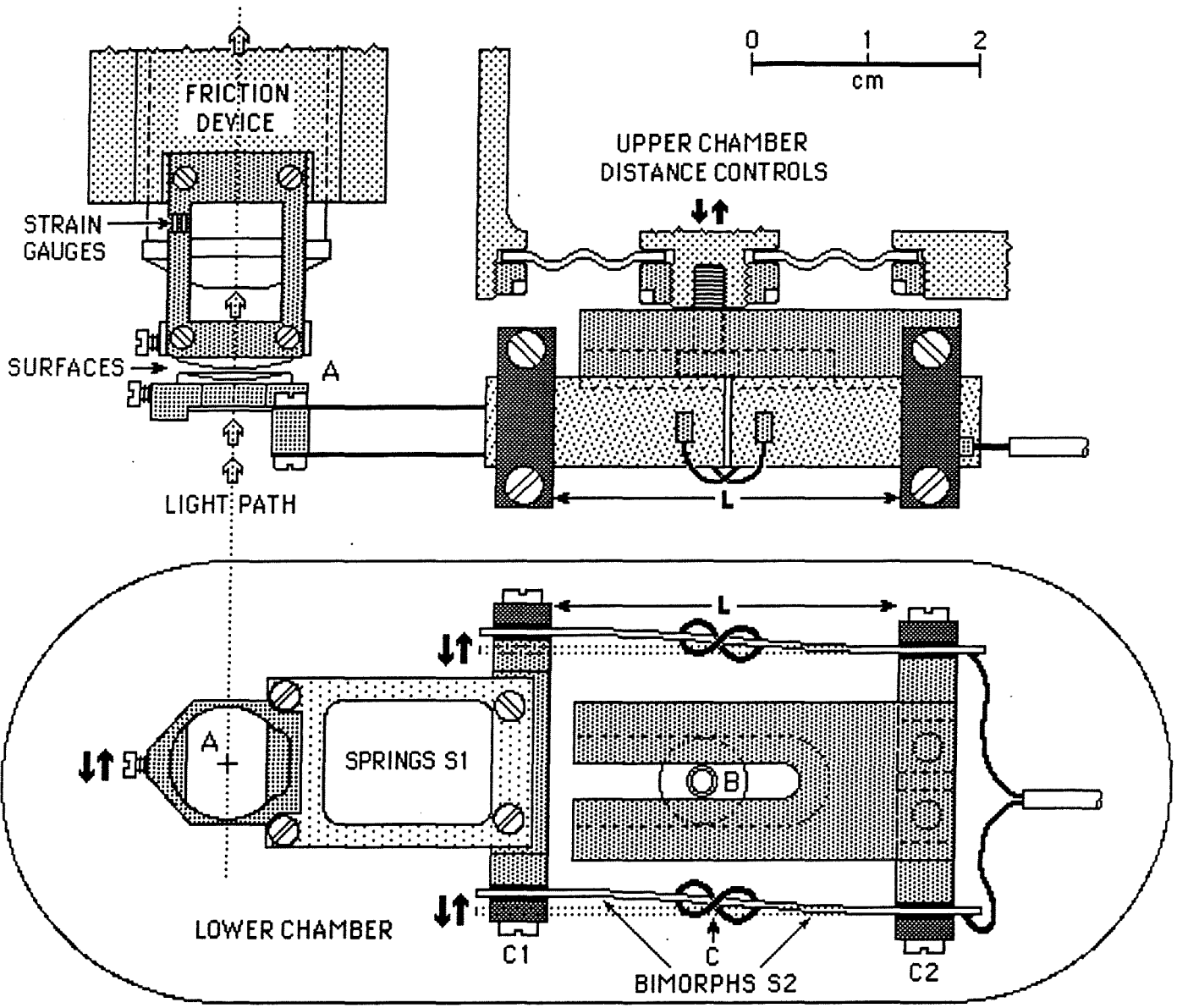


**Figure 46.** The Bimorph Slider attachment has been designed for making friction and shear measurements over a large range of sliding velocities or driving frequencies.

**Operation and description of the Bimorph Slider**

The lower surface is supported at the end of a double-cantilever spring (Figure 46 – S1) used for measuring the normal forces between the surfaces. Lateral movement is accomplished with two (or – for increased driver stiffness – four) parallel piezoelectric bimorph strips S2. Bimorphs are ‘piezoelectric couples’ made of two thin sheets of piezoelectric ceramic bonded together by a thin layer of hard conducting material. The two outer faces of each bimorph are coated with thin conducting layers of metal (usually of silver or nickel), which provide

protection and serve as suitable electrode surfaces for electrical connections, such as the soldering of connecting wires. Before two piezoelectric sheets are bonded to form a bimorph, their polarity is reversed relative to each other, so that when a DC voltage is applied across the bimorph, one sheet expands lengthways as the other contracts, resulting in a net bending of the bimorph. For low applied voltages (<100V) the bending, or lateral displacement of each end, is proportional to the applied voltage  $V$ . Bimorphs are capable of producing much larger displacements than piezoelectric crystals for the same applied voltage. Bimorphs also work in reverse, as force sensors. Thus, when a force is applied to one end, a large voltage develops across the two outer electrode faces, which can be easily measured. (Bimorphs have long been used in SFA force measurements, both as displacement transducers and as force sensors.) The bimorphs used in the Bimorph Slider are typically PZT 4, 0.023 inches thick, 6 cm long, silver coated; from Morgan Matroc Corp.

To convert the pure bending motion of a bimorph into a linear displacement, one may create a 'sectored' bimorph by scraping away a thin strip of the conducting metal coat from the center of each face **C** and then electrically connecting the two pairs of diagonally opposite faces as shown in Figure 46. This splits the direction of the applied voltage across the two halves (sectors) of the bimorph, making each half bend in the opposite direction. If the two halves are of equal length, the resulting effect is a pure linear displacement of the two ends relative to each other, just as occurs with a double-cantilever spring, with no net rotation or bending component. By using two or more parallel bimorphs in this way, a highly robust linear displacement transducer is produced, and this mechanism is used to drive the lower surface, as shown in Figures 46–48. In addition, normal vertical motion of the whole slider assembly and lower surface **A** is produced by a three-stage mechanical translation mechanism composed of micrometers and springs located in the Upper Chamber.

The active length,  $L$ , of the sectored bimorph can be adjusted by moving the two clamps, **C1** and **C2**, closer or farther apart. This changes the stiffness of the bimorphs (in proportion to  $1/L^3$ ). The increased stiffness or decreased  $L$  also results in a decreased range of travel for a given applied voltage (proportional to  $L^2$ ), and to an increased natural frequency of the lower surface 'drive' (proportional to  $1/L^{3/2}$ ). Since the two clamps, **C1** and **C2**, have to be spaced symmetrically about the strip **C**, changing the clamping positions also changes the horizontal position of the lower surface, **A**. To keep the horizontal distance **A–B** constant, the whole bimorph mount may be relocated by shifting it to the left or right and then relocking it to the Upper Chamber with screw **B**.

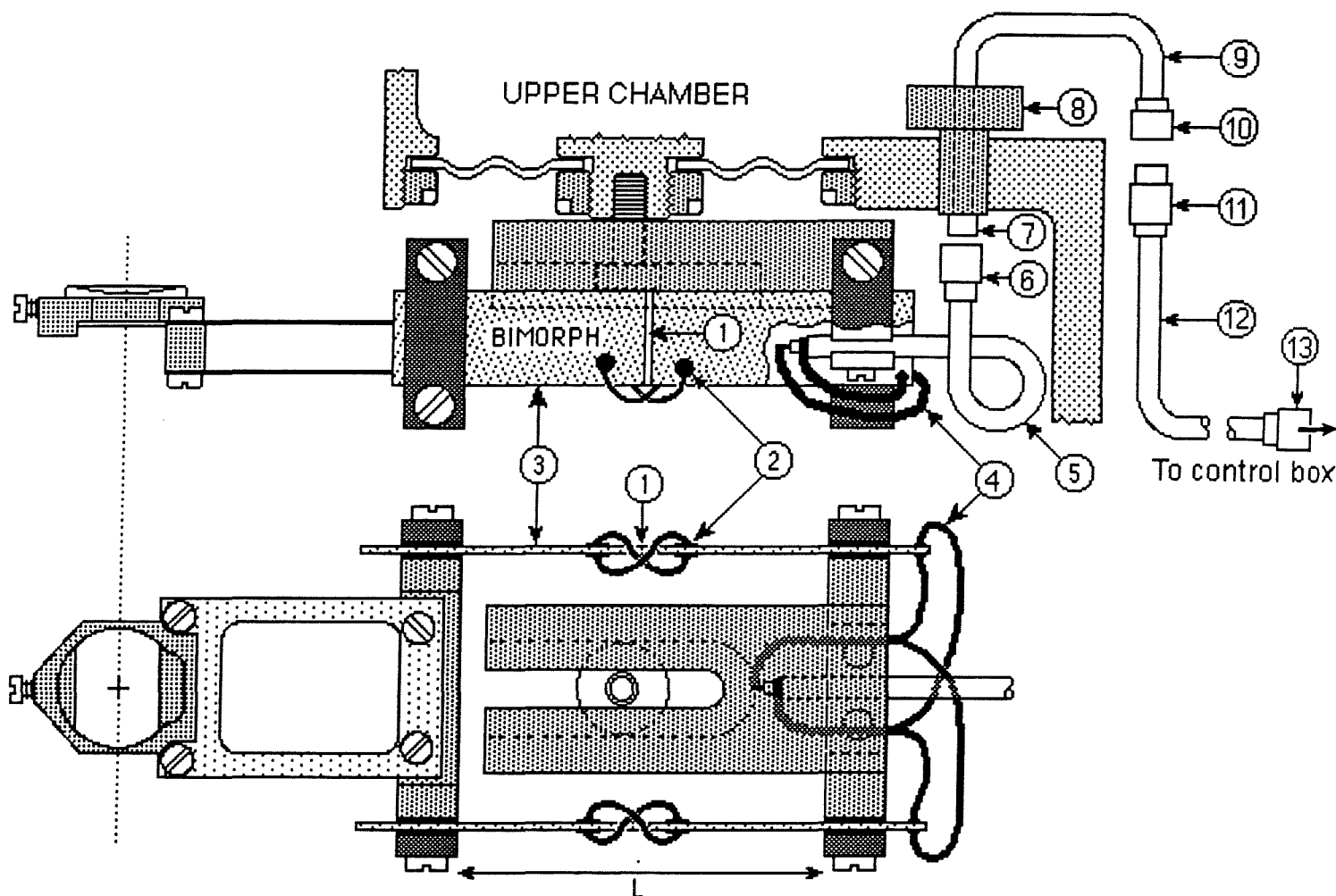


**Figure 47.** Electrical wiring and connections of Bimorph Slider.

Lateral motion of the lower surface A is produced by applying a DC or AC voltage to the bimorphs through a coaxial cable connected to the outside of the Lower Chamber via a Teflon-sealed Lemo-type connector. In most cases, it is desirable to have a 'drive' that (i) can travel over a large distance, (ii) is very rigid (stiff), and (iii) has a high natural frequency (see Theoretical Section below). For a typical PZT bimorph of active length  $L = 30$  mm, the range of travel (at  $\pm 100$  V DC across the bimorph) is about  $\pm 50 \mu\text{m}$ , and the stiffness of a double-bimorph slider is  $K_x \approx 10^4$  N/m (Figure 47). The effective mass of the lower surface support or 'drive' is  $m_x \approx 8$  g, which determines the upper limit for dynamic measurements (corresponding to the resonant frequency of the drive) at approximately  $\nu_x \approx (1/2\pi)(K_x/m_x)^{1/2} \approx 200$  Hz. Higher travel distances, up to 1 mm p-p, can be attained by increasing the active bimorph length,  $L$ , using clamps C1 and C2, but at the cost of a decreasing stiffness. Alternatively, higher stiffnesses  $K_x$  and resonant frequencies  $\nu_x$  can be attained by reducing the

active bimorph length, but this also lowers the travel distance for a given (maximum safe or linear) voltage. Thus, some compromise is always required. The ability to readily change the active bimorph length provides sufficient flexibility for optimizing the system parameters for most types of experiments.

In sliding experiments, it is often desirable to have surfaces moving (shearing) at some *constant* speed or shear rate rather than sinusoidally. This can be achieved with the bimorph slider by applying a triangular voltage signal. This produces constant velocity motion in one direction until the turning point, and then in the reverse direction, repeatedly. In this way, very low or very high constant velocities can be achieved. For example, using the above operating parameters ( $L=30$  mm), the range of practical speeds attainable using a function generator that provides a 1–100V peak-to-peak triangular signal (corresponding to 0.7–70  $\mu\text{m}$  total travel per cycle) is from 0.1 nm/s at a driving frequency of  $\nu=10^{-6}$  Hz to 10 mm/s at  $\nu=10^2$  Hz. For a film thickness of 10 nm, these speeds correspond to shear rates that can be varied from  $\dot{\gamma} = 10^{-4}$  to  $10^6$   $\text{s}^{-1}$  – a range of ten orders of magnitude.

Finally, since bimorphs can both induce and detect motion, the bimorph slider may also be used as a friction force-measuring spring.

#### **Using the Bimorph Slider and Friction device together**

When used together with the Bimorph Slider, the Friction Device can be used as the 'receiver' (Figure 48). One can change the mass and spring dimensions of the Friction Device to optimize it for use with the Bimorph Slider. For example, the mass  $m_y$  of the upper surface or 'stage', and the dimensions of the friction force-measuring springs (length, width and thickness), can be optimized to provide (i) high force sensitivity (bridge output voltage vs. friction force), or (ii) high displacement sensitivity (bridge output voltage vs. lateral displacement), and (iii) high natural frequency  $\nu_y$  of the 'stage'. The latter property is desirable for obtaining a high dynamic range and the ability to measure rapid transient effects such as stick-slip friction. Typical middle of the range operating values are:  $K_y \approx 10^3$  N/m,  $m_y \approx 2.2$  g,  $\nu_y \approx 120$  Hz. When used with a strain-gauge amplifier (MEASUREMENTS GROUP, Model 2311) and chart recorder (SOLTEC, Model 1242) or storage scope recorder (TEKTRONIX, Model 2232), the DC friction force sensitivity should be better than  $\sim 50$   $\mu\text{N}$  ( $\sim 5$  mg), corresponding to lateral displacements of the friction spring of 50  $\text{\AA}$ . Enhanced sensitivities can be obtained when measurements are made in AC mode with a lock-in amplifier (Stanford Research Systems digital two-phase lock-in amplifier Model SR830) which also allows independent measurements of the in-phase and out-of-phase components of the output signal.

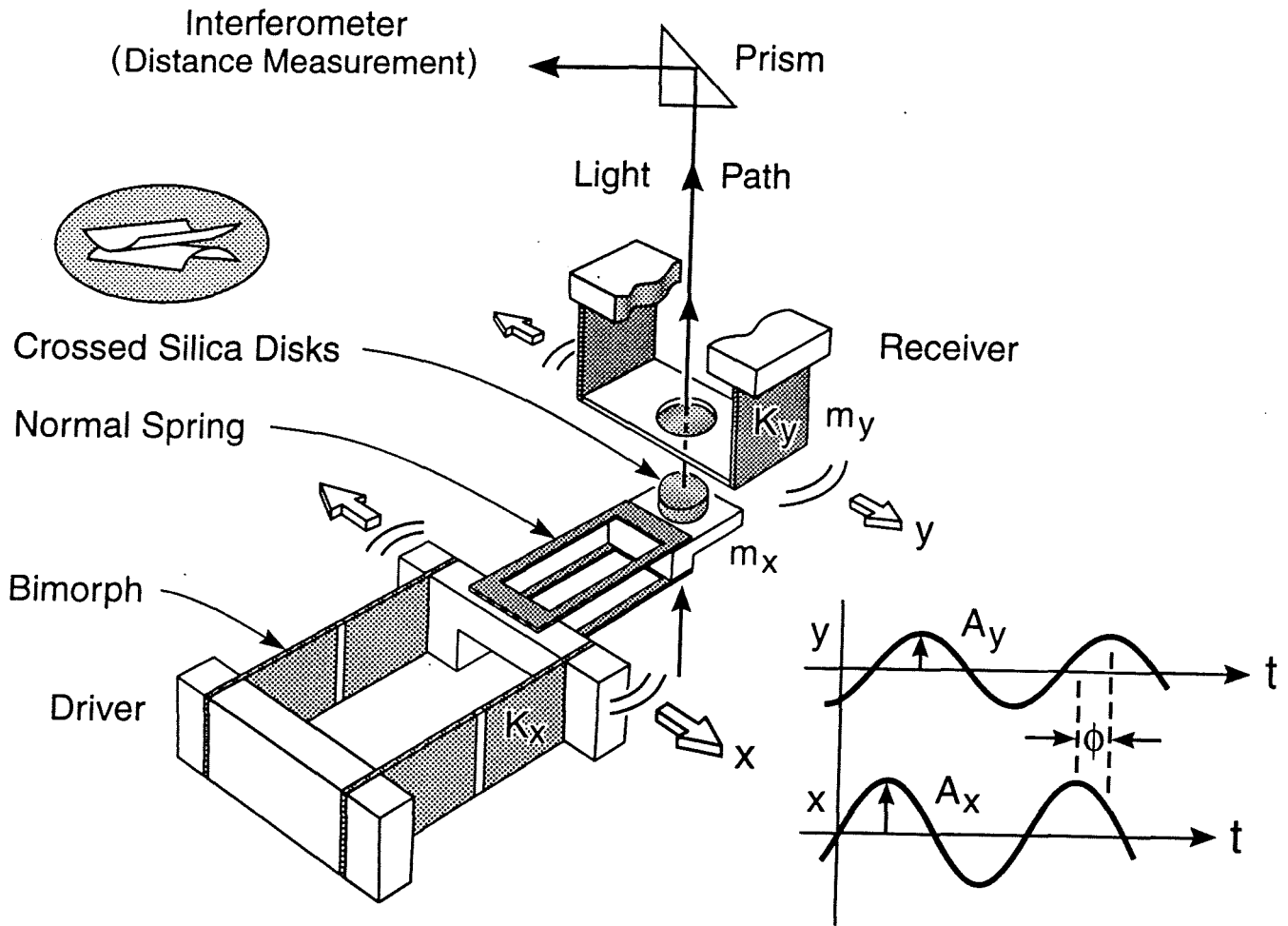


Figure 48. Shear elements of the Bimorph Slider attachment.

In principle, it should also be possible to measure the motion of the friction spring using a capacitance or optical technique, for example, laser light interferometry, instead of strain-gauges. Strain gauge measurements of spring deflections do not have the sensitivity of capacitance or optical techniques but they do have the advantage of fast response times and simplicity of construction and use. Capacitance measurements introduce unwanted forces between the plates, and optical interferometric techniques can be unreliable when used over large distances ( $D \gg \lambda$ ).

The Friction Device also has the capability of driving the upper surface (the stage) at a constant speed using a mechanical drive that is powered by a variable speed DC motor with an encoder readout. The total distance of travel is much larger than can be attained with bimorphs:  $\sim 5$  mm instead of 0.1–1 mm. However, the range of sliding speeds attainable is much more limited, and sinusoidal motions are not feasible as they are with the Bimorph Slider. Nevertheless, when used in this way, the upper friction attachment serves as a complete, self-contained unit, capable of both generating movement and measuring the resulting friction forces. The lower

(bimorph) attachment is only capable of generating movement, and so must be used in combination with the Friction Device whenever friction forces need to be measured as well.

It is also possible to use the Bimorph Slider as a displacement sensor, recording the output voltage produced by the bimorphs when they are disturbed. When used in this way, the motor on the Friction Device is used to move the upper surface (which now becomes the drive), and the lower surface now becomes the stage. This set-up is not as practical as the first one described above because the motor cannot provide AC motion and piezoelectric bimorphs, because they are lossy, are unreliable as DC sensors at low frequencies or driving speeds.

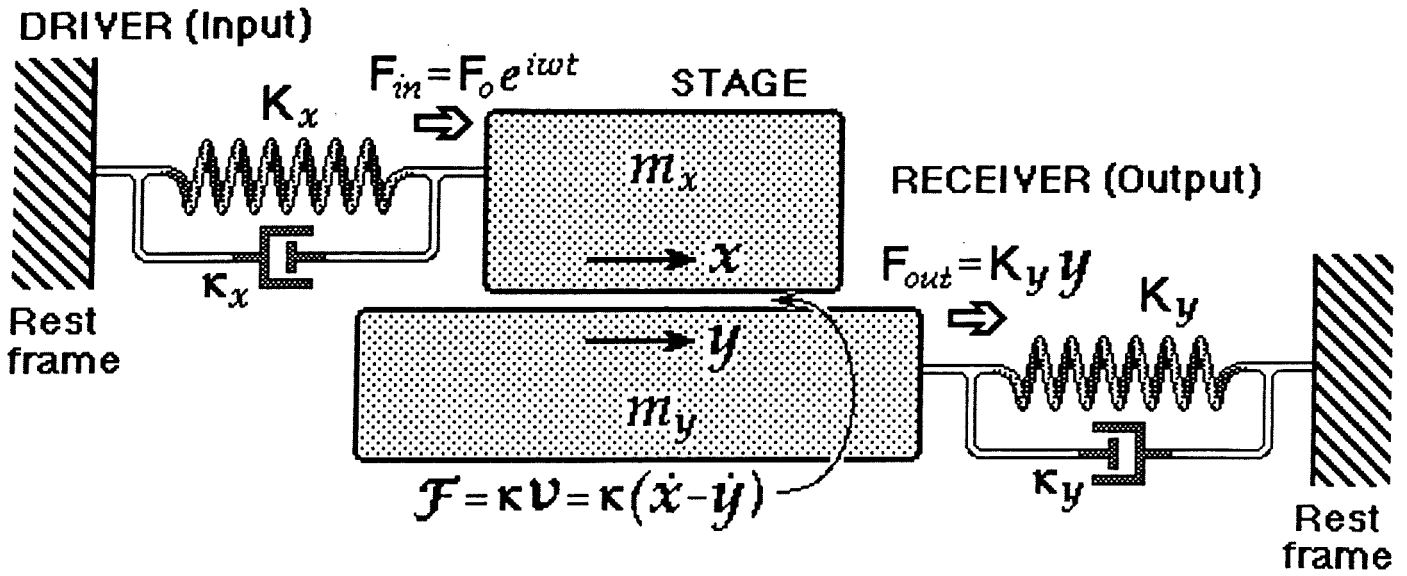
### Equations of motion for Bimorph Slider in AC mode (refer to Figs 48 and 49)

When undergoing forced oscillations, the mechanical system may be described in terms of two coupled, damped, forced harmonic oscillators (Figure 49, top):

$$\begin{aligned} m_x \ddot{x} + K_x x + \kappa_x \dot{x} + \kappa(\dot{x} - \dot{y}) &= F_0 e^{i\omega t} \\ m_y \ddot{y} + K_y y + \kappa_y \dot{y} - \kappa(\dot{x} - \dot{y}) &= 0 \end{aligned} \quad (13)$$

where  $(x - y)$  is the relative lateral displacement of the lower and upper surfaces. The subscripts  $x$  and  $y$  refer to the **drive** (bimorph slider) and **receiver** (stage and strain gauges),  $F_0$  is the driving force, and  $\kappa(\dot{x} - \dot{y}) \equiv \kappa v = \mathcal{F}$  is the real friction force between the two surfaces defined in terms of  $\kappa$ , the damping of the lubricating fluid between the two surfaces. The coefficient  $\kappa$  contains all the information on the friction force between the surfaces, and thus depends on the geometry of the surfaces, on the relative velocity  $v$ , and for non-Newtonian lubrication it will also depend on other factors such as time and previous history. At periodic driving frequencies  $\omega = 2\pi\nu$  much lower than the resonance frequencies  $\omega_0$  of the drive and receiver the inertial terms  $m_x \ddot{x}$  and  $m_y \ddot{y}$  can be neglected. Likewise, we may neglect the two independent damping terms of the drive and stage,  $\kappa_x$  and  $\kappa_y$ , which are both much less than  $\kappa$ , and mainly affect the amplitude of the oscillations close to resonance ( $\omega \approx \omega_0$ ). The glue layers supporting the substrate surfaces are generally much more rigid than the other compliant parts of the system and their contributions are automatically incorporated into  $K_x$  and  $K_y$ . If required, this contribution can be independently calibrated with the two surfaces rigidly clamped together with a metal rod. If the stiffness of the bimorph drive  $K_x$  is greater than that of the friction force-measuring spring  $K_y$  ( $K_x > K_y$ ) the above equations simplify to

$$\begin{aligned} x &= (F_0 / K_x) e^{i\omega t} = A_0 e^{i\omega t} \\ K_y y - \kappa v &= 0 \end{aligned} \quad (14)$$



(A) Reynold's lubrication geometry

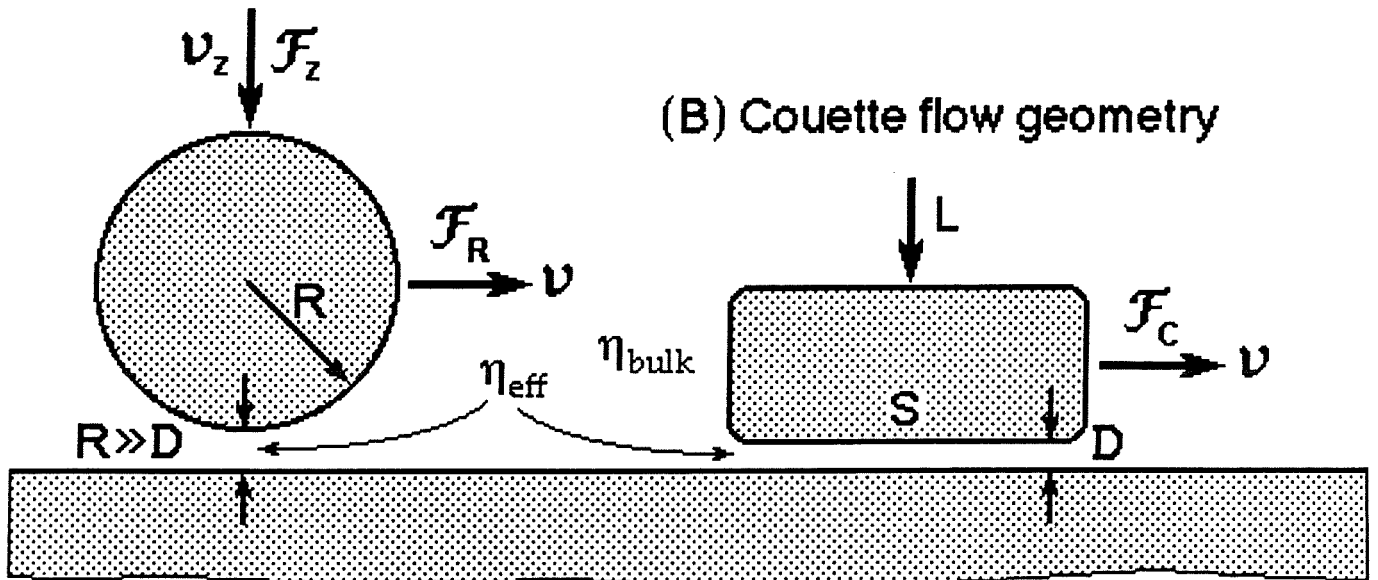


**Figure 49.** Equivalent mechanical circuit of the Bimorph Slider and Friction Device (top). The geometry and direction of motion of the surfaces determines the hydrodynamics of the problem, for example, whether sphere on flat (A) or flat on flat (B), as described in the text.

The forced movement of the lower surface  $x$  is thus transmitted via the friction force to the upper surface where it is measured by the strain gauges as a displacement,  $y$  (Figure 48). The oscillatory response is of the form

$$y = A_y \exp[i(\omega t + \phi)] \quad (15)$$

where the amplitude and phase of the upper surface are given by

$$A_y = \frac{A_0}{[1 + K_y^2 / (\omega^2 \kappa^2)]^{1/2}}$$

$$\tan \phi = -\frac{K_y}{\omega \kappa} \quad (16)$$

From the above, the damping coefficient is given by

$$\kappa = \frac{K_y}{\omega [(A_0 / A_y)^2 - 1]^{1/2}} = \frac{K_y}{\omega \tan \phi} \quad (17)$$

We may note that all the parameters on the RHS of the above equations are known or directly measurable. The above solution is similar to one which applies to two surfaces undergoing normal vibrations along the z-direction [Israelachvili, J. N., Kott, S. J. and Fetters, L. J., *J. Polym. Sci., Polym. Phys. Ed.* **1989**, 27, 489.]. The main difference between normal and shearing motion is in the damping coefficient,  $\kappa$ , which depends on different surface geometry parameters (grouped in  $\Omega$ ) and the viscosity. For example, for a sphere moving towards or away from a flat surface in a simple Newtonian liquid with shear viscosity  $\eta$  (Figure 49A), we have

$$\mathcal{F} = \kappa v \equiv \Omega \eta v = 6\pi R^2 \eta v / D \quad (18)$$

whereas for a (non-rotating) sphere moving parallel to a flat surface surface†

$$\mathcal{F} = \kappa v \equiv \Omega \eta v = 6\pi R \eta v \left[ \frac{8}{15} \log \left( \frac{2R}{D} \right) + \dots \right] \quad (19a)$$

$$\approx \frac{16}{5} \pi R \eta v \log \left( \frac{2R}{D} \right) \quad \text{for } R \gg D \quad (19b)$$

where  $R$  is the radius of the sphere and  $D$  is the closest distance of separation in both cases. For two crossed cylinders, the geometry adopted here, the effective hydrodynamic radius  $R$  is related to the cylinder radii  $R_1$  and  $R_2$  by (Chan, D. Y. C. and Horn, R. G., *J. Chem. Phys.* **1985**, 83, 5311)

$$R^2 = 2(R_1 R_2)^{3/2} / (R_1 + R_2) \quad (20)$$

when  $R_1 = R_2$ , we may put  $R = R_1 = R_2$  and the geometry is equivalent to a sphere of radius  $R$  near a flat surface.

† O'Neill, M. E. *Mathematica* **1964**, 11, 67.

O'Neill, M. E.; Stewartson, K. J. *Fluid. Mech.* **1967**, 27, 705.

Goldman, A. J.; Cox, R. G.; Brenner, H. *Chem. Eng. Sci.* **1967**, 22, 637.

Another important geometry that was also studied is that of two flat parallel surfaces (Figs 1 and 49B). If one surface of area  $S$  is moving laterally past the other at a fixed surface separation  $D$ , the situation corresponds to Couette flow and the viscous force is given by

$$\mathcal{F} = \kappa v \equiv \Omega \eta v = \frac{\text{Area} \times \text{viscosity} \times \text{velocity}}{\text{Film thickness}} = \frac{S \eta v}{D} \quad (21)$$

We should emphasize again that the above relations hold only for Newtonian fluids. In some cases, when film thicknesses approach molecular dimensions and fluids cease to be Newtonian, we shall use the above equation to compute an effective viscosity,  $\eta_{\text{eff}}$ , defined by

$$\eta_{\text{eff}} = FD/Sv \quad (22)$$

where all the parameters on the RHS are measured values.

If we deal with a viscoelastic liquid, the viscosity  $\eta$  may be represented by a complex function  $\eta = \eta' - i\eta''$  where  $\eta'$  is the viscosity component that is in phase with the rate of strain, and  $\eta''$  is the component that is 90 degrees out of phase. Solving Eq. 14 for the case of linear viscoelasticity, we obtain

$$\begin{aligned} \eta' &= \frac{K_y f \sin \phi}{\omega \Omega [f^2 - (2f \cos \phi - 1)]} \\ \eta'' &= \frac{K_y (f \cos \phi - 1)}{\omega \Omega [f^2 - (2f \cos \phi - 1)]} \end{aligned} \quad (23)$$

where  $f = (A_x/A_y)$ . The magnitude of the viscosity is given by

$$\eta = \sqrt{\eta'^2 + \eta''^2} = \frac{K_y}{\omega \Omega [f^2 - (2f \cos \phi - 1)]^{1/2}} \quad (24)$$

and the 'storage' and 'loss' shear moduli are, respectively

$$G' = \omega \eta'', \quad G'' = \omega \eta' \quad (25)$$

which together define the complex 'shear' modulus  $G = G' + iG''$ . We should note that  $\eta''$  and  $G'$  are proportional to the energy stored elastically in the system, whereas  $\eta'$  or  $G''$  are proportional to the energy lost per cycle through irreversible viscous (thermal) dissipation. When the viscosity is different from the bulk value, as occurs in thin films, the 'effective viscosity',  $\eta_{\text{eff}}$ , as measured by use of the hydrodynamic equations 18–22 and defined by Eq. 24 is used instead of  $\eta$  in all of the above equations.

It is also useful to know the shear rates, the shear strains and the shear stresses. When using sinusoidal signals the shear rate can be calculated from

$$\dot{\gamma} = V/D = \frac{i\omega[A_0 - A_y \exp(i\phi)]\exp(i\omega t)}{D} \quad (26)$$

In general, we will refer to the maximum shear rate, given by

$$\dot{\gamma} = \frac{\omega \sqrt{(A_y \sin \phi)^2 + (A_0 - A_y \cos \phi)^2}}{D} \quad (27)$$

Using Eq. 24, this can be transformed into

$$\dot{\gamma} = \frac{K_y A_y}{\eta \Omega D} \quad (28)$$

The maximum shear strain,  $\gamma$ , is consequently

$$\gamma = \dot{\gamma} / \omega \quad (29)$$

It is now straightforward to calculate the maximum shear stress,  $\sigma$ , imposed on the sample using the general viscoelastic relations:

$$\sigma \equiv F_0 / S_{eff} = \eta_{eff} \dot{\gamma} \quad (31)$$

Equation 22 allows us to calculate an effective area of shear,  $S_{eff}$  in any geometry.

All the above equations assume that the response  $y$  is directly proportional to  $x$ , which is the case in the absence of yield points as occurs in the tribological regime. They also assume that the viscosities  $\eta'$  and  $\eta''$ , and shear moduli  $G'$  and  $G''$  depend only on the frequency and not on the amplitude of the stress or strain, which has indeed been verified in experiments with thicker films [Luengo, et al., *Macromolecules* (submitted, 1996)].

## BIMORPH VIBRATOR

### MAIN FEATURES

- ☆ Detects vertical displacements of the lower surface, especially oscillatory.
- ☆ Can be used to measure thin film viscosity and rheological properties.
- ☆ Versatile mount that can receive other types of attachments, including a fixed-stiffness force-measuring spring.

### DESCRIPTION

The BIMORPH VIBRATOR (see Figures 17 and 28) is an attachment for vibrating one surface (vertically) while measuring – for example, with a lock-in amplifier – the amplitude and phase of the vibrations induced in the other surface. This attachment is useful for measuring rheological and visco-elastic properties of fluids and thin fluid films near surfaces or between two surfaces. For experiments with the bimorph totally immersed in a liquid such as water (Figure 50), it is possible to chemically and electrically seal the bimorph surfaces and its attached wires by dipping slowly into HUMISEAL Protective Coating type 1A20, then withdrawing at 1 cm/min, then allowing to dry overnight. In this way a semi-hard, chemically inert 15-20  $\mu\text{m}$  thick polyurethane film protects the surfaces, while exhibiting sufficient flexibility (elasticity) so that the mechanical characteristics of the bimorph are not impaired.

The equations of motion of the bimorph vibrator are similar to those of the Bimorph Slider, detailed above, except that the oscillatory motion is normal rather than lateral (cf. Figure 49). This means that the liquid film experiences squeeze flow rather than shear flow, so that the response is much more sensitive than in the case of the Slider. The Bimorph Vibrator has provided some important results on the viscosity of thin fluid films and the location of the slipping plane that cannot be obtained with other techniques. See, for example:

1. **Measurements of Dynamic Interactions in Thin Fluid Films: the Transition from Simple to Complex (Non-Newtonian) Behavior.**  
J. N. Israelachvili, S. J. Kott, L. Fetters, *J. Polymer Sci., Part B: Polymer Physics* **27** (1989) 489-502.
2. **Measurements and Relation Between the Dynamic and Static Interactions Between Surfaces Separated by Thin Liquid and Polymer Films.**  
J. N. Israelachvili, *Pure & Appl. Chem.* **60** (1988) 1473-1478.
3. **Shear Properties and Structure of Simple Liquids in Molecularly Thin Films: the Transition from Bulk (Continuum) to Molecular Behavior with Decreasing Film Thickness.**  
J. N. Israelachvili, S. J. Kott, *J. Colloid Interface Sci.* **129** (1989) 461-467.

The Bimorph Vibrator also comes with a number of additional attachments, including one for mounting a fixed stiffness spring (which takes up very little volume and so can be used with very small quantities of liquid), and a general-purpose mounting connector suitable for fitting new attachments that one may wish to design and incorporate in the future.

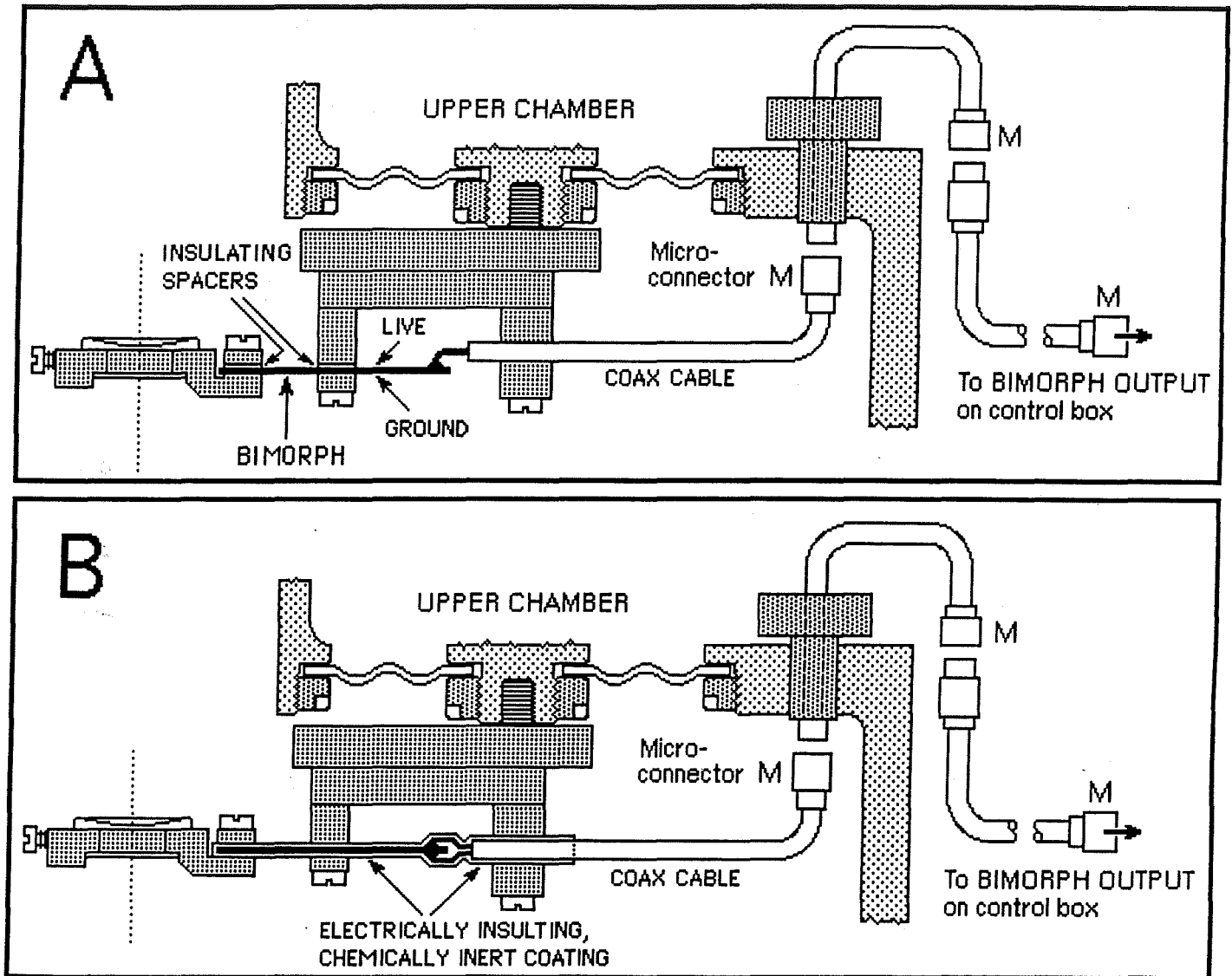


**Figure 50.** Schematic drawing of BIMORPH VIBRATOR assembly. (A) Unsealed bimorph for 'droplet' experiments in vapors. (B) Sealed bimorph for experiments in liquids. Note: when handling the micro-connectors (M), do not push or pull the coaxial cable – always connect and disconnect by turning and pushing or pulling the brass hex head.

## **OTHER FEATURES, INCLUDING OPTIONAL ATTACHMENTS AND CUSTOMIZED MODIFICATIONS**

Various additional attachments and modifications are available for use with the SFA3. Others are in a stage of development. Custom-built and specialized attachments can always be made for, or constructed by, the user since the SFA3 is a modular apparatus, designed to have its parts interchanged and added to (an excellent book that provides useful hints on designing small machine components is *Foundations of Ultraprecision Mechanism Design* by S. T. Smith and D. G. Chetwynd, Gordon and Breach Science Publishers, Amsterdam, 1992, 1994). Examples of the types of additional attachments or modifications that are available are as follows:

### **☆ Customized modifications**

Purchasers can specify certain customized 'modifications' for their SFA, for example, the dimensions of the certain parts, the mass of the moving surfaces in friction experiments, the stiffness of the friction-force-measuring-spring, etc. One or other of these options and modifications could be very important for optimizing certain types of experiments.

### **☆ Experiments with small volumes of liquid**

The capacity of the SFA3 chamber is about 75 ml, depending on which attachment is being used. A special lower chamber for doing experiments with small quantities of liquids (about 25 ml) is available (see Figure 51). This chamber also has an adjustable-height window for the incoming light beam to allow for nearly opaque liquids to be studied.

### **☆ Variable friction force-measuring spring**

An attachment is available that allows the stiffness (inertia) of the 'stage' in friction measurements to be adjusted from outside the apparatus during experiments, without the need to open the apparatus. Stiffnesses can be varied over a range of two orders of magnitude, which can be very useful in certain types of shear experiments.

### **☆ Installing surfaces 'under water' for biological experiments**

The retractable side window in the Lower Chamber of the SFA3 has been so designed to allow for its easy removal so that pre-prepared surfaces can be installed into the chamber 'under water' without removing them from solution. This is important when surfaces that have been pre-coated with delicate biological molecules in a Langmuir-Trough, for example, must be transferred into the apparatus without removing them from water. Installation is achieved as follows: place the filled apparatus on its side, remove the

window, fit the 'deposition cell' to the window (this Teflon cell or bath, which has to be specially made, is filled with liquid that immerses two small beakers containing the ready-to-be-installed surfaces), remove the 'plug' of the cell and insert the two disks. Special dove-tailed disks are available that can be inserted into the apparatus straight through the side window. These must be used with special dove-tailed disk mounts on the Piezo Mount and force-measuring spring, as shown in Figure 52.

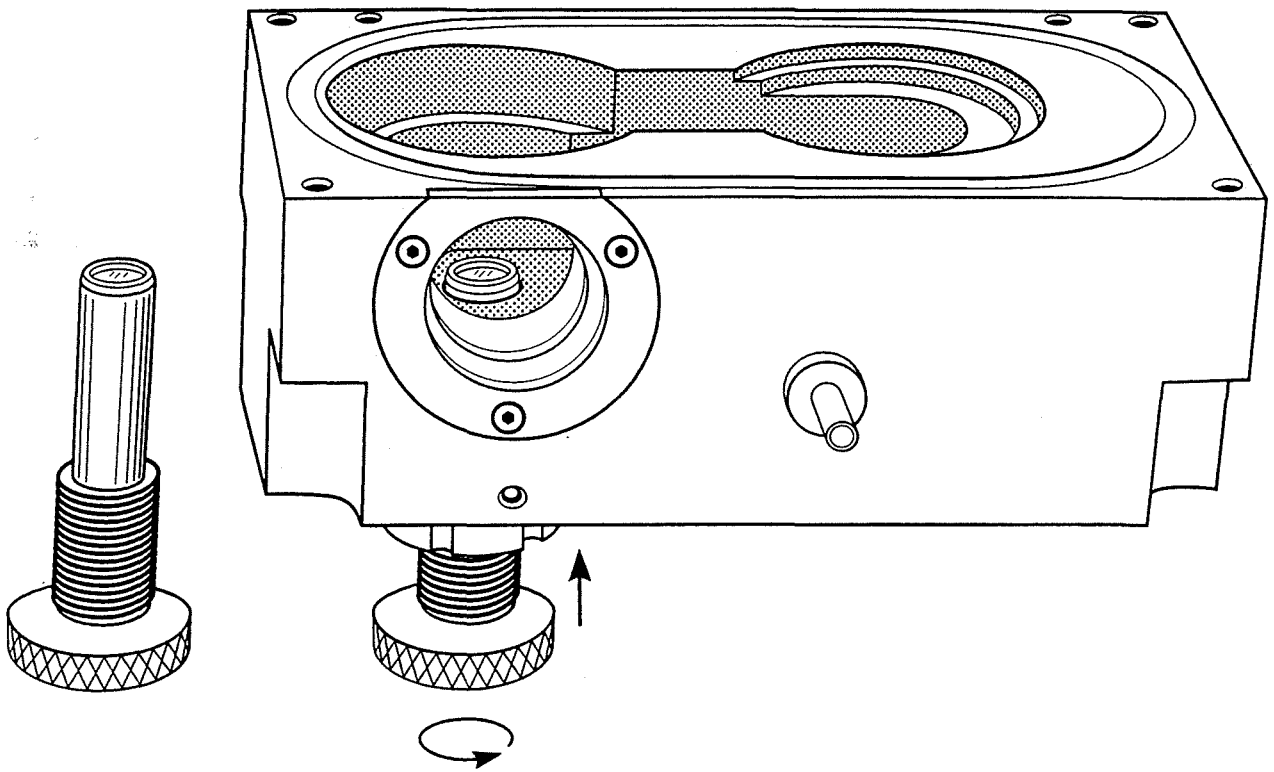


**Figure 51.** Small volume bath with height-adjustable lower window.

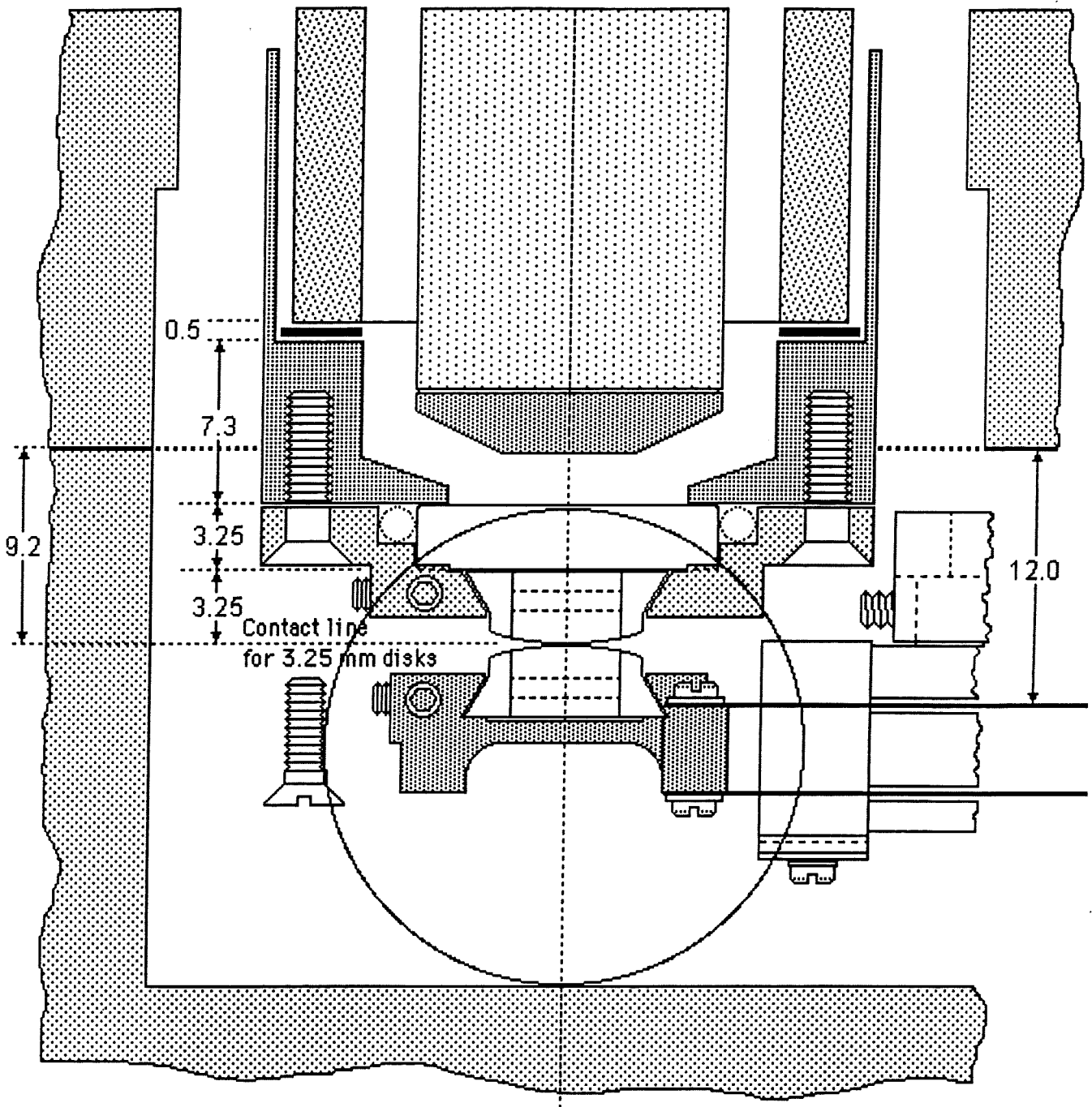


**Figure 52.** Dove-tailed disks and disk mounts, and view through side window.

END OF PART 3

# **PART IV**

## **FURTHER INFORMATION, SPECIFICATIONS & REFERENCES**

## PERFORMANCE SPECIFICATIONS OF SFA 3 AND ATTACHMENTS

The following values are approximate, and should be calibrated for each instrument and attachment before use as described in the User's Manual. It is also advisable to check these calibrations periodically or before critical experiments. This is because some properties, for example, of piezoelectric crystals and bimorphs, can age with time and anyway depend on the temperature and humidity.

### Power requirements

100 to 240 V and 50 or 60 Hz (specify when ordering).

### SFA 3 Basic Unit<sup>1</sup>

Sensitivity of measuring normal and adhesion forces: 10 nN (1 millidyne).

Distance resolution: 0.1 nm (1 Å)<sup>2</sup>

Lateral distance resolution: 1 μm.<sup>3</sup>

Range of force-measuring spring stiffnesses attainable: 50 – 5x10<sup>5</sup> N/m (4 decades).

Maximum compressive pressure attainable (using curved surfaces of radii

0.5–1 mm and a thin layer of hard glue): 0.5 MPa (5,000 atm).

Thermal drift: <0.1 Å/sec (after 1 hr equilibration in a room or enclosure that is temperature stabilized to ±0.1°C).

### Friction Device (semi-conductor type)

Sensitivity of measuring lateral, shear and frictional forces: 1–10 μN = 0.1–1 dyne.<sup>4</sup>

Friction spring stiffness: 10<sup>10</sup> N/m = 10<sup>7</sup> dyn/cm (other stiffnesses available).

Lateral distance sensitivity: approx. 10 Å.<sup>4</sup>

Resolution of measuring Friction Coefficients: 0.0001.<sup>4</sup>

Range of lateral sliding speeds: 0.05 to 5 μm/s using a *single* motor, but range can be increased almost indefinitely up or down by exchanging motors with different gearheads.

### Bimorph Slider

Maximum recommended applied voltage (peak to peak): ±50 V (100 V p-p).

Maximum lateral displacement (at maximum voltage): ≈ 1 mm.

Stiffness of bimorphs: 10<sup>7</sup> mN/m.<sup>5</sup>

Range of lateral sliding speeds attainable: 10<sup>-8</sup> to 1 cm/s.

Resonant frequency of bimorphs and support: ≈ 250 Hz.<sup>5</sup>

Recommended range of driving frequencies: 10<sup>-6</sup> to 200 Hz (or up to resonance).

Maximum shear rates attainable: 10<sup>5</sup> s<sup>-1</sup> in squeeze mode (much higher rates are attainable in shear/sliding mode depending on the test fluid).

- <sup>1</sup> All stainless steel parts of internal surfaces are 316 or 316L chemically non-corrosive, non-magnetic steel. Other internal parts are either silica, PTFE (Teflon) or Kel-F.
- <sup>2</sup> Assumes a medium sized spectrometer (1/4 to 1/2 meter type). There is no theoretical limit to the distance resolution. Using special image analysis techniques, Kyle and Davis [Reference] have shown that surface separations can be measured reproducibly to ±0.15 Å.
- <sup>3</sup> Much smaller particles trapped between two surfaces can be "detected" due to the much larger elastic deformations they produce on the surrounding surfaces.
- <sup>4</sup> Depends on the sensitivity and quality of the strain gauge amplifier/bridge, and on the type of strain gauge being used. Values quoted are for semi-conductor gauges. Resistance strain gauges are about 100 times less sensitive.
- <sup>5</sup> Depends on number of bimorphs used (double or quadruple). Stiffness and hence resonant frequency can be varied up or down by changing the bimorphs' active clamping length, which is adjustable.

**TABLE II: COMPLETE LIST OF PARTS & SUPPLY ITEMS**

The following Table is a complete inventory of all the PARTS in each UNIT and their accompanying SUPPLY items. Numbers in brackets refer to the number of parts and supply items, including spares, provided per unit (if more than 1).

PART No.	NAME (No. PER UNIT)	ACCOMPANYING SUPPLY ITEMS
<b>01000 UPPER CHAMBER</b>		
01010	UPPER CHAMBER	Main O-ring (3), top O-ring (3), shaft O-ring (3), male Luer connector (2), female Luer connector (2), female Luer cap (2).
01030	CANTILEVER SPRING	Long screws (4), short screws (2), assembly spatula, screw driver.
01040	TRANSFER SPRING	Flathead screws (2).
01050	SPRING HANGER	
01060	SPRING CARRIER	Screws (2), washers (2).
01070	HANGER BUTTON	
01080	SPRING GUIDE	
01090	GUIDE PINS (2)	
01100	OUTER RING	
01110	INNER RING	
01120	DOVETAIL SCREW	
01130	WIDE KEY	
01140	NARROW KEY	
01150	MICROMETER NUT	Differential micrometer – attached.
01160	SEALING NUT	
01170	LOCKING SCREW	
01180	GEARS STOP	Screws (2).
01190	FRONT PLATE	Screws (3).
01200	BACK PLATE	Screws (4).
01210	TRANSFER LEVER	Roller bearings w. washers (2) – attached.
01220	BEVEL GEAR	Set screws (2).
01230	PINION SHAFT	
01240	GEARS MOUNT	Mitre & bevel gears, matching pair – attached.
01250	GEAR SHAFT	
01260	GEAR WHEEL	Set screw.
01270	COUPLING CONNECTOR	Set screw (2).
01280	---	
01290	TEFLON BELLOWS (2)	
01300	ANTIBACKLASH SPRING	Medium-sized serrated forceps.
01310	COMPRESSION SPRING	

00040	MOTOR HOUSING	Micrometer head, O-ring, flexible coupling, DC motor with gearbox and encoder, 6-pin electric cable, low voltage DC motor power supply, encoder display counter, limit switches (2) screwed on board with scale, small screw with washer.
00050	MOTOR BUSHING	Dowel pins (2) – attached, flathead screws (2).
<b>02000</b>		<b>LOWER CHAMBER</b>
02010	LOWER CHAMBER	Silica window – attached, side window O-ring (2), inlet O-ring (3), thermistor O-ring (4), syringe port O-ring (3), heaters (2) with electric cable, male Luer connector (2), female Luer connector (2), m-m Luer coupling (1), m-f Luer coupling (2), f-f Luer coupling (2), female Luer cap (2), PTFE valve, Teflon tubing (2), 50 ml syringe.
02030	ENTRANCE FRAME	Silica window – attached.
02040	VIEWING FRAME	Silica window, flathead screws (4).
02050	CHAMBER SCREWS (4)	
02060	HINGE	Ovalhead screws (2).
02070	THERMISTOR HOLDER	Thermistor (2).
02080	THERMISTOR PLUG	
<b>03000</b>		<b>BASE</b>
03010	BASE PLATE	Grounding screw, circular spirit level.
03020 A	BASE HINGES A (2)	Flathead screws (8).
03020 B	BASE HINGES B (2)	
03020 C	HINGE PINS C (4)	
03030 A	LEG EXTENSION (3)	Hex nut (3), washer (3).
03030 B	LEG NUT (3)	
03030 C	BASE LEG (3)	
03040	RUBBER PADS (3)	neoprene rubber – attached, steel balls (3) – attached.
03050 A	LOCATING DISK A	Wood screws (6).
03050 B	LOCATING DISK B	
03050 C	LOCATING DISK C	
<b>04000</b>		<b>VARIABLE SPRING</b>
04010	DOVETAIL SLIDE	
04020	SLIDER MOUNT	Screw.
04030	SLIDER NUT	Flathead screws (2).
04040	UPPER SLIDE	
04050	LOWER SLIDE	
04060	SADDLE	Flathead screws (2).
04070	UPPER RETAINER	
04080	LOWER RETAINER	Screws (2).
04090	LEAD SCREW	Bevel gear with pin & washer.
04100	CLAMP SHIM	
04110	CLAMP PIN (2)	
04120	FORCE SPRING (2 + 2 SPARE)	
04130	DOVETAIL SCREW	
00020	DISC MOUNT	Screws (4 +2 spare), silica discs (2).
00030 A	DISK SCREW (1+ 2 spare)	
00030 B	SCREW TIP (1+ 2 spare)	

<b>05000</b>		<b>PIEZO MOUNT</b>
05010	CRYSTAL MOUNT	Piezo crystal tube – attached, wire inserts – attached, cable with Lemo connector.
05020	DISC MOUNT	
05050	EXIT FRAME	Silica window – attached.
05060 A	PIEZO INSULATOR A	
05060 B	PIEZO INSULATOR B	
00030 A	DISK SCREW (1+ 2 spare)	
00030 B	SCREW TIP (1+ 2 spare)	
00080	CLAMPING RING	Long screws (2).
<b>06000</b>		<b>MIRROR</b>
06010	UPPER BASE	This UNIT usually comes fully assembled. Remote control cables (3).
06020	MIRROR BASE	Flathead screws (4), helical spring with screw.
06030	MIRROR SLIDER	Ball bearings (36) – attached, remote control cable.
06040	MIRROR SWIVEL	Screws (2), flathead main screw, remote control cable.
06050	SLIDER GUIDE (2)	
06060	SCREW HEAD	Roller bearing.
06070	MIRROR MOUNT	Rectangular mirror – attached, ball bearings (2), spring with screw,
06080	MIRROR TURNTABLE	Flathead screw.
06090	PIVOT PINS (2)	
06100	PIN	
<b>07000</b>		<b>OPTICS STAND</b>
07010	OPTICS BASE	
07020	SWIVEL RING	Large screw.
07030	SWIVEL ROD	
07040	LOCKING KNOB (2)	
07050	LOCKING SCREW (2)	
07060	MICROSCOPE PLATE	Flathead screws (3), motor screws (2), reversible motor with cable, belt, large gear wheel, small gear wheel.
07070	MOTOR MOUNT	Top screw, bolting screws (2), reversible motor w. cable, belt, gear wheel.
07080	MICROMETER MOUNT	Set screw, bolting screws (4), micrometer head.
07090	MICROMETER NUT	Set screw.
07100	ARM ROD	Glass plate – attached, flathead screws (2).
07110	ARM PLATE	Thumb screw.
07120	PLATFORM	
07130	PRISM DOVETAIL	
07140	DOVETAIL PIN	Helical spring.
07150	MICROSCOPE DOVETAIL	Flathead bolting screws (4), microscope stage.
07160	END PLATE	Bolting screws (2).
07170	CONTROL SCREW	
07180	CONTROL KNOB	
07190	PRISM SUPPORT	Screw, nut & washer (2), small screw, nut & washer (2).
07200	MICROSCOPE TUBE	Thrust bearing (1) with washers (2).
07210	TURNTABLE	

07220	ARM HOLDER	Set screw (2), clamping screw.
07230	SOCKET SCREW	
07240	PRISM TABLE	Prism.
07250	PRISM SCREW	
07260	SPRING ARM	Helical spring.
07270	WHEEL AXLE	
07280	---	
07290	MICROSCOPE TUBE	Objective lens.
<b>08000 SYRINGE INJECTOR</b>		
08010	SYRINGE SUPPORT	Small syringe, syringe needles (2).
08020	SYRINGE BALL	
08030	CHECK NUT	
08040	SYRINGE SLEEVE	
08050	RECEPTACLE	Luer connectors.
08060	BALL HOLDER	
08070	BALL RETAINER	
08080	PORT PLUG	
08090	PORT STUDS (3)	
08100	HEX NUTS (3)	
08110	RECEPTACLE HOLDER	Bolting screws (3).
<b>11000 FRICTION DEVICE</b>		
11010	RING HOLDER	Bolting screw.
11020	SPRING HOUSING	Teflon sealing plugs (2) – attached, O-ring.
11030	COUPLING	Bolting screws (2).
11040	MICROMETER CONNECTOR	Set screws (2), O-ring.
11050	TRANSLATION STAGE	4-pin connector, wired – attached.
11060	FLAT DISK	
11070	COMPRESSION SPRING	
11080	TRANSLATION SPRING (2)	Bolting screws (8).
11090	SPRING CLAMP A (2)	
11100	SPRING CLAMP B (2)	
11110	FRICTION TUBE	Bolting screws (4), 4-pin connector, wired – attached.
11120	FRICTION SPRING (2 + 2 spare)	Bolting screws (4), semi-conductor or resistance strain gauges, temperature compensated, mounted & wired.
11130	TUBE CLAMPS (2)	
11140	DISK SUPPORT	Bolting screws (4), silica disk (2), disk screw (2).
11150	SUPPORT CLAMPS (2)	
11160	FRICTION COVER	Silica window – attached, O-ring (2), extra long clamping screws (2).
11171	ELECTRIC CONNECTOR	O-ring, 4-pin Lemo receptacle.
11180	MICROSCOPE TUBE	Objective lens.
00040	MOTOR HOUSING	Micrometer head, O-ring, flexible coupling, DC motor with gearbox and encoder, 6-pin electric cable, low voltage DC motor power supply, encoder display counter, limit switches (2) screwed on board with scale, small screw with washer.
00050	MOTOR BUSHING	Dowel pins (2) – attached, flathead screws (2).

<b>12000</b>		<b>BIMORPH SLIDER</b>
12010	SLIDER MOUNT	Bimorphs, wired w. connector (2 + 2 spare).
12020	CABLE CLAMP	Screws (2).
12030	LOCKING SCREW	
12040	SPRING MOUNT	
12050	BIMORPH CLAMP (4)	Screws (8).
12060	MICA SPACERS (8)	
12070	SLIDER SPRING A (2) SLIDER SPRING B (2)	Bolting screws (4).
00090	SEALING CONNECTOR	Coax cable with miniature end-connector.
00020	DISC MOUNT	Screws (4 +2 spare), silica discs (2).
00030 A	DISK SCREW (1+ 2 spare)	
00030 B	SCREW TIP (1+ 2 spare)	
<b>13000</b>		<b>BIMORPH VIBRATOR</b>
13010	BIMORPH MOUNT	Bolting screws (4)
13020	BIMORPH SUPPORT	Bimorph strip, wired with connector (1 + 1 spare).
13030	CLAMP A	Screws (2)
13040	CLAMP B	Screws (2)
13050	LENS HOLDER	Screws (4)
13060	FIXED MOUNT	
13070	BIMORPH SPRING (4)	Screws (4)
13080	LOCKING SCREW	
00020	DISC MOUNT	Silica discs (2).
00090	SEALING CONNECTOR	Coax cable (no need if already provided with SLIDER)
00030 A	DISK SCREW (1+ 2 spare)	
00030 B	SCREW TIP (1+ 2 spare)	
<b>15000</b>		<b>ACCESSORIES</b>
15010	CONTROL BOX	Connecting cables.
15020	PACKING CASE	
15030	TOOL KIT (assembly)	Screw driver set, Allen keys, tweezers, forceps, spatula.
15040	MISC. SUPPLIES	Glue (Epon Resin 1004, 1007, 1009), spirit level
15050	MANUAL	
15060	VIDEOS	

## REFERENCES TO SFA TECHNOLOGY AND LITERATURE ON FORCE MEASUREMENTS

### Description of SFA3

- "Adhesion and Short-Range Forces Between Surfaces – New Apparatus for Surface Force Measurements", J. N. Israelachvili, P. M. McGuigan, *J. Mater. Res.* **5** (1990) 2223-2231.

### Description of SFA Mk 2

- "Measurement of Forces Between Two Mica Surfaces in Aqueous Electrolyte Solutions in the Range 0-100 nm", J. N. Israelachvili, G. E. Adams, *J. Chem. Soc., Faraday Trans. I* **74** (1978) 975-1001.

### Description of the optical interference (FECO) technique

- Tolansky, S., "*Multiple Beam Interferometry of Surfaces and Films*", Oxford University Press, 1948; "*An Introduction to Interferometry*", Longmans, Green & Co., London, 1955.
- **Review of modern deposition techniques:** Hass, G., Heaney, J. B. and Hunter, W. R., *Physics of Thin Films*, **12**, 1 (1982).
- "Thin Film Studies Using Multiple Beam Interferometry", J. Israelachvili, *J. Colloid Interface Sci.* **44** (1973) 259-272.
- **Papers showing photos of FECO fringes:** See above paper, as well as "Role of Hydrophobic Forces in Bilayer Adhesion and Fusion", C. A. Helm, J. N. Israelachvili, P. M. McGuigan, *Biochemistry* **31** (1992) 1794–1805. One can employ a second camera at the same time as looking at the FECO fringes by simply splitting the emerging beam by 90° using a normal 50-50 beam-splitter. The vertical (undeflected) beam can then be directed to a "top-view" camera, such as a CCD camera or fluorescence microscope, and the horizontal (deflected) beam is directed to the spectrometer, as in normal operations. For a description, with pictures, of how to combine normal optical microscopy with FECO interferometry see "Direct Visualization of Cavitation and Damage in Ultrathin Liquid Films", T. Kuhl, M. Ruths, Y-L. Chen, J. Israelachvili, *Journal of Heart Valve Disease* **3** (1994) S117–S127.
- **FECO spectroscopy (extension to non-uniform and absorbing media):** "Enhanced absorption within a cavity: a study of thin dye layers with the Surface Forces Apparatus", C. Müller, P. Mächtle and C. A. Helm, *J. Phys. Chem.* **98** (1994) 11119–11125. "A thin absorbing layer at the center of a Fabry-Pérot interferometer", P. Mächtle, C. Müller and C. A. Helm, *J. Phys. II France* **4** (1994) 481–500.

### Using surfaces other than mica in SFA studies

- **Sapphire:** Horn, R.G., Clarke, D.R., and Clarkson, M.T., "Direct Measurements of Surface Force Between Sapphire Crystals in Aqueous Solutions", *J. Mater. Res.* **3** (1988) 413-416.
- **Zirconia:** "Effect of substrate on shearing properties of ultrathin polymer films", S. J. Hirz, A. M. Homola, G. Hadziioannou & C. W. Frank, *Langmuir* **8** (1992) 328–333.

- **Alumina:** "Van der Waals Epitaxial Growth of  $\alpha$ -Alumina Nanocrystals on Mica", S. Steinberg, W. Ducker, G. Vigil, C. Hyukjin, C. Frank, M. Tseng, D. Clarke, J. Israelachvili, *Science* **260** (1993) 656–659.
- **Silica:** "Surface Forces and Viscosity of Water Measured Between Silica Sheets", R. G. Horn *et al.*, *Chem. Phys. Lett.* **162** (1989) 404–408.
- **Silica:** "Interactions of Silica Surfaces", G. Vigil, Z. Xu, S. Steinberg, J. Israelachvili, *J. Colloid Interface Sci.* **165** (1994) 367–385.
- **Biological surfaces:** "The surface forces apparatus – a tool for probing molecular protein interactions", D. Leckband, *Nature* **376** (1995) 617–618.

### **Measurements of viscosity and rheology of thin liquid films**

- "Surface Forces and Viscosity of Water Measured Between Silica Sheets", R. G. Horn *et al.*, *Chem. Phys. Lett.* **162** (1989) 404–408.
- "Measurement of the Viscosity of Liquids in Very Thin Films", J. N. Israelachvili, *J. Colloid and Interface Sci.* **110** (1986) 263–271.
- Peachey, J.; Van Alsten, J.; Granick, S. *Rev. Sci. Instrum.* **1991**, *62*, 463.

### **Tribological measurements using the SFA**

- "Measurements of and Relation between the Adhesion and Friction of Two Surfaces Separated by Molecularly Thin Liquid Films", A. M. Homola, J. N. Israelachvili, M. L. Gee, P. M. McGuiggan, *J. Tribology* **111** (1989) 675–682.
- Granick, S., "Motions and Relaxations of Confined Liquids", *Science*, **253** (1991) 1374–1379. Hu, H-W. and Granick, S., "Viscoelastic Dynamics of Confined Polymer Melts", *Science* **258** (1992) 1339–1342.

### **SFA coupled to other techniques**

- **Simultaneous X-ray synchrotron and SFA measurements:** "The X-Ray Surface Forces Apparatus: Structure of a Smectic Liquid Crystal under Confinement and Flow", S.H.J. Idziak, C.R. Safinya, R. Hill, K.E. Kraiser, M. Ruths, H. Warriner, S. Steinberg, K.S. Liang, J. Israelachvili, *Science* **264** (1994) 1915–1918.
- **Coupling surfaces forces with charge-transfer interactions:** "Contact Electrification and Adhesion between Dissimilar Materials", R. G. Horn, D. T. Smith, *Science* **256** (1992) 362–363.
- **FECO spectroscopy:** "Enhanced absorption within a cavity: a study of thin dye layers with the Surface Forces Apparatus", C. Müller, P. Mächtle and C. A. Helm, *J. Phys. Chem.* **98** (1994) 11119–11125.

## Reviews and miscellaneous applications

- **Ceramics:** "Surface Forces and their Action in Ceramic Materials", R. G. Horn, *J. Am. Ceram. Soc.* **73** (1990) 1117-1135.
- **Polymers:** "Surface Forces with Adsorbed Polymers", J. Klein, *Macromol. Chem. Macromol. Symp.* **1** (1986) 125-137.
- **Polymers:** "Measurement of Forces Between Surfaces in Polymer Fluids", S. S. Patel and M. Tirrell, *Annu. Rev. Phys. Chem.* **40** (1989) 597-635.
- **Attaining high local pressures (0.5 GPa):** Briscoe, B. J. and Evans, D. C., "The Shear Properties of Langmuir Blodgett Layers", *Proc. Roy. Soc. London*, **A380** (1982) 389-407.

## ADDITIONAL INFORMATION MATERIAL

- **Instructional films:** A number of videos are available on procedures for doing SFA experiments – preparation of surfaces, installation into the apparatus, etc. – and the optical technique. In this video one can see moving fringes as they appear in different types of systems and interactions, which can be invaluable for getting a feel for the full potential of the optical technique.

# APPENDIX 1

Copy of original paper describing the SFA3

## **Adhesion and Short-Range Forces Between Surfaces: New Apparatus for Surface Force Measurements**

J. N. Israelachvili, P. M. McGuiggan  
*J. Mater. Res.* 5, No. 10 (1990) 2223-2231

# Adhesion and short-range forces between surfaces.

## Part I: New apparatus for surface force measurements

Jacob N. Israelachvili and Patricia M. McGuiggan

*Materials Department, and Department of Chemical and Nuclear Engineering, University of California, Santa Barbara, California 93106*

(Received 15 March 1990; accepted 27 June 1990)

A new miniature Surface Forces Apparatus (SFA Mark III) is described for measuring the forces between surfaces in vapors and liquids. The apparatus employs similar techniques to those used in current SFAs, but it is easier to operate and is generally more user-friendly. Four stages of increasingly sensitive distance controls replace the three control stages of previous apparatuses. The first three stages allow for rapid manual control of surface separation to within 10 Å, while the fourth piezo-control stage has a sensitivity of better than 1 Å. All four distance controls have been specially designed to produce perfectly linear displacements of the surfaces. In addition, the SFA Mk III is more robust, less susceptible to thermal drifts, easier to clean, and requires smaller quantities of liquid than conventional SFAs. The high performance of this new instrument is illustrated in the succeeding paper (Part II), which describes the subtle effects of surface lattice mismatch on the oscillatory forces in water in the distance regime from 0 to 10 Å.

### I. INTRODUCTION

#### A. Early surface forces apparatuses

We briefly review the current state of direct surface forces measuring techniques, describe their limitations, and discuss why it was felt necessary to develop a new apparatus. In 1969 Tabor and Winterton,<sup>1</sup> and later Israelachvili and Tabor,<sup>2</sup> developed Surface Forces Apparatuses (SFAs) for directly measuring the van der Waals forces between surfaces in air or vacuum. These were successfully used for measuring van der Waals forces in the distance regime 1.5–130 nm with a distance resolution of 0.1–0.2 nm. In 1976, Israelachvili and Adams<sup>3</sup> designed a new apparatus (later known as SFA Mk I) for measuring the forces between surfaces in liquids as well as in vapors, allowing control and measurement of the surface separation to within 0.1 nm. The SFA Mk I enabled the first detailed measurements to be made of the two fundamental forces of colloid science. These are the repulsive electrostatic double-layer forces and the attractive van der Waals forces, which exist between any two charged surfaces immersed in an electrolyte solution. These two forces make up the so-called DLVO Theory, which forms the basis of analyzing the long-range interactions of colloidal and biological structures in solution.<sup>4</sup>

The principles on which Mk I operates are simple<sup>3</sup>: one of the surfaces (the upper) is rigidly mounted at the end of a piezoelectric crystal tube while the lower surface, which faces the upper, is suspended at the end of a force-measuring spring. The surfaces can be moved toward or away from each other using a three-stage sys-

tem of controls of increasing accuracy. First, a coarse control micrometer drive allows for positioning to within about 500 nm over a range of 1 cm. The second level of control, the medium control, employs a micrometer-driven differential spring having an accuracy of 1 nm over a range of 10 μm. The third or fine control involves applying a voltage to the piezoelectric crystal allowing for final (vibration-free) positioning to an accuracy of 0.1 nm over a linear range of a few thousand angstroms. An optical technique (described more fully below) is used to measure the separation between the surfaces to ±0.1 nm.

The force is measured by moving the two surfaces toward or away from each other using one of the above controls, e.g., by applying a voltage to the piezoelectric crystal, and simultaneously measuring the deflection of the force-measuring spring using the optical technique. This gives the force at any particular surface separation. As mentioned above, the principles used in making direct force measurements are usually very simple; the main challenge has always been in the design of a mechanical device that would successfully apply these principles at the angstrom level.

#### B. Surface forces apparatus: Mk II

Following the success of Mk I, it was modified and improved, and became known as Mk II.<sup>5</sup> In particular, various attachments were developed that could be added to Mk II which greatly extended its scope and versatility.<sup>6</sup> For example, the replacement of the original single-cantilever force-measuring spring by a

variable-stiffness double-cantilever spring greatly extended the range of the forces that could be measured to more than six orders of magnitude. A small bath attachment was constructed that could be inserted into the main chamber to allow for much less liquid to be used than the full capacity of the chamber (about 350 ml), and more recently various attachments have been introduced<sup>6</sup> for making dynamic, as opposed to static or equilibrium, measurements (e.g., of the viscosity and shear properties of very thin liquid films).

Over the last few years a number of other successful, and often simpler, surface forces apparatuses have also been built based on similar principles as Mks I and II and using the same optical technique for the distance measurements. Thus, Klein<sup>7</sup> developed a circular glass apparatus and Parker *et al.*<sup>8</sup> developed a circular steel apparatus (SFA Mk IV), both of which are simpler to assemble and use than Mk II. Other optical<sup>9,10</sup> and capacitance<sup>11</sup> techniques for measuring surface separations have also been recently introduced in surface force measurements. All of these are now being regularly used to measure a whole variety of forces and interfacial phenomena in both vapors and liquids at the molecular level, and their use is expected to continue and expand into new areas.<sup>12</sup>

However, the systems and phenomena being studied are rapidly growing in complexity; these now include multicomponent polymeric and lubricant systems, the deformation and fusion of surfactant or lipid bilayers, dynamic and time-dependent interactions, molecular relaxations in thin films, tribological phenomena, etc.<sup>6</sup> These studies often require greater accuracy, stability, versatility, and control than can be attained with existing force-measuring apparatuses, even with the new attachments added. Thus a whole generation of new phenomena could be studied if only some of these deficiencies or limitations could be overcome. Our primary aim here was the identification of these limitations, and the design and construction of a new device that did not suffer from these limitations. This will now be described.

### C. Limitations of existing surface forces measuring apparatuses

The most serious drawbacks of Mk II are listed below, together with their causes and how they limit the types of measurements that can be made or reduce their accuracy (these also apply to other surface forces apparatuses):

(1) The two surfaces are prone to thermal drifts which can greatly diminish the accuracy of the forces measured below the theoretically attainable limit of at least  $10^{-8}$  N ( $10^{-6}$  g). These thermal drifts arise from the long mechanical path between the two surfaces, often passing outside the main body of the apparatus

where it is not thermally insulated by the thermal inertia of the apparatus and chamber. Consequently, even small differential thermal gradients outside the apparatus can lead to slow drifts of the two surfaces relative to each other. These drifts can usually be minimized by thermostating the apparatus or the experimental room to 0.1 °C, but they preclude accurate measurements of forces that take a long time to reach equilibrium, time-dependent adhesion effects, hydrodynamic interactions, etc.

(2) The maximum attainable stiffness is not very high even when the variable-stiffness force-measuring spring is fully clamped.<sup>5</sup> This, too, is a consequence of the unnecessarily long mechanical path between the two surfaces even at full clamping. This precludes certain types of measurements to be made that require high rigidity, for example, of strongly attractive hydrophobic and capillary forces at small separations.

(3) The coarse control which employs a screw-thread and/or dovetailed slide mechanism is basically incapable of the perfectly linear friction-free motion that is required at the submicroscopic level. This can cause erratic motion, backlash, irreversibility, and undesirable shear motion. Such erratic motion is unavoidable whenever linear motion depends entirely on a screw-thread or dovetail mechanism, regardless of how well the parts are machined. These effects can lead to unreliable control of distance and, at worst, to surface damage on separating two adhering surfaces.

(4) The three distance controls do not adequately cover the required range from about 0.5 cm to 0.1 nm, i.e., a range of more than seven orders of magnitude. A fourth distance control, like a fourth gear in a car, would greatly facilitate measurements.

(5) Most surface forces apparatuses need to be disassembled for the bathing chamber to be properly cleaned, and the chambers are often difficult to clean because of their large volumes and internal surface areas. The whole process is thus cumbersome and time-consuming. In addition, as the chamber or bath is filled with liquid it is difficult to keep the liquid surface clean by aspiration as it approaches, then contacts (i.e., wets), and finally passes across the two solid surfaces. It is thus difficult to prevent a monolayer or submonolayer of some foreign material from being deposited onto the surfaces as the meniscus passes them. This can result in contaminated surfaces even before an experiment is properly underway. Fortunately, such material often dissolves in the immersing liquid, but one cannot always be totally certain of this.

It was decided to design a new and more user-friendly apparatus that did not have any of the drawbacks mentioned above and with some additional features making it suitable for new types of measurements. This new surface forces apparatus (SFA Mk III)

was developed and successfully tested and used during 1985–89 in a series of different experiments, including these described in the following paper. It is shown in Figs. 1 and 3 and will now be described.

## II. SURFACE FORCES APPARATUS: Mk III

Figure 1 shows a section through Mk III. Note that Mk III is smaller and more compact than previous models. Forces are measured between the two mica or mica coated surfaces supported on two cylindrical silica disks. The upper disk is attached to the piezoelectric PZT-5A crystal tube which is mounted on a support that can be moved laterally and rotated before it is clamped tightly to the top of the apparatus. The apparatus has two separate parts, an upper (control) chamber, and a lower (bathing) chamber. The control chamber handles the four distance controls, the force-measuring spring adjustment, and the positioning and clamping of the two surfaces. Its workings are totally sealed from the lower chamber via the teflon bellows B. The lower chamber acts as a simple bath that can be bolted underneath the upper chamber and then filled with liquid. It is thus completely sealed both from the outside environment as well as from the mechanical controls of the upper chamber. This design feature of Mk III is similar to that of the surface forces apparatus designed by Klein.<sup>7</sup> The lower and upper chambers are made of 316 stainless steel. The lower chamber can also be made entirely of teflon (PTFE) or some other inert fluorocarbon material such as Kel-F. It is easy to clean and can be readily replaced by another bathing cham-

ber. At no point during or between experiments does the control chamber have to be opened or dismantled; indeed, once the control chamber has been assembled it requires no further attention.

The four distance controls of the upper chamber will now be described. As shown in Fig. 1, there are three mechanical controls and one piezoelectric control. The three mechanical controls are based on a new spring translation assembly, located roughly at the center of the control chamber (T), whose main design features are shown in Fig. 2. The main part of this assembly is the vertical-motion translation stage (part T<sub>1</sub>). This is machined from a single block of Cu–Be alloy and consists of four equal double-cantilever spring systems. This type of design ensures that if the two end parts (A) are fixed, i.e., bolted inside the control chamber (see Fig. 1), then the displacement of the middle part (B) will be perfectly vertical and linear, with no possible movement in any other, e.g., lateral, direction. The eight cantilever springs of this unit also ensure that there is no possibility of any wobble or rotation, or any other type of unwanted movement as occurs with dovetailed slides or screw-thread drives. To ensure further that there is also no buckling of the springs, it can be shown that the vertical force inducing the displacement must be applied through an axis passing through the center of the spring system, i.e., along the direction defined by the vertical arrow drawn through T<sub>1</sub>.

The full translation assembly includes another Cu–Be part (Fig. 2, part T<sub>2</sub>), which is attached to the translation stage (T<sub>1</sub>) by bolting parts C and B together via

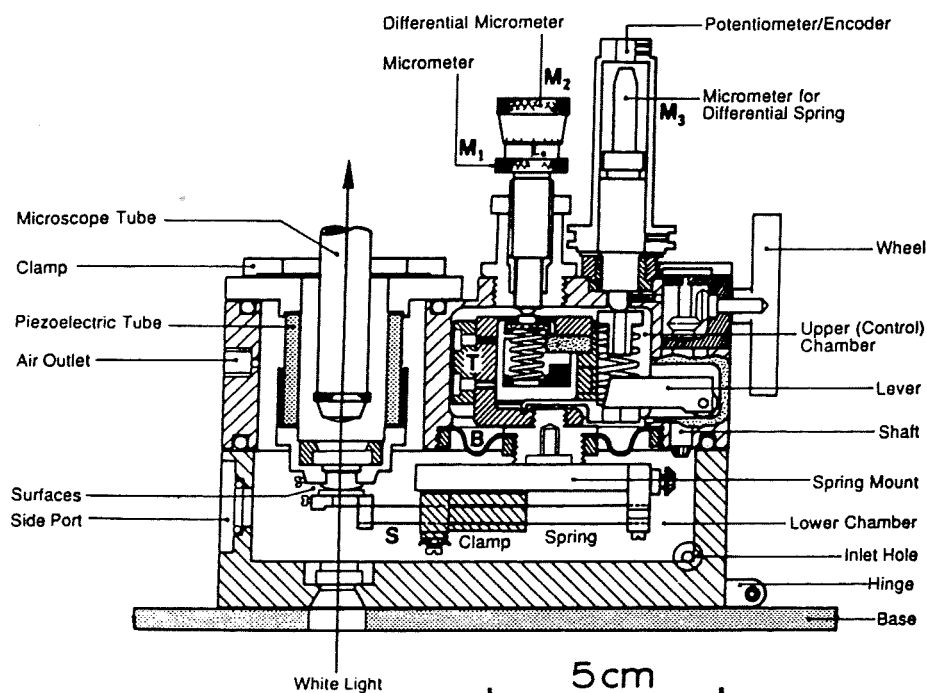


FIG. 1. New Surface Forces Apparatus (SFA Mk III) for measuring the forces between two molecularly smooth surfaces. The figure shows a section through the center of the apparatus. There are four distance controls: normal micrometer (M<sub>1</sub>), differential micrometer (M<sub>2</sub>), differential spring control (M<sub>3</sub>), and piezoelectric tube. The lower surface is mounted at the end of a variable-stiffness double-cantilever force-measuring spring (S) which is connected via the spring mount to the distance controls of the upper (control) chamber via a teflon bellows (B). The wheel and shaft unit are used for laterally moving the spring clamp and thereby changing the stiffness of the force-measuring spring. The lower chamber is bolted to the underside of the upper chamber from which it is completely sealed by the bellows, as well as being sealed with teflon O-rings from the outside. The main translation stage unit (T) is described in Fig. 2 and a photograph of the apparatus is shown in Fig. 3.

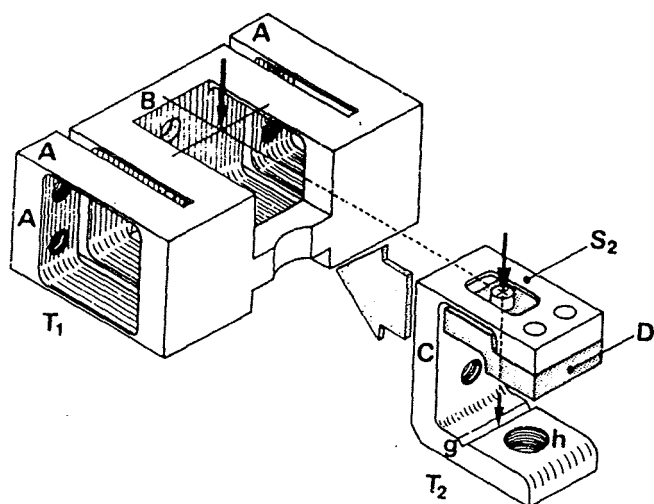


FIG. 2. Basic spring assembly unit (or translation stage) ensuring that the two surfaces move vertically and perfectly linearly relative to each other with no displacement or rotation in any other direction. The main part of the translation stage  $T_1$  is bolted to the inside of the control chamber (Fig. 1). The second part,  $T_2$ , is bolted to  $T_1$  so that the positions of the two arrows coincide. The arrows define the vertical axis passing through the center of the four double-cantilever spring system of  $T_1$ , the single-cantilever spring  $S_2$ , and the groove  $g$  on  $T_2$ . The micrometer shaft of  $M_1$  and  $M_2$  presses vertically down on the small steel disk on top of part  $D$ , as shown in Fig. 1. The workings of the spring assembly are described in the text. All the spring parts were machined from Cu-Be alloy before they were heat treated (tempered).

two bolts. Once assembled, the two arrows shown on  $T_1$  and  $T_2$  coincide and define the vertical axis through the center of the double-cantilever spring systems of  $T_1$ . The assembled unit of these two parts fits inside the control chamber via four bolts through parts  $A$ , as shown in Fig. 1. At the bottom of  $T_2$  there is a threaded hole ( $h$ ) to which the bellows  $B$  and the force-measuring

spring mount are attached (cf. Figs. 1 and 2). The spring mount protrudes into the lower chamber, and the teflon bellows  $B$  isolates the two chambers from each other.

### A. Characteristics of positioning and force-measuring springs

Table I gives the spring characteristics of the various springs used to perform the following three functions: position the two surfaces (distance control), measure forces, and avoid backlash. In each case the spring type, its stiffness, range of operation, and elastic limit were designed for optimum performance. These are further described in the following sections.

### B. Control of surface separation

*Coarse controls:* There are three mechanical distance controls (two coarse and one medium) and one piezoelectric (fine) control. The coarse controls work as follows. A differential micrometer ( $M_1$  and  $M_2$ : modified from a micrometer obtained from *Microcontrol*, Cat. No. 385 034) is bolted to the top of the apparatus. The micrometer axis is along the line of the arrow in Fig. 2. It presses down against the polished flat surface of a small hardened steel disk attached to the stainless steel part ( $D$ ) on top of the translation stage assembly. Turning the micrometer causes parts  $T_2$ ,  $B$ , and hence the spring mount in the lower chamber to move along a perfectly vertical axis, and in this way the normal distance between the two surfaces can be moved over a total range of about 6 mm ( $\pm 3$  mm about the mean position) with control to 500 nm (using the normal micrometer,  $M_1$ ) and 50 nm (using the differential micrometer  $M_2$ ). This positioning can be done by hand. A stiff helical spring located inside  $T_2$  (see Fig. 1)

TABLE I. Spring specifications.<sup>a</sup>

Function and location	Spring type	Stiffness (N/m)	Operating range (length)	Range of loads
1st and 2nd (coarse) distance control ( $T_1$ )	Unit of four double-cantilevers	$3.6 \times 10^3$	0– $\pm 3.5$ mm	<Elastic limit
Anti-backlash for $T_1$ (under $M_1, M_2$ )	Helical	$4.3 \times 10^3$	7–14 mm	1.7–4.7 Kg
3rd (medium) distance control (under $M_3$ )	Helical	$1.5 \times 10^3$	9–24 mm	0.3–1.8 Kg
3rd distance control ( $S_2$ ) (in series with above)	Cantilever	$1.5 \times 10^6$	0– $\pm 10$ $\mu$ m	<Elastic limit
Force-measuring ( $S$ ) (variable stiffness)	Double-cantilever	$30\text{--}5 \times 10^5$	Clamping: 0–32 mm Vertical: 0– $\pm 1$ mm	$10^{-6}$ g–100 g

<sup>a</sup>The first four springs are located within the upper (control) chamber and are made of machined Cu-Be alloy that is later hardened by heat-treatment. The force-measuring spring ( $S$ ) located inside the lower chamber is made of noncorrosive stainless steel since it contacts various solvents. The stiffness of the force-measuring spring is related to its variable clamping length  $L$  via Eq. (3). The bellows  $B$  has a negligible elastic stiffness compared to the other positioning springs. The 4th (fine) distance control is done via a piezoelectric crystal tube.

presses against the underside of D along the main translation axis defined by the arrows and acts as an antibacklash spring (see Table I).

**Medium control:** The third (medium) distance control is via a differential spring mechanism. Here a helical spring is compressed by a motor-driven nonrotating micrometer ( $M_3$ ). The spring presses against a lever which in turn presses down on  $T_2$  at the groove (g) which, as mechanically required, is also located along the vertical axis passing through the center of the spring translation assembly. The force acting on  $T_2$  from the action of this spring deflects a cantilever spring ( $S_2$ ) located on top of  $T_2$  (this spring is also symmetrically displaced about the main translation axis). The deflection of  $S_2$  therefore causes B and hence the spring mount to be displaced vertically, but by a very small amount: the stiffness of  $S_2$  is about 1000 times greater than that of the helical spring under  $M_3$  (see Table I), and the lever ratio is about 2:1. Thus the movement of the micrometer  $M_3$  over a total range of 15 mm is reduced by a factor of about 2000. (Note that spring  $S_2$  is actually acting in parallel with the springs of  $T_1$ , but the effect of  $T_1$  on the reduction ratio is negligible since, as shown in Table I,  $S_2$  is about 500 stiffer than  $T_1$ . However,  $T_1$  does help ensure that the surface displacement remains along a vertical axis.) This third control therefore enables the micrometer displacement, which covers a range of 15 mm with an accuracy of  $\sim 1 \mu\text{m}$ , to be reduced to a range of  $7.5 \mu\text{m}$  with a positioning accuracy about 0.5–1 nm between the two surfaces.

**Fine control:** The final, nonmechanical control of surface separation is effected by changing the dc (or ac) voltage across the inner and outer silver-coated walls of the piezoelectric tube that supports the upper surface. The outer wall is grounded (earthed), while the inner wall is the active surface. The tube expands by about 1.0 nm per volt, so that when working from  $-500 \text{ V}$  to  $+500 \text{ V}$  the surfaces can be moved over a range of about  $1 \mu\text{m}$  with an accuracy of better than 0.1 nm—this accuracy now being limited by factors such as the background vibrations and thermal drift of the two surfaces relative to each other (discussed below) and the performance of the piezoelectric material. Most commercial piezoelectric crystals are rated to withstand many thousands of volts, but we have found that their motion is linear and creep-free only below about 500 V (corresponding here to a total movement of  $\pm 500 \text{ nm}$ ). We have also found that there is no lateral displacement of the piezoelectric tube when it is expanded vertically, so long as it is properly glued into place, i.e., with its axis perfectly vertical.

To summarize, the four distance controls have the following resolution and workable range: normal micrometer (500 nm over a range of 6 mm); differential

micrometer (50 nm over a range of 0.1 mm); differential spring (1 nm over a range of  $5 \mu\text{m}$ ); and piezo control ( $<0.1 \text{ nm}$  over a range of  $1 \mu\text{m}$ ).

The three micrometer controls,  $M_1$ ,  $M_2$ , and  $M_3$ , are conveniently positioned for manual control, but any one of them can also be controlled by a variable-speed reversible 24 V dc motor and gear-box (Philips 4322 010 75143 and 9912 200 02036) via a gear wheel and belt. The differential spring facility of  $M_3$  is similar to the lower motor control of Mk I and II,<sup>3,5</sup> and the displacement of the spring can likewise be measured from a resistance potentiometer or encoder attached to the top of  $M_3$ .

### C. Control of stiffness of force-measuring spring

The stiffness of the double-cantilever force-measuring spring ( $S$ ) can be adjusted by sliding the spring-loaded clamp laterally along the spring supporting mount. This clamp is attached to a dovetailed slide and has a screw thread passing throughout its length. The clamp can be moved by rotating this screw at the point where it protrudes from the spring mount at its right end. To accomplish this adjustment the O-ring-sealed shaft and wheel are unlocked and, by holding the wheel, manually lowered until the two bevel gears engage. The wheel is then turned until the desired clamping position is attained. Each turn corresponds to 0.5 mm displacement, and the range of clamping of this spring is from 0 to 32.5 mm (65 turns of the wheel). After the desired clamping position has been reached, the wheel and shaft are raised and locked back into place (the locking mechanism is not shown in Fig. 1 but it is essentially a screw that can be turned by hand so that it presses against the wheel assembly; this screw is seen in Fig. 3 as the circular knob that protrudes from the front of the apparatus just to the left of the wheel). The whole process of changing the spring stiffness takes no more than 1 min. The range of stiffnesses attainable is from below 30 N/m to about  $5 \times 10^5 \text{ N/m}$  (see Table I). This is about 4 orders of magnitude. Since at each stiffness one can usually measure 3–4 orders of force, the Mk III can measure a force-law over a range of 6–7 orders of magnitude.

### D. Experimental procedure

The mica sheets are first cut, silvered, glued onto the cylindrical silica disks, pretreated with some desired surface coating (if needed), and installed into position in the apparatus so as to face each other as shown in Fig. 1. The lower chamber is then placed underneath the upper chamber and bolted to it.

Optimization of the optics (see below) is carried out more or less as for Mk I and II,<sup>1-3</sup> except that with Mk III the three micrometers  $M_1$ ,  $M_2$ , and  $M_3$  are all

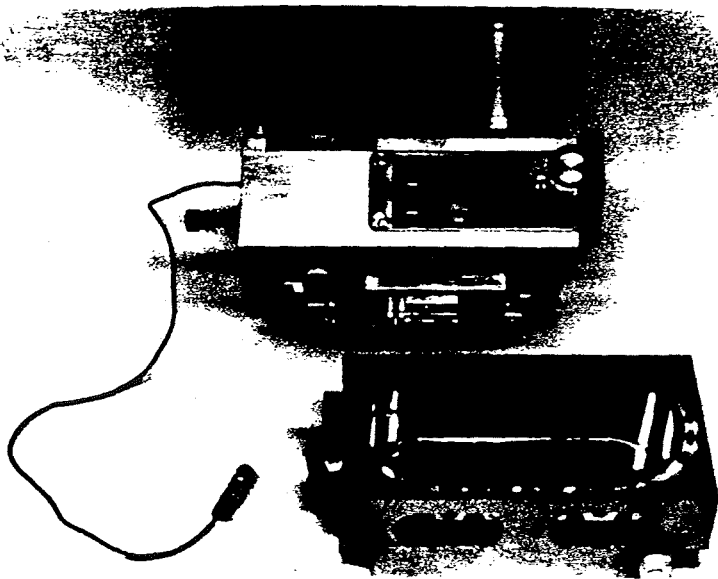


FIG. 3. Photograph of Mk III with the upper and lower chambers disconnected. A matchbox on the left gives an idea of the size of the apparatus.

accessible by hand so that it is possible to make very fine adjustments manually before tightening the belt around the micrometer  $M_2$  or  $M_3$ . The desired spring stiffness can be obtained by moving the spring clamp as described above, and the apparatus (or lower chamber) is now ready for filling with liquid.

By tilting the apparatus clockwise about the hinge (see Fig. 1) until it is almost vertical, one may fill the chamber through the inlet hole. The capacity of the chamber is 50–60 ml, so that it can be filled with a syringe. As the liquid level rises and approaches the two solid surfaces, its surface can be continuously aspirated through the side port on the left wall of the lower chamber, while gently purging the atmosphere with clean  $N_2$  gas through the air outlet port. Once filled, the apparatus is lowered back onto its base and force measurements can proceed as described below.

#### E. Measuring distances and surface profiles using the FECO technique

Surface separations and profiles can be measured to within about 0.1 nm by monitoring the movement of multiple beam interference fringes known as Fringes of Equal Chromatic Order (FECO).<sup>13–15</sup> These sharp fringes are produced when a beam of white light is made to pass through the two mica sheets (Fig. 1). The transparent mica sheets are of equal thickness (about 1–3  $\mu\text{m}$ ) and are each coated with a 98% reflecting layer of silver (thickness  $\sim 550$  Å) before they are glued, silvered sides down, onto the cylindrically curved silica disks. The interference fringes are produced by multiple reflections of light between the two silvered layers, so that only certain wavelengths (which interfere con-

structively) emerge from the other side of the sheets. The emerging beam is focused onto the slit of a normal grating spectrometer which separates out the different colors (interference fringes). Depending on the shapes of the two surfaces, these fringes appear as sharp lines or curves at the exit of the spectrometer<sup>13–18</sup> and can be viewed by eye through a normal microscope eyepiece or recorded on film or a video camera.

From the positions and shapes of the FECO fringes one can determine not only the surface separation but also their shapes and the refractive index of the medium between them. Equations describing how one translates the measured wavelengths to surface separations and refractive indices have been given by Israelachvili<sup>15</sup> together with photos of FECO fringes and a working example of how these can be used to measure the thickness and refractive index of thin films.

More recently, the FECO technique has been used to measure the capillary condensation of liquids,<sup>17</sup> the elastically deformed shapes of contacting surfaces,<sup>16</sup> and the fusion of surfactant films.<sup>18</sup> These papers may be referred to for pictures of the FECO fringes and further details of the optical technique.

There are two major advantages of using this technique over other techniques (such as a capacitance technique). The first is that the surface separation is actually measured at the point of closest approach of the two surfaces; i.e., the separation is measured where one actually wants to know it. Most other techniques measure the displacement of a spring or balance arm at some point away from the interaction zone, and in this way any elastic deformations of the surfaces occurring around the contact zone become mixed in with the

measured distance displacement. With the FECO method, the distances between the two surfaces and any deformations of the materials are unambiguously distinguishable and independently measurable. The second advantage is that one can measure the surface profile, and in particular the local radius of curvature  $R$  of the two apposing surfaces. This is important when one wants to compare the measured forces with theory or when one needs to translate adhesion forces to surface energies [see Eq. (5)].

### F. Measuring forces

Given the facility for moving the surfaces toward or away from each other and independently measuring their separation, each with a sensitivity or resolution of about 0.1 nm (1-Å), the force measurements themselves now become straightforward. The force is measured by expanding or contracting the piezoelectric crystal by a known amount and then measuring optically how much the two surfaces have actually moved. Any difference in the two values when multiplied by the stiffness of the force-measuring spring gives the force difference between the initial and final positions. Thus if the surfaces are initially at  $D_0$  where the force between them is  $F(D_0)$ , and the piezoelectric crystal is expanded by  $\Delta D_p$  so that the surface separation changes by  $\Delta D_s$  to  $D$ , the force at  $D$  is related to the force at  $D_0$  by

$$F(D) = F(D_0) + (\Delta D_p - \Delta D_s)K \quad (1)$$

where  $K$  is the stiffness of the force-measuring spring. Thus, if  $\Delta D_p = \Delta D_s$ , we have  $F(D) = F(D_0)$ , so that if the force is zero at  $D_0$ , it is also zero at  $D$ . However, if  $\Delta D_p > \Delta D_s$ , we have  $F(D) > F(D_0)$  and the force at  $D$  is repulsive, whereas if  $\Delta D_p < \Delta D_s$ , we have  $F(D) < F(D_0)$  and the force at  $D$  is attractive. In this way, by starting at some large separation where there is no detectable force and working systematically toward smaller separations both repulsive and attractive forces can be measured with a sensitivity of about  $10^{-6}$  g (see Table I) and a full force-law can be obtained over any distance regime.

As an example, we consider a typical experimental run where there is a monotonically repulsive force between the two surfaces in a liquid at separations below 15.0 nm. The piezoelectric tube is first calibrated at large distances ( $>15$  nm) where there is no detectable force using the optical technique. This calibration yields, say, 1.0 nm/V. The two surfaces are now brought to a separation of 20.0 nm and the voltage across the piezoelectric tube is changed by 5.0 V, corresponding to  $\Delta D_p = 5.0$  nm. This results in an inward displacement of the surfaces, as measured from the shift in the FECO fringes, from 20.0 nm to 15.0 nm, corresponding to  $\Delta D_s = 5.0$  nm. Thus,  $\Delta D_p = \Delta D_s$ , so

that  $F(D = 15 \text{ nm}) = F(D = 20 \text{ nm}) = 0$ . Next, the surfaces are brought to  $D = 15.0$  nm, and the process is repeated. This time, however, the surfaces are found to move to 11.0 nm, so that  $\Delta D_s = 4.0$  nm. The net force at  $D = 11.0$  nm is therefore repulsive and, using Eq. (1), is equal to  $K(5.0 - 4.0) \times 10^{-9}$  N. The spring constant,  $K$ , can be calibrated at the end of the experiment by replacing the silica disks with small weights and measuring the deflection using a micrometer eyepiece or traveling microscope.<sup>1-3</sup> For example, if the value obtained for  $K$  is 100 N/m, then the repulsive force at  $D = 11.0$  nm is  $10^{-7}$  N ( $10^{-2}$  dynes or  $10^{-5}$  g).

The force-measuring spring can be varied during an experiment by a factor of up to 10 000 (see Table I), so that both very weak and very strong forces may be measured. When strongly attractive forces are measured, instabilities can occur wherein the surfaces suddenly jump from one stable position to another. This is analogous to bringing a magnet suspended from a spring down toward a block of iron where at some point it will jump into contact with the block. Both inward and outward jumps can occur (cf. the outward jump from contact when the spring attached to the magnet is pulled back). Instabilities occur whenever the gradient of the force exceeds the spring stiffness, i.e., when  $\partial F/\partial D > K$ , and is common whenever complicated force laws are being measured, such as oscillatory forces.<sup>3,19</sup> Note that Eq. (1) still applies when instabilities occur, though certain distance regimes now become inaccessible to force measurements (these being regions where no stable equilibrium can occur). However, by increasing the spring stiffness these regions can become accessible, though at the cost of reduced sensitivity.

### G. Measuring adhesion forces

Measuring outward jumps from contact is a particularly suitable way of measuring adhesion forces. For example, with  $K = 100$  N/m, as before, an outward jump of 15  $\mu\text{m}$  implies an adhesion force of  $1.5 \times 10^{-3}$  N (0.15 g). Alternatively, using a higher spring stiffness of  $K = 10^4$  N/m, the jump apart corresponding to the same adhesion force would now be only 150 nm. This is just as easy to measure as 15  $\mu\text{m}$ , and it has the advantage that the whole operation can be done much more quickly with the piezoelectric control (no moving mechanical parts), and then repeated many times to test for reproducibility just as quickly.

Using a stiffer spring setting for measuring large forces also has the advantage that the lateral displacement (shearing) of the two surfaces can be reduced as they are being pulled apart. If the active length of the double-cantilever force-measuring spring (S) is  $L$ , then it can be shown that a vertical displacement of  $\Delta D$  at the point of contact of the two surfaces results in a lat-

eral displacement of the surfaces by  $\Delta x$ , where

$$\Delta x = \frac{2\Delta D^2}{3L}. \quad (2)$$

Further, the stiffness (or spring constant),  $K$ , of a double-cantilever spring is given by

$$K = 2YbT^3/L^3 \propto 1/L^3 \quad (3)$$

where  $Y$  is the Young's modulus,  $b$  the spring width, and  $T$  the spring thickness. Since the adhesion force is related to the spring constant  $K$  and deflection  $\Delta D$  by  $F = K\Delta D$ , we obtain for a double-cantilever spring with variable clamping length  $L$ :

$$\Delta x \propto \Delta D^2/L \propto (F/K)^2/L \propto (FL^3)^2/L \propto F^2L^5. \quad (4)$$

Equations (2) and (4) are important for determining the shear displacement of two surfaces when forces of magnitude  $F$  between them are being measured with a double-cantilever spring of length  $L$  and stiffness  $K$ . Equation (4) shows that to reduce  $\Delta x$  (at a given  $F$ ) one must use a shorter spring length  $L$ . This can be achieved with the Mk III by reducing the clamping distance of the force-measuring spring during an experiment. It is worth mentioning that it is possible to design a nonshearing force-measuring spring,<sup>5,6</sup> but it is not easy to design one whose stiffness can also be varied during an experiment.

Returning to the above example where an adhesion force of  $F = 1.5 \times 10^{-3}$  N was measured using spring constants of either  $K = 10^2$  N/m or  $K = 10^4$  N/m, these correspond to spring lengths of  $L = 2.1$  cm and 0.45 cm, respectively (see Table I). With the weaker spring setting we have  $\Delta D = F/K = 1.5 \times 10^{-5}$  m, so that the lateral displacement is given by Eq. (2) as  $\Delta x = 7.1$  nm, which may introduce unwanted frictional forces during pull-off. However, with the stiffer spring setting Eq. (4) shows that the shear displacement falls to  $\Delta x = 0.003$  nm (0.03 Å), which is totally acceptable. It is with these stiffer spring settings that the adhesion forces, described in Part II,<sup>29</sup> were measured.

There is a well-known expression, known as the Derjaguin approximation,<sup>4</sup> which relates the force between two curved surfaces to the energies of flat surfaces. In particular, the adhesion energy (otherwise known as the surface or interfacial free energy)  $E$  per unit area between two flat surfaces is simply related to  $F$  by:

$$E = F/2\pi R. \quad (5)$$

Thus, in the above example where  $F = 1.5 \times 10^{-3}$  N, if the radius of the surfaces were  $R = 10^{-2}$  m (1 cm), the surface energy would be  $E = 25 \times 10^{-3}$  mJ/m<sup>2</sup> (25 erg/cm<sup>2</sup>).

## H. Performance characteristics of Mk III

Mk III is much more stable against thermal drifts, and is easier to operate and keep clean than previous models. The thermal drift of the two surfaces has been found to depend mainly on the temperature stability of the room (apparatus environment), and is typically less than 0.1 nm/min if the ambient temperature is controlled to within 0.1 °C. The improved thermal stability of the apparatus is due to its compactness and because all the critical moving parts are internalized. In addition, the mechanical path between the two surfaces is very short and does not go outside the apparatus (as in previous models). All these factors reduce the susceptibility of the apparatus to transient temperature gradients.

The replacement of the dovetailed slide and screw threads by the purely spring-loaded translation assembly of Fig. 2 has also helped to ensure linear motion and significantly reduced backlash and other erratic motions of the two surfaces.

The four distance controls now make it easy to quickly bring the surfaces together manually within a few hundred angstroms and then, depending on the strength of the forces, to measure these using either the piezoelectric crystal, the differential spring, or the differential micrometer; i.e., there are three rather than two choices for measuring forces. The short path between the two surfaces also allows for a higher stiffness to be attained with Mk III than with existing apparatuses.

Finally, the ability to have the surfaces immersed in a passivated stainless steel or an all-TEFLON bath allows for very clean work to be done, and the aspiration capability during filling significantly reduces the chances of having contaminated surfaces.

## I. Additional features and attachments

Mk III has been designed to be as versatile as possible, and to easily accept new attachments. As an example of the former, note that the lower chamber may be readily removed (without disturbing the two surfaces) and replaced by a different chamber. This allows for different types of baths to be used for different experiments; for example, one bath for experiments with surfactant-coated surfaces using the Langmuir-Blodgett technique, another bath for experiments in vapors of controlled vapor pressures, and yet another bath whose walls are well thermostated suitable for experiments over a wide range of temperatures.

The new SFA Mk III can also be used with a variety of different attachments, as can its predecessor.<sup>6</sup> Typically, these attachments would be secured to the bottom of the translation stage  $T_2$ , replacing the spring mount. Two attachments currently in the design stage

are (1) a sliding facility for shearing two surfaces laterally past each other, suitable for friction measurements and for studying various tribological phenomena, and (2) a constant-force electromagnetic balance attachment, for making accurate measurements of truly equilibrium forces across thin liquid films regardless of thermal drifts and the time it takes to reach equilibrium. Finally, for the experiments reported in the following paper a new attachment was developed for measuring the dependence of adhesion and short-range forces in liquids on the twist angle between the two interacting surface lattices.<sup>13</sup>

#### ACKNOWLEDGMENTS

We thank Allan Reading and Robert Hill for their excellent technical expertise, Dr. Roger Horn for his valuable comments, and the United States Department of Energy for financial support under DOE grant DE-FG03-87ER45331, although this support does not constitute an endorsement by DOE of the views expressed in this article.

#### REFERENCES

- <sup>1</sup>D. Tabor and R. H. S. Winterton, *Proc. R. Soc. London, Ser. A* **312**, 435 (1969).
- <sup>2</sup>J. N. Israelachvili and D. Tabor, *Proc. R. Soc. London A331*, 19 (1972).
- <sup>3</sup>J. N. Israelachvili and G. E. Adams, *Nature* **262**, 774 (1976); *J. Chem. Soc., Faraday Trans. I* **74**, 975 (1978).
- <sup>4</sup>J. N. Israelachvili, *Intermolecular and Surface Forces* (Academic Press, London and New York, 1985).
- <sup>5</sup>J. N. Israelachvili, *Proc. Natl. Acad. Sci. U.S.A.* **84**, 4722 (1987).
- <sup>6</sup>J. N. Israelachvili, *Chemtracts—Analytical and Physical Chemistry* **1**, 1 (1989).
- <sup>7</sup>J. Klein, *J. Chem. Soc., Faraday Trans. I* **79**, 99 (1983).
- <sup>8</sup>J. L. Parker, H. K. Christenson, and B. W. Ninham, *Rev. Sci. Instrum.* **60**, 3135–3138 (1989).
- <sup>9</sup>D. C. Prieve, F. Luo, and F. Lanni, *Faraday Discuss. Chem. Soc.* **83**, 297 (1987); S. G. Bike and D. C. Prieve, *Langmuir* (in press).
- <sup>10</sup>R. Erlandsson, G. M. McClelland, C. M. Mate, and S. Chiang, *J. Vac. Sci. Technol. A* **6**, 266 (1988); Y. Martin, C. C. Williams, and H. K. Wickramasinghe, *J. Appl. Phys.* **61**, 4723 (1987); S. Alexander, L. Hellemans, O. Marti, J. Schneir, V. Elings, P. K. Hansma, M. Longmire, and J. Gurley, *J. Appl. Phys.* **65**, 164 (1989); A. L. Weisenhorn, P. K. Hansma, T. R. Albrecht, and C. F. Quate, *Appl. Phys. Lett.* **54**, 2651 (1989).
- <sup>11</sup>A. Tonck, J. M. Georges, and J. L. Loubet, *J. Colloid Interface Sci.* **126**, 150 (1988).
- <sup>12</sup>"Frontiers in Chemical Engineering," Chairman: Neal Amundson, National Academy Press, Washington, DC (1988).
- <sup>13</sup>S. Tolansky, *Multiple Beam Interferometry of Surfaces and Films* (Oxford University Press, 1948).
- <sup>14</sup>S. Tolansky, *An Introduction to Interferometry* (Longmans, Green & Co., London, 1955).
- <sup>15</sup>J. N. Israelachvili, *Nature-Phys. Sci.* **229**, 85 (1971); *J. Colloid Interface Sci.* **44**, 259 (1973).
- <sup>16</sup>J. N. Israelachvili, E. Perez, and R. K. Tandon, *J. Colloid Interface Sci.* **78**, 260 (1980); R. G. Horn, J. N. Israelachvili, and F. Pribac, *J. Colloid Interface Sci.* **115**, 480 (1987).
- <sup>17</sup>L. R. Fisher and J. N. Israelachvili, *J. Colloid Interface Sci.* **80**, 528 (1981); *Colloids & Surfaces* **3**, 303 (1981).
- <sup>18</sup>C. A. Helm, J. N. Israelachvili, and P. M. McGuiggan, *Science* **246**, 919 (1989).
- <sup>19</sup>R. G. Horn and J. N. Israelachvili, *J. Chem. Phys.* **75**, 1400 (1981).
- <sup>20</sup>P. M. McGuiggan and J. N. Israelachvili, *J. Mater. Res.* **5**, 2232 (1990).

## APPENDIX 2

Example of SFA Experiment to measure forces between two surfactant-coated surfaces immersed in a hydrocarbon liquid



## CALCIUM SULPHONATE ACROSS WHITE OIL

This is a record and analysis of a real experiment, the first using Ca-sulphonate surfactant.

Aim: To measure forces between calcium-benzene-sulphonate surfactant monolayer adsorbed on mica in white oil (Blandol), and to test effect of water on the forces.

Materials: Calcium-benzene-sulphonate was from Exxon (SA 119) commonly used to stabilize colloids in lubricating oils (lube oils). The oil was Blandol, a mixture of mainly branched hydrocarbons with carbon numbers between 12 and 36. The oil had been previously dried, centrifuged and kept with 4A molecular sieves. The surfactant had been purified by recrystallization following the method of John Marsh and Isabelle McDonald.

18 JULY 1988

3pm. Mica sheets from JMI 7/5/88 A3 and A4 were glued onto two 5mm discs with 1004 glue. Small beakers of pure water ready. Water surface touched with surfactant then aspirated. One disc dipped into beaker, then after a few minutes slowly withdrawn (all this time surfactant was in contact with water surface). Surface came out dry. Disc dried. Repeated with second disc. Discs placed in apparatus, Mk II, then purged with  $N_2$  for 30 minutes.

left overnight in dark room for temperature drifts to equilibrate. All controls checked and found to be working (motors, prism, focus, multimeters, flash light, dove prism, system, tape ready, temperature setting, etc.) <sup>video</sup>

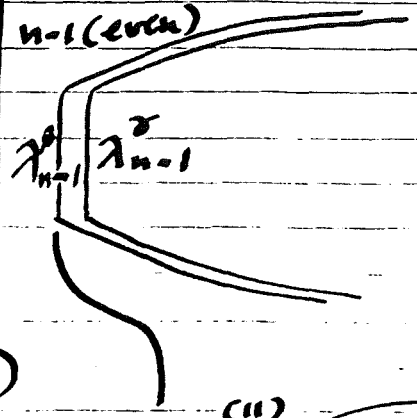
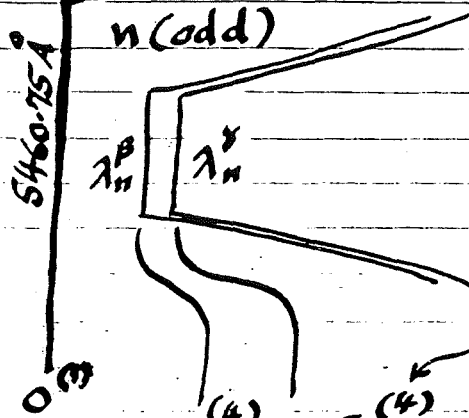


Contact in dry N<sub>2</sub>

Polaroid removed.

Hg green line

Hg yellow lines

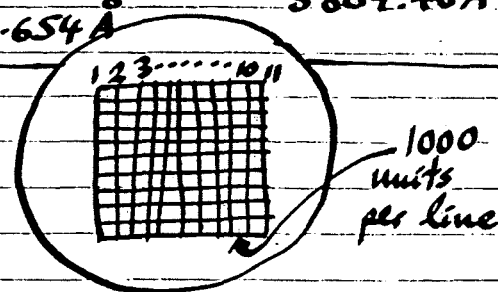


0 <sup>(3)</sup>	+243 <sup>(4)</sup>	-15 <sup>(4)</sup>
...	+243	-18
...	+244	-12
0 <sup>(1)</sup>	+243 <sup>(4)</sup>	-15 <sup>(4)</sup>
↓	↓	↓
0 <sup>(1)</sup>	-2757 <sup>(1)</sup>	-3015 <sup>(1)</sup>
↓	↓	↓
5460.75 Å	5551.25 Å	5559.72 Å

-50 <sup>(11)</sup>	-621 <sup>(11)</sup>
...	-620
...	-622
-50 <sup>(11)</sup>	-621 <sup>(11)</sup>
↓	↓
-10,050 <sup>(11)</sup>	-10,621 <sup>(11)</sup>
↓	↓
5790.654 Å	5809.40 Å

encoder units measured with 11th line

∴ DISPERSION:  $\frac{5790.654 - 5460.75}{10,050 - 0} = 0.03282627 \text{ Å/unit}$



∴  $\left. \begin{aligned} \lambda_n^\beta &= 5551.25 \text{ Å} \\ \lambda_n^\delta &= 5559.72 \text{ Å} \\ \lambda_{n-1}^\beta &= 5809.40 \text{ Å} \end{aligned} \right\} n^{\text{th}} \text{ fringe}$

$$\Delta\mu = \mu \Delta\lambda / \lambda = 1.60 (\lambda_n^\beta - \lambda_n^\delta) / (\lambda_n^\beta + \lambda_n^\delta)$$

$$= 1.60 \times 8.47 / 5555.5 = 0.0024$$

∴  $\mu_n^\beta (\lambda = \infty) = 1.5835 - 0.0012 = 1.5823$   
 and  $\mu_n^\delta (\lambda = \infty) = 1.5835 + 0.0012 = 1.5847$

$\frac{1}{nF_n} = \frac{5809.40 - 5551.25}{5809.40} = 0.04444, \therefore nF_n = 22.50$   
 try  $n(\text{odd}) = 21, \therefore F_n \approx 1.024 + \frac{1}{21} = 1.0716$   
 $n \approx 22.50 / 1.0716 = 21.002 \rightarrow 21 \text{ odd}$



19 JULY 1988

9 AM

Purged with  $N_2$  for 30'  
Newton's rings circular, contact and  
separation fine.

10 AM

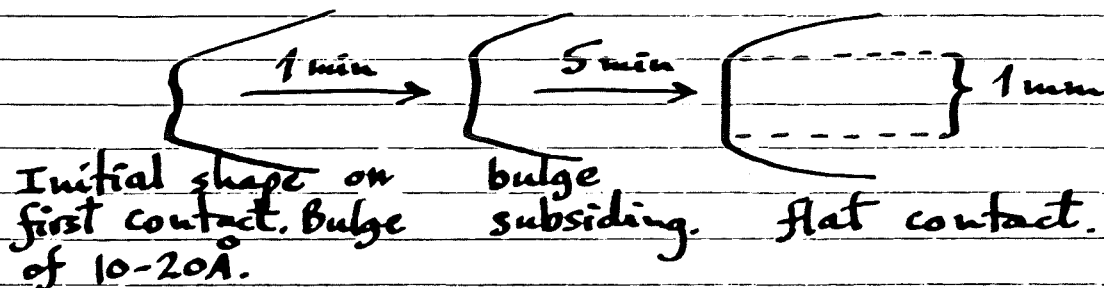
$P_{205}$  put into small receptacle.  
 $N_2$  purge stopped.

2 PM

FECO contact excellent.  
Almost zero birefringence, polaroid used.  
Symmetry of odd and even fringes checked.  
Flat contact on scanning checked.  
Surfaces separated: nice jump apart until adjacent  
fringes 3.6 mm apart.

2:15

Surfaces brought into contact again, pressed  
together until contact diameter  $\phi \approx 1$  mm.  
Noticed that:



Never seen this before - suggests fluid monolayers.

Optics optimized: mirror controls, focus, centering, prism table controls, slit, dove prism, Hg line, polaroid, etc.



$$D \approx n F_n \delta \lambda_n / 2 \mu_{\text{mica}}$$

$$\approx 22.50 \times 0.0328 / 2 \times 1.60 = 0.231 \text{ \AA / unit.}$$

Now put following values into HP 15C storage registers:

register	store
0	5460.75 ← Hg reference line $\lambda(\text{\AA})$
1	0 ← encoder reading of above
2	$\ominus 0.03282627$ ← dispersion ( $\text{\AA}/\text{unit}$ )
3	5551.25 ← $\lambda_n^B$
4	5809.40 ← $\lambda_{n-1}^B$
5	1.467 ← ref. index of medium (oil)
6	1.5823 ← $\mu_n^P (\lambda = \infty)$

Check the program by pressing in  $+2757$  or  $+2758$  to get  $D \approx 0$ , and  $+2857$  to get  $23.1 \text{ \AA}$ .

also check by pressing  $+10,621$  to get  $\frac{\lambda_{n-1}^B}{2 \mu_{\text{medium}}}$

$$\frac{5809.4}{2 \times 1.467} = 1,980 \text{ \AA}$$

Surfaces separated. Jumped apart to where adjacent fringes  $3.6 \text{ mm}$  apart, as before.  
 $\leftarrow 3600 \text{ units}$

Put  $\mu_{\text{medium}} = 1.00$  into register 5

Enter -3600

Press D

→ gives  $D_{\text{jump}} = 8.93 \mu\text{m}$   
 ↙ jump

Now  $R = 0.45 \text{ cm}$  (see later)

$K = 1.52 \times 10^5 \text{ dyne/cm}$  (calibrated at end)

$$\therefore F = 8.93 \times 10^{-4} \times 1.52 \times 10^5 = 4\pi R \delta$$

$$\therefore \delta = 24.0 \text{ cm}^2/\text{cm}^2 \text{ (or } 32 \text{ cm}^2/\text{cm}^2 \text{ if use } F = 3\pi R \delta).$$



20 JULY 1989

Insert 1.467 into 5.

11:45 AM

droplet of

Injected white oil with surfaces apart.  
Purged with  $N_2$  during injection. Surfaces did not come into contact during injection. Brought surfaces together with upper motor. Came to flattened "contact" at  $+233^{(4)}$   $\rightarrow 2.5 \text{ \AA}$   
Hg green line checked.

Separated with lower motor.

Jumped apart from  $+178^{(4)}$   $\rightarrow 15 \text{ \AA}$   
to  $-5050^{(1)}$   $\rightarrow 537 \text{ \AA}$

$$K/R = 3.38 \times 10^5$$

$$F/R = -1.76 \frac{\text{dyne}}{\text{cm}}$$

Repeat jump apart more gently with piezo (PZT).

Jumped from  $181^{(4)}$   $\rightarrow 14 \text{ \AA}$ by  $1 \mu\text{m}$   
 $\rightarrow 250 \text{ \AA}$ 

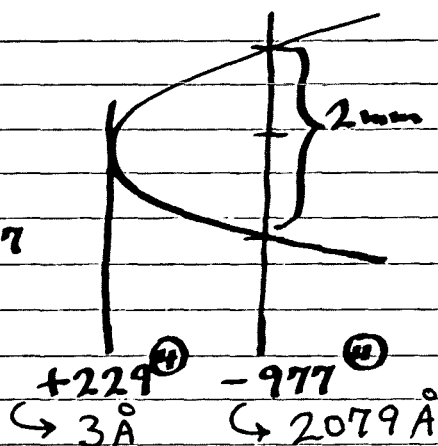
after a short time in contact

$$F/R = -0.80 \frac{\text{dyn}}{\text{cm}} = \frac{\text{mN}}{\text{m}}$$

RADIUS CALIBRATION

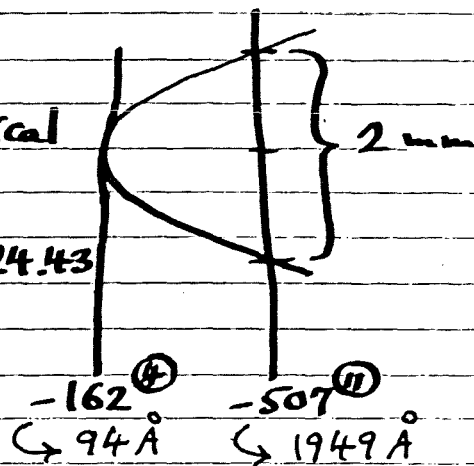
Normal prism

mag. = 23.17



Hysterical prism

mag. = 24.43



$$R_N = \frac{(0.1/23.17)^2}{2 \times 2079 \times 10^{-8}}$$

= 0.45 cm

$$R_H = \frac{(0.1/24.43)^2}{2 \times 1855 \times 10^{-8}}$$

= 0.45 cm

$$\therefore \bar{R} = \sqrt{R_N R_H} = 0.45 \text{ cm}$$

$$K = 1.52 \times 10^5 \text{ dyne/cm.}$$

$$\therefore K/R = 3.38 \times 10^5 \text{ dyne/cm}^2.$$



Surfaces brought into flattened contact at  $+233^{\circ}$   $\rightarrow 2.5 \text{ \AA}$

Hg line checked.

12 PM

Lower motor reversed until contact rounded, then measured forces with lower motor on way out.

$k\Omega$	$D(\text{units})$	$D(\text{\AA})$	$F/R(\text{dyne/cm})$
18.675	$+233^{\circ}$ $\hookrightarrow 2.767^{\circ}$	2.3	
12.589	$+220$	5.3	
10.030	208	8.1	
5.715	200	9.9	
0.740	192	11.8	
14.982	176-180	15.0	<span style="border: 1px solid black; padding: 2px;">-1.10</span>
↓ Jump (with motor)			
	$-1172^{\circ}$	329	0

not used

Measure outward jumps with piezo (carefully)

Jumped from  $+180^{\circ}$  (1 min contact)  $\rightarrow$   $14.6 \text{ \AA}$  to  $-1258^{\circ}$   $\rightarrow$   $4258^{\circ}$   $\rightarrow$   $F/R = -1.20$  (1 min)  $\rightarrow$   $349 \text{ \AA}$

Jumped from  $+178^{\circ}$  (1 min)  $\rightarrow$   $1510 \text{ \AA}$  to  $-1184^{\circ}$   $\rightarrow$   $332 \text{ \AA}$   $\rightarrow$   $F/R = -1.12$  (1 min)

12:15 PM Brought gently with piezo to  $+210^{\circ}$   $\rightarrow$   $7.6 \text{ \AA}$  and left there for 20 min. then jump out from  $+195^{\circ}$   $\rightarrow$   $11 \text{ \AA}$  to  $-1774^{\circ}$   $\rightarrow$   $471 \text{ \AA}$   $\rightarrow$   $F/R = -1.55$  (20 min)

Brought together again with piezo then separated within ~1 minute. Jumped from  $+185$   $\rightarrow$   $13.4 \text{ \AA}$  to  $-1260$

30 sec contact:  $+176 \rightarrow -789 \rightarrow F/R = -0.81$  (30s)  $\rightarrow$   $15.5 \text{ \AA}$

1/2 min contact:  $+176 \rightarrow -1340 \rightarrow F/R = -1.25$  (1/2 min)  $\rightarrow$   $15.5 \text{ \AA}$

$F/R = -1.20$  (1 min)



Definitely looks like the adhesion increases with the time the surfaces remain close to contact (in the potential minimum), but not so much on how close or compressed they are.

25 sec contact: 168  $\rightarrow$  -904  $\rightarrow$  F/R = -0.90 (25s)  $\rightarrow$  17.3 Å  
 1 min contact: 190  $\rightarrow$  -1144  $\rightarrow$  F/R = -1.10 (1min)  $\rightarrow$  12.2 Å

Could be that under high compression it actually takes longer for the molecules to relax.  
 Hg line checked.

FORCE RUN WITH PIEZO

K/R = 3.38

used Piezo: 5.648 Å/V (see next page)

VOLTS	D (units)	D (Å)	F/R *	
-195	-6001 $\rightarrow$ 9001	1,540	0	} 5.68 Å/V
-98	-3893 $\rightarrow$ 6893	989	0	
+10	-1393 $\rightarrow$ 4393	381	0	
+115	+180 $\rightarrow$ 2820	14.6	+0.77	not equilibrated?
277	+216	6.2	+3.8	* Analysis based on $\Delta F = \frac{K}{R} \Delta D$ then adding $\frac{\Delta F}{R}$ from the previous point to get F at each D.
499	228	3.5	+8.0	
736	230	3.0	+12.5	
1013	233	2.3	+17.8	
1013			+17.0	
Reverse				
736	228	3.5	+11.7	
499	226	3.9	+7.19	
277	212	7.2	+2.97	
215	207	8.3	+1.79	
151	197	10.6	+0.58	
78	187	13.0	-0.77	
48	+180	14.6	-1.34	
				↓ jump
48	-1526 $\rightarrow$ 945?	412	0	} 5.66 Å/V
-50	-3805	967	0	

Immediate return to 20 sec contact. Jump out from  $\rightarrow$  -948  $\rightarrow$  F/R = -0.93 (20 sec)



## PIEZO CALIBRATION

Fringe passing  $+243^{\circ}$ , viz.  $\Delta D = 1892 \text{ \AA}$ .  
 $\hookrightarrow 5551.25 / 2 \times 1.467 \rightarrow$

14 volts  $\xrightarrow{\text{forward}}$  348 volts (+1 fringe)

12 volts  $\xleftarrow{\text{return}}$

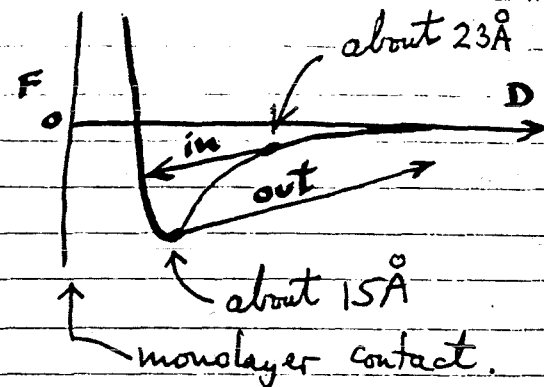
$\therefore 1 \text{ V} = 5.648 \text{ \AA}$  (good)

## Measuring jumps into "contact"

Difficult to measure since very sluggish and jump distance obviously small.

Estimate: from  $\sim +143^{\circ}$  (min. D)

$\therefore D \approx 23 \text{ \AA}$



If we assume that the jump is due to van der Waals forces between the mica surfaces across the surfactant and oil (which both have the same refractive index) we obtain for the Hamaker constant

$$\frac{dF}{dD} = K = \frac{AR}{3D^3} \rightarrow A = \frac{3KD^3}{R}$$

$$A = 3 \times 1.52 \times 10^5 \times (30 + 23)^3 \times 10^{-24} / 0.45$$

$\leftarrow 2 \times \text{monolayer thickness, see later.}$

$$= 8.1 \times 10^{-14} \text{ erg}$$

Is this reasonable?



It was noticed that after a high adhesion the subsequent adhesion was also high if measured soon after the separation, but was lower if the surfaces were kept apart for  $>10$  min. For example, for 1 minute contacts or less, jumps out were  $\sim 1\mu\text{m}$  ( $F/R < 1.0$ ) if the surfaces kept apart for a long time between separations. But if surfaces brought together again within 1-2 minutes, the adhesion rose and remained high as long as adhesions measured repetitively (all after 1 min contact times).

4<sup>40</sup> PM

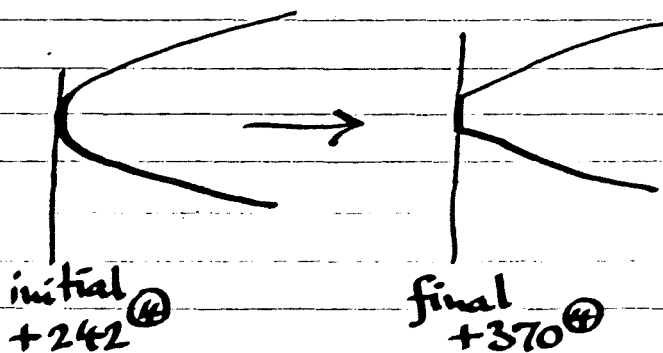
P<sub>2</sub>O<sub>5</sub> replaced by pure WATER.  
Left overnight.

21 JULY 1988

Brought in gently with upper motor.

Came to  $\sim +242^\circ$  then after  $\sim 1$  min slowly moved in to  $\overset{D \approx 0}{\text{more}}^{\circ}$  adhesive flat contact at 360-370.

$\rightarrow D \approx -29^\circ$ .



Monolayer thickness  $\sim 15\text{\AA}$ .

Jump apart on separation until fringes 3.3 mm apart,\* viz.  $D_j = 58,840^\circ$   
 $\therefore \gamma \approx 16 \text{ erg/cm}^2$ .

\* Means separated by 3.3 mm as seen in the eyepiece graticule.

Repeated above: first surfaces stopped at 242 then moved in to 370 then have jump out as above.



Damage.

New position found.

Brought in with motor, gently to hard wall at +232.

↳ 2.5 Å

Separate: jump out from +214 by 300 v of piezo.

Repeat: " " " +203 " 380 V " "  
 +196 " 320 V  
 +200 " 350 V  
 +209 " 345 V

mean: 204 340 V

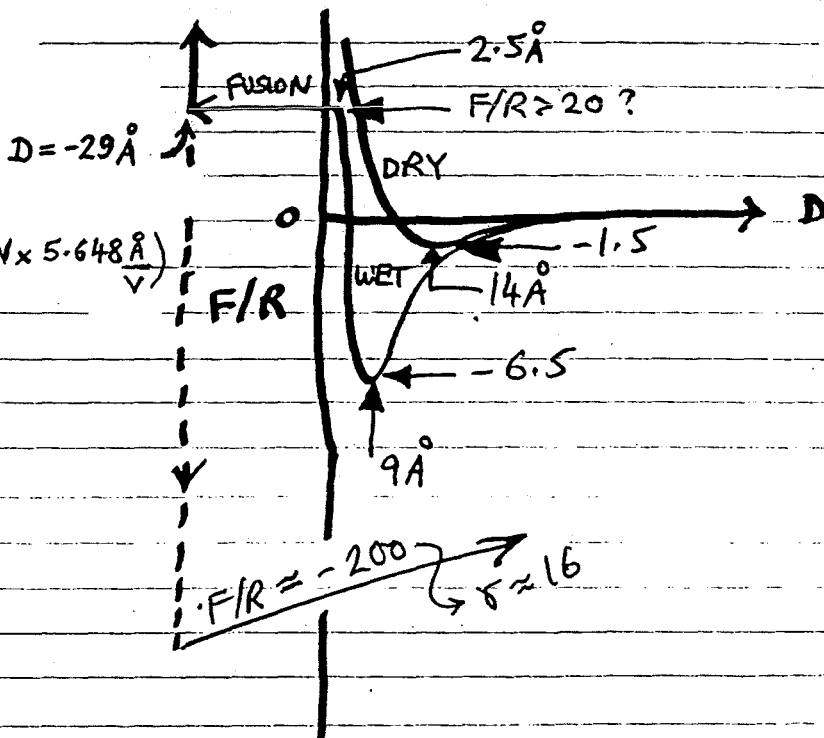
↳ D = 9 ± 2 Å      ↳ F/R = -6.5 \*

\*

$$\frac{\Delta F}{R} = \frac{k \Delta D}{R}$$

$$= 3.38 \times 10^5 \frac{\text{dyn}}{\text{cm}^2} \times \left( 9 \text{ \AA} - 340 \text{ V} \times 5.648 \frac{\text{ \AA}}{\text{V}} \right)$$

$$= -6.46 \text{ dyn/cm.}$$



Proceed in with upper motor: ↔ ↔ ↔ ↔  
 Ease of breakthrough suggests fluid monolayer.      breakthrough separate

Jump apart to where surfaces 3.5 mm apart.

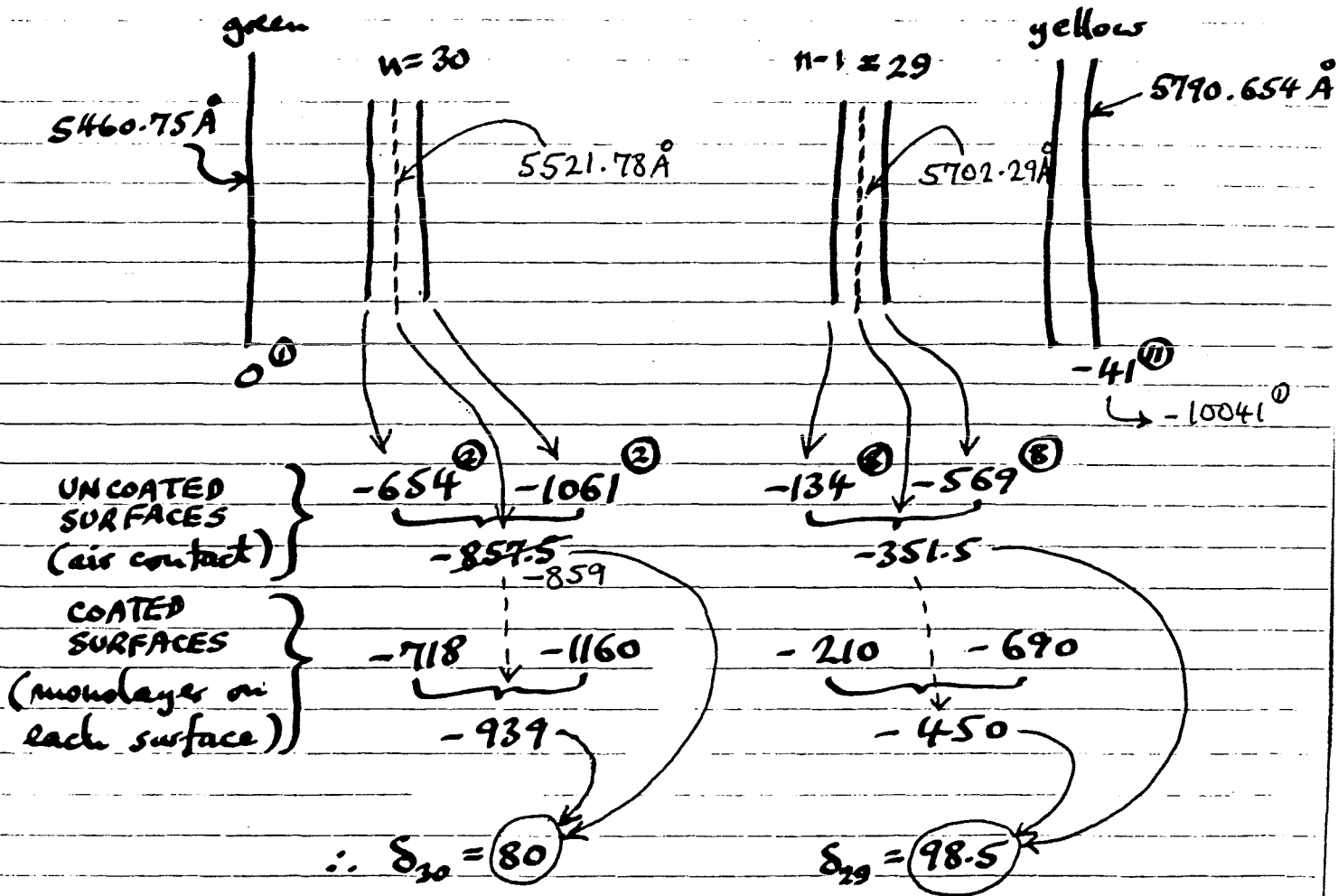
END

Calibrate at k = 1.52 × 10<sup>5</sup> dyn/cm.



# THICKNESS & REF. INDEX OF Ca-Sulphonate\*

Two identical silvered mica sheets used. On one, Ca-sulphonate SA 119 deposited by retraction from distilled water. Two test pieces were prepared, one with the surfactant deposited and one without. Test pieces mounted onto test piece "jig" and FECo fringes optimized until fringes are maximum to the right (red end of the spectrum).



DISPERSION:  $329.904 / 10041 = 0.0328557 \text{ \AA/unit}$

$$\frac{1}{nF_n} = \frac{\lambda_{n-1} - \lambda_n}{\lambda_{n-1}} = \frac{5702.29 - 5521.78}{5702.29} = \frac{1}{31.59}$$

Try  $n=30^*$ ,  $1.024 + 1/30 = 1.0573$ ,  $31.59 / 1.0573 = 29.9 \checkmark$

For  $n=29$ ,  $nF_n = 29(1.024 + 1/29) = 30.70$

∴  $D = nF_n S \lambda_n / 2 \times 1.60 = 30.70 \times 98.5 \times 0.0328 / 3.2 = 31.0 \text{ \AA}$

∴ Monolayer thickness = 15.5 \AA

Refractive index of monolayer:  $\sqrt{\frac{nF_n \delta_n}{n-1 F_{n-1} \delta_{n-1}}} (1.60) = 1.46$

Note: can also use program C on calculator.

Note change to even fringe for n.

(SA-119) Ca Sulphonate - Blandol

$R = 0.145 \text{ cm}$      $K = 1.52 \times 10^5$

Ca Sulphonate monolayer prepared by dipping once and retracting from water in beaker with surfactant in contact with surface.

Contact in air: lenses which flatten out - suggests fluid bilayer (see original notes).  
 $\gamma_{\text{AIR}} = 24 \text{ erg/cm}^2$   
 P205 in chamber

- 0 Force run with piezo
- x after forced contact with upper water at 2.5A
- ⊗ after 1 minute contact, unforced
- + after ~20 min contact, unforced
- ⊠ after ~30 sec contact, unforced

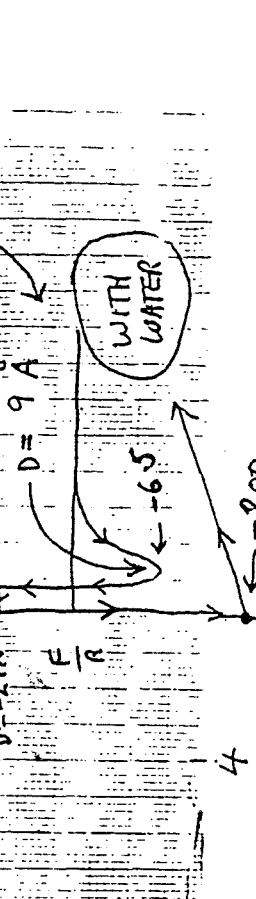
Adhesion high after long time in contact, increasing force at contact, decreasing time between measurements.

P205 replaced by water (overnight equilibration).

Surfaces now come easily to  $D \approx 0 \text{ A}$ , and the squeeze out monolayers coming to  $D \approx -29 \text{ A}$ , i.e.  $\sim 15 \text{ A}$  removed per surface (c.f. 18-19A for 2 dips).

Adhesion: From  $D = -29 \text{ A}$ ,  $F/R = -200$  (twice)  
 From  $D = 2.5 \text{ A}$ ,  $F/R = -6.5$  (5 readings)

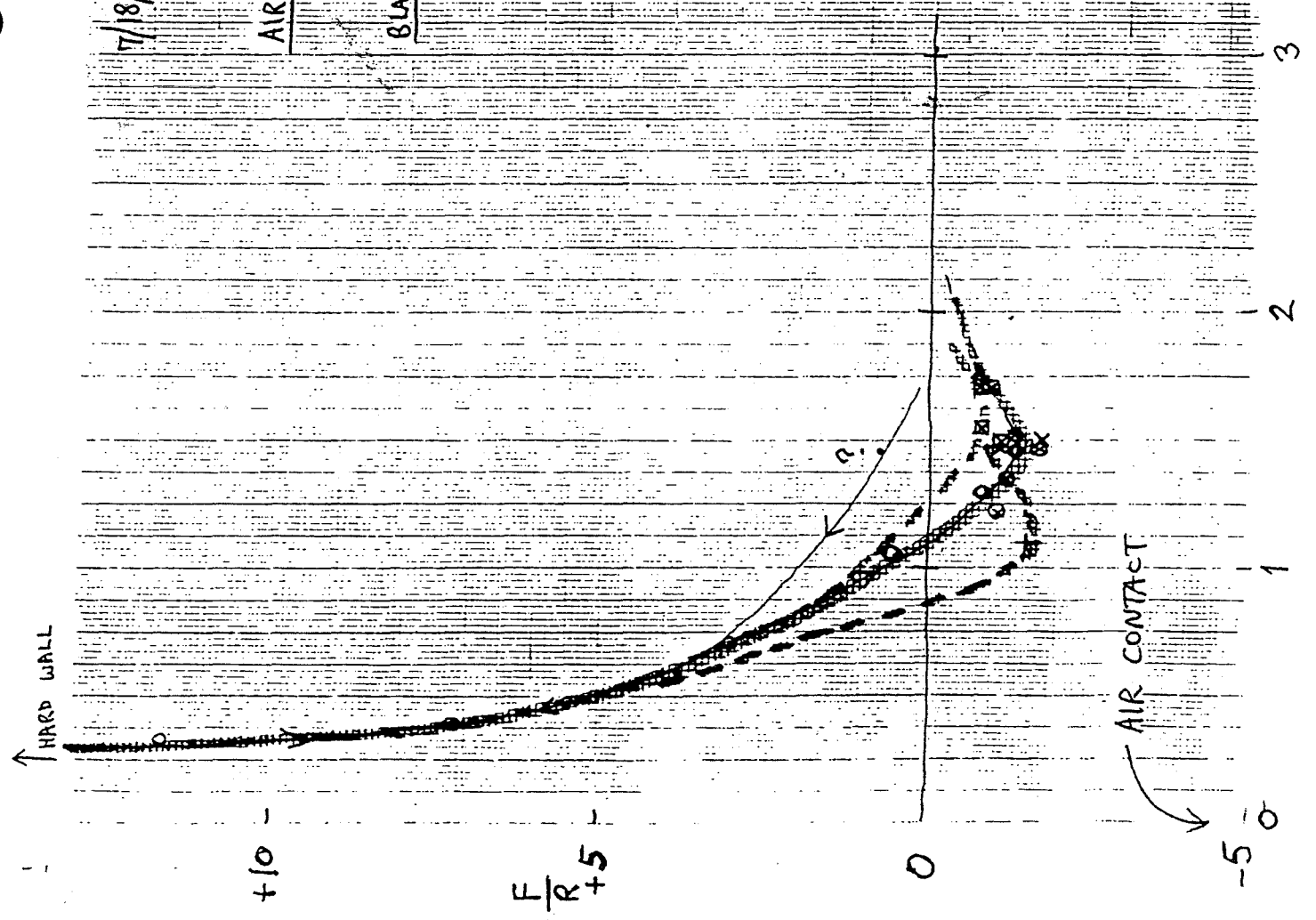
Again suggests fluid monolayer



7/18/88

AIR

BLANDOL



## APPENDIX 3

### Force-measuring capabilities of the SFA and AFM compared

The AFM and SFA are quite different when it comes to force measurements. The AFM cannot measure true force-distance profiles. This may sound surprising because AFM data is often presented in exactly this way – as a plot of force *versus* distance. However, the “distance” in an AFM measurement is not what is normally meant by the “distance” in a force-distance plot: the former refers to the displacement of a spring far from the interaction zone, the latter refers to the separation between two surfaces. The SFA technique allows one to measure the force and, independently and unambiguously, the geometry and separation between two surfaces. The AFM technique uses the measured force to infer all three. This is elaborated in more detail below.

The AFM was originally designed as a microscope rather than a force-measuring instrument: it uses the force between a tip and a surface to obtain an image of the surface. However, it can also be used in reverse – to accurately measure an adhesive force, say, the force needed to detach a tip from a surface, but so long as the distance-dependence of the interaction is not required. To quantitatively measure a *force-law* or interaction potential (i.e., the force as a function of the surface separation), one has to be able to measure not only the force but also the geometry of the interacting surfaces and their absolute distance of separation. While the AFM can measure a force, it cannot independently measure the geometry nor the surface separation, that is, it cannot measure a true force-distance or energy-distance curve without making assumptions about the nature of the force and compliance of the surfaces. The AFM technique becomes more reliable at large separations, where the forces are weak, but again the surface separation is only known to within an unknown correction factor.

In contrast, the SFA (Surface Forces Apparatus) was designed right from the start to measure not only forces, but also the local surface geometry of the interacting surfaces and the exact separation between them. The SFA can do all this because the FECO optical interference technique used in the SFA measures the surface separation and surface shape profiles precisely at the point where the interaction occurs. The AFM, on the other hand, does not measure the absolute distance between the two interacting surfaces (the tip and a flat surface). Instead, it measures the displacement of a cantilever spring at some point away from the interaction zone, and there is no way of unambiguously telling whether a  $10\text{\AA}$  deflection measured corresponds to a  $10\text{\AA}$  deflection between the surfaces. It could be that the surfaces are already in contact but are elastically flattening under the influence of an attractive short-range adhesion force, in which case the measured  $10\text{\AA}$  deflection corresponds to *zero* change in the surface separation, as illustrated in Figures 53A and B. Similar problems arise with capacitance measurements of surface separations. Furthermore, the local tip geometry in the interaction zone is never known in an AFM experiment, and since all elastic surfaces (especially soft organic, polymer and biological surfaces) generally deform during an interaction, this further complicates interpretation of the results.

**Figure 53A.**

Typical “spring deflection-displacement” curve measured by AFM when one surface is made to approach the other, which is interpreted as a “force-distance” curve. Figure 53B illustrates the ambiguity of this interpretation.

Measured displacement (force)

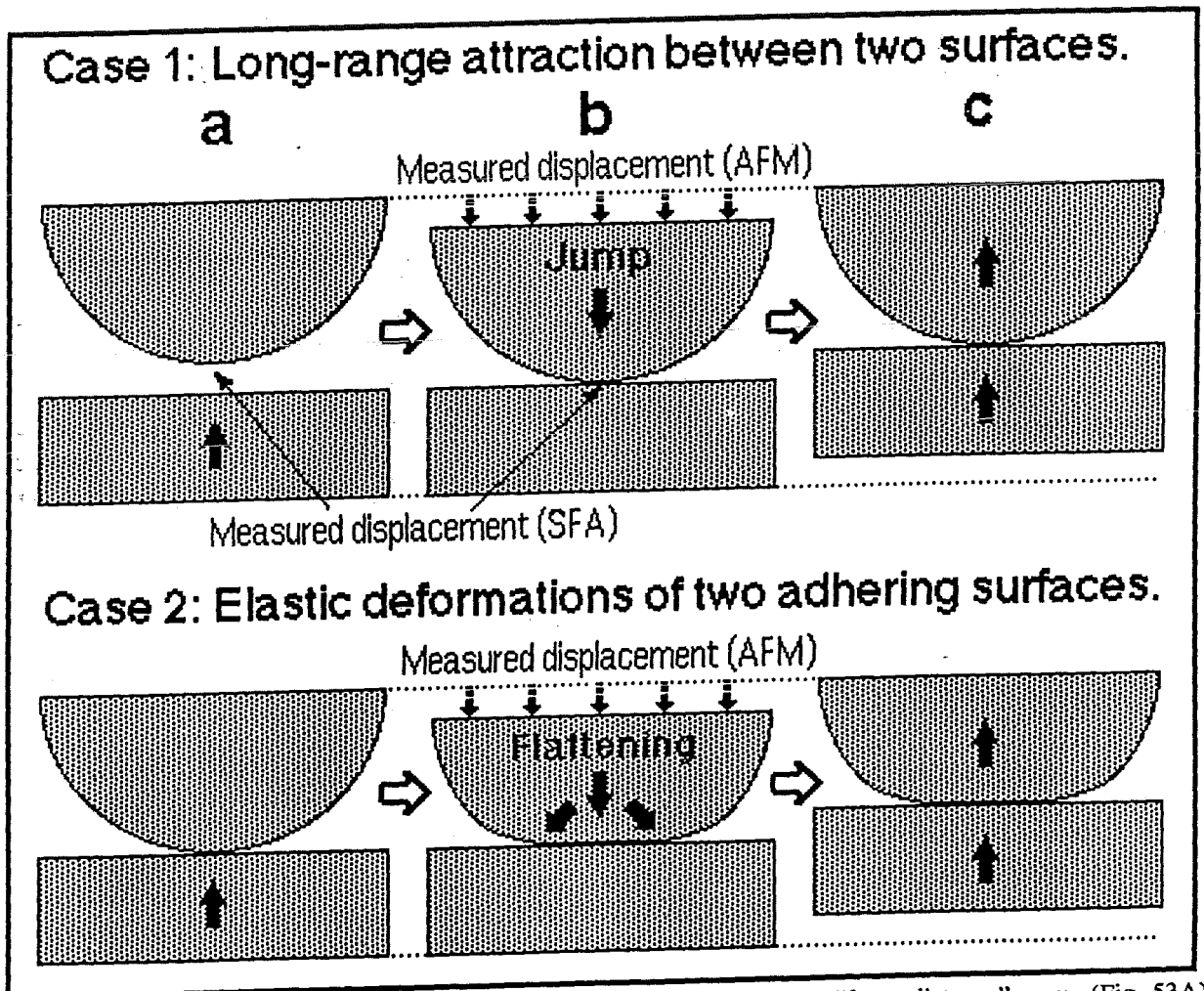
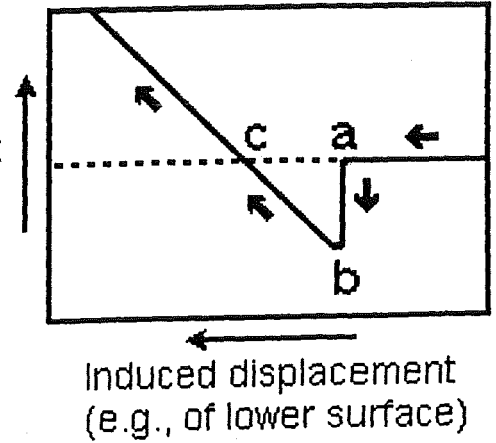


**Figure 53B.** Two very different interactions that nevertheless give the same “force-distance” curve (Fig. 53A) when measured by the AFM. In Case 1, a real long-range force causes the two surfaces to jump into contact (a → b). In Case 2, the surfaces are already in contact when an apparent jump occurs. In Case 1, the distance between the two surfaces has changed during the jump, but in Case 2 it has not, yet the AFM method of measuring displacements will record indistinguishable force-distance curves for these two very different situations. On the other hand, the FECO optical technique will record the true change in surface separation during the jump (finite change in Case 1, no change in Case 2) and also give the exact change in shape and contact area of the two surfaces in Case 2.

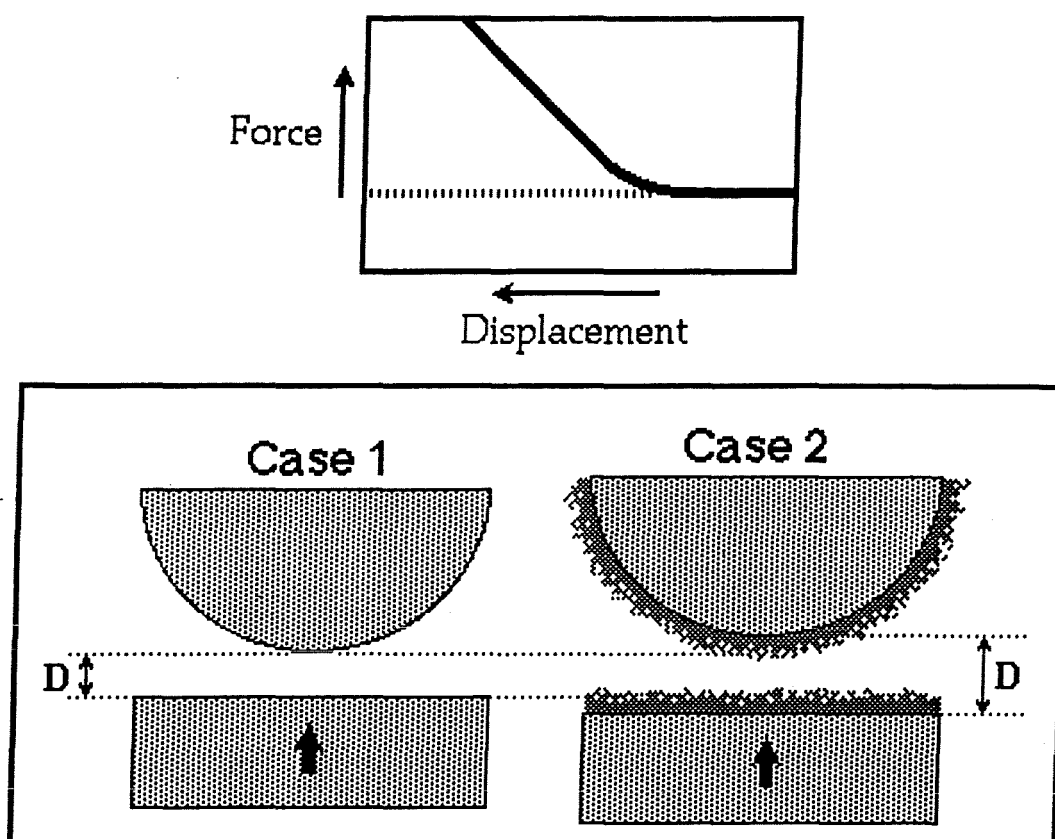


**Figure 53C.** This shows a different scenario where again the AFM will produce erroneous results. In this case, the recorded force *vs* distance between two surfaces (or a tip and a surface) in aqueous electrolyte solution may look like the one shown in the top of Figure 53C. Such a curve could be generated by an exponential electrostatic (double-layer) repulsion between two charged surfaces, but the same curve could arise from an adsorbed layer of polyelectrolyte polymer where the tail-end of the force is the same as the double-layer force, but where closer-in there is a sharp steric “hard-wall” repulsion. The AFM will not be able to distinguish between these two very different forces and will not show that there is a polymer layer of finite thickness on the surfaces (which could be a contaminant layer).

One more example illustrating the power of the FECO optical technique in SFA experiments concerns forces measured in sliding (or AFM scanning) experiments. Consider one surface moving laterally across a perfectly smooth surface that is chemically heterogeneous: for example, a surface with hydrophobic and hydrophilic groups at different positions. The AFM will not be able to distinguish a change in surface topography from a variation in the local intermolecular interactions. The resulting “image” could be interpreted either way, with no way of knowing which is correct. Again, SFA measurements of lateral forces can distinguish changes in surface separation from changes in both normal and lateral (friction or lubrication) forces.

Last, but by no means least, the SFA lets you know when you have a contaminant layer or unwanted particle between your two surfaces – the range and magnitude of the forces, together with the irregular surface deformations occurring on approach, clearly indicate when “something is wrong”.

END OF PART 4 (END OF SFA3 MANUAL)



# SurForce™ Corporation

2233 Foothill Lane, Santa Barbara, CA 93105, USA.  
Tel. 805-899 9292, Fax. 805-899 9190.

April 1997

## SFA3™ MANUAL UPDATES

The following material is provided free for customers of SurForce™ Corporation.

### SETTING UP A BASIC (NO FRILLS) SURFACE FORCES MEASUREMENT LAB

#### Location of SFA lab

Ideally, your laboratory should be located in a basement or ground floor – well away from vibration-producing machinery such as large pumps or air-conditioning units. The walls, furniture and floor should never be coated or cleaned with oil-based polishes that give off surface active contaminants into the atmosphere (these can usually be smelled if present). All laboratory surfaces, including floors and work benches, should be cleaned with warm water only. The dark room(s) should be thermostatically controllable, to  $\pm 0.1^\circ\text{C}$  if possible. The thermostating air-conditioning or air-ducting system should not be connected to other laboratories so as not to introduce air-borne contamination into the lab atmosphere. Ideally, the air pressure of the laboratory should be slightly higher than that of the adjoining rooms, ensuring a steady flow of (clean and thermostatted) air from that room outwards.

#### Recommended laboratory hardware and fittings for basic SFA measurements

Your SFA3™ package should arrive in a condition ready for immediate use in experiments – all necessary apparatus parts, basic supplies, assembly tools, electrical items and cables being provided with your unit. However, a number of additional laboratory hardware items (not provided in the package) are needed for carrying out basic experiments. These are listed in the following Table.

Some labs will already have some of the equipment listed, for example, a vacuum chamber. Other equipment and electronic devices such as video and CCD cameras, function generators, strain-gauge bridges, chart recorders, storage O-scopes, Langmuir-Blodgett deposition cell, etc., may be required for specialized tribological or biological experiments (see SFA3™ Manual for a complete list of possible items).

It is assumed that the laboratory is well-equipped with standard lab furniture and disposable items, such as work benches (fume hood), sinks, essential materials (mica) and laboratory supplies such as glassware, chemicals, liquids (distillation unit), filters, etc. A source of pure (and dry) high pressure nitrogen gas is also required, either from boil-off (liquid nitrogen source) or from a pressurized cylinder.

<b>EQUIPMENT ITEM</b> [and possible supplier*]	<b>REQUIRED FOR</b>	<b>PRICE</b> \$
<b>OPTICAL ITEMS</b>		
<b>Grating spectrometer [Spec]</b> 1/2 or 1/4 meter, with adjustable width entrance slit, first exit port modified for wide-field viewing eyepiece on translation stage with manual drive encoder (travel distance: 15 mm), second exit port for video camera. Recommended dispersion: 32 Å/mm – 1200 grooves/mm, 550 nm blaze.	Measuring surface separations, surface shapes, thin film thickness and refractive index using FECO fringe interferometry.	6,000 to 11,000
<b>Prism turntable [Newport]</b> with 3-axis rotation/tilting controls.	For holding prism at spectrometer entrance slit.	450
<b>Wide field Eyepiece</b> 10X adjustable focus, with 10 mm X10 mm sq. grid reticule / graticule.	For mounting on translation stage at spectrometer exit port.	250
<b>Display Counter [Newport]</b> with power supply.	For translation stage encoder output at spectrometer exit port.	600
<b>White light source</b> 12V, 100W Tungsten-Halogen lamp, or Xenon Arc Lamp, with focusing (collimating) lens and IR heat filter.	White light source for SFA box.	1,000 to 2,000
<b>IR filter (hot mirror)</b>	For absorbing/reflecting IR light from white light source.	50 to 100
<b>Dove prism</b> in rotary holder	For rotating image from SFA box before it goes into spectrometer.	75 to 250
<b>Yellow Filter</b> (or sodium lamp)	For observing Newton's rings with white light (instead of Na lamp).	65
<b>Mercury Lamp</b> thin pen-ray type (~5 W)	Wavelength standard calibration (also for curing certain glues)	500
<b>Stage micrometer</b>	For calibrating lateral magnification of spectrometer output image	50
<b>VACUUM COATING UNIT</b>		
<b>Vacuum Coating Unit / Evaporator</b> with 18" high bell jar	Deposit silver, silica, etc., on mica.	11,000
<b>Thickness monitor</b>	Measuring thickness of deposited films on mica (or other) surfaces.	2,000 to 3,000

<b>EQUIPMENT ITEM [and possible supplier*]</b>	<b>REQUIRED FOR</b>	<b>PRICE \$</b>
<b>MICA CUTTING AND GLUING</b>		
<b>Mica cutting stage [Prior]</b> XYZ translation stage with platinum wire, low voltage DC power supply.	For cutting thin mica sheets by melting through them (mica sheet supported on two metal blocks).	1,200
<b>Small Hot-Plate</b> Use with low voltage power supply. Can be constructed in-house.	For melting thermosetting glues, used for gluing mica sheets to silica disks.	NA
<b>ELECTRICAL ITEMS</b>		
<b>Low Voltage DC Power Supply</b> Dual Outputs: 0 to $\pm 24V$ , 5 Amp.	For 100 W lamp, mica cutting stage, and small gluing hot-plate.	300 to 400
<b>Multimeter (5 digit)</b>	AC/DC V-I-R measurements.	1,500
<b>Voltage amplifier [Trek]</b>	Amplify outputs from Control Centre to piezo and bimorphs.	1,500 to 2,500
<b>MISCELLANEOUS</b>		
<b>Pressure rinsers [Gelman]</b> or ethanol squirt guns	For high pressure ethanol squirt cleaning of SFA parts.	500
<b>Laminar Flow Cabinet</b> or Work Station: Outward horizontal air-flow type	For cutting mica, apparatus assembly, and other preparations under dust-free conditions.	5,000
<b>Glass Desiccators</b>	For storing mica sheets, samples, etc.	500
<b>Anti-vibration table</b>	For placing apparatus (optional, but essential for laboratories located above ground-level).	2,500
<b>Oil-less pumps</b>	Aspirating liquids, evacuating desiccators.	1,000

\* In the Table, we have sometimes included specific supplies and suppliers. SurForce™ Corporation is not promoting or advertising, nor is it affiliated with, any supplier, in any way whatsoever. The information contained herein is purely meant for guidance and is based on lists of suppliers and supplies we have used in the past and this may change at any time. Note also that all prices are approximate, based on 1996 price lists, and do not include TAXES, SHIPPING and HANDLING.

## **BEFORE THE FIRST EXPERIMENT**

Before the first experiment with a new apparatus, it is advisable to clean it thoroughly, especially all screw threads and threaded holes. In addition, ensure that all the metal parts that come into contact with liquid in the lower chamber are indeed made of non-corrosive stainless steel (type 304 or 316). All these parts, including all screws and washers, should be left in water for a few hours. Any corrosive metal can be recognized from the (usually brownish) coloring of the aqueous solution that slowly develops near its surface.

## **GROUND LOOPS (EARTH LOOPS)**

Ground loops can give rise to noisy electric output signals and voltage spikes during experiments, especially when sensitive electric signals are being recorded as often occurs during friction and dynamic measurements. Large transient voltage spikes can be particularly annoying and even damaging. These typically appear when high voltage circuits, such as the 110 or 220 Volt optics control circuits are switched on or off. If this occurs, you should test for ground loops in your electric connections and cables. First check that there is only one common ground terminal, e.g., the strain gauge bridge. If the noise and spikes persist, check that the apparatus walls and all connector casings and outer cable shields are indeed electrically connected to the common ground (you can do this with a multimeter – the resistance readings should always be well below 1 Ohm). Devices that detect weak signals – such as the Friction Device output cable and the Bimorph Vibrator coaxial cable – should be checked particularly thoroughly.

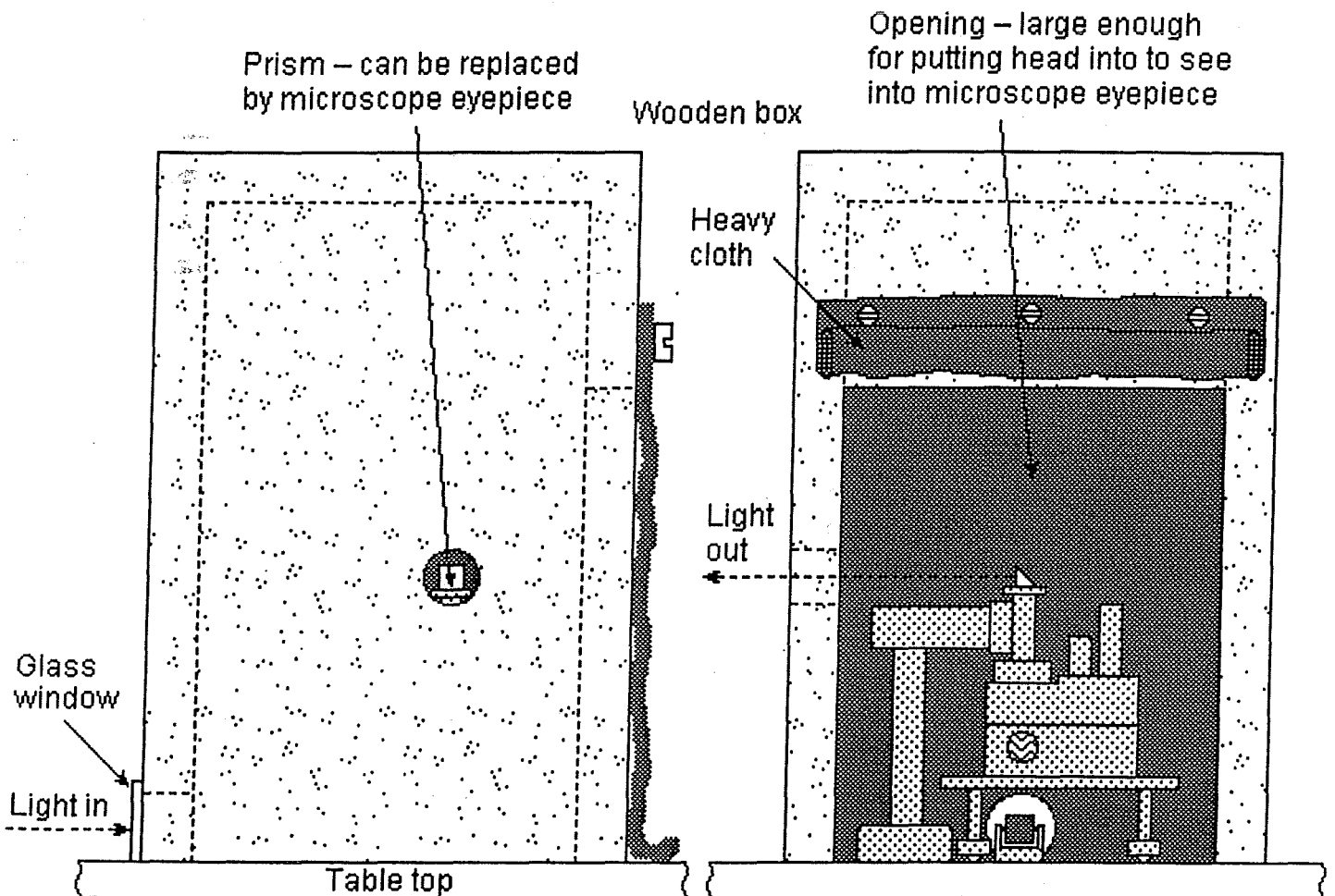
If unexpected noise and spikes suddenly appear, the most likely reason is that the shielding or outer connection of one of the output cables has become detached from its metal receptacle/connector because someone had recently disconnected it by pulling the cable rather than the connector. The problem, once the source has been found, is always easy to fix.

## **DRIFTS**

Allow to settle for at least one hour after changing anything, such as filling, injecting liquid, finding a new position, or switching on the light. If a drift persists, check the following: (1) that the coarse nut on the differential micrometer is tight, (2) that a heat-reflecting or absorbing mirror/window, or a 6" water bath, is in the path of the light, (3) that your thermostating air-conditioning system has not broken down, (4) insert a filter or two in series to the air outlet (to allow the pressure outside and inside the chamber to equilibrate rapidly – in case the atmospheric air pressure is changing rapidly), (5) reduce the intensity of the lamp by lowering the voltage through the bulb. Also, did you tighten the spring-clamping screw and two small

Philips screws on the variable spring mount? Did you check that both silica disks were firmly tightened into place? Did you tighten the piezo mount evenly in place? It is also possible that the piezo crystal tube has become loose; this sometimes happens if the epoxy glue layer that bonds it to the steel support has deteriorated (due to prolonged exposure to humid or certain organic atmospheres). To check that the crystal mount is 'robust', hold it firmly with gloved fingers at either end, then gently (without over stressing) twist or bend it to see if the glue layer is loose or 'gives'.

Is your apparatus enclosed in a (wooden) box inside the thermostatted room? Such an enclosure, with an opening on one side which can be covered with a heavy cloth when the apparatus is in use, can be very useful for preventing drafts and further reducing thermal drifts (and vibrations – see below).

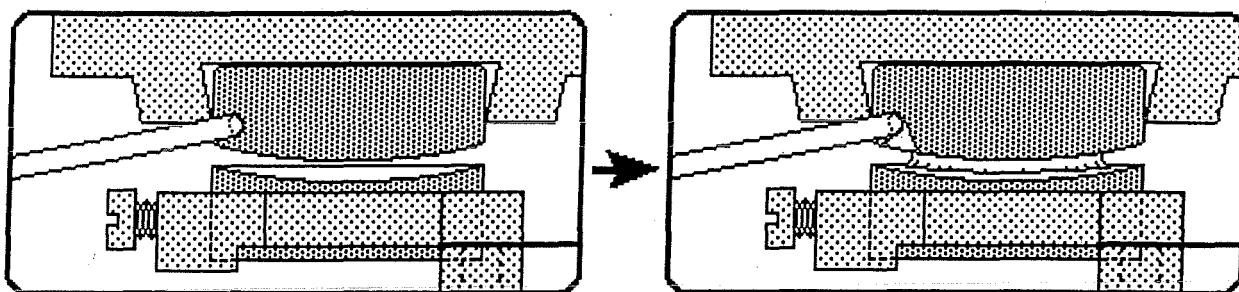


Drifts are more pronounced in droplet experiments (see Figure below). This is because the droplet may be slowly evaporating or because of contact angle hysteresis. Evaporation is a common problem, especially when using volatile liquids such as low MW hydrocarbons, alkanes, organic liquids and even water. Evaporation causes drift because the effective mass of the lower surface is constantly decreasing with time, resulting in a steady inward drift. The second effect (contact angle hysteresis) causes drift after the surfaces are moved towards or away from each other because the meniscus is still relaxing well after the piezo or motor have stopped moving. Such drifts can persist for a long time after a distance adjustment in a direction determined by the previous history of approach and separation of the surfaces. Liquids that wet the surfaces (have zero contact angle) do not exhibit this effect, but can cause drifts due to evaporation. Evaporation can be reduced by saturating the measuring chamber with the liquid's vapor, either by filling the small bath in the syringe injector port or by simply injecting a few drops of the liquid into the chamber (in this case, however, you will not be able to remove the liquid during the experiment except, perhaps, by a prolonged purge with clean nitrogen gas). The rate of evaporation depends on the temperature of the droplet between the surfaces relative to that of the vapor. When light is passing through the surfaces and droplet, they heat up by  $\sim 1^\circ\text{C}$  above the surrounding which enhances the evaporation rate. This effect can be reduced by following some of the procedures listed above. In addition, one may also completely cover the floor of the lower chamber with a  $\sim 1$  mm layer of the liquid; this will also ensure that part of the liquid is also heated by the light coming through the lower window, which raises the vapor pressure. If possible, it is always better to fill the box with liquid than do droplet experiments.

In most cases it is impossible to completely eliminate all drift, the best that can be hoped for is a drift of the order of  $1\text{-}2 \text{ \AA}/\text{sec}$ . This may be negligible if the time between force measurements (data points taken at different separations) is  $15\text{-}30$  sec, as is usually the case. Additionally, since the drift rate is usually fairly constant over a fairly long time period (many minutes to hours) this constancy can be used to advantage by making force measurements in a time-consistent way. The following two examples illustrate how this can be done depending on the type of force being measured and the system relaxation time: (1) Apply a ramp voltage to the piezo to exactly offset the drift during the more crucial measurements. (2) Measure forces between two points by both increasing and decreasing the voltage on the piezo, i.e., both on going in and going out, and take the average. Use the same times to equilibrate at each position, both on going in and going out. You may also need to calibrate the piezo separately on going in and going out. Similarly for measurements with the DC motor (Motor 1).

## INJECTING A LIQUID DROP BETWEEN THE SURFACES

It is not necessary to separate the surfaces by more than a few microns before injecting a small droplet of liquid between them. Just aim the tip of the syringe needle gently at the upper silica surface and let the injected liquid flow down where it will immediately be sucked between the surfaces by capillary forces, as shown below (however, you should calculate in advance whether the surfaces might come into contact by these forces given the spring stiffness you are using at the time). Immediately after the droplet has spread between the surfaces, move them rapidly towards each other, but not yet into contact, to prevent any possible dust or contamination from settling on them. By keeping the surfaces close together at all times, you can also see the FECO fringes on your video screen during the whole process.



## VIBRATIONS

An anti-vibration or optics table is essential for really vibration-free work. If vibrations persist, first check that the three base legs are not wobbly – that they are all screwed tightly to the base at one end and to the rubber foot at the other, and that the brass thumb screws are also tight. Make similar checks to those when drifts occur (see DRIFTS above). Each apparatus, depending on its construction and mass, has its own spectrum of resonance frequencies that it is particularly susceptible to. Your SFA3 may be sensitive to the frequencies being generated by, for example, a nearby flow hood, in which case do not have the flow hood running during experiments since this may cause the surfaces to vibrate, especially in air. These vibrations can reach the apparatus through the air (sound waves) so that having a good vibration isolation table will not prevent this. You can isolate the apparatus in a wooden box (see DRIFTS above) as well as change its resonant frequency by adding weights (ballast) to the base plate, such as lead weights underneath it.

## FLOW OF LIQUID DURING TEMPERATURE CHANGES

Whenever the heaters are on and heating up the liquid, unavoidable flow patterns are set up within the chamber. These convections produce regular low-frequency oscillations of the

surfaces. However, they should only be there when the temperature is *changing*. Once the temperature has stabilized, and especially once the heaters are turned off, the oscillations should die down very rapidly, during which time one can make accurate measurements (of course, if the heaters are "off" the temperature will be slowly falling). One can also insert baffles or other obstacles (e.g., glass beads) into the chamber to block or break up the flow currents.

### **SYRINGE INJECTOR – VAPOR PRESSURE CONTROL BATH**

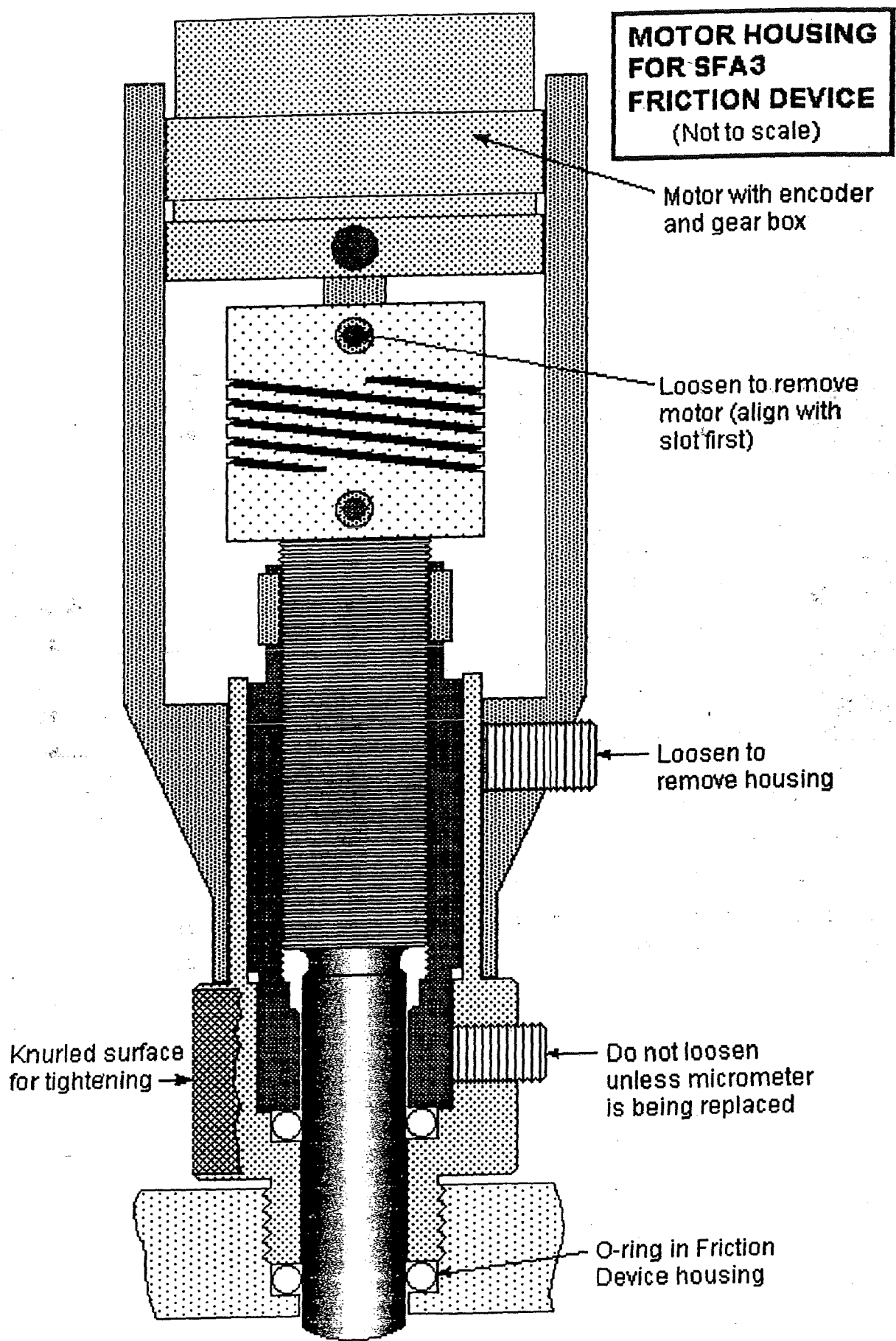
To install the liquid bath (page 37, Fig. 25, left) first insert a Teflon -012 O-ring into the syringe injector opening on the left of the Lower Chamber, then insert the Kel-F bath through the steel mount, then push the bath through the O-ring until the steel lip goes into the O-ring groove. This presses the O-ring both against the Kel-F bath and the groove walls to seal all around. The more you tighten the three hex screws, the better the seal, but you should not need to tighten them much to obtain a good seal.

### **BIMORPH SLIDER / VIBRATOR.**

The outer wire (cladding or shield) of the coaxial cable to the bimorph slider and vibrator is not supposed to connect all the way through. It simply shields the coax up until it reaches the apparatus. This avoids 'earth loops' problems (see page 43) because the outer shield is connected to ground (earth) via the BNC output of the amplifier or function generator, and the apparatus is connected to ground via the terminal on the front of the base plate. However, one must ensure that the (earthed) surface of the bimorph is indeed connected to earth through its internal contact with the apparatus (see Figure 50, page 120).

### **MOTOR HOUSING**

The following page shows a drawing of the Motor Housing (both for Motor 1 and Motor 2) which may be helpful when dismantling it or changing the motors.



## NEW ITEMS

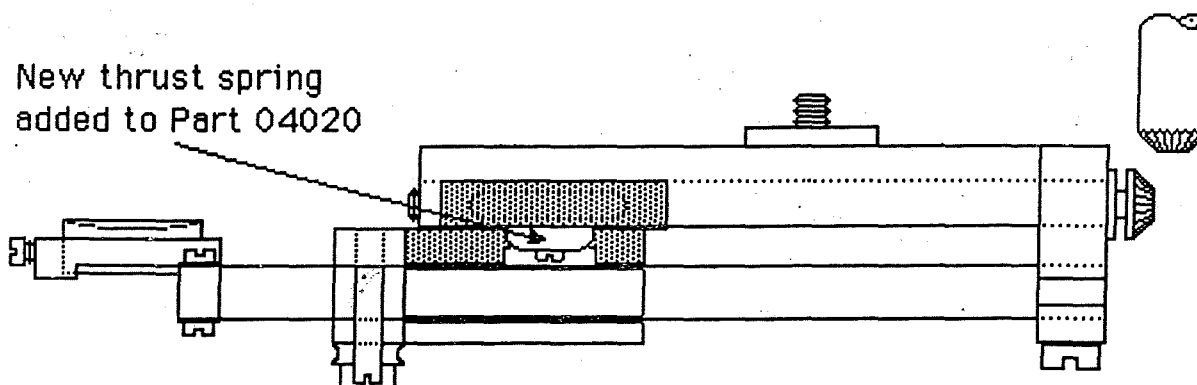
If you are interested in any of the following new developments, please ask.

**Silica disks.** ESCO Optical Products, Inc. is now recommended for their excellent workman in making silica disks and windows of any shape or size. They are also much cheaper and faster than any previous suppliers that we have dealt with. Their address: 171-T Oak Ridge Road, Oak Ridge, NJ 07438. Phone: 800-327 1399 or 201-697 3700, fax: 201-697 3011. SurForce Corporation is planning to purchase the more commonly used disk sizes in bulk (which is cheaper), and provide them to customers when needed at roughly the same cost.

**Disks for mounting surfaces 'under water'.** A new "Universal Disk Mount" has been perfected for both the upper and lower disks. These new disk supports can take both cylindrical disks and a new type of rectangular dove-tail disk that can be inserted 'under water' through the front window, without removing the Lower Chamber. The rectangular disks, when held by specially shaped self-locking tweezers, can have monolayers deposited on them in an Langmuir Blodgett or Langmuir-Schaeffer trough, and then inserted directly into the SFA3. Please contact SurForce™ Corporation if you are interested in these disks.

**Motor speed control card.** A new speed-control card (cost ~\$100) can be added to the circuitry of MOTOR 2 (friction motor) which greatly increases the range of sliding speeds that can be attained to 3.5 orders of magnitude. A 10K 10-turn potentiometer is also required to provide the required speed-control sensitivity. This can also be done with MOTOR 1, but such a large range of speed is usually not needed for this motor. If your Control Box does not have this card, it will be provided free of charge with instructions on how to install it into the Control Box.

**Additional anti-backlash thrust spring for sliding clamp.** An additional spring has been added to the slider (part 04020) of the variable stiffness spring which greatly improves the stability of the force-measuring spring. If your slider does not have this (see figure below) it will be provided free of charge.



© Copyright SurForce™ Corporation, 1997.  
All rights reserved.